

Topological Quantum Many-Body Physics

Lecture Notes • Summer Term 2025

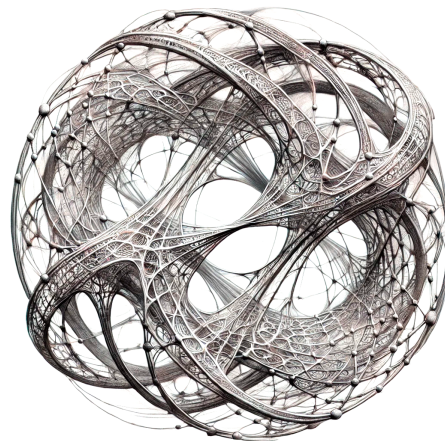
Nicolai Lang*

*Institute for Theoretical Physics III
University of Stuttgart*

Updated June 20, 2025

Version (Git Commit): 4389b57

Check for Updates: → itp3.info/tqp



How DALL·E imagines “the braiding of anyons” in 2025.

*nicolai.lang@itp3.uni-stuttgart.de

Contents

Contents	ii
Preliminaries	v
Requirements for this course	v
Literature recommendations	v
Goals of this course	viii
Notes on this document	ix
Symbols & Scientific abbreviations	x
0. Setting the Stage	1
0.1. Motivation: Transferring energy with pendulums	1
0.2. The Big Picture	7
0.3. Quantum phases and quantum phase transitions	9
0.4. Spontaneous symmetry breaking	13
0.5. Extending Landau's paradigm: Topological phases	15
0.6. Overview and Outlook	25
I. Topological Phases of Non-Interacting Fermions	29
1. The Integer Quantum Hall Effect	30
1.1. From the classical to the quantum Hall effect	31
1.2. Landau levels	34
1.2.1. Landau gauge	35
1.2.2. \ddagger Symmetric gauge	36
1.3. Berry connection and Berry holonomy	38
1.3.1. Berry phase and Chern number	42
1.4. Quantization of the Hall conductivity	47
1.4.1. The Kubo formula	47
1.4.2. The TKNN invariant	51
1.5. The role of disorder	58
1.6. Edge states	61
1.7. Notes on classification	66

2. The Quantum Anomalous Hall Effect	68
2.1. Preliminaries	68
2.1.1. Lattice models with two bands	69
2.1.2. Time-reversal symmetry (TRS)	74
2.1.3. Dirac fermions	80
2.2. The Qi-Wu-Zhang Model	82
2.3. The Haldane Model	86
2.4. ‡ Experiments	92
3. The Topological Insulator	93
3.1. Construction of the Kane-Mele model	94
3.2. Phase diagram	98
3.3. Vorticity of the Pfaffian and the \mathbb{Z}_2 -Index	100
3.4. Edge modes	109
3.5. ‡ Experiments	112
4. The Su-Schrieffer-Heeger Chain	113
4.1. Preliminaries: Sublattice symmetry	113
4.2. The Su-Schrieffer-Heeger chain	116
4.3. Diagonalization	118
4.4. A new topological invariant	119
4.5. Breaking the symmetry	122
4.6. Edge modes	123
4.7. ‡ Experiments	128
5. The Majorana Chain	129
5.1. Preliminaries: Particle-hole symmetry and mean-field superconductors	129
5.2. The Majorana chain	131
5.3. Symmetries and topological indices	135
5.4. Majorana fermions	139
5.5. Edge modes	141
5.6. ‡ Application as topological quantum memory	144
5.7. ‡ Experiments	154
6. Classification	155
6.1. Generic symmetries and the tenfold way	155
6.2. The periodic table of topological insulators and superconductors	160
6.3. Frameworks for classification	161
6.4. Consequences of interactions	165
II. Symmetry-Protected Topological Phases of Interacting Spins	169

III. Intrinsic Topological Order and Long-Range Entanglement	170
Bibliography	171

Preliminaries

Important

This script is in development and continuously updated. To download the latest version:

➔ itp3.info/tqp

If you spot mistakes or have suggestions, send me an email:

➔ nicolai.lang@itp3.uni-stuttgart.de

Requirements for this course

I assume that students are familiar with the following concepts:

- Non-relativistic quantum mechanics and second quantization
Fermions, bosons, spins, ...
- Basics of condensed matter theory
Band theory, quasi particles, Fermi sea, ...
- Basics of quantum information theory
Qubits, quantum gates, ...
- Basics of group theory
(Non-)abelian groups, linear representations, ...

Literature recommendations

This course follows no particular textbook but draws its inspiration from various sources.

Topological phases of non-interacting fermions (Part I):

- Bernevig & Hughes: *Topological Insulators and Topological Superconductors* [1]
ISBN 978-0691151755
Accessible introduction to topological phases of non-interacting fermions.
- Asbóth *et al.*: *A Short Course on Topological Insulators: Band Structure and Edge States in One and Two Dimensions* [2]
ISBN 978-3319256054
Accessible brief introduction to topological phases of non-interacting fermions.
- Franz & Molenkamp *et al.*: *Topological insulators* [3]
ISBN 978-0444633187
Accessible and comprehensive introduction to topological insulators in two and more dimensions.

- Shen: *Topological Insulators: Dirac Equation in Condensed Matters* [4]
 ISBN 978-3642328589
 Accessible introduction to topological insulators and superconductors.
- Moessner & Moore: *Topological Phases of Matter* [5]
 ISBN 978-1107105539
 Comprehensive introduction to topological phases of matter (including topological order).

Symmetry-protected topological phases of interacting bosons (Part II):

- Chen *et al.*: *Classification of gapped symmetric phases in one-dimensional spin systems* [6]
 Original research on the classification of interacting spin systems in one dimension.
 (Quite accessible, in particular the first sections of the paper.)
- Verresen *et al.*: *One-dimensional symmetry protected topological phases and their transitions* [7]
 Original research on the classification of interacting systems of spins and fermions in one dimension.
 (Quite accessible, in particular the introduction to the paper.)

Intrinsic topological order and long-range entanglement (Part III):

- Simon: *Topological Quantum* [8]
 ISBN 978-0198886723
 Thorough and modern introduction to many aspects of topological order (anyons, TQFTs, ...).
 I highly recommend this book!
- Pachos: *Topological Quantum Computation* [9]
 ISBN 978-1107005044
 Accessible introduction to anyon models and topological quantum computation.
- Moessner & Moore: *Topological Phases of Matter* [5]
 ISBN 978-1107105539
 Contains chapters on topological order and topological quantum computing (among others).
- Wen: *Quantum Field Theory of Many-Body Systems* [10]
 ISBN 978-0199227259
 Focus on field theory methods to describe quantum many-body systems.
- Wang: *Topological Quantum Computation* [11]
 ISBN 978-0821849309
 Very mathematical treatment of anyon models and topological quantum computation.

Mathematical Background

- Nakahara: *Geometry, Topology and Physics* [12]
 ISBN 978-0750306065
 Extensive, mathematically rigorous treatment of topology for physicists.

Milestones & Nobel Prizes

There are three nobel prizes directly related to the subject of this course:

- **NOBEL PRIZE IN PHYSICS 1985:**

The Nobel Prize in Physics 1985 was awarded to KLAUS VON KLITZING “for the discovery of the quantized Hall effect.”

Related milestone paper:

- [13] K. v. Klitzing, G. Dorda, M. Pepper
New Method for High-Accuracy Determination of the Fine-Structure Constant Based on Quantized Hall Resistance
 Physical Review Letters, Vol. 45, p. 494-497 (1980)
 Von Klitzing discovers the quantized Hall effect.

• **NOBEL PRIZE IN PHYSICS 1998:**

The Nobel Prize in Physics 1998 was awarded jointly to ROBERT B. LAUGHLIN, HORST L. STÖRMER and DANIEL C. TSUI “for their discovery of a new form of quantum fluid with fractionally charged excitations.”

Related milestone papers:

- [14] D. C. Tsui, H. L. Störmer, A. C. Gossard
Two-Dimensional Magnetotransport in the Extreme Quantum Limit
 Physical Review Letters, Vol. 48, p. 1559-1562 (1982)
 Tsui and Störmer discover the fractional quantum Hall effect.

- [15] R. B. Laughlin
Anomalous Quantum Hall Effect: An Incompressible Quantum Fluid with Fractionally Charged Excitations
 Physical Review Letters, Vol. 50, p. 1395-1398 (1983)
 Laughlin describes the fractional quantum Hall effect in terms of fractional charges.

• **NOBEL PRIZE IN PHYSICS 2016:**

The Nobel Prize in Physics 2016 was awarded with one half to DAVID J. THOULESS, and the other half to F. DUNCAN M. HALDANE and J. MICHAEL KOSTERLITZ “for theoretical discoveries of topological phase transitions and topological phases of matter.”

Related milestone papers:

- [16] J. M. Kosterlitz, D. J. Thouless
Ordering, metastability and phase transitions in two-dimensional systems
 Journal of Physics C: Solid State Physics, Vol. 6, No. 7 (1973)
 Kosterlitz and Thouless use methods from topology to describe the KT phase transition.
- [17] D. J. Thouless *et al.*
Quantized Hall Conductance in a Two-Dimensional Periodic Potential
 Physical Review Letters, Vol. 49, p. 405-408 (1982)
 Thouless and coworkers explain the quantization of the Hall conductivity.
- [18] F. D. M. Haldane
Nonlinear Field Theory of Large-Spin Heisenberg Antiferromagnets: Semiclassically Quantized Solitons of the One-Dimensional Easy-Axis Néel State
 Physical Review Letters, Vol. 50, p. 1153-1156 (1983)
 Haldane uses methods from topology to describe the 1D Heisenberg antiferromagnet.
- [19] F. D. M. Haldane
Model for a Quantum Hall Effect without Landau Levels: Condensed-Matter Realization of the “Parity Anomaly”
 Physical Review Letters, Vol. 61, p. 2015-2018 (1988)
 Haldane predicts the anomalous quantum Hall effect without external magnetic fields.

Goals of this course

The goal of this course is to gain a thorough understanding of topological concepts in modern quantum many-body physics. You acquire the mathematical tools needed to describe topological quantum phases, understand the physical features that characterize these systems, and learn about potential applications.

In particular (★ optional):

(Gray topics are not yet covered by the script.)

Topological phases of non-interacting fermions (Part I):

- Integer quantum Hall effect
- Berry connection, Berry holonomy, Chern number
- Anomalous quantum Hall effect (Haldane model)
- Quantum spin Hall effect, topological insulators (Kane-Mele model)
- Pfaffian topological invariant
- Winding numbers, sublattice symmetry, edge modes (SSH model)
- Topological superconductivity (Majorana chain)
- Tenfold way and periodic table of topological insulators/superconductors
- Effects of interactions
- Topological bands in classical systems (topological metamaterials ...) ★

Symmetry-protected topological phases of interacting bosons (Part II):

- Tensor network states, matrix product states, PEPS
- Projective representations and (twisted) cohomology groups
- Classification of bosonic topological phases in one dimension
- Haldane chain and AKLT model

Intrinsic topological order and long-range entanglement (Part III):

- Statistics of indistinguishable particles in 2+1 dimensions (Braid group)
- Toric code (anyonic excitations, topological entanglement entropy, ...)
- Topological quantum memories
- Fibonacci anyons
- String-net condensates ★
- Topological quantum computation (non-abelian anyons, braiding, fusion, ...)
- Mathematical framework
(Modular tensor categories, pentagon & hexagon relations, quantum dimension, topological spin, ...)
- Application to foundational questions of high-energy physics (fermions, ...) ★

Notes on this document

- This document is not an extension of the material covered in the lectures but the script that I use to prepare them.
- Please have a look at the given literature for more comprehensive coverage. References to primary and secondary resources are also given in the text.
- The content of this script is color-coded as follows:
 - Text in black is written to the blackboard.
 - Notes in red should be mentioned in the lecture to prevent misconceptions.
 - Notes in blue can be mentioned/noted in the lecture if there is enough time.
 - Notes in green are hints for the lecturer.
- One page of the script corresponds roughly to one covered panel of the blackboard.
- Enumerated lists are used for more or less rigorous chains of thought:
 - 1 | This leads to ...
 - 2 | this. By the way:
 - i | This leads to ...
 - ii | this leads to ...
 - iii | this.
 - 3 | Let's proceed ...
- In the bibliography (p. 171 ff.) you can find links ([Download](#)) to download most papers referenced in this script. As most of these papers are not freely available, you need a password to do so; this password is made available to students of my classes. Papers that are open access are highlighted green ([Download](#)) and do not require a password.
- This document has been composed in **Vim** on **Arch Linux** and is typeset by **Lua^ATeX** and **BibTeX**. Thanks to all contributors to free software!
- This document is typeset in **Equity**, **Concourse** and **MathTimeProfessional**.

Acknowledgements

- Thanks to Tobias Maier for finding typos and creating animations of the Berry curvature of the QWZ model.

Symbols & Scientific abbreviations

The following abbreviations and glyphs are used in this document:

<i>cf</i>	confer (“compare”)
<i>dof</i>	degree(s) of freedom
<i>eg</i>	exempli gratia (“for example”)
<i>etc</i>	et cetera (“and so forth”)
<i>et al</i>	et alii (“and others”)
<i>ie</i>	id est (“that is”)
<i>viz</i>	videlicet (“namely”)
<i>vs</i>	versus (“against”)
<i>wlog</i>	without loss of generality
<i>wrt</i>	with respect to
<i>iff</i>	if and only if
\triangleleft	“consider”
\rightarrow	“therefore”
!	“Beware!”
$\overset{\circ}{=}$	non-obvious equality that may require lengthy, but straightforward calculations
$\overset{*}{=}$	non-trivial equality that cannot be derived without additional input
$\overset{\circ}{\rightarrow}$	“it is easy to show”
$\overset{*}{\rightarrow}$	“it is <i>not</i> easy to show”
\Rightarrow	logical implication
\wedge	logical conjunction
\vee	logical disjunction
\square	repeated expression
\blacksquare	anonymous reference
w/o	“without”
w/	“with”
\rightarrow	internal forward reference (“see below/later”)
\leftarrow	internal backward reference (“see above/before”)
\uparrow	external reference to advanced concepts (“have a look at an advanced textbook on...”)
\downarrow	external reference to basic concepts (“remember your basic course on...”)
\Leftrightarrow	reference to previous or upcoming exercises
\star	optional choice/item
$\ast\ast$	implicit or explicit definition of a new technical term (“so called ...”)
\ddagger	Aside
\equiv	Synonymous terms
$:=$	Definition

The following scientific abbreviations are used in this document:

2DEG	2-Dimensional Electron Gas
AC	Alternating Current
BEC	Bose-Einstein Condensate
CFT	Conformal Field Theory
CS	Chern-Simons
DC	Direct Current
DMRG	Density Matrix Renormalization Group
FQHE	Fractional Quantum Hall Effect
IQH	Integer Quantum Hall
IQHE	Integer Quantum Hall Effect
ITO	Invertible Topological Order
KT	Kosterlitz-Thouless
LL	Luttinger Liquid / Landau Level
LLL	Lowest Landau Level
LU	Local Unitary
MPS	Matrix Product State
PTB	Physikalisch Technische Bundesanstalt
QCD	Quantum Chromo Dynamics
QFT	Quantum Field Theory
QHE	Quantum Hall Effect
SET	Symmetry-Enriched Topological
SI	Système International (d'unités)
SPT	Symmetry-Protected Topological
SSB	Spontaneous Symmetry Breaking
SSH	Su-Schrieffer-Heeger
TIM	Transverse-field Ising Model
TKNN	Thouless-Kohmoto-Nightingale-Nijs
TO	Topological Order
TP	Topological Phase
TQC	Topological Quantum Computation
TQFT	Topological Quantum Field Theory
TQM	Topological Quantum Memory
TQO	Topological Quantum Order
YM	Yang-Mills

0. Setting the Stage

◆ Topics

- Motivation: A classical system with topological edge modes
- Localization within physics: Where we are on the energy ladder
- Introduce our objects of interest: Quantum phases and phase transitions
- Sketch the Landau paradigm: Spontaneous symmetry breaking
- Concepts beyond the Landau paradigm: Topological phases
- Sketch different types of topological phases

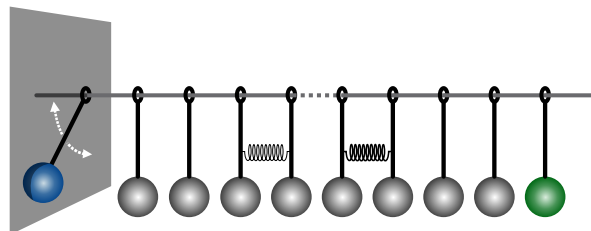
0.1. Motivation: Transferring energy with pendulums

To get you hooked (hopefully!), we start with a series of simple *classical mechanics* “experiments” (= computer simulations). The point of this adventure is to highlight some of the surprising effects *topological* features can have (where exactly topology enters is not obvious and will be discussed in due time):

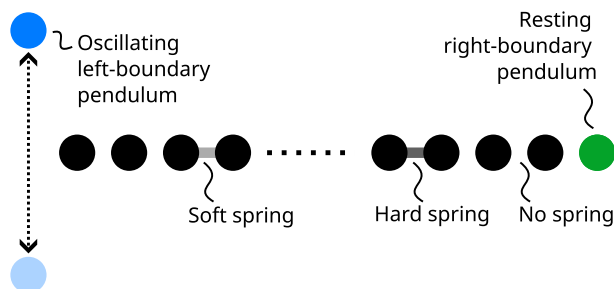
The following is inspired by on one of my papers [20].

Beamer and internet connection required!

1 | < 1D chain of N identical pendulums, coupled by *tunable* springs:



→ Schematic view from bottom:



We encode the strength of springs by their color:
White: no spring / Light: soft spring / Dark: stiff spring

2 | **Goal:** Transfer oscillation energy from one boundary to the other:

$$\underbrace{\vec{x}(t < 0) = (1, 0, \dots, 0) \cdot e^{i\omega t}}_{\text{Left pendulum excited}} \xrightarrow[\text{How??}]{\text{Time evolution}} \underbrace{\vec{x}(t > T) = (0, \dots, 0, 1) \cdot e^{i\omega t}}_{\text{Right pendulum excited}} \quad (0.1)$$

Here, $x_i(t)$ denotes the displacement of pendulum i at time t ; our protocol starts at $t = 0$ and ends at $t = T$. The eigenfrequency of the (identical) pendulums is ω .

3 | **Time evolution** → Classical equation of motion:

$$\ddot{\vec{x}} + \mathbb{D}(t)\vec{x} = 0 \quad (0.2)$$

This is the Newtonian equation of motion for N coupled harmonic oscillators.

$\mathbb{D}(t) \in \mathbb{R}^{N \times N}$: Time dependent coupling matrix

4 | **Rules:**

- We can choose the stiffness for each spring independently.
- We can modify the stiffness of an arbitrary subset by *a single* time dependent factor.
- We can choose the time dependence of this factor freely.

→ Allowed form of the coupling matrix:

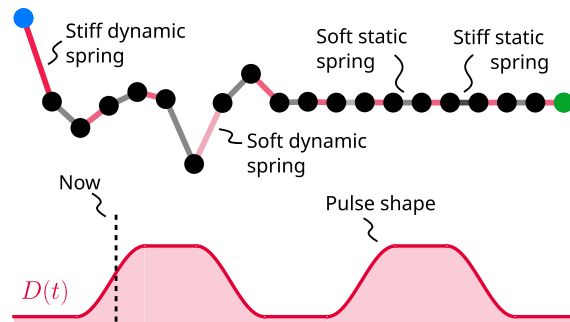
$$\mathbb{D}(t) = \underbrace{\begin{pmatrix} \omega_1^2 & s_1 & & & \\ s_1 & \omega_2^2 & s_2 & & \\ & s_2 & \omega_3^2 & & \\ & & & \ddots & \end{pmatrix}}_{\text{Static springs \& pendulums}} + D(t) \underbrace{\begin{pmatrix} 0 & d_1 & & & \\ d_1 & 0 & d_2 & & \\ & d_2 & 0 & & \\ & & & \ddots & \end{pmatrix}}_{\text{Time dependent springs}} \quad (0.3)$$

With ...

- $\omega_i = \sqrt{g/l_i} \equiv \omega$: Frequency of pendulums (uniform and fixed)
- s_j : Static stiffness of spring coupling pendulums i and $i + 1$
- $D(t) \cdot d_j$: Time dependent stiffness of spring coupling pendulums i and $i + 1$
- Global time dependence of spring stiffness:

$$D(t) = \begin{cases} 0 & t < T \\ P(t) & 0 \leq t \leq T \\ 0 & t > T \end{cases} \quad \text{with pulse shape } P(t) : [0, T] \rightarrow [0, 1] \quad (0.4)$$

→ Schematic view:



We color static (tunable) springs in shades of black (red). The shape of $D(t)$ is plotted below the pendulum chain; the current point in time is marked by a vertical line in this plot.

5 | Questions:

- How to choose the spring couplings s_i and d_i ?
- How to choose the pulse shape $P(t)$?

6 | Experiments:

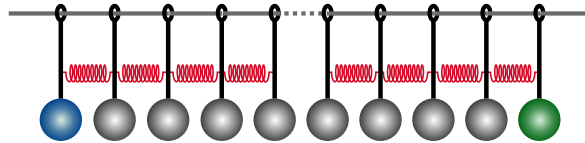
The simulations below are based on numerical integration of Eq. (0.2) with initial configuration (0.1):

[↪ Download Mathematica notebook](#)

i | Variant 1:

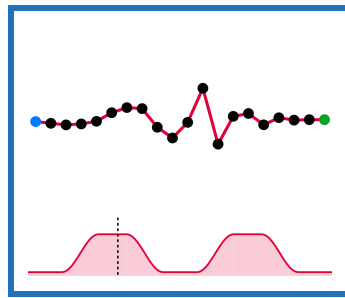
$$s_i = 0 \quad \text{and} \quad d_i = d > 0 \quad \text{for all} \quad i = 1, \dots, N - 1 \quad (0.5)$$

In this approach, we couple all pendulums *uniformly* by springs of *time dependent* stiffness:



As pulse $P(t)$ we choose a smoothed-out rectangular double pulse to transfer the excitation from left to right and back. The latter is of course not necessary; it allows us to amplify the effects of a single transfer. We normalize the pulse such that $\max_t P(t) \approx 1$.

→ Simulation: [Click on figure \(internet required\)](#).



<https://itp3.info/pendulumv1>

→ Result: No perfect transfer possible! ☹

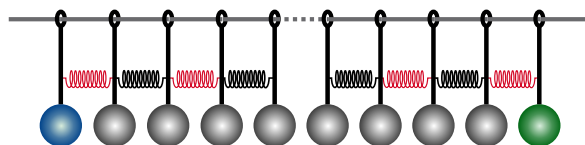
The reason is quite obvious: The boundary excitation is transferred via an elastic wave that travels through the bulk. Because of \downarrow *dispersion*, this excitation cannot be relocalized on the other boundary; we loose inevitably energy to bulk excitations.

ii | Variant 2: (We assume N to be even!)

$$s_i = 0 \quad \text{and} \quad d_i = d > 0 \quad \text{for odd} \quad i = 1, 3, \dots, N - 1 \quad (0.6a)$$

$$s_i \approx 2 \times d \quad \text{and} \quad d_i = 0 \quad \text{for even} \quad i = 2, 4, \dots, N - 2 \quad (0.6b)$$

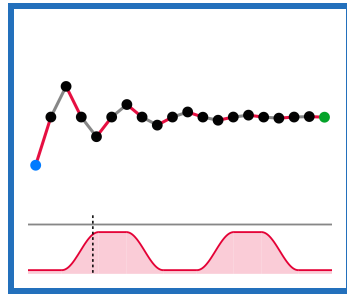
Now we couple pendulums *alternating* with weak & dynamic and strong & static springs:



- We use the same pulse $P(t)$ as for **Variant 1** above. Now it affects only every other spring, of course!

- If you wonder *how* one might come up with this contraption: This is why you should attend this course 😊.

→ Simulation:



<https://itp3.info/pendulumv2>

→ Result: (Almost) perfect transfer possible! 😊😊

- The video above is “stroboscopic”, i.e., the pendulums are oscillating with a much higher frequency; the visible oscillations are therefore determined by the actual frequency and the chosen frame times (↓ *beat frequency*). The transfer also works with lower frequencies (as in the **Variant 1** video above), but would then take much longer.
- The reason why this approach works perfectly is not obvious. In particular, its robustness to certain types of disorder (→ *next*) are not trivial to understand. We need to introduce quite a bit of machinery to tackle this problem (→ *much later*).

What happens to this method if the constituents of our contraption have *Imperfections*?

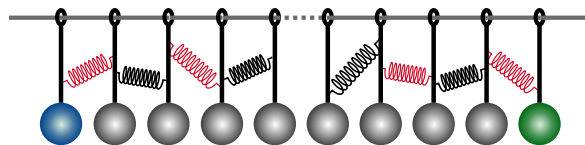
a | < Imperfect springs:

$$s_i = 0 \quad \text{and} \quad d_i \in \mathcal{N}(d, \sigma_d) \quad \text{for odd } i \quad (0.7a)$$

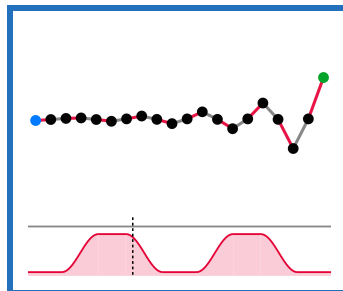
$$s_i \in \mathcal{N}(2d, \sigma_s) \quad \text{and} \quad d_i = 0 \quad \text{for even } i \quad (0.7b)$$

- $\mathcal{N}(\mu, \sigma)$ denotes the ↓ *normal distribution* with mean μ and standard deviation σ .
- We choose $\sigma_d \approx 0.1 \times d$ and $\sigma_s \approx 0.1 \times 2d$, i.e., tolerances of about 10%.

→ We modify all non-zero spring couplings randomly by a small amount:



→ Simulation:



<https://itp3.info/pendulumv2a>

→ Result: Still perfect transfer possible! 😊

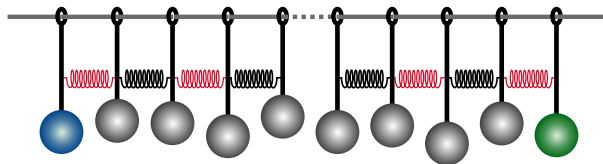
- ¡! This is not what one typically expects for an imperfect system. In particular for rather large imperfections of about 10%.
- To achieve perfect transfer, one has to tune the pulse slightly (either its height or its duration). However, one always finds an appropriately tuned pulse that achieves (almost) perfect transfer.
- Note that even if the pulse is not tuned, there is (almost) no energy loss to bulk modes. A non-optimal pulse therefore leads to an incomplete transfer but not to losses.
- If you look closely, there actually are weak excitations of the pendulum pairs in the bulk after the double transfer. This is a consequence of weak adiabaticity breaking; an ideal transfer would take infinitely long.

b | < Imperfect pendulums:

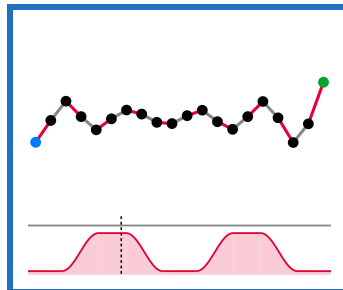
$$\text{Eq. (0.6) together with } \omega_i \equiv \omega \mapsto \omega_i \in \mathcal{N}(\omega, \sigma_\omega) \quad (0.8)$$

We choose $\sigma_\omega \approx 0.1 \times \omega$, i.e., tolerances of about 10%.

→ We modify all frequencies (= lengths of pendulums) ω_i randomly by a small amount:



→ Simulation:



<https://itp3.info/pendulumv2b>

→ Result: No perfect transfer possible! ☹

- This is the typical effect one might expect for an imperfect system.
- If one optimizes over the pulse length (or height), one typically does *not* find a pulse that achieves perfect transfer.
- Note that there is still no energy loss to bulk modes. This means that for small-enough imperfections, the time-evolution remains almost adiabatic.
- That the two boundary pendulums oscillate with drastically different periods is a consequence of the frequency imperfections (which of course also affect the boundary pendulums) in combination with the “stroboscopic” visualization.

7 | → Many questions ...

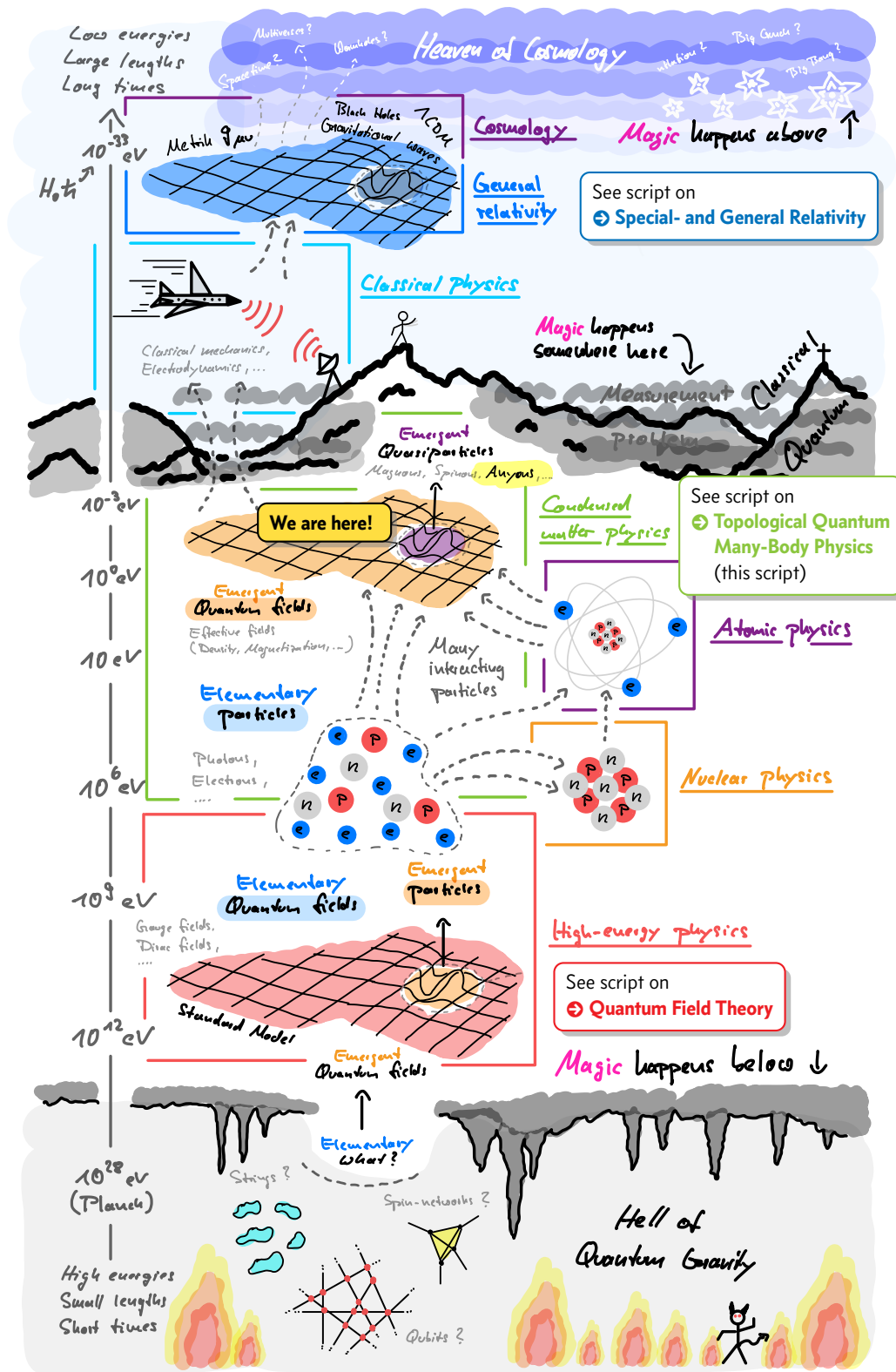
1. Why does **Variante 2** work? Where do these “boundary modes” come from?
2. Why is this procedure robust against one type of disorder, but not the other?
3. What has this to do with *topology*?
4. What has this to do with *quantum mechanics*?

Answers: → *Later*

For the impatient: The first three questions will be answered in ???. How some features of topological quantum phases translate to classical systems is discussed in ???.

0.2. The Big Picture

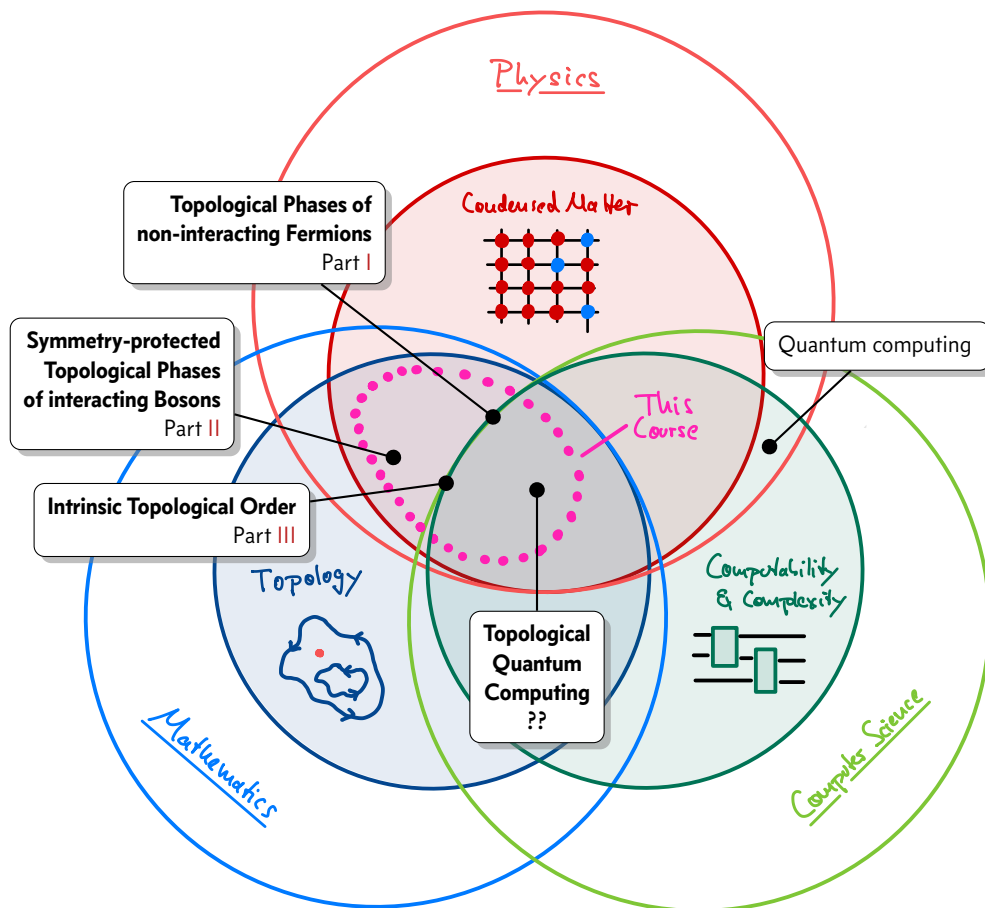
Physics strives for an objective, operational description of nature. To do so systematically, it is convenient to slice reality into layers separated by energy-, time- and length scales:



Comments:

- In this course we neither study the very small (\uparrow *high-energy physics*) nor the very large (\downarrow *relativity*). Thus we are not concerned with *fundamental* physics but with *emergent* phenomena.
- While this course is clearly focused on the *mathematics* and *conceptual foundations* that underlie the phenomenology of topological quantum phases, there will be connections to both experiments and applications along the lines. In particular the applications differentiate this course from more fundamental topics close to the extremes of the energy scale.
- At the very end (\rightarrow ??), we will briefly discuss a scenario where some of these emergent properties (related to topological order) might be of relevance for fundamental questions of high-energy physics. Maybe the realm of particle physics is emergent as well, and the theory of topological quantum many-body physics has something to say about questions that conventional high-energy physics is silent about? (For example, why there are fermions to begin with?)

The topics covered in this course can also be located with respect to adjacent scientific disciplines:



- \uparrow *Topology* is the area of mathematics that deals with properties of spaces (e.g. manifolds) that are robust against smooth deformations of these spaces. For example, the topology of a torus (= donut) is characterized by the fact that it has a single “hole”; its exact shape (e.g. its size and local bumps on the surface) are part of its *geometry* but not relevant for its *topology*.
- Which, why, and how concepts of topology are instantiated in particular quantum phases is the main focus of this course.

0.3. Quantum phases and quantum phase transitions

1 | In this course, we are interested in the following concepts:

✱ Definition: Quantum phases and phase transitions

- **Quantum phase** \Leftrightarrow Phase of matter at $T = 0$ (= no thermal fluctuations)
 - \Leftrightarrow Ground state manifold of

$$\left\{ \begin{array}{c} \text{scalable} \\ \text{local} \\ \text{many-body} \end{array} \right\} \text{ Hamiltonian in the } \textit{thermodynamic limit}$$
 - “*Scalable*”: The Hamiltonian is actually a *family* of Hamiltonians H_L parametrized by the system size L (e.g., number of modes/atoms/spins in each spatial direction).
 - “*Local*”: The Hamiltonian is a sum of operators that act only on a finite number of adjacent degrees of freedom (i.e., no long-range interactions).
 - “*Many-body*”: The Hamiltonian describes the interactions of extensively many degrees of freedom (spins, particles).
 - “*Thermodynamic limit*”: We are interested in the ground state properties for infinitely large systems, i.e., in the limit $L \rightarrow \infty$.
- In this course, we are mostly interested in a particular subclass of quantum phases:
 - Gapped quantum phase** \Leftrightarrow Ground state manifold of
Hamiltonian with a *stable bulk gap*
 - “*Bulk gap*”: Spectral gap between the ground state manifold and the first excited states of a system with periodic boundaries. Systems *with* boundaries may have eigenstates that cross this gap.
 - “*Stable*”: The gap remains finite in the thermodynamic limit $L \rightarrow \infty$.
- Naturally, we are also interested in transitions *between* quantum phases:
 - Quantum phase **transition** \Leftrightarrow Transition between different quantum phases
(in the thermodynamic limit)
 - \Leftrightarrow *Qualitative* change of *macroscopic* properties triggered by *small* changes of *microscopic* parameters

Comments:

- ¡! In this course we consider exclusively quantum phases; hence we drop the term “quantum” in the expressions defined above in many cases.
- Quantum phases are characterized by properties that *emerge* from many particles that interact quantum-mechanically. We are therefore interested how *macroscopic* quantum properties emerge from *microscopic* quantum interactions.
- Thus, the study of quantum phases and phase transitions is particularly challenging, because computing the ground state(s) of large, interacting quantum systems is hard if not impossible. (The Hilbert space dimension grows exponentially with the system size L !)

Broadly speaking, there are four attack vectors:

- (1) Solve models *analytically* ...
 - (a) ...with exact methods.
(↑ *Bethe ansatz*, → *Stabilizer formalism*, → *Quadratic theories*, ...)
 - (b) ...with approximate methods.
(↓ *Perturbation theory*, ↑ *Mean-field theory*, ↑ *Quantum field theory*, ...)
- (2) Solve models *numerically* (on classical computers).
(↓ *Exact diagonalization*, → *DMRG*, ↑ *Quantum Monte Carlo*, ...)
- (3) Perform *quantum simulations*.
(→ *Analog quantum simulation*, ↑ *Digital quantum simulation*, ...)
- (4) Last but not least: conduct *experiments*.

Here we focus on approach (1a); in some exercises you will make contact with approach (2).

- Quantum phase transitions are triggered by changes of parameters in the Hamiltonian (e.g. interaction strengths, chemical potentials, hopping rates, ...). (Quantum) phase *diagrams* are therefore plotted as functions of *parameters* of the Hamiltonian, and not temperature or pressure [as you learned in your course on ↓ (*classical*) *statistical physics*].
- Quantum phases at $T = 0$ are properties of *pure quantum states* without entropy. By contrast, *classical phases* (like crystalline phases of solids, or the liquid phase of water), are properties of statistical *ensembles* of states with finite entropy; in the framework of quantum mechanics, these are described by *density matrices* [for example, the Gibbs state $\rho = e^{-\beta H} / Z$ of the ↓ *canonical ensemble*].
- Classical *thermodynamic* phase transitions (e.g., the boiling of water) are driven by *thermal fluctuations* that modify the statistical ensemble of microstates, such that its macroscopic observables change qualitatively. By contrast, *quantum* phase transitions are driven by *quantum fluctuations* (due to non-commuting terms in the Hamiltonian, → *below*). These modify the *amplitudes* of basis states in the (pure!) ground state of the system, thereby changing its quantum-mechanical properties qualitatively (correlations, entanglement structure, ...).
- ¡! Quantum fluctuations are *not* dynamical fluctuations in time. The ground state is an *eigenstate* and therefore *time-independent*. However, if you would initialize the system in a classical product state which is not an eigenstate (in particular, not the ground state), then it would fluctuate in time, because the ground state is actually a *superposition* of many different such classical product states.

2 | Examples of quantum phases that exist in nature and/or can be experimentally realized:

- ↓ *Superconductors*
- ↓ *Superfluids* (e.g. superfluid Helium ...)
- ↑ *Supersolids* (have been recently realized in experiments [21–23])
- ↓ *Bose-Einstein condensates* (BEC)
- ↓ *Fermi liquids*
- → *Quantum Hall states*
- ...

While these are important examples, they are typically hard to describe and understand theoretically. It is therefore advisable to focus on a simple “toy model” that is exactly solvable:

↓ Lecture 2 [11.04.25]

3 | Paradigmatic example:

i | ≪ Periodic 1D chain of L spin- $\frac{1}{2}$ with Hamiltonian:

⌘⌘ *Transverse-field Ising model (TIM):*

$$H_{\text{TIM}} = -J \sum_{i=1}^L \sigma_i^z \sigma_{i+1}^z - h \sum_{i=1}^L \sigma_i^x \quad (0.9)$$

where ...

- $J \geq 0$: ferromagnetic coupling strength
- $h \geq 0$: *transverse* magnetic field

“*Transverse*” since h points in x -direction, which is transverse to the z -direction of the ferromagnetic Ising interactions.

ii | Observation:

$$[\sigma_i^z \sigma_{i+1}^z, \sigma_i^x] \neq 0 \quad (0.10)$$

→ The Ising interactions and the magnetic field terms *cannot* be diagonalized simultaneously!

→ *Quantum fluctuations*

→ Ground state(s) = (entangled) *superpositions* of product states $|\uparrow\downarrow\dots\rangle$ for $h \neq 0$

Product states of the form $|\uparrow\downarrow\dots\rangle$ are eigenstates of the classical Ising interaction $\sigma_i^z \sigma_{i+1}^z$.

iii | Two **qualitatively different** parameter regimes:

a | $J \ll h$:

$J \approx 0 \rightarrow$ *Gapped* phase with *unique* ground state:

$$|\Omega_+\rangle \approx |+\dots+\rangle \quad (0.11)$$

≪ Spin-spin correlations:

$$\langle \Omega_+ | \sigma_i^z \sigma_j^z | \Omega_+ \rangle \xrightarrow{|i-j| \rightarrow \infty} 0 \quad (0.12)$$

→ ⌘⌘ *Paramagnetic phase* (=disordered phase)

- Note that $\langle \Omega_+ | \sigma_i^z | \Omega_+ \rangle = 0$, i.e., measuring any spin yields ± 1 with equal probability. The vanishing of spin-spin correlations (0.12) means that there is no correlation between these random outcomes for distant spins. That is, there is *no order* in the ground state.
- For $J = 0$ and $h > 0$ the system has a stable bulk gap of $\Delta E = 2h$, independent of L (the energy cost of flipping a single spin from $|+\rangle$ to $|-\rangle$).

b | $J \gg h$:

$h \approx 0 \rightarrow$ Gapped phase with *two-fold degenerate* ground state manifold:

$$|\Omega\rangle \approx \alpha \underbrace{|\uparrow\uparrow \dots \uparrow\rangle}_{|\Omega_\uparrow\rangle} + \beta \underbrace{|\downarrow\downarrow \dots \downarrow\rangle}_{|\Omega_\downarrow\rangle} \quad (0.13)$$

\triangleleft Spin-spin correlations:

$$\langle \Omega | \sigma_i^z \sigma_j^z | \Omega \rangle \xrightarrow{|i-j| \rightarrow \infty} 1 \quad (0.14)$$

This is true for arbitrary amplitudes α and β !

\rightarrow **** Ferromagnetic phase (ordered phase)**

- Note that now $\langle \Omega | \sigma_i^z | \Omega \rangle \geq 0$ depends on the particular values of α and β ; for the “classical” product states it is $\langle \Omega_{\uparrow\downarrow} | \sigma_i^z | \Omega_{\uparrow\downarrow} \rangle = \pm 1$. However, the non-vanishing correlations (0.14) imply in any case that z -measurements of distant spins are correlated. That is, there is *order* in the ground state.
- For $J > 0$ and $h = 0$ and periodic boundaries, the system has a stable bulk gap of $\Delta E = 4J$, independent of L (the energy cost of flipping a contiguous domain of spins, e.g., $|\uparrow\uparrow\uparrow\uparrow\rangle \mapsto |\uparrow\downarrow\downarrow\uparrow\rangle$).

iv | \rightarrow The z -magnetization σ_i^z is a **** local order parameter for the ferromagnetic phase**:

$$\lim_{|i-j| \rightarrow \infty} \langle \sigma_i^z \sigma_j^z \rangle = 0 \quad \text{in the paramagnetic (disordered) phase} \quad (0.15a)$$

$$\lim_{|i-j| \rightarrow \infty} \langle \sigma_i^z \sigma_j^z \rangle \neq 0 \quad \text{in the ferromagnetic (ordered) phase} \quad (0.15b)$$

- The very fact that there is a local order parameter that characterizes the ferromagnetic phase makes this particular kind of order locally testable, i.e., by looking at a finite patch of the system, you can decide whether you are in the ferromagnetic or the paramagnetic phase. This makes the ferromagnetic phase a *counterexample* of a *topological* phase (\rightarrow later).
- Note that $[H, \sigma_i^z] \neq 0$, i.e. correlations of this observable at two distant points are a non-trivial phenomenon.

v | Comments:

- So far we only made heuristic arguments regarding the ground states of the TIM Hamiltonian (0.9). Fortunately, this model *can* be solved exactly! Despite the simplicity of the Hamiltonian, this calculation is not straightforward and requires quite a bit of machinery; you solve the model on \rightarrow Problemset 7 \rightarrow later.
- While the TIM Hamiltonian clearly has a stable bulk gap in the two extreme cases ($J = 0$ and $h > 0$ vs. $J > 0$ and $h = 0$), it is not clear what happens when one adds small perturbations. For example, whether the gap stays open for $J > 0$ and $0 < h \ll J$ is not obvious. The problem is that the gap ΔE is of order unity, but the total operator norm of the magnetic field perturbation goes like $h \times L$, which diverges in the thermodynamic limit $L \rightarrow \infty$ for *arbitrarily small* perturbations $h > 0$. In general, bulk gaps can therefore vanish under infinitesimally small perturbations! [For the TIM this does *not* happen, and the gap remains open for up to some critical value h_c of the magnetic field, but this must be proven (\rightarrow Problemset 7).]

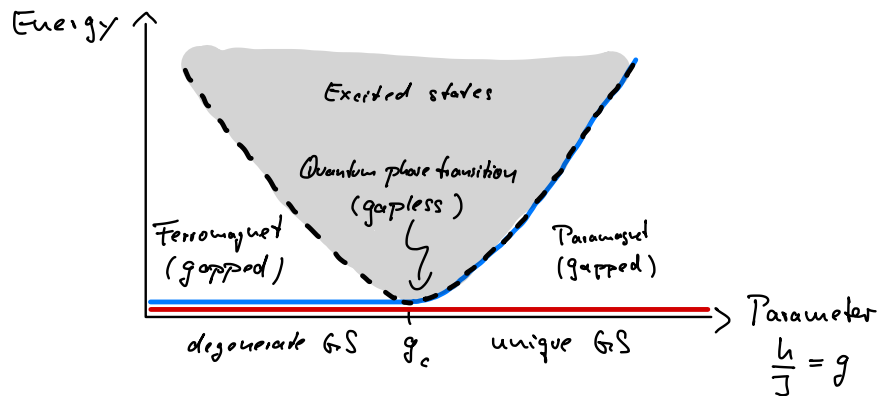
0.4. Spontaneous symmetry breaking

vi | What happens between the two gapped phases for $J \ll h$ and $J \gg h$?

Since the ground state degeneracy of the two gapped phases is different, the gap must close at some critical ratio $g_c = h/J$.

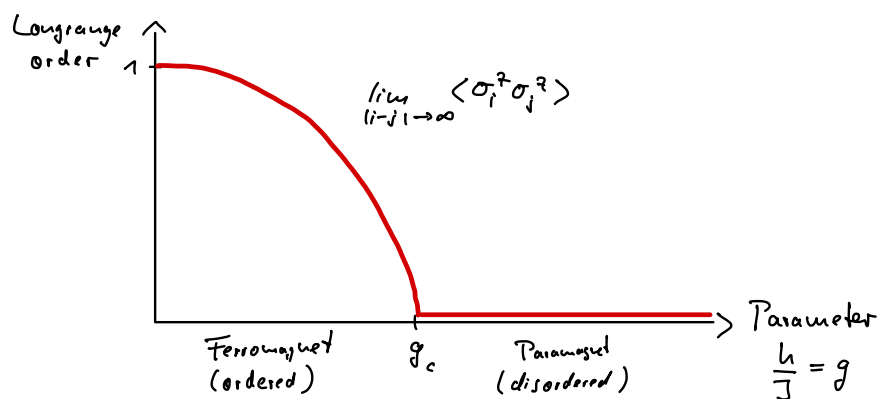
As noted above, we cannot exclude $g_c = 0$ or $g_c = \infty$ with our current knowledge. Here we assume that $0 < g_c < \infty$ (which turns out to be correct).

→ Schematic spectrum:



You compute this spectrum exactly later on → Problemset 7.

vii | Tentative Phase diagram:



→ Order parameter *continuous* at phase transition

Again, this is not obvious; but solving the model exactly shows that it is true.

viii | → *Continuous (second-order) phase transition:

This is the most typical situation (at least for the models studied in this course), with the following features at the phase transition:

- Bulk gap closes
- Long-range fluctuations and self-similarity (= quantum fluctuations on all length scales)
- Effective conformal field theory (CFT) description
- Algebraic decay of correlations (As compared to exponential decay in gapped phases.)

ix | What characterizes the phase transition?

LEV LANDAU: *Spontaneous symmetry breaking!*

LANDAU was awarded the Nobel Prize in Physics 1962 for his pioneering work on describing quantum phases of matter, especially the superfluid phase of liquid Helium.

(1) \triangleleft Symmetry group G_S of the TIM Hamiltonian (0.9):

$$G_S = \{1, X\} \simeq \mathbb{Z}_2 \quad \text{with} \quad X := \prod_{i=1}^L \sigma_i^x \quad (0.16)$$

X realizes a global flip of all spins: $|\uparrow\rangle \leftrightarrow |\downarrow\rangle$.

Check that $[H_{\text{TIM}}, X] = 0$. Note that $X^2 = 1$ so that $G_S \simeq \mathbb{Z}_2$.

(2) \triangleleft Symmetry groups G_E of the TIM ground states Eqs. (0.11) and (0.13):

- Paramagnetic phase:

$$G_E^{(\text{para})} = \{1, X\} = G_S \quad \text{since} \quad X|\Omega_+\rangle = |\Omega_+\rangle \quad (0.17)$$

→ $**$ Symmetric phase

- Ferromagnetic phase:

$$G_E^{(\text{ferro})} = \{1\} \subsetneq G_S \quad \text{since} \quad X|\Omega_\uparrow\rangle = |\Omega_\downarrow\rangle \neq |\Omega_\uparrow\rangle \quad (0.18)$$

→ $**$ Symmetry-broken phase

! Important

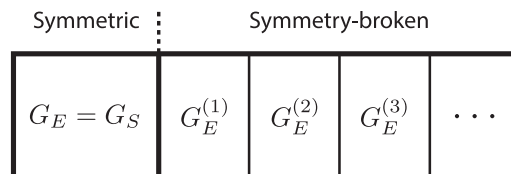
In the ferromagnetic phase, the ground states $|\Omega_{\uparrow/\downarrow}\rangle$ spontaneously break the symmetry group G_S of the Hamiltonian H_{TIM} .

→ $**$ Spontaneous symmetry breaking (SSB)

Landau’s paradigm (Spontaneous symmetry breaking)

4 | This concept extends to many quantum phases and their phase transitions (e.g. superconductors/-superfluids where the particle number symmetry $G_S = U(1)$ is spontaneously broken) and is also applicable to classical phases and phase transitions (e.g. the transition from liquid to solid where rotation and translation symmetry are broken down to crystallographic subgroups).

→ Phases are characterized by the symmetries they break & preserve:



Labels of phases = Subgroups $G_E^{(i)}$ of symmetry group G_S

- This concept covers many (quantum and classical) phases and phase transitions, but in the realm of quantum mechanics there is more than just symmetry breaking—there is *entanglement!* This will become important → *below ...*

- For the TIM the symmetry group G_S has only itself and the trivial group as subgroups. In general, G_S can be much larger so that many non-trivial subgroups exist (and therefore many different phases are possible). For example, if $G_S = E(3)$ is the Euclidean group of three-dimensional space (continuous rotations and translations), then G_S contains all possible space groups (symmetry groups of crystals) as subgroups.

5 | Comments:

- Note that the spontaneous symmetry breaking of the TIM in 1D is *not* forbidden by the \uparrow Mermin-Wagner theorem because the broken symmetry is *discrete* (\mathbb{Z}_2).
- In *one* dimension, the spontaneous symmetry breaking (and the ferromagnetic phase) does *not* survive at finite temperatures $T > 0$. (Recall that the *classical* Ising model does not have a thermodynamic phase transition in one dimension, i.e., there is no ferromagnetic phase in a classical 1D Ising chain since domain walls can move without energy penalty.) The quantum phase transition of the 1D TIM is therefore a genuine quantum phenomenon, without classical counterpart.
- By contrast, in *two* dimensions (and above) the spontaneous symmetry breaking (and the ferromagnetic phase) *does* survive at finite temperatures $T > 0$. (Recall that the classical 2D Ising model has a thermodynamic phase transition at a critical temperature T_c below which it enters a ferromagnetic phase that breaks ergodicity.)
- A note on “symmetry breaking” in the quantum case:

The ground state (for $h = 0$ and $J > 0$)

$$|\Omega_s\rangle := \frac{1}{\sqrt{2}}|\Omega_\uparrow\rangle + \frac{1}{\sqrt{2}}|\Omega_\downarrow\rangle = \frac{1}{\sqrt{2}}|\uparrow\uparrow \dots \uparrow\rangle + \frac{1}{\sqrt{2}}|\downarrow\downarrow \dots \downarrow\rangle \quad (0.19)$$

is clearly *symmetric* under global spin-flips: $X|\Omega_s\rangle = |\Omega_s\rangle$. So what about the symmetry *breaking*? (Note that this is something without analog in a classical setting where you cannot superimpose arbitrary ground states to form new ground states.)

Mathematically, the two symmetry breaking states $|\Omega_\uparrow\rangle$ and $|\Omega_\downarrow\rangle$ belong to different \uparrow *superselection sectors* in the thermodynamic limit (they don’t live in the same Hilbert space). As a consequence, the “symmetric state” $|\Omega_s\rangle$ is not a state in the Hilbert space of the *infinite* system (strictly speaking, this is the mathematical manifestation of SSB); \uparrow Refs. [24–26].

Physically, the symmetry-broken states $|\Omega_{\uparrow/\downarrow}\rangle$ behave very differently than the symmetry-invariant states $|\Omega_\uparrow\rangle \pm |\Omega_\downarrow\rangle$: Local measurements (of σ_i^z) immediately collapse the latter into a mixture of the former. I.e. the symmetric states are extremely *fragile* (in contrast to the symmetry-broken states). Thus, in an experiment, one would always observe the *symmetry-broken* states, so that the notion of “spontaneous symmetry breaking” effectively carries over to the quantum realm.

0.5. Extending Landau’s paradigm: Topological phases

- 6 | To understand the deficits of Landau’s paradigm, and the conceptual possibility of topological phases, we first need a mathematically more rigorous definition of quantum phases (without spontaneous symmetry breaking!):

**** Definition: Gapped quantum phases (formal version)**

\triangleleft Gapped, local Hamiltonians H_a and H_b with unique ground states $|\Omega_a\rangle$ and $|\Omega_b\rangle$.

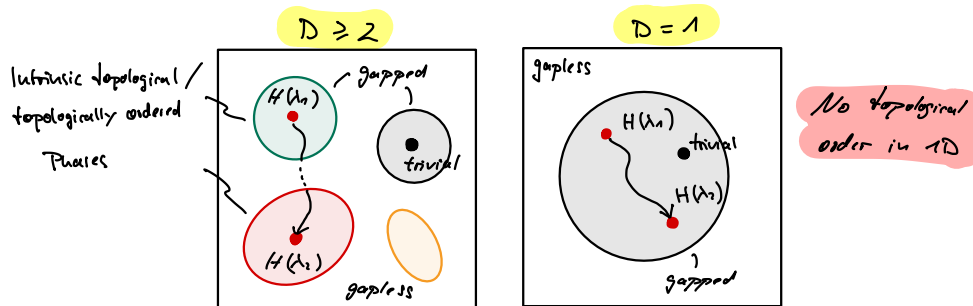
These two many-body ground states belong to the same quantum phase if and only if there is a family of *gapped* and *local* Hamiltonians $\hat{H}(\alpha)$ (which depends continuously on a parameter

$\alpha \in [0, 1]$ such that

$$H_a = \hat{H}(0) \quad \text{and} \quad H_b = \hat{H}(1). \quad (0.20)$$

- The two constraints “gapped” and “local” ensure that the macroscopic properties of the ground states only change gradually along the path. (This precludes the traversal of phase boundaries where macroscopic properties change qualitatively.)
- ¡ Note that, strictly speaking, the two Hamiltonians H_a and H_b [and the family $\hat{H}(\alpha)$] are meant to be *sequences* of Hamiltonians for increasing system sized $L \rightarrow \infty$. The condition that the gap remains open along the parameter path thus refers to the *thermodynamic limit* $L \rightarrow \infty$, and not to any finite system. (Note that every finite system has a trivial gap that separates its ground state manifold from the first excited states!)
- The above definition can be extended in a straightforward way to systems with finite (but non-extensive) ground state degeneracies. This allows for an extension of the following concepts to symmetry-broken phases as well (\rightarrow below).

7 | \leftarrow Parameter-space of local Hamiltonians (without SSB, $G_E = G_S$):



* \rightarrow In $D \geq 2$ dimensions the parameter space decomposes into “islands” of gapped Hamiltonians that cannot be connected without closing the gap:

- *Trivial phase:* Ground state = disentangled product state (e.g. $|\Omega_+\rangle = |+\rangle \otimes |+\rangle \otimes \dots$ or $|\Omega_\uparrow\rangle = |\uparrow\rangle \otimes |\uparrow\rangle \otimes \dots$)
- *Topological phase:* Ground state = long-range entangled state (different patterns of long-range entanglement = different topological phases)

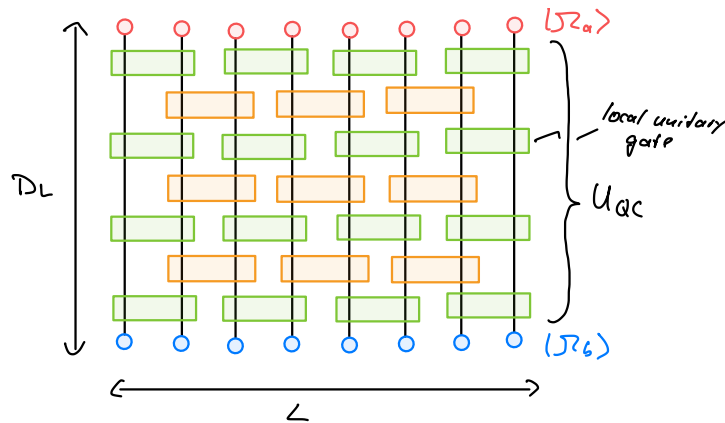
Comments:

- The fact that one-dimensional systems cannot have intrinsic topological order is not obvious. It follows because the ground states of gapped 1D Hamiltonians (without SSB) are short-range correlated and feature an area law (the entanglement entropy between different parts of the system is constant) [27, 28]. One can therefore encode these states as (short-range correlated) \rightarrow matrix-product states (MPS) with finite \rightarrow bond dimension. It then follows that states of this form can always be mapped to a product state by a quantum circuit of finite depth (\rightarrow below) [6].
- ¡ In this course, we often distinguish between *fermionic* systems and *bosonic* systems. Since in our context bosonic systems make only sense with interactions (\rightarrow below), we also count *spin* systems to this class and often use the terms interchangeably. What makes (interacting) systems *bosonic* is therefore not so much the existence of an infinite-dimensional bosonic Fock space, but rather that the operator algebras of local degrees of freedom commute. Note

that spin- $\frac{1}{2}$ (or \downarrow qubits) are equivalent to \downarrow hard-core bosons (\Rightarrow Problemset 1), i.e., bosons with an infinite, repulsive on-site interaction.

- This splitting can also occur for Hamiltonians with SSB and a fixed subgroup G_E . We will not discuss this case in this course (\rightarrow below).
 - Strictly speaking, the statement that there is no topological order in 1D is only true for bosonic systems (or spin systems). For 1D systems of fermions, there is a single non-trivial topological phase realized by the \rightarrow Majorana chain (Chapter 5) [29]. The subtle distinction between 1D bosonic and fermionic systems can be traced back to the non-locality of the \rightarrow Jordan-Wigner transformation that translates between them, and the fact that parity is a locality constraint for fermionic systems.
- 8 | There is an alternative (but mathematically equivalent) definition of quantum phases in terms of local unitary circuits with constant depth:

\leftarrow $\star\star$ Local unitary (LU) circuit of depth D_L :



\rightarrow \star $|\Omega_a\rangle$ and $|\Omega_b\rangle$ belong to the same quantum phase, if and only if

$$|\Omega_a\rangle = U_{QC}|\Omega_b\rangle \tag{0.21}$$

where U_{QC} is a local quantum circuit of constant depth $D_L = \text{const}$ for $L \rightarrow \infty$.

- This characterization clarifies that two states belong to the same quantum phase if they share the same “pattern of long-range entanglement” since this pattern can only be modified by long-range unitary gates (and not a LU-circuit of constant depth).
- With this characterization, it follows that a ground state $|\Omega_a\rangle$ is long-range entangled (= topologically ordered) iff it cannot be transformed into a trivial product state $|\uparrow\uparrow\uparrow \dots\rangle$ by a constant-depth quantum circuit that is local wrt. the geometry of the system.
- This definition can be shown to be equivalent to the one given in the definition above [30]. The unitary can be explicitly expressed as

$$U_{QC} = \mathcal{P} \exp \left[-i \int_0^1 d\alpha \tilde{H}(\alpha) \right] \tag{0.22}$$

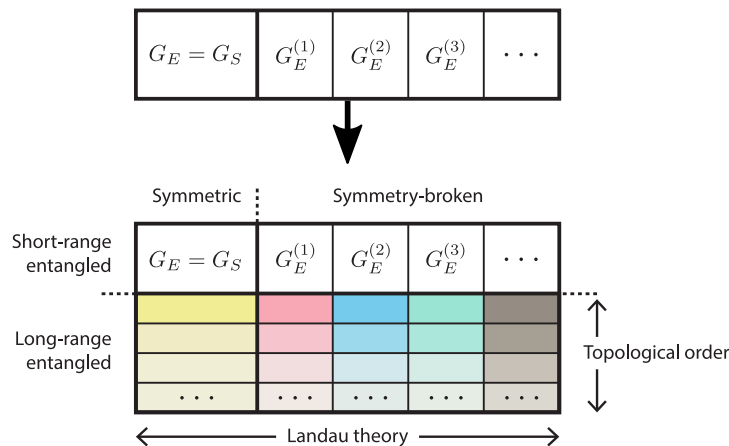
where \mathcal{P} denotes the path-ordered exponential and $\tilde{H}(\alpha)$ is a sum of local Hermitian operators that is related (but generally not identical) to the gapped path $\hat{H}(\alpha)$.

- This makes the preparation of topologically ordered states experimentally challenging for quantum computers and quantum simulators with locality constraints: Quantum computers

must apply quantum circuits with a depth (= run time) that scales with the systems size. Similarly, quantum simulators that rely on adiabatic preparation schemes must cross a topological phase transition – which requires the duration of the preparation protocol to scale with the system size as well.

First extension of Landau’s paradigm: (Intrinsic) Topological order

- 9 | The concept of long-range entanglement and equivalence via LU-circuits suggests the following extension of the classification of (gapped) quantum phase of matter:



This motivates the definition:

**** Definition: Topological order (TO)**

** (Intrinsic) Topological order := Patterns of long-range entanglement

- We discuss this concept at the end of this course: → Part III
- ¡! Sometimes the term “topological order” is used sloppily in the literature to refer to any phase of matter with some topological characteristics (e.g., → *symmetry-protected topological phases*). Then the modifier “intrinsic” is used to refer to states with non-trivial long-range entanglement. In this course “topological order” *always* refers to long-range entangled states; however, we still might add “intrinsic” to emphasize this point. By contrast, the term “topological phase” is used much broader and refers to any quantum phase with topological features.

↓ Lecture 3 [17.04.25]

10 | Examples for topologically ordered systems that exist in nature (or in laboratories):

- Fractional quantum Hall states

Yes, this is all we actually know of (except for some special cases, see below)! There is a plethora of *theoretical* models, some of which are actively studied in labs; but none of them have been experimentally realized and characterized to the degree that fractional quantum Hall states have. Examples of promising models that are theoretically known to be topologically ordered and actively experimentally studied include ↑ *topological quantum spin liquids* like the → *toric code* (→ ??) [31, 32], ↑ *Kitaev materials* [33], and ↑ *fractional Chern insulators* [34].

- But actually, that’s not quite correct:

Integer quantum Hall states, first observed in 1980 by KLAUS VON KLITZING [13], are also long-range entangled, i.e., cannot be transformed into product states via constant-depth LU circuits [35]. However, their long-range entanglement is of a particularly simple type (so called *invertible* topological order, → *below*) that does *not* give rise to anyonic excitations and topological ground state degeneracies (→ *Part III*, see also Ref. [36]) which makes non-invertible topological orders like fractional quantum Hall states so interesting. This is why some use a different nomenclature where “topologically ordered” only refers to non-invertible topological order with anyonic excitations and non-vanishing → *topological entanglement entropy* [37].

- But *aaactually* ...that’s also not quite correct:

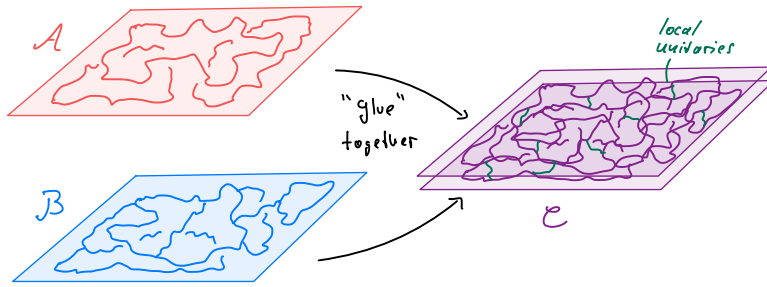
Surprisingly, conventional *s*-wave superconductivity in 3D systems (discovered in 1911 by HEIKE KAMERLINGH ONNES) is also an example of intrinsic topological order [35, 38]. This is not true for simplistic models like the BCS-Hamiltonian where the electromagnetic gauge field is treated as a non-dynamical background. In the real world, however, the gauge field *is* dynamical and a superconductor is described by the interactions between charged particles (electrons) with themselves (which gives rise to pairing) and with the dynamical electromagnetic field (which gives rise to string-like excitations, namely quantized ↑ *flux tubes*, and massive photons). The combined system of charges and electromagnetic field turns out to be topologically ordered [39, 40] and is described by a ↑ *topological quantum field theory* called ↑ *BF-theory* [41]. The excitations of such systems are (1) Bogoliubov quasiparticles (“broken Cooper pairs”), (2) flux lines/loops, and (3) massive photons. The Bogoliubov quasiparticles have non-trivial braiding statistics with the flux lines/loops – which demonstrates the (non-invertible) topological order of such systems.

11 | ‡ Invertible topological orders (ITO):

With our definition of gapped quantum phases, one can define a “multiplication” of such phases:

◁ Two topological phases \mathcal{A} and \mathcal{B} (in the same dimension):

$$\underbrace{\mathcal{A} \boxtimes \mathcal{B}}_{\text{Stacking two TOs}} = \underbrace{\mathcal{C}}_{\text{New TO}} \tag{0.23}$$



Observation: Trivial phase \mathcal{E} (= product states) acts as identity:

$$\mathcal{A} \boxtimes \mathcal{E} = \mathcal{A} \tag{0.24}$$

→ Commutative monoid of quantum phases [42]

In mathematics, a \downarrow *monoid* is a set with an associative binary operation and an identity. It is commutative if the binary operation is abelian. Elements are not required to have inverse elements (if all elements have inverse elements, the monoid becomes a group).

◁ Class of topological phases that have an *inverse element*:

✱ Definition: Invertible topological order (ITO)

$$\text{✱ Invertible TOs (ITO)} := \{ \mathcal{A} \mid \exists \mathcal{A}^{-1} : \mathcal{A} \boxtimes \mathcal{A}^{-1} = \mathcal{E} \}$$

- The class of ITOs forms a *group* within the monoid of TOs.
- If they exist, the inverse phases are given by a time-reversal operation [43].
- In words: A topologically ordered ground state is invertible if and only if you can find another ground state (of a gapped, local Hamiltonian) such that the combination of both can be transformed into a product state by a constant-depth LU circuit.

* → The entanglement patterns of ITOs are of a particularly simple kind [42, 43]:

$$\text{ITO} \Leftrightarrow \begin{cases} \text{No} \rightarrow \text{anyons} \\ \text{Vanishing} \rightarrow \text{topological entanglement entropy} \end{cases}$$

In that sense, ITOs are a rather “boring” type of long-range entanglement, which is why some do not refer to ITOs as topologically ordered in the first place (in this course, we do).

Examples [35, 44]:

- → *Integer quantum Hall states* in 2D (Chapter 1)
- → *Haldane model* in 2D (Chapter 2)
- → *Kane-Mele model (Topological insulator)* in 2D (Chapter 3)
(This is the only example in this list that is truly short-range entangled.)
- → *Majorana chain* in 1D (Chapter 5),

So despite their lack of fancy anyonic statistics, ITOs are not so boring after all and we will study them in detail (and discover much interesting physics).

12 | But wait! There is more ...

Adding patterns of long-range entanglement to our labeling scheme produces a more fine-grained classification of quantum phases. However, it can be useful to make this classification *even more fine-grained* by adding additional symmetry constraints.

We can motivate this rationale by a classical analog:

★ **Interlude: Restrictions on perturbations**

◁ Phase diagram of water:

(This argument draws inspiration from classical thermodynamic phases, not quantum phases.)

→ Restrictions on allowed paths can be useful! (depending on the system ...)

13 | → Restrict Hamiltonians by (*protecting*) symmetries $G_P \subseteq G_S$:

✱ **Definition: Symmetry-protected quantum phases**

◁ Gapped, local Hamiltonians H_a and H_b with unique ground states $|\Omega_a\rangle$ and $|\Omega_b\rangle$, and a symmetry group G_P (represented by unitaries U_g on the Hilbert space) with $[H_x, U_g] = 0$ for all $g \in G_P$ and $x = a, b$.

The ground states belong to the same *symmetry-protected quantum phase* if and only if there exists a family of *gapped* and *local* Hamiltonians $\hat{H}(\alpha)$ that depends continuously on $\alpha \in [0, 1]$ such that

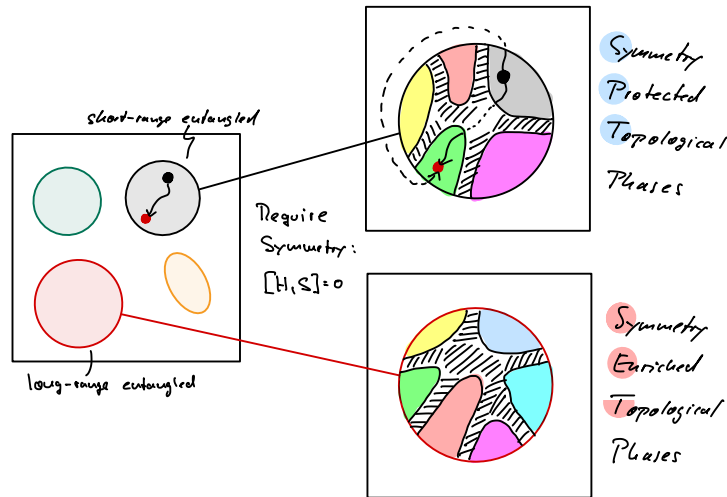
$$H_a = \hat{H}(0) \quad \text{and} \quad H_b = \hat{H}(1) \tag{0.25}$$

and

$$[\hat{H}(\alpha), U_g] = 0 \quad \text{for all } g \in G_P \text{ and } \alpha \in [0, 1]. \tag{0.26}$$

14 | → Phases with the *same entanglement pattern* can *split* further:

In particular short-range entangled phases that belong to the trivial phase!



→ Conventional nomenclature:

**** Definition: SPT and SET phases**

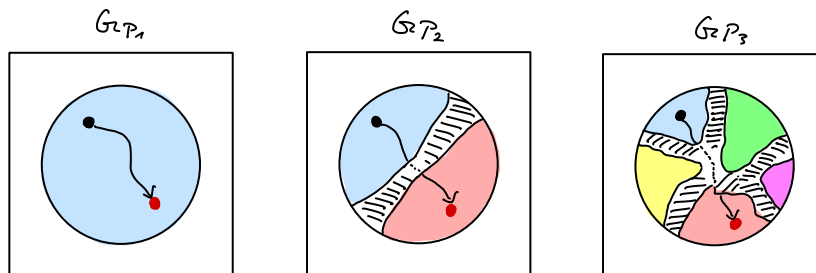
- **** Symmetry-protected topological (SPT) phases** := Short-range entangled phases protected by symmetries
- **** Symmetry-enriched topological (SET) phases** := Long-range entangled phases with additional symmetries

We use the terms “SPT(s)” and “SET(s)” to mean “symmetry-protected/enriched topological quantum phase(s)” whenever the context requires it.

Comments:

- Typical examples for SPT phases are the → *SSH chain* in 1D (Chapter 4) and the → *topological insulator* in 2D (Chapter 3).
- Typical examples for SET phases are ↑ *fractional quantum Hall states* with protected U(1) symmetry (= particle number conservation) [35].
- We will not study SET phases in this course!
- Since SPT phases are LU-equivalent to product states (when ignoring symmetries), they belong to the equivalence class \mathcal{E} of “trivial” phases; in particular, they are ← *invertible topological orders* (of a special kind, namely without any long-range entanglement).

15 | Important: Possible SPTs (and SETs) depend on the protecting symmetry G_P :

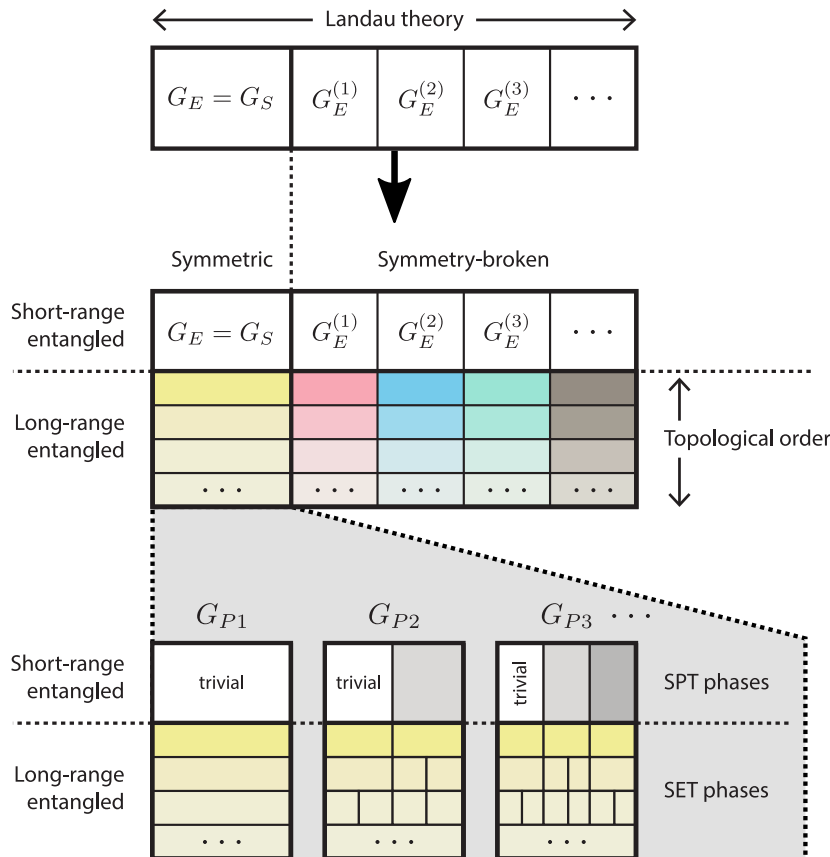


! Note that SPTs (and SETs) are not properties of ground states (like intrinsic topological order) but rather classifications of ground states with respect to a prescribed class of allowed Hamiltonian

deformations (or a restricted class of constant-depth LU circuits). The relevance of this class typically derives from physical considerations (recall the motivation above).

Second extension of Landau’s paradigm: Symmetry-protected topological phases

16 | These insights lead us to a second extension of our classification scheme:



! In this course we only study phases without SSB.

17 | *Question:* How to characterize SPT phases?

We cannot label them by patterns of long-range entanglement nor by the symmetries they break!

Answer: Complicated! (also: subject of ongoing research!)

→ Make simplifying assumptions: Consider restricted classes of models/Hamiltonians:

- < Non-interacting fermions → Part I

The benefit of non-interacting fermions is that such models can be solved exactly. This provides us with powerful tools to classify them systematically. Note that some of these models will turn out to be invertible topological orders (we will not find *non*-invertible TOs with anyons etc. for this class of Hamiltonians).

- < Interacting bosons/spins (in 1D) → Part II

Interacting systems of bosons/spins in 1D are usually not exactly solvable. However, since there is no topological order in these systems, such models realize true SPT phases with a powerful description in terms of matrix-product states (which again makes a systematic classification possible).

Let me comment on a few questions that might come up at this point:

- Why not *interacting* fermions?

In 1D, this classification derives (via Jordan-Wigner transformation) from the classification of interacting spin systems (also in 1D) [29]. In higher dimensions, there are approaches to classify interacting fermions (this is ongoing research [45]), but this goes beyond the scope of this course.

- Why not *non-interacting* bosons?

Because non-interacting bosons form a Bose-Einstein condensate (which is a well-understood non-topological quantum phase). Thus topological phases for bosons *require* interactions (in contrast to fermions).

- Why not interacting bosons in *higher dimensions*?

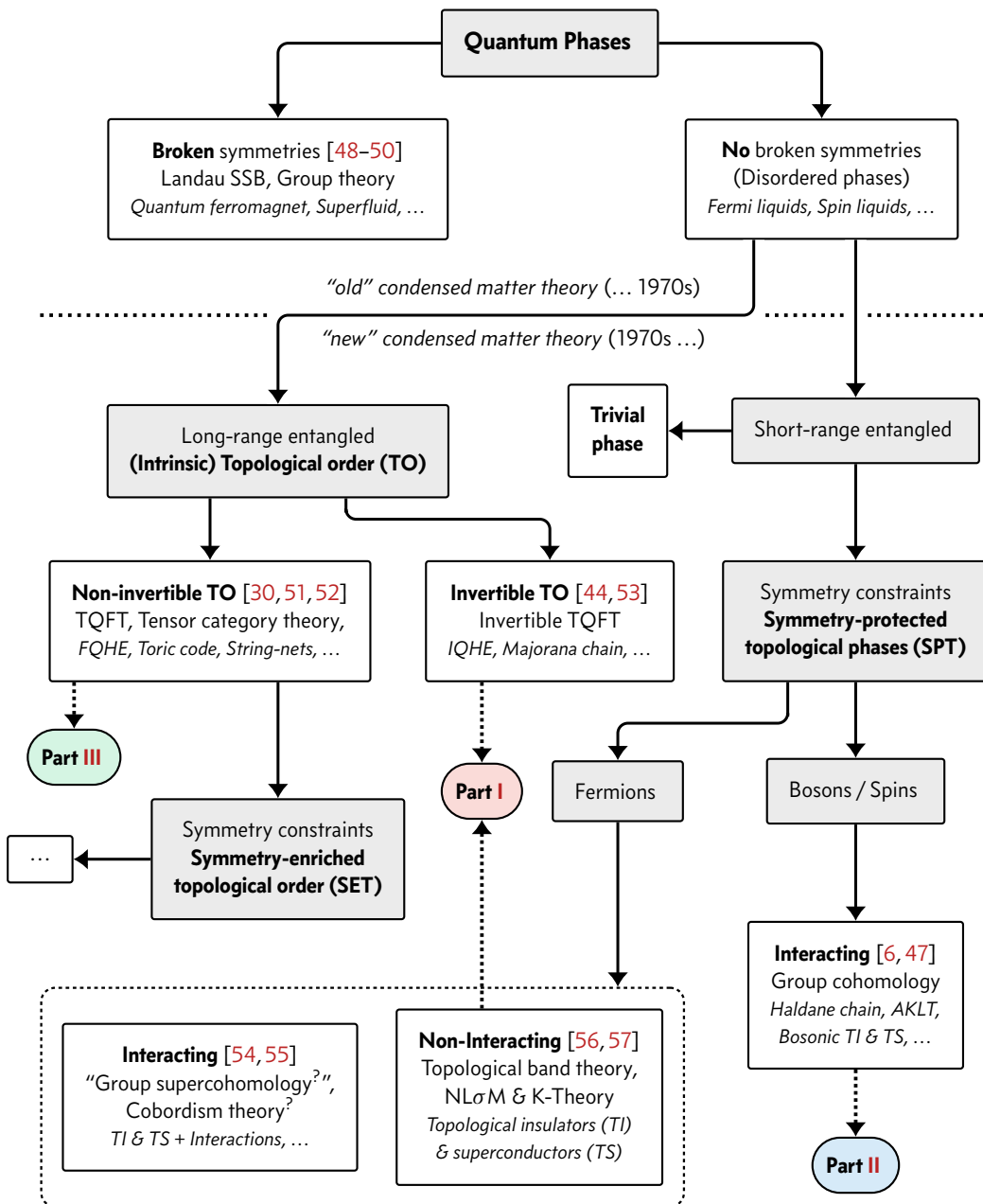
This can be done with a generalization of the mathematical methods that we will discuss for the 1D case (Part II) [46, 47]. We will not discuss these generalizations in this course.

0.6. Overview and Outlook

We can combine all these concepts into a flowchart:

Highlight the three classes that we will discuss in this course.

(A few important original references are given that establish the various concepts.)



✱✱ Definition: Nomenclature

In this course, gapped quantum phases that ...

- (1) do not break any symmetries
- (2) and are either ...
 - (2a) *topologically ordered (TO)* or
(invertible and non-invertible, with and without additional protecting symmetries)
 - (2b) *symmetry-protected (SPT)*

...will jointly be referred to as *topological phases (TP)*.

Note the difference between “topologically ordered phases” (which are long-range entangled) and “topological phases” (which can also refer to short-range entangled SPT phases)!

So far, we discussed topological phases on an abstract level. To further motivate these concepts, let us briefly list a few features of these intriguing phases of matter. Note that not every topological phase exhibits all these features! Some of them necessarily require long-range entanglement, some don't. Conversely, long-range entanglement does not necessarily imply all these features. It is quite a mess and we will study various models in this course to shed light on these features and their origins.

Some features of topological phases

- TPs cannot be characterized by local order parameters
(all correlations of local operators decay exponentially, cf. our discussion of the TIM).
This is the defining property of topological phases and applies to intrinsic topological order and SPT phases alike.
- For some TPs, the ground state degeneracy on closed manifolds depends on their topology (whether it is a sphere, a torus, etc.) and is robust in the presence of perturbations [58].
This is true for non-invertible topological orders (like fractional quantum Hall states), but not for SPT phases and invertible topological orders (topological insulators, integer quantum Hall states).
- Some TPs feature exponentially localized excitations (*quasiparticles*) that obey neither fermionic nor bosonic statistics – they are *anyons* and obey *fractional or anyonic statistics* [59, 60].
The presence of anyons is closely related to the topological degeneracy mentioned above. For example, integer quantum Hall states and topological insulators do not have anyonic quasiparticles, but fractional quantum Hall states do.
- These quasiparticles can carry fractionalized charges (e.g. a fraction of the electron charge) [15].
Fractional charges are a consequence of additional symmetries (for example, particle number conservation). Fractional charges are therefore a consequence of anyonic excitations in the presence of a conserved symmetry, i.e., SET order. Fractional quantum Hall states with $U(1)$ particle number conservation are an example.
- Some TPs have an effective low-energy description in terms of a *topological quantum field theory (TQFT)* [61] (a quantum field theory defined by an action that is a topological invariant).

This is closely related to features of intrinsic topological orders (topological degeneracy, anyonic excitations). Invertible topological orders are described by \uparrow *invertible TQFTs*.

- In some TPs, (lattice) **defects** can exhibit anyonic statistics as well (**under continuous deformations of the Hamiltonian**).

This can happen even for invertible topological phases like the Majorana chain in 1D and the $p_x + i p_y$ superconductor in 2D. Note that such defects are *not* intrinsic quasiparticle excitations but deformations of the Hamiltonian.

- Some TPs feature robust, gapless edge states on manifolds with boundaries that allow for scattering-free transport [62].

This can happen for invertible topological phases and even SPT phases. Examples are the famous chiral edge states of integer quantum Hall systems.

- The linear response of TPs can be *quantized* to a remarkable degree (**even in the presence of disorder!**).

This can happen for invertible and non-invertible topological orders (like integer and fractional quantum Hall states) and even SPT phases (like topological insulators). The quantization requires some additional symmetry (like particle number conservation), even if the phase itself does not require any symmetry protection.

† Note: Why topology?

After this introductory info-dump you might wonder:

Why are topological phases called “topological”?

Where does topology enter the picture?

The answer to these questions is, as usual, complicated and cannot be fully appreciated at this point (answering these questions is the purpose of this course). However, we can make a few high-level comments to set your expectations:

First, remember that \downarrow *topology* is the field of mathematics that is concerned with the formalization of deformation-invariant properties of spaces. Topology is therefore considered with rather “robust” qualities of (potentially abstract) objects – in contrast to *geometry* that is concerned with concepts like distances and angles (for which one requires a metric). For instance, a donut (bagel) is topologically equivalent to a coffee mug because you can continuously deform these two shapes into each other (such a deformation is called a \downarrow *homotopy*):

➔ Example of a homotopy (Source: Wikipedia)

We say that the donut and the coffee mug are *topologically equivalent* but *geometrically distinct*. Formalizing the concept of “topological equivalence” and studying its implications is the core subject of topology.

Generally speaking, topological phases are called “topological” because various (!) concepts from topology play a role in their description. It is important to appreciate that the term “topology” can refer to *different* topological concepts and their application in physics. Broadly speaking, there are two very distinct such applications in the realm of topological quantum many-body physics:

- “Classical topology”:

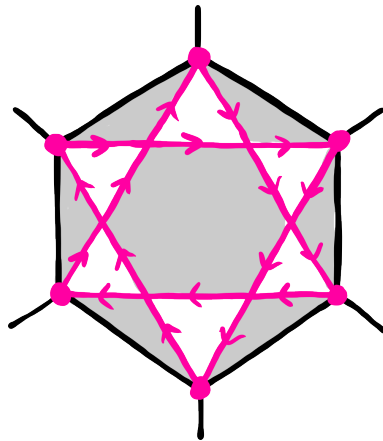
Our first encounter of topological concepts will concern so called \rightarrow *topological invariants* that can be used to characterize certain manifolds (parametric paths, Brillouin zones, band structures, ...) that describe *non-interacting* quantum systems (Part I). This is an application of topology to *single-particle* quantum mechanics (with many-body ramifications like the quantized Hall conductivity). As such, some (not all!) of these phenomena translate to classical systems (\rightarrow *topological edge modes*) with several applications in engineering (??). The SPT phases of non-interacting fermions (topological insulators and superconductors) are an example of “classical topology” at play.

- “Quantum topology”:

A completely different application of methods from topology concerns the description of long-range entangled quantum many-body phases, i.e., *intrinsic topological order*. The low-energy physics of quantum phases in general can be described by \uparrow *quantum field theories* (QFT). It turns out that the quantum field theories of systems with topological order are of a particularly elegant type: they are so called \uparrow *topological quantum field theories* (TQFT). These are QFTs that do not depend on the metric of the space on which the fields live; hence their degrees of freedom only depend on the *topology* of this space. The algebraic properties of TQFTs capture all the fascinating properties of topologically ordered systems (anyonic excitations, topological ground state degeneracies, ...). This application of topology is a genuine feature of *quantum* systems and has no classical counterpart, hence “quantum topology”.

Part I.

**Topological Phases
of Non-Interacting Fermions**



1. The Integer Quantum Hall Effect

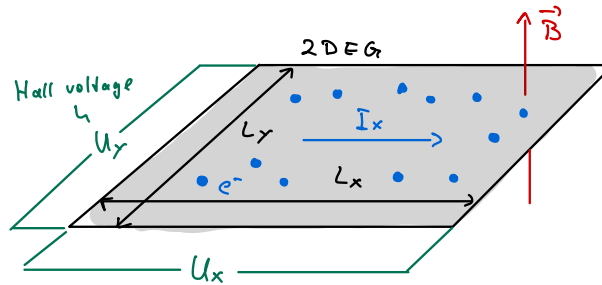
◇ Topics

- Review the classical & (integer) quantum Hall effect
- Derive Landau levels
- Motivate & define the Berry connection & holonomy
- Motivate & define the Berry curvature & phase
- Motivate & define the Chern number as a topological invariant
- Derive the Kubo formula and the TKNN formula for the Hall conductivity
- Comment on the role of disorder and edge states
- Locate the integer quantum Hall states in our classification of topological phases

- We start our discussion with topological phases that can be realized by *non-interacting fermions*. Such systems can be solved exactly in terms of single-particle Hamiltonians, the spectrum of which defines a ↓ *band structure*. The many-body ground states are then given by a ↓ *Fermi sea* of “filled bands” (in first-quantized language, the ground state is given by a ↓ *Slater determinant* of single-particle eigenstates). The resulting quantum phases will be symmetry-protected (SPT) phases and invertible topological orders. We will not encounter non-invertible topological orders (with anyons etc.) within this family of quantum many-body systems.
- Historically, the study of topological phases was kick-started by the experimental observation of the integer quantum Hall effect by KLAUS VON KLITZING in 1980 [13] who was awarded the 1985 Nobel Prize in Physics for his seminal discovery. The theoretical explanation of the effect by Thouless *et al.* in 1982 [17] highlighted the pivotal role that topological concepts can play in quantum many-body physics. For these theoretical contributions (among others) DAVID J. THOULESS (jointly with F. DUNCAN M. HALDANE and J. MICHAEL KOSTERLITZ) was awarded the 2016 Nobel Prize in Physics. We will use the integer quantum Hall effect and its theoretical description as motivation and starting point for the exploration of topological phases of non-interacting fermions in general.
- In the following, we have a quite detailed look at some aspects of the integer quantum Hall effect, especially the mathematics that underlies the quantization of the Hall conductivity. However, the integer quantum Hall effect is not the main focus of this course, and we will not cover the subject to its full extend (to do so would merit its own dedicated course!). If you are interested in more details, have a look at the textbook *Field Theories of Condensed Matter Systems* by Fradkin [63] (Chapter 12 and 13) or the *Lectures on the Quantum Hall Effect* by David Tong [64] on which parts of this chapter are based. You may also have a look at the collection [65] by Prange *et al.*

1.1. From the classical to the quantum Hall effect

1 | < 2D electron gas (2DEG) in perpendicular magnetic field $\mathbf{B} = B\mathbf{e}_z$:



Our sample is wired such that a current I_x can flow from a connection on the left boundary to a connection on the right boundary (there is no source/drain on the boundaries in y -direction, $I_y = 0$). There are voltage probes on all four boundaries to measure the voltages U_x and U_y .

2 | Drude model: (= Electrons as billiard balls)

$$m \frac{d}{dt} \mathbf{v} = \underbrace{-e\mathbf{E} - e\mathbf{v} \times \mathbf{B}}_{\text{Lorentz force}} - \underbrace{\frac{m}{\tau} \mathbf{v}}_{\text{Scattering}} \tag{1.1}$$

τ : scattering time (due to electrons bouncing of much heavier crystal ions)

3 | < Equilibrium $\frac{d}{dt} \mathbf{v} = \mathbf{0}$

Define the current density $\mathbf{J} = -ne\mathbf{v}$ (n : electron density) $\vec{\circ}$

Note that $I_x = L_y J_x$ and $U_y = L_y E_y$.

$$\underbrace{\mathbf{J} = \sigma \mathbf{E}}_{\text{Ohm's law}} \quad \text{with} \quad \underbrace{\sigma = \begin{bmatrix} \sigma_{xx} & \sigma_{xy} \\ \sigma_{yx} & \sigma_{yy} \end{bmatrix}}_{\text{Conductivity tensor}} \stackrel{\circ}{=} \frac{\sigma_0}{1 + \omega_B^2 \tau^2} \begin{bmatrix} 1 & -\omega_B \tau \\ \omega_B \tau & 1 \end{bmatrix} \tag{1.2}$$

Note that $\sigma_{xx} = \sigma_{yy}$ and $\sigma_{xy} = -\sigma_{yx}$ is a consequence of the *rotation symmetry* of the system about the perpendicular z -axis.

with

$$\omega_B = \frac{eB}{m} \quad \text{** cyclotron frequency} \tag{1.3}$$

and $\sigma_0 = ne^2\tau/m$ the ** DC conductivity (conductivity w/o magnetic field).

4 | $\vec{\circ}$ ** Resistivity tensor:

$$\rho \equiv \begin{bmatrix} \rho_{xx} & \rho_{xy} \\ \rho_{yx} & \rho_{yy} \end{bmatrix} := \sigma^{-1} = \frac{1}{\sigma_0} \begin{bmatrix} 1 & \omega_B \tau \\ -\omega_B \tau & 1 \end{bmatrix} \quad \text{with} \quad \mathbf{E} = \rho \mathbf{J} \tag{1.4}$$

Note that Hall *resistance* and Hall *resistivity* are (up to a sign depending on convention) the same:

$$R_{xy} := \frac{U_y}{I_x} = \frac{\cancel{L_y} E_y}{\cancel{L_y} J_x} = \frac{E_y}{J_x} = -\rho_{xy} \tag{1.5}$$

(Here we used $J_y = 0$ due to our experimental setup.)

This is *not* true for longitudinal resistance and resistivity:

$$R_{xx} := \frac{U_x}{I_x} = \frac{L_x E_x}{L_y J_x} = \frac{L_x}{L_y} \rho_{xx} \quad (1.6)$$

This already suggests that the Hall resistance is in some sense more robust than the longitudinal (ohmic) resistance as the former is independent of the sample geometry whereas the latter is not.

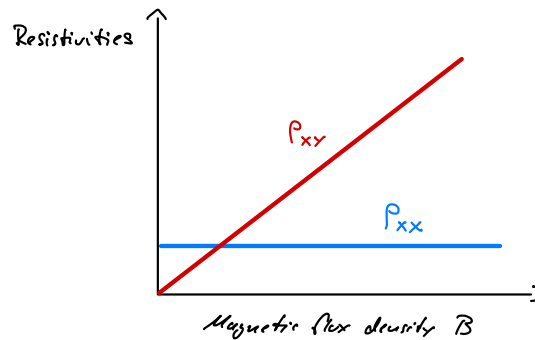
→ In particular:

$$\rho_{xy} = \frac{\omega B \tau}{\sigma_0} = \frac{B}{ne} \quad \text{Independent of } \tau \text{ (= no dissipation) !} \quad (1.7a)$$

$$\rho_{xx} = \frac{m}{ne^2 \tau} \quad (1.7b)$$

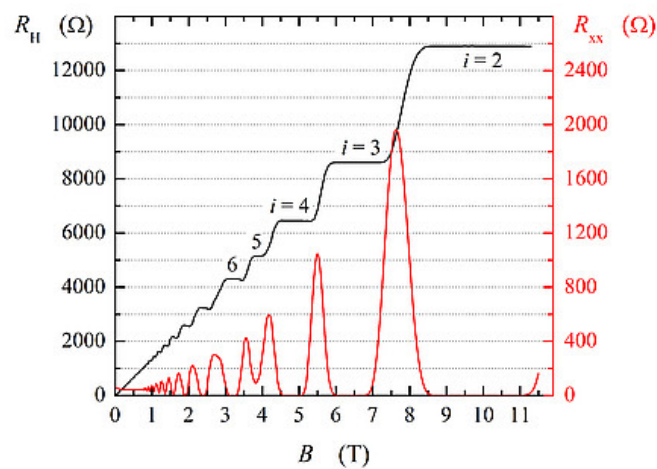
This implies that the Hall resistivity [and via Eq. (1.5) the Hall resistance] does not depend on the microscopic interactions of electrons with crystal ions and lattice defects (which determines the scattering time τ).

5 | → Classical prediction:



6 | Observation:

- ✓ Valid for high temperatures & weak magnetic fields ($\hbar\omega_B \ll k_B T$).
- ✗ Not valid for low temperatures & strong magnetic fields ($\hbar\omega_B \gg k_B T$):



- Note how the plot resembles the classical predictions in the lower-left corner (i.e., for weak magnetic fields).

- These results are from the electrical quantum metrology division of the PTB (the national metrology institute of Germany) and taken from this website; here $R_H = R_{xy} = L_y/L_x \cdot \rho_{xy} = \rho_{xy}$ and $R_{xx} = L_x/L_y \cdot \rho_{xx}$ and $i = \nu$ (see below). This phenomenon was first observed by KLAUS VON KLITZING in [13] for which he was awarded the 1985 Nobel Prize in Physics.
- The oscillations of the longitudinal resistance R_{xx} are called ↑ *Shubnikov-de Haas oscillations*. Here we are interested in the → *Hall plateaus* of the transversal resistance R_{xy} (→ below).

7 | → *Quantized* plateaus for Hall resistivity:

$$\rho_{xy} = \underbrace{\frac{h}{e^2}}_{R_K} \frac{1}{\nu} \quad \text{with } \nu \in \{1, 2, 3, \dots\} \quad (1.8)$$

R_K : ✨ *von Klitzing constant* or *quantum of resistivity* ($R_K \approx 25.8 \text{ k}\Omega$)

At this point, Eq. (1.8) is an observational fact and a theoretical miracle!

Note: By the revision of the SI system of units in 2019, the numerical values of h and e are now fixed. Consequently, the value of the von Klitzing constant R_K is also fixed by definition and does not have to be measured. The integer quantum Hall effect can then be used as a universal (and defining) resistance measurement device (that's why the BIPM is measuring the Hall resistance, see above). In particular, the quantization of the first → *Landau level* is perfect by definition: $\nu = 1.000\dots$ (Using your ohmmeter to measure this quantization would be as if using your balance to measure the weight of the primary kilogram in Paris before the revision of the SI. With one big difference: the primary kilogram was a unique artifact. By contrast, the integer quantum Hall effect is a universal phenomenon that can be reproduced everywhere with the right equipment. Thus “bootstrapping” universal units for measurements is much easier when artifacts are not involved. This was the motivation behind the 2019 revision of the SI system in the first place.)

- 8 | Historically, the miracle of the quantized Hall response and its “topological explanation” [17] (→ below) kick-started the study of topological phases in the first place:

! Important

The *exact quantization* of the (macroscopic) Hall resistivity in *disordered samples* of a 2DEG is a remarkable and unexpected feature that demands for an explanation!

With “exact quantization” one refers to the extraordinary precision to which the experimentally measured Hall resistivity of *different* samples coincides: the relative variations are of order 10^{-10} ! A miracle indeed.

1.2. Landau levels

Up to now we used *classical* physics to describe the Hall effect – and we failed to explain the quantization of the Hall resistance. It is time for quantum mechanics to flex its muscles ...

! Important

The *integer* quantum Hall effect can be understood in the context of *non-interacting fermions*. Therefore we focus on *single-particle wavefunctions* in the following.

This is *not* true for the ↑ *fractional quantum Hall effect*!

1 | < Same setup as before, but now we quantize the system!

→ Single-particle Hamiltonian of an electron in a magnetic field:

$$H = \frac{1}{2m} \underbrace{(\mathbf{p} + e\mathbf{A})^2}_{\boldsymbol{\pi}} \quad (1.9)$$

$\boldsymbol{\pi}$: *kinetic* momentum (gauge independent)

\mathbf{p} : *canonical* momentum (gauge dependent)

$\mathbf{A}(\mathbf{x})$: gauge potential with $\nabla \times \mathbf{A} = B\mathbf{e}_z$ (we do not yet fix a gauge!)

2 | Canonical quantization:

$$[x_i, p_j] = i\hbar\delta_{ij} \quad (1.10)$$

→ $[\pi_x, \pi_y] \stackrel{\circ}{=} -ie\hbar B$

Remember that the (static) gauge potential $\mathbf{A}(\mathbf{x})$ depends on the position (operator) \mathbf{x} , and that the canonical momentum (operator) that satisfies Eq. (1.10) is $p_i = -i\hbar\frac{\partial}{\partial x_i}$ (↑ *Stone-von Neumann theorem*).

→ The magnetic field couples the movement in x - and y -direction, so that the kinetic momenta form a pair of conjugate observables.

3 | This immediately suggests the introduction of ↓ *ladder operators*:

$$a := \frac{1}{\sqrt{2e\hbar B}}(\pi_x - i\pi_y) \quad \text{and} \quad a^\dagger = \frac{1}{\sqrt{2e\hbar B}}(\pi_x + i\pi_y) \quad (1.11)$$

→ These satisfy as usual $[a, a^\dagger] = 1$ and we find with Eq. (1.9) →

$$H \stackrel{\circ}{=} \hbar\omega_B \left(a^\dagger a + \frac{1}{2} \right) \quad (1.12)$$

→ Discrete spectrum $E_n = \hbar\omega_B \left(n + \frac{1}{2} \right)$ with $n = 0, 1, 2, \dots$

→ ✱ *Landau levels* (LL)

The term “Landau levels” refers to both the quantized *eigenenergies* E_n and the corresponding (degenerate) *eigenspaces* within the single-particle Hilbert space.

4 | Eigenstates? Degeneracy?

Note that we only used *one* degree of freedom (= one harmonic oscillator) although we started with *two* independent degrees of freedom (an electron moving in a 2D plane). The Landau levels must therefore be extensively degenerate to harbor all the needed states! So see this, we must first fix a gauge ...

We stress that here the gauge field A is *not* a dynamical degree of freedom (like when you quantize the electromagnetic field). Thus gauge fixing is really just a classical inconvenience and does not lead to fundamental problems like negative norm states etc.

1.2.1. Landau gauge

Here we proceed with the particularly simple *Landau gauge* (which comes with a price: it breaks the rotational symmetry of the problem); the alternative *symmetric gauge* is discussed in Section 1.2.2 → *below*. Since these are gauges, their choice does not affect physical conclusions; however, they lead to different basis states in the Landau levels that paint different (but equivalent) pictures of the physics within them.

5 | < Gauge choice $A := xBe_y$

This gauge breaks translation symmetry in x -direction and rotation symmetry in the plane. This is of course a mathematical artifact: the physics remains completely invariant under these transformations.

Eq. (1.9) → Hamiltonian:

$$H = \frac{1}{2m} [p_x^2 + (p_y + eBx)^2] \tag{1.13}$$

6 | < Translation symmetry in y -direction

Here we assume either periodic boundaries in y -direction or take the limit $L_y \rightarrow \infty$.

→ Ansatz: $\Psi_k(x, y) = e^{iky} f_k(x)$

In Eq. (1.13) → *Shifted* harmonic oscillator:

$$H_k \stackrel{\circ}{=} \frac{1}{2m} p_x^2 + \frac{m\omega_B^2}{2} (x + kl_B)^2 \tag{1.14}$$

with

$$l_B = \sqrt{\frac{\hbar}{eB}} \quad \text{** magnetic length} \tag{1.15}$$

The magnetic length is the relevant length scale for electrons in a magnetic field (it is the length scale of their cyclotron orbits).

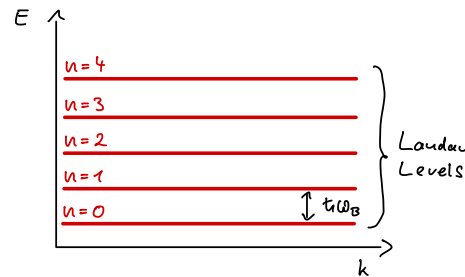
7 | → Eigenfunctions: (of H_k for each y -momentum k)

$$\Psi_{n,k}(x, y) = \mathcal{N} \underbrace{e^{iky}}_{\substack{\text{Plane wave} \\ \text{in } y\text{-direction}}} \underbrace{H_n(xl_B^{-1} + kl_B)}_{\text{Hermite polynomials}} \underbrace{e^{-\frac{1}{2}(xl_B^{-1} + kl_B)^2}}_{\text{Harmonic oscillator wavefunctions in } x\text{-direction}} \tag{1.16}$$

with $n = 0, 1, 2, \dots$ the Landau level index and $k = \frac{2\pi}{L_y}\mathbb{Z}$ the y -momentum.

Note that the eigenspaces of H (and the eigenfunctions) are *physical* and therefore gauge independent. What is *unphysical* is the choice of a basis (and the labeling of the basis wavefunctions by “good” quantum numbers). Since the Landau gauge preserves translation symmetry in y -direction, the basis above can be labeled by momenta in y -direction. In other gauges (see below), this is not the case. However, the eigenspaces that are spanned by these wavefunctions are the same for all gauges (of course) and you can linearly combine basis functions of one gauge with basis functions of another.

- 8 | Spectrum: $E_n = \hbar\omega_B \left(n + \frac{1}{2}\right)$ (degenerate in the k quantum number!)



The Landau levels are prototypes for *perfectly flat bands*. If a LL is only partially filled, the many-body properties of the electrons that occupy this level are determined by their (Coulomb) interactions. This is crucial to understand the long-range entanglement (topological order) of \uparrow *fractional quantum Hall states*.

- 9 | Degeneracy: $0 \leq x \leq L_x \rightarrow$ Restricted y -momenta $k: -L_x/l_B^2 \leq k \leq 0$

(Since the wavefunctions (1.16) are exponentially localized around $x_k = -kl_B^2$.)

→ Number of states in each Landau level:

$$N = \frac{L_x/l_B^2 - 0}{2\pi/L_y} = \frac{L_x L_y}{2\pi l_B^2} = \frac{AB}{\Phi_0} = \frac{\Phi}{\Phi_0} \quad (1.17)$$

$\Phi_0 = 2\pi\hbar/e$: \star *quantum of flux* (cf. $R_K = 2\pi\hbar/e^2$ the *quantum of resistivity*)

$A = L_x L_y$: area of the sample

→ Extensive degeneracy of each Landau level (as expected)

In particular, the number of electrons N than can be crammed into each Landau level increases with the magnetic flux through the sample (one electron per quantum of flux). This implies that if we fix the electron density and increase the magnetic flux density, fewer and fewer Landau levels will be needed to distribute all electrons, until for very large B all electrons fit into the lowest Landau level (LLL). Conversely, at “every day” weak-field conditions, Landau levels up to very large indices n are occupied by fermions.

1.2.2. \ddagger Symmetric gauge

You will do these calculations on \rightarrow Problemset 2.

In contrast to the \leftarrow *Landau gauge*, the *symmetric gauge* breaks translation invariance in *both* directions but retains the two-dimensional rotation invariance of the system. Thus, instead of k , we should expect a basis labeled by *angular momentum quantum numbers* m :

10 | < Gauge choice

$$\mathbf{A} := -\frac{1}{2} \mathbf{r} \times \mathbf{B} = -\frac{yB}{2} \mathbf{e}_x + \frac{xB}{2} \mathbf{e}_y \quad (1.18)$$

11 | Hamiltonian: [recall Eq. (1.12)]

$$H = \frac{\pi^2}{2m} = \hbar\omega_B \left(a^\dagger a + \frac{1}{2} \right) \quad (1.19)$$

with a, a^\dagger defined via π_x and π_y [recall Eq. (1.11)]

So far, this procedure does not depend on the gauge choice since the kinetic momentum is a gauge independent quantity.

12 | Define additional “momentum”: (which does not show up in the Hamiltonian!)

$$\tilde{\pi} := \mathbf{p} - e\mathbf{A} \quad \Rightarrow \quad [\tilde{\pi}_x, \tilde{\pi}_y] \stackrel{\circ}{=} i\hbar B \quad (1.20)$$

(Recall that $\pi = \mathbf{p} + e\mathbf{A}$.)

Important: In *symmetric gauge* (1.18) the two momenta are independent: $[\pi_i, \tilde{\pi}_j] \stackrel{\circ}{=} 0$

This is not so in other gauges!

13 | → Define additional ladder operators:

$$b := \frac{1}{\sqrt{2e\hbar B}} (\tilde{\pi}_x + i\tilde{\pi}_y) \quad \text{and} \quad b^\dagger = \frac{1}{\sqrt{2e\hbar B}} (\tilde{\pi}_x - i\tilde{\pi}_y) \quad (1.21)$$

→ $[b, b^\dagger] = 1$ and $[a, b] = 0$ (The latter is only true in symmetric gauge!)

14 | → Eigenstates:

$$|n, m\rangle := \frac{a^{\dagger n} b^{\dagger m}}{\sqrt{n!m!}} |0, 0\rangle \quad \text{with} \quad a|0, 0\rangle = b|0, 0\rangle = 0 \quad (1.22)$$

$n = 0, 1, 2, \dots$: Landau level index

$m = 0, 1, 2, \dots$: Angular momentum index (→ below)

In symmetric gauge, m replaces the y -momentum k and generates the degeneracy of the LLs.

15 | < Complex coordinates:

The unconventional sign makes the functions below holomorphic instead of antiholomorphic.

$$z := x - iy \quad \text{and} \quad \bar{z} := x + iy \quad (1.23)$$

and the corresponding ↓ Wirtinger derivatives

$$\partial := \frac{1}{2} (\partial_x + i\partial_y) \quad \text{and} \quad \bar{\partial} := \frac{1}{2} (\partial_x - i\partial_y) \quad (1.24)$$

Then $\partial z = \bar{\partial} \bar{z} = 1$ and $\partial \bar{z} = \bar{\partial} z = 0$. A function of complex variables is then holomorphic (= satisfies the Cauchy-Riemann equations) if and only if $\bar{\partial} f = 0$, i.e., $f = f(z)$.

16 | Use $p_i = -i\hbar\partial_i$ & Eqs. (1.18), (1.20), (1.21), (1.23) and (1.24) →

$$a = -i\sqrt{2} \left(l_B \bar{\partial} + \frac{z}{4l_B} \right) \quad \text{and} \quad a^\dagger = -i\sqrt{2} \left(l_B \partial - \frac{\bar{z}}{4l_B} \right) \quad (1.25a)$$

$$b = -i\sqrt{2} \left(l_B \partial + \frac{\bar{z}}{4l_B} \right) \quad \text{and} \quad b^\dagger = -i\sqrt{2} \left(l_B \bar{\partial} - \frac{z}{4l_B} \right) \quad (1.25b)$$

17 | \leftarrow Lowest Landau level wave functions $\Psi_0(z, \bar{z})$:

$$a\Psi_0 = 0 \quad \Leftrightarrow \quad \bar{\partial}\Psi_0 = -\frac{z}{4l_B^2}\Psi_0 \quad \Leftrightarrow \quad \Psi_0(z, \bar{z}) = f(z)e^{-z\bar{z}/4l_B^2} \quad (1.26)$$

$f(z)$: arbitrary holomorphic function

18 | \leftarrow Unique state with $m = 0$: (within the lowest Landau level)

$$b\Psi_0 = 0 \quad \Leftrightarrow \quad \partial\Psi_0 = -\frac{\bar{z}}{4l_B^2}\Psi_0 \quad \xleftrightarrow{(1.26)} \quad \partial f(z) = 0 \quad \Leftrightarrow \quad f(z) = \text{const} \quad (1.27)$$

$\rightarrow \Psi_{0,0}(z, \bar{z}) \propto e^{-|z|^2/4l_B^2}$ (Gaussian state)

19 | \leftarrow Other states in the LLL \rightarrow Apply b^\dagger to $\Psi_{0,0}$: (Remember that $\bar{\partial}z = 0$.)

$$\Psi_{0,m} \propto b^{\dagger m}\Psi_{0,0} \propto \left(l_B\bar{\partial} - \frac{z}{4l_B}\right)^m e^{-z\bar{z}/4l_B^2} \propto \left(\frac{z}{l_B}\right)^m e^{-|z|^2/4l_B^2} \quad (1.28)$$

\rightarrow Holomorphic monomials \times Gaussian

Since all wave functions $\Psi_{0,m}$ are degenerate, one can form arbitrary linear combinations of these holomorphic monomials (times a Gaussian) to form more general holomorphic polynomials.

20 | \rightarrow In the LLL, m is an angular momentum quantum number:

$$J\Psi_{0,m} = \hbar m\Psi_{0,m} \quad \text{with} \quad \underbrace{J = i\hbar(x\partial_y - y\partial_x)}_{\text{Angular momentum operator}} = \hbar(z\partial - \bar{z}\bar{\partial}) \quad (1.29)$$

with $m = 0, 1, 2, \dots$

Note: In 2D there is only one generator of angular momentum $J = J_z$ and the Lie algebra that generates the rotation group $\text{SO}(2) \simeq U(1)$ (namely $\mathfrak{u}(1) \simeq \mathbb{R}$) is abelian. Consequently, there is no algebraic reason for spin to be quantized (as in 3D where spin can take only half-integer values) and all irreducible representations are one-dimensional. Thus there is only *one* spin quantum number needed (to label the irrep) but none to label distinct basis states of an irrep, i.e., $J = m$. So Eq. (1.29) is all there is to say about spin in this context. Note that the abelian “angular momentum algebra” in 2D has also consequences for particles with anyonic statistics which do not only feature “fractional charges” and “fractional statistic” but also “fractional spin” (\rightarrow Part III).

1.3. Berry connection and Berry holonomy

We now take a step back and discuss some rather abstract (and high-level) concepts of quantum mechanics. We return to the integer quantum Hall effect \rightarrow later.

The following concepts are very generic and play a role in many areas of modern physics; they are also important throughout this course. Their application to the quantized Hall conductivity \rightarrow below is only one of many examples.

The following derivation is quite common and leads to physically important (and valid) conclusions. However, it is mathematically not rigorous and uses hidden assumptions on the \uparrow connection of the full \uparrow Hilbert bundle on which the parametric family of Hamiltonians is defined, see Ref. [66] for a mathematical treatment of the problem geared towards physicists.

1 | < Setting:

- Continuous family of gapped Hamiltonians $H(\Gamma)$ with k parameters $\Gamma = (\Gamma_1, \Gamma_2, \dots, \Gamma_k)$ and n -fold degenerate ground state space $\mathcal{V}(\Gamma) \equiv \mathcal{V}(H(\Gamma))$
 Since $H(\Gamma)$ is continuous and gapped, the dimension of $\mathcal{V}(\Gamma)$ is constant.
 We set $H(\Gamma)|\Psi\rangle = 0$ for $|\Psi\rangle \in \mathcal{V}(\Gamma)$ and all Γ , i.e., the ground state energy is zero.
- Slow “parameter path” $\Gamma(t)$ for $0 \leq t \leq T$
 “Slow” compared to the (inverse) of the smallest energy gap along the path $\Gamma(t)$.
- Initial ground state $|\Psi_0\rangle \in \mathcal{V}(\Gamma_0)$

2 | Question: What happens with $|\Psi_0\rangle$ as $H(\Gamma(0))$ evolves to $H(\Gamma(T))$?

3 | To answer this question, we use the following well-known fact:

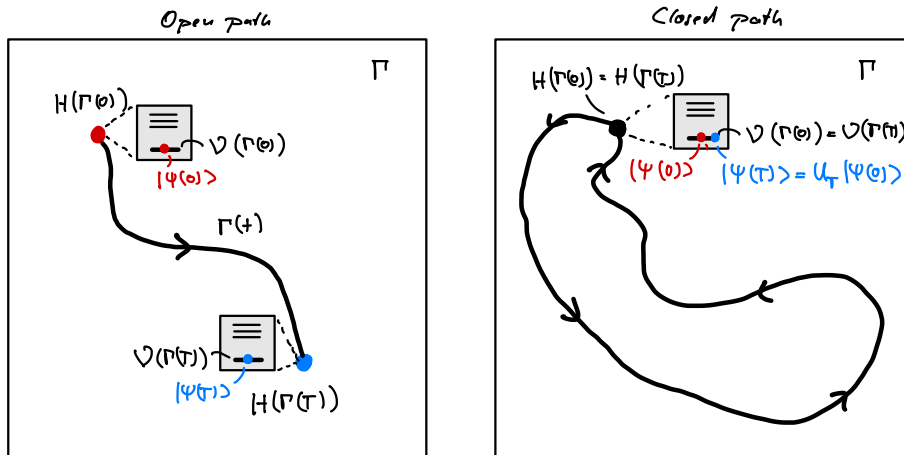
! Important: Adiabatic theorem

A physical system remains in its instantaneous eigenstate if a given perturbation is acting on it slowly enough and if there is a gap between the eigenvalue and the rest of the Hamiltonian’s spectrum.

This fundamental insight is due to MAX BORN and VLADIMIR FOCK [67].

4 | Solution:

Here is a sketch of the scenario/task that we want to solve:



We proceed step by step:

i | Pick a basis $\{|v_i(\Gamma)\}_{i=1, \dots, n}$ of $\mathcal{V}(\Gamma)$ for every Γ

This choice is not unique and leads to a $U(n)$ gauge degree of freedom (\rightarrow below). Here we assume that the choice is differentiable (and therefore continuous) along the path Γ . This makes it less arbitrary but leaves a lot of arbitrariness to choose from. Note that a choice that is globally continuous is often impossible. Then one follows the arguments below on local patches in parameter space on which such a choice is possible.

ii | < Time-dependent Schrödinger equation:

$$\underbrace{i\hbar\partial_t}_{(L)}|\Psi(t)\rangle = \underbrace{H(\Gamma(t))}_{(R)}|\Psi(t)\rangle \tag{1.30}$$

↓ Lecture 5 [25.04.25]

iii | < Adiabatic theorem

→ Initial state remains in the ground state manifold: $|\Psi(t)\rangle \in \mathcal{V}(\Gamma(t)) \rightarrow$

(L) $|\Psi(t)\rangle = \sum_{i=1}^n \Psi_i(t) |v_i(\Gamma(t))\rangle \rightarrow$

$$\partial_t |\Psi(t)\rangle = (\partial_t \Psi_i(t)) |v_i(\Gamma(t))\rangle + \Psi_i(t) [\partial_{\Gamma_l} |v_i(\Gamma(t))\rangle] (\partial_t \Gamma_l(t)) \quad (1.31)$$

We omit sum symbols; sums over repeated indices are implied (Einstein notation).

(R) $H(\Gamma(t))|\Psi(t)\rangle = 0$ (Remember that we set the ground state energy to zero.)

This assumption is not crucial for the derivation that follows; it simply removes any dynamical phase from the evolution, so that only a geometric phase remains (which is what we are interested in). If you do not set the ground state energy to zero, use $H(\Gamma(t))|\Psi(t)\rangle = E_0(\Gamma(t))|\Psi(t)\rangle$ instead and track the additional term. Its effect is to add an additional, energy-dependent dynamical phase to the evolution of the wave function (which is not a new & interesting insight ...).

iv | Apply $\langle v_j(\Gamma(t))|$ and use Eq. (1.30):

$$\partial_t \Psi_j(t) = -\Psi_i(t) \langle v_j(\Gamma(t)) | \partial_{\Gamma_l} |v_i(\Gamma(t))\rangle (\partial_t \Gamma_l(t)) \quad (1.32)$$

v | This suggests the definition of the

$$\ast\ast \text{ Berry connection } [\mathcal{A}_l(\Gamma)]_{ji} := -i \langle v_j(\Gamma) | \partial_{\Gamma_l} |v_i(\Gamma)\rangle \in \mathfrak{u}(n) \quad (1.33)$$

Think of the \mathcal{A}_l as Γ -dependent Hermitian $n \times n$ -matrices, one for each of the $l = 1, \dots, k$ parameters.

vi | With this definition, we can write $[\Psi \equiv (\Psi_j)_{j=1,\dots,n}]$

$$\partial_t \Psi(t) = -i \underbrace{(\partial_t \Gamma_l(t)) \mathcal{A}_l(\Gamma(t))}_{\text{Time-dependent matrix}} \Psi(t) \quad (1.34)$$

vii | This equation can be solved with a ↓ Time- (\mathcal{T}) or path-ordered (\mathcal{P}) exponential:

$$\Psi(T) = \mathcal{T} \exp \left[-i \int_0^T \mathcal{A}_l(\Gamma(t)) \partial_t \Gamma_l(t) dt \right] \Psi_0 \quad (1.35a)$$

$$= \underbrace{\mathcal{P} \exp \left[-i \int_{\Gamma} \mathcal{A} d\Gamma \right]}_{\equiv U_{\Gamma} \text{ (Unitary matrix)}} \Psi_0 \quad (1.35b)$$

Here, $\mathcal{A} = (\mathcal{A}_l)$ should be seen as a $\mathfrak{u}(n)$ -valued vector field on the parameter space (a 1-form). I.e., \mathcal{A} can be integrated along parameter paths which, after (path ordered) exponentiation, produces a unitary $U(n)$ that describes the geometric part of the adiabatic evolution on the ground state space.

- 5 | \leftarrow Change of local basis by unitary $\Omega(\Gamma) \in U(n)$: $|v'_i(\Gamma)\rangle := \Omega_{ij}(\Gamma)|v_j(\Gamma)\rangle$

Note that the choice of basis is a gauge choice: it cannot have physical significance!

$$\overset{\circ}{\rightarrow} \mathcal{A}'_l = \Omega \mathcal{A}_l \Omega^\dagger - i \frac{\partial \Omega}{\partial \Gamma_l} \Omega^\dagger \quad (1.36)$$

If you attended a course on quantum field theory, you might recognize this as the gauge transformation of a non-abelian $U(n)/SU(n)$ Yang-Mills gauge theory (like QCD). The difference is that here the gauge (Berry) connection \mathcal{A}_l does not live on Minkowski spacetime but on an abstract “parameter space.” Gauge transformations arise from “parameter-local” basis transformations in the degenerate ground state space of a Hamiltonian (family).

$$\overset{\circ}{\rightarrow} U'_\Gamma = \Omega(\Gamma(T)) U_\Gamma \Omega^\dagger(\Gamma(0)) \quad (1.37)$$

To show this, consider an infinitesimal piece $d\Gamma$ of the path Γ and linearize U_Γ along this piece to derive the above transformation. Then use that the path-ordered exponential is defined as the product of such infinitesimal pieces. The identity $\Omega \frac{\partial \Omega^\dagger}{\partial \Gamma_l} = -\frac{\partial \Omega}{\partial \Gamma_l} \Omega^\dagger$ might help (prove this!).

- 6 | \leftarrow Open path $\Gamma \rightarrow U_\Gamma$ is gauge dependent \rightarrow Cannot contain physical information!

To see this let $\Omega(\Gamma(0)) = \mathbb{1}$. Then $U'_\Gamma = \Omega(\Gamma(T)) U_\Gamma$ can be chosen (almost) *arbitrary* since $U(n)$ is a group and $\Omega(\Gamma(T))$ can be chosen (almost) arbitrary (just connect it smoothly to the identity, i.e., its determinant must be one). This means that U_Γ cannot contain physical information as it can be transformed into any other unitary U'_Γ (with the same determinant) by parameter-local basis transformations.

\rightarrow \leftarrow Closed loops Γ in parameter space

I.e., $H(\Gamma(0)) = H(\Gamma(T))$ and $\mathcal{V}(\Gamma(0)) = \mathcal{V}(\Gamma(T))$ such that U_Γ is an *automorphism* on $\mathcal{V}(\Gamma(0))$ and described the geometric transformation of ground states due to cyclic (and adiabatic) deformations of the Hamiltonian.

- 7 | Then the

$$\text{** Berry holonomy } U_\Gamma = \mathcal{P} \exp \left[-i \oint_\Gamma \mathcal{A} d\Gamma \right] \in U(n) \quad (1.38)$$

is gauge covariant: [This follows from the continuity of $\Omega(\Gamma)$ and $\Gamma(T) = \Gamma(0)$.]

$$U'_\Gamma = \Omega(\Gamma(0)) U_\Gamma \Omega^\dagger(\Gamma(0)) \quad (1.39)$$

Note that the argument from above breaks down since both unitaries $\Omega(\Gamma(T)) = \Omega(\Gamma(0))$ are necessarily the same (since the parameter path is closed). U_Γ can still be changed, but not arbitrarily: It is unique up to unitary basis transformations (for instance, its spectrum is independent of basis changes!). This quantity *can* encode physical properties of the system. Note the difference between gauge *invariant* ($U'_\Gamma = U_\Gamma$) and gauge *covariant* [Eq. (1.39)].

- 8 | There is another important *gauge covariant* quantity (that we will use \rightarrow below):

$$\text{** Berry curvature } \mathcal{F}_{lm} := \frac{\partial \mathcal{A}_l}{\partial \Gamma_m} - \frac{\partial \mathcal{A}_m}{\partial \Gamma_l} - i [\mathcal{A}_l, \mathcal{A}_m] \in \mathfrak{u}(n) \quad (1.40)$$

This is the “field-strength” of the gauge field \mathcal{A} , the non-abelian generalization of the field-strength tensor $F_{\mu\nu} = \partial_\mu A_\nu - \partial_\nu A_\mu$ in electrodynamics (where $A_\mu \in \mathfrak{u}(1) \simeq \mathbb{R}$ so that the commutator vanishes identically).

→ \mathcal{F}_{lm} is gauge covariant:

$$\mathcal{F}'_{ij}(\Gamma) \doteq \Omega(\Gamma) \mathcal{F}_{ij}(\Gamma) \Omega^\dagger(\Gamma) \quad (1.41)$$

Notes:

- This is the field strength tensor known from ↑ *non-abelian Yang-Mills gauge theories*. The Yang-Mills Lagrangian takes the trace of the field strength tensor, thereby converting a gauge *covariant* quantity into a gauge *invariant* quantity: $\text{Tr}[F_{\mu\nu} F^{\mu\nu}]$. (Note that the summation over μ and ν is not related to gauge but Lorentz invariance for YM theories; as we do not have generic symmetries on the *parameter space*, we do not have an analog of this symmetry in the current situation.)
- If Eq. (1.40) seems abstract but you know about ↓ *general relativity*, there is some insightful connection (☺) to be drawn. Remember that the ↓ *Riemann curvature tensor* can be expressed as [68, Section 10.2.3]

$$R^i{}_{jlm} = \partial_l \Gamma^i{}_{jm} - \partial_m \Gamma^i{}_{jl} + \Gamma^i{}_{nl} \Gamma^n{}_{jm} - \Gamma^i{}_{nm} \Gamma^n{}_{jl} \quad (1.42)$$

in terms of ↓ *Christoffel symbols* $\Gamma^i{}_{jm}$, which are the (coordinate-dependent) connection coefficients of the (metric-induced) ↓ *Levi-Civita connection* on the spacetime manifold. Let us interpret the first two indices of the Christoffel symbols as indices of a $D \times D$ matrix (where D is the spacetime dimension), $[\Gamma_m]_{ij} \equiv \Gamma^i{}_{jm}$, and do the same for the Riemann curvature tensor: $[R_{lm}]_{ij} \equiv R^i{}_{jlm}$. In this notation, Eq. (1.42) reads

$$R_{lm} = \partial_l \Gamma_m - \partial_m \Gamma_l + \Gamma_l \Gamma_m - \Gamma_m \Gamma_l = \partial_l \Gamma_m - \partial_m \Gamma_l - [\Gamma_m, \Gamma_l] \quad (1.43)$$

which is (up to prefactors) completely analogous to Eq. (1.40). This explains why the Berry curvature is called “curvature”: it describes a generalized (and rather abstract) curvature of the vector bundle defined by the ground state spaces $\mathcal{V}(\Gamma)$ on the parameter manifold \mathcal{M} .

Note that in general relativity, the vector space at each point of the spacetime manifold is given by the ↓ *tangent space* – which has the same dimension as the manifold itself. This is why it is convenient to treat all four indices of the Riemann tensor on the same footing. In our context, the parameter manifold is k -dimensional and has nothing to do with the attached ground state spaces $\mathcal{V}(\Gamma)$ that are n -dimensional. Hence we prefer the matrix notation in Eq. (1.40) where the indices that correspond to the Hilbert space are suppressed.

1.3.1. Berry phase and Chern number

We now want to focus on the important special case w/o degeneracy ($n = 1$). In this case, we can make use of the Berry curvature to calculate the Berry holonomy (which is for $n = 1$ just a phase known as → *Berry phase*):

- 9 | < Special case $n = 1$: $\mathcal{V}(\Gamma) = \text{span}\{|v(\Gamma)\rangle\}$ (= systems w/o ground state degeneracy)

In this special case, the quantities introduced above simplify as follows:

$$\text{Berry connection: } \mathcal{A}_l(\Gamma) = -i \langle v(\Gamma) | \partial_{\Gamma_l} | v(\Gamma) \rangle \in \mathfrak{u}(1) \simeq \mathbb{R} \quad (1.44a)$$

$$\text{Berry holonomy: } U_\Gamma = \exp \left[-i \oint_\Gamma \mathcal{A} d\Gamma \right] \equiv e^{i\gamma(\Gamma)} \in \text{U}(1) \quad (1.44b)$$

$$\text{Berry curvature: } \mathcal{F}_{lm} = \frac{\partial \mathcal{A}_l}{\partial \Gamma_m} - \frac{\partial \mathcal{A}_m}{\partial \Gamma_l} \in \mathfrak{u}(1) \simeq \mathbb{R} \quad (1.44c)$$

→ Ground state can only change by a phase!

10 | Gauge transformation: $\Omega(\Gamma) = e^{i\xi(\Gamma)} \rightarrow$

The gauge transformation of the Berry connection is similar to electrodynamics:

$$\mathcal{A}' = \mathcal{A} + \nabla_{\Gamma} \xi \tag{1.45a}$$

$$U'_{\Gamma} = U_{\Gamma} \quad (\text{gauge invariant}) \tag{1.45b}$$

$$\mathcal{F}'_{lm} = \mathcal{F}_{lm} \quad (\text{gauge invariant}) \tag{1.45c}$$

11 | This motivates the following definition:

✱✱ **Definition: Berry phase**

For $n = 1$, the exponent of the Berry holonomy is called ✱✱ *Berry phase*:

$$\gamma(\Gamma) = -\oint_{\Gamma} \mathcal{A} d\Gamma = i \oint_{\Gamma} \langle v(\Gamma) | \partial_{\Gamma_l} | v(\Gamma) \rangle d\Gamma_l \in \mathbb{R} \tag{1.46}$$

The nomenclature is sometimes a bit vague: $\gamma(\Gamma)$ and $e^{i\gamma(\Gamma)}$ are both called “Berry phase.”

- The Berry phase is a ✱✱ *geometric phase* – as compared to the usual \downarrow *dynamical phases* accumulated by wave functions in quantum mechanics. Remember that an eigenstate with energy E collects the phase $e^{-\frac{i}{\hbar} E \Delta t}$ in the time interval Δt due to the unitary evolution governed by the Schrödinger equation. Such phases are called *dynamical phases*. By contrast, the Berry phase is *not* a consequence of the energy of the system (recall that we set the ground state energy to zero for all parameters!); it is rather a *geometric property* of the parametric path Γ over the \uparrow *vector bundle* \mathcal{V} of ground state spaces.
- The Berry phase was first discussed by MICHAEL BERRY in 1984 [69].
- The Berry phase follows from the Berry connection. But where does the Berry connection “come from”? It seems that it is somehow hidden in the Hamiltonian family $H(\Gamma)$, but this can only be partially true as the latter only defines a projector onto its ground state manifold. This provides us with the Hilbert sub-bundle $\mathcal{V}(\Gamma)$ on which the Berry connection is defined. But a projection does not magically produce a connection. Actually, we start from the full Hilbert bundle (its fibers are the Hilbert spaces on which the Hamiltonians act) and (silently) assume that it is trivialized $\mathcal{M} \times \mathcal{H}_0$ with some reference Hilbert space \mathcal{H}_0 . A trivialized bundle has a natural connection, namely the trivial (or constant) connection. Starting from this connection, the ground state projection provided by a Hamiltonian then induces a connection on the sub-bundle $\mathcal{V}(\Gamma)$ – and this is the Berry connection. If there is no canonical (or physically motivated) trivialization of the full Hilbert bundle, the choice of the connection on this bundle leads to potentially distinct Berry connections and thereby distinct Berry phases; for details on this subtlety see Ref. [66].

12 | Examples of systems with non-trivial Berry phase:

- Spin- $\frac{1}{2}$ in a variable magnetic field (↻ Problemset 2 and \uparrow Ref. [69])
- Aharonov-Bohm effect (\uparrow [69])
- Foucault pendulum (\uparrow [70, 71])

The concept of parallel transport with non-trivial holonomies is not restricted to quantum mechanical systems!

13 | < Effect of gauge transformations on the Berry phase:

$$\gamma'(\Gamma) = -\oint_{\Gamma} \mathcal{A}' d\Gamma = -\oint_{\Gamma} (\mathcal{A} + \nabla_{\Gamma} \xi) d\Gamma = \gamma(\Gamma) - [\xi(\Gamma(T)) - \xi(\Gamma(0))] \quad (1.47)$$

Note that here $\xi(\Gamma(T))$ should be read as $\lim_{\epsilon \rightarrow 0} \xi(\Gamma(T - \epsilon))$ and $\xi(\Gamma(0))$ is shorthand for $\lim_{\epsilon \rightarrow 0} \xi(\Gamma(0 + \epsilon))$, which explains why Eq. (1.48) below makes sense even though $\Gamma(T) = \Gamma(0)$.

Continuity of the gauge transformation: $\Omega(\Gamma(0)) = \Omega(\Gamma(T)) \rightarrow$

Recall that Γ is a closed path: $\Gamma(T) = \Gamma(0)$. Note that continuity of the gauge transformation $e^{i\xi(\Gamma(0))} = \Omega(\Gamma(0)) = \Omega(\Gamma(T)) = e^{i\xi(\Gamma(T))}$ does not imply continuity of $\xi(\Gamma)$!

$$\text{Eq. (1.45b)} \Rightarrow \xi(\Gamma(T)) - \xi(\Gamma(0)) = 2\pi m \quad \text{for } m \in \mathbb{Z} \quad (1.48)$$

→ $\gamma(\Gamma)$ is gauge invariant up multiples of 2π

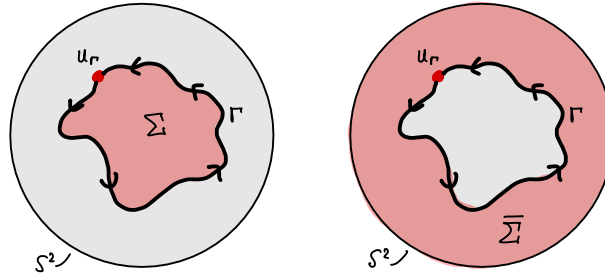
→ For $\gamma(\Gamma) \notin 2\pi\mathbb{Z}$, the Berry phase *cannot* be gauged away and can have physical consequences!

14 | < Special case k=2: $\Gamma = (\Gamma_1, \Gamma_2)$

This is the most important case for us because the parameter space we are interested in will be the 2D ↓ Brillouin zone (which is a torus).

→ Computation of the Berry phase for $k = 2$ on a compact manifold \mathcal{M} (sphere, torus):

- i | < Closed path Γ on sphere $\mathcal{M} = S^2$
- < Submanifolds with $\Sigma \cup \bar{\Sigma} = \mathcal{M}$ and $\partial\Sigma = \Gamma = \partial\bar{\Sigma}$:



! Important

In general it is *not* possible to choose a gauge that is continuous (= non-singular) everywhere on \mathcal{M} !

Hence we must be careful when integrating the Berry connection \mathcal{A} along paths on \mathcal{M} ! In the following, we assume that we *can* find continuous gauges for every simply connected, open submanifold of \mathcal{M} though:

- ii | < Continuous gauge \mathcal{A}_1 on $\Sigma \rightarrow$ Stokes' theorem valid on $\Sigma \rightarrow$

$$\oint_{\Gamma} \mathcal{A}_1 d\Gamma \stackrel{\text{Stokes}}{=} \int_{\Sigma} \mathcal{F}_{lm} d\sigma^{lm} \quad (1.49)$$

σ^{lm} is the differential area element (a 2-form that is antisymmetric in l and m , just as \mathcal{F}_{lm}).

For a reformulation in terms of differential forms see the comments → below.

iii | < Continuous gauge \mathcal{A}_2 on $\bar{\Sigma}$ → Stokes' theorem valid on $\bar{\Sigma}$ →

$$\oint_{\Gamma} \mathcal{A}_2 d\Gamma \stackrel{\text{Stokes}}{=} - \int_{\bar{\Sigma}} \mathcal{F}_{lm} d\sigma^{lm} \quad (1.50)$$

The sign is due to the opposite orientation of the boundary for $\bar{\Sigma}$.

iv | Using Eq. (1.48) \wedge Eq. (1.49) \wedge Eq. (1.50) →

$$\int_{\mathcal{M}} \mathcal{F}_{lm} d\sigma^{lm} = \underbrace{\oint_{\Gamma} \mathcal{A}_1 d\Gamma}_{\gamma(\Gamma)+2\pi m_1} - \underbrace{\oint_{\Gamma} \mathcal{A}_2 d\Gamma}_{\gamma(\Gamma)+2\pi m_2} = 2\pi m \quad \text{with } m \in \mathbb{Z} \quad (1.51)$$

Here we used that the closed loop integrals of the Berry connection are unique up to integer multiples of 2π .

15 | This motivates the following definition:

Definition: Chern number

For a compact, closed two-dimensional parameter space \mathcal{M} with Berry curvature \mathcal{F} , the **(first) Chern number** is an integer and defined as

$$C := \frac{1}{2\pi} \int_{\mathcal{M}} \mathcal{F}_{lm} d\sigma^{lm} \in \mathbb{Z} \quad (1.52)$$

This is our first example of a *topological invariant*.

- We will meet the Chern number again in Section 1.4 where we compute the Hall conductivity.
- $!$ Following the argument above, it is clear that whenever there exists a gauge that is non-singular on the *complete* parameter space, the Chern number is necessarily zero. [Because you can then choose $\mathcal{A}_1 = \mathcal{A}_2$ such that the difference in Eq. (1.51) vanishes.] Conversely, whenever the Chern number does *not* vanish, there must be singularities in all gauges! You will encounter an example of this in \odot Problemset 2.

16 | \ddagger Comments:

- Differential forms:

The proper way to formulate the application of Stokes' theorem is in terms of *differential forms*. In this framework

$$\mathcal{A} := \sum_{l=1}^k \mathcal{A}_l d\Gamma_l \quad (1.53)$$

is a *1-form* that can be integrated along paths:

$$\gamma(\Gamma) = - \oint_{\Gamma} \mathcal{A}. \quad (1.54)$$

The Berry curvature is then the *2-form* given by the *exterior derivative* of \mathcal{A} (this is only true for $n = 1$, i.e., abelian gauge fields):

$$\mathcal{F} := d\mathcal{A} = \sum_{1 \leq l, m \leq k} \underbrace{(\partial_m \mathcal{A}_l - \partial_l \mathcal{A}_m)}_{\mathcal{F}_{lm}} \underbrace{\frac{1}{2} d\Gamma_m \wedge d\Gamma_l}_{d\sigma^{lm}} = \mathcal{F}_{lm} d\sigma^{lm} \quad (1.55)$$

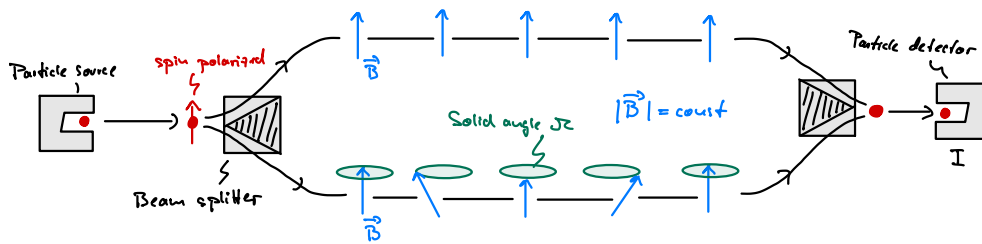
where the last expression is just a shorthand notation. (For *non-abelian* gauge fields it is $\mathcal{F} = d\mathcal{A} + \mathcal{A} \wedge \mathcal{A}$; note that \mathcal{A} is a 1-form with values in a non-abelian Lie algebra so that the wedge product does not vanish in general.)

Finally, Stoke's theorem for differential forms states that

$$\oint_{\Gamma=\partial\Sigma} \mathcal{A} = \int_{\Sigma} d\mathcal{A} = \int_{\Sigma} \mathcal{F}. \tag{1.56}$$

- Observation of the Berry phase:

◀ Spin-polarized particles on beam splitter in magnetic field with constant amplitude:

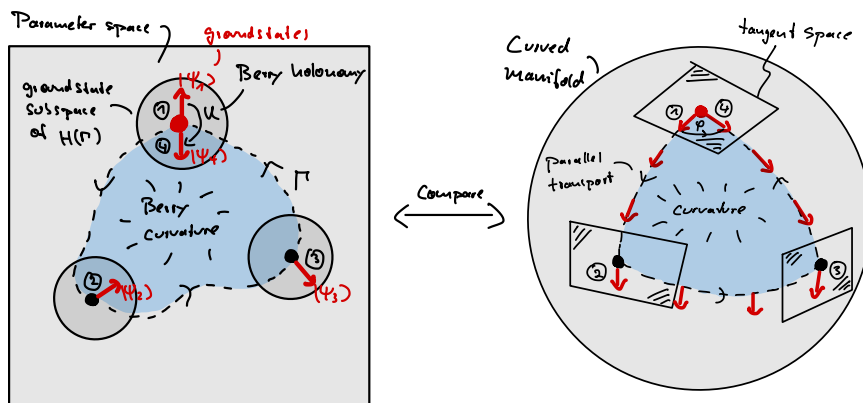


→ Interference pattern: $I = |1 + e^{i\gamma(\Gamma)}|^2$ where $e^{i\gamma(\Gamma)} = e^{i\Omega/2}$ with solid angle $0 \leq \Omega \leq 4\pi$. You will calculate the dependency of the Berry phase on the solid angle traced out by the magnetic field in → Problemset 2. This experiment was already proposed and studied by Berry in his original work [69].

To the best of my knowledge, there has been no experiment that implemented exactly Berry's proposal (due to experimental issues controlling additional dynamical phases). However, there have been multiple other experimental verifications of the Berry phase in quantum systems since its prediction in 1984 [72, 73]. (Note that the historically first reporting [74] was later disputed [75] because it can be explained classically, without invoking quantum mechanics.)

- Geometric interpretation of the Berry curvature:

In general, the parameter space can be multi-dimensional. For obvious reasons we only draw two of them:



The Berry holonomy can be compared to the rotation of a vector when carried (“parallel transported”) around a closed curve on a curved space (like the shown sphere). The analog to the ↓ *Riemann curvature* is the Berry curvature, the role of the ↓ *Levi-Civita connection* is played by the Berry connection. The Chern number equals the ↑ *Euler characteristic* of a compact 2D manifold, and the relation that gives the Chern number in terms of the

Berry curvature is then known as \uparrow *Gauss-Bonnet theorem* (more precisely: \uparrow *Chern-Gauss-Bonnet theorem*, a generalization of the classic Gauss-Bonnet theorem to even-dimensional Riemannian manifolds). This “real space analog” may be known from your lectures on \downarrow *general relativity*. Note that in general relativity one is interested in the \uparrow *tangent bundle* where a tangential space is attached to every point of the (spacetime) manifold. Here we are *not* interested in the tangent bundle of the parameter manifold but more general \uparrow *fiber bundles* where the local fibers are given by ground state spaces $\mathcal{V}(\Gamma)$ or Lie groups $U(n)$ that act on them.

1.4. Quantization of the Hall conductivity

With these new mathematical insights, we now return to the integer quantum Hall effect and its Hall plateaus. Our goal is to find a relation between the Hall conductivity and the Chern number. This remarkable relation between a *physical quantity* and a *topological invariant* is one of the most important insights in contemporary condensed matter physics and explains the quantization of the Hall conductivity.

The following discussion is based on David Tong’s lecture notes on the quantum Hall effect [64]. For a more detailed (and much more technical) discussion, see Chapter 3 of Bernevig’s textbook [1]; another account can be found in Chapter 12 of Fradkin’s textbook [63]. You might also want to have a look at the original manuscript by Thouless *et al.* [17] and the follow-up [76].

1.4.1. The Kubo formula

As a preparation, we compute the linear response of a quantum mechanical system at $T = 0$ for a time-dependent, external perturbation. Here we focus on the special case where the perturbation is a time-dependent electric field and the response is a current of charged particles. The approach is generic and valid for general (in particular: interacting) Hamiltonians. The resulting \rightarrow *Kubo formula* has many applications beyond computing the quantized Hall conductivity.

- 1 | \leftarrow Unperturbed Hamiltonian H_0 with Eigenstates $|m\rangle$ and Eigenenergies E_m
 \leftarrow Time-dependent perturbation $\Delta H(t)$
 $\rightarrow H(t) = H_0 + \Delta H(t)$ (Schrödinger picture!)
- 2 | It is convenient to absorb the unperturbed time evolution into operators:
 $\rightarrow \downarrow$ *Interaction picture*:

$$\Delta H_I(t) := U_0^\dagger(t) \Delta H(t) U_0(t) \quad \text{and} \quad |\Psi(t)\rangle_I := U(t, t_0) |\Psi(t_0)\rangle_I \quad (1.57)$$

with unperturbed time evolution operator $U_0(t) := e^{-\frac{i}{\hbar} H_0 t}$ and

$$U(t, t_0) := \mathcal{T} \exp \left[-\frac{i}{\hbar} \int_{t_0}^t \Delta H_I(t') dt' \right] \quad (1.58)$$

Here \mathcal{T} denotes the time-ordered exponential. It is easy to check that the states $|\Psi(t)\rangle_I$ satisfy the Schrödinger equation in the interaction picture:

$$i\hbar \frac{d}{dt} |\Psi(t)\rangle_I = \Delta H_I(t) |\Psi(t)\rangle_I. \quad (1.59)$$

To show the unitary equivalence between the interaction picture and the conventional Schrödinger picture, you must show that $U(t, t_0) \doteq U_0^\dagger(t - t_0)U_S(t, t_0)$ with the full Schrödinger evolution

$$U_S(t, t_0) := \mathcal{T} \exp \left[-\frac{i}{\hbar} \int_{t_0}^t H(t') dt' \right]. \quad (1.60)$$

- 3 | Prepare system for $t_0 \rightarrow -\infty$ in ground state $|0\rangle$ of H_0 (or some other eigenstate)
- 4 | \triangleleft Expectation value of arbitrary (interaction picture) operator $\mathcal{O}_I(t) = U_0^\dagger \mathcal{O} U_0$:

$$\langle \mathcal{O}(t) \rangle = \underbrace{\langle 0 | U_S^\dagger(t, -\infty) \mathcal{O} U_S(t, -\infty) | 0 \rangle}_{\text{Schrödinger picture}} \quad (1.61a)$$

$$= \underbrace{\langle 0 | U^\dagger(t, -\infty) \mathcal{O}_I(t) U(t, -\infty) | 0 \rangle}_{\text{Interaction picture}} \quad (1.61b)$$

$$\stackrel{1.58}{\approx} \langle 0 | \left\{ \mathcal{O}_I(t) + \frac{i}{\hbar} \int_{-\infty}^t [\Delta H_I(t'), \mathcal{O}_I(t)] dt' \right\} | 0 \rangle \quad (1.61c)$$

This linearization is the core of *linear response* theory.

Note that time ordering is not important in linear order (only one time integral!).

→

**** Kubo formula:**

$$\delta \langle \mathcal{O}(t) \rangle \equiv \langle \mathcal{O}(t) \rangle - \langle \mathcal{O} \rangle = \frac{i}{\hbar} \int_{-\infty}^t \langle 0 | [\Delta H_I(t'), \mathcal{O}_I(t)] | 0 \rangle dt' \quad (1.62)$$

- This is the linear response of the system to the perturbation $\Delta H(t)$. Note that $\langle \mathcal{O} \rangle = \langle 0 | \mathcal{O} | 0 \rangle = \langle 0 | \mathcal{O}_I(t) | 0 \rangle$ is not a dynamic response but the static expectation value of \mathcal{O} in the initial state (remember that $|0\rangle$ is a eigenstate of H_0). In the following, we will set it to zero.
- The Kubo formula was first presented by RYOGO KUBO in 1957 [77].

↓ Lecture 6 [02.05.25]

5 | < Special case: Coupling to uniform electric field $E(t) = E e^{-i\omega t}$

i | Choose gauge such that $E(t) = -\partial_t A(t)$ (i.e. $A_t = \phi = \text{const}$)

Remember that in general $E = -\nabla\phi - \partial_t A$ and $B = \nabla \times A$.

$$\rightarrow A(t) = E e^{-i\omega t} / (i\omega)$$

ii | < Perturbation Hamiltonian:

$$\Delta H_I(t) = -\mathbf{J}(t) \cdot \mathbf{A}(t) \tag{1.63}$$

with (total) current operator $\mathbf{J}(t)$

- At this point we do not want to fix the unperturbed Hamiltonian H_0 that describes the charge carriers without the field. Hence we do not know the form of $\mathbf{J}(t)$ in the interaction picture. We therefore play it safe and carry a potential time-dependence along.
- This is a linearized version of the true coupling Hamiltonian that describes the effect of the electromagnetic field on electrical charges. For instance, a free particle with charge q (and with $\phi = \text{const} = 0$) is described by the Hamiltonian

$$H = \frac{1}{2m} (\mathbf{p} - q\mathbf{A})^2 = \underbrace{\frac{\mathbf{p}^2}{2m}}_{\sim H_0} - \underbrace{\frac{q\mathbf{p}}{m} \cdot \mathbf{A}}_{\sim \Delta H(t)} + \mathcal{O}(A^2). \tag{1.64}$$

There is also a quadratic term A^2 which does not contribute to the Hall conductance (so we can safely drop it).

- In terms of the ↓ current density $\mathbf{j}(\mathbf{r}, t)$ the Hamiltonian reads

$$\Delta H_I(t) = - \int d^2r \mathbf{j}(\mathbf{r}, t) \cdot \mathbf{A}(\mathbf{r}, t) \tag{1.65}$$

with the usual current density $\mathbf{j} = \frac{q}{2m} \sum_i [p_i \delta(\mathbf{r} - \mathbf{r}_i) + \delta(\mathbf{r} - \mathbf{r}_i) p_i]$ for many particles indexed by i . With a homogeneous electric field, this becomes

$$\Delta H_I(t) = -\mathbf{J}(t) \cdot \mathbf{A}(t) \quad \text{with total current} \quad \mathbf{J}(t) = \int d^2r \mathbf{j}(\mathbf{r}, t). \tag{1.66}$$

For a homogeneous current, the total current is $\mathbf{J} = L_x L_y \mathbf{j} = A \mathbf{j}$ where $A = L_x L_y$ denotes the area of the sample.

iii | < Current as observable: $\mathcal{O} = J_i \rightarrow$

(Remember that we set the static expectation value to zero: $\langle 0 | J_i | 0 \rangle = 0$.)

$$\langle J_i(t) \rangle \stackrel{1.62}{=} -\frac{1}{\hbar\omega} \int_{-\infty}^t \langle 0 | [J_j(t'), J_i(t)] | 0 \rangle E_j e^{-i\omega t'} dt' \tag{1.67a}$$

Time-translation invariance of H_0 ; Substitution $t'' = t - t'$

$$\stackrel{\circ}{=} \underbrace{\left\{ -\frac{1}{\hbar\omega} \int_0^\infty \langle 0 | [J_j(0), J_i(t'')] | 0 \rangle e^{i\omega t''} dt'' \right\}}_{=: \sigma_{ij}(\omega) A} E_j e^{-i\omega t} \tag{1.67b}$$

with $\ast\ast$ conductivity tensor $\sigma_{ij}(\omega)$

The sample area $A = L_x L_y$ shows up because the conductivity tensor relates, by definition, the current density j_i to the electric field, and not the total current $J_i = A j_i$.

To show the second equality, use that $J_j(t') = e^{\frac{i}{\hbar} H_0 t'} J_j e^{-\frac{i}{\hbar} H_0 t'}$ [and similar for $J_i(t)$] and that $|0\rangle$ is an eigenstate of H_0 .

iv | → Hall conductivity:

$$\sigma_{xy}(\omega) = -\frac{1}{\hbar\omega A} \int_0^\infty \langle 0 | [J_y(0), J_x(t)] | 0 \rangle e^{i\omega t} dt \quad (1.68)$$

This is the *AC Hall conductivity* as it is still frequency dependent.

v | Set $t_0 = 0$ and use $U_0(t) = \sum_n e^{-iE_n t/\hbar} |n\rangle\langle n|$ and $J_i(t) = U_0^\dagger(t) J_i U_0(t)$:

→

$$\sigma_{xy}(\omega) = -\frac{1}{\hbar\omega A} \int_0^\infty \sum_n \left\{ \begin{array}{l} \langle 0 | J_y | n \rangle \langle n | J_x | 0 \rangle e^{i(E_n - E_0)t/\hbar} \\ - \langle 0 | J_x | n \rangle \langle n | J_y | 0 \rangle e^{i(E_0 - E_n)t/\hbar} \end{array} \right\} e^{i\omega t} dt \quad (1.69a)$$

Integrate (using a regularization $\omega + i\varepsilon$ to make the integral convergent)

$$= -\frac{i}{\omega A} \sum_{n \neq 0} \left\{ \frac{\langle 0 | J_y | n \rangle \langle n | J_x | 0 \rangle}{\hbar\omega + E_n - E_0} - \frac{\langle 0 | J_x | n \rangle \langle n | J_y | 0 \rangle}{\hbar\omega + E_0 - E_n} \right\} \quad (1.69b)$$

vi | Take DC limit $\omega \rightarrow 0$ and use $\frac{1}{\hbar\omega + E_n - E_0} = \frac{1}{E_n - E_0} - \frac{\hbar\omega}{(E_n - E_0)^2} + \mathcal{O}(\omega^2)$:

(Note the i/ω that must be canceled to render the expression finite!)

$$\sigma_{xy} \stackrel{\circ}{=} \frac{i\hbar}{A} \sum_{n \neq 0} \frac{\langle 0 | J_y | n \rangle \langle n | J_x | 0 \rangle - \langle 0 | J_x | n \rangle \langle n | J_y | 0 \rangle}{(E_n - E_0)^2} \quad (1.70)$$

This is the Hall conductivity expressed in terms of current matrix elements. Our \rightarrow next project will be a (quite tedious) reformulation of this expansion with the goal to re-express it in terms of a topological invariant, namely the \leftarrow Chern number.

vii | Comment on the constant term:

For the derivation of Eq. (1.70) it is crucial that

$$\sum_{n \neq 0} \frac{\langle 0 | J_y | n \rangle \langle n | J_x | 0 \rangle + \langle 0 | J_x | n \rangle \langle n | J_y | 0 \rangle}{E_n - E_0} = 0 \quad (1.71)$$

which makes the constant terms of the Taylor expansion cancel (this avoids the divergence for $\omega \rightarrow 0!$).

One way to see this is from *rotation invariance* of the system in the x - y -plane (a quantum Hall system should be rotation invariant about the axis of the magnetic field). In particular, σ_{xy} should be invariant under the $\pi/2$ -rotation $J_x \mapsto J_y$ and $J_y \mapsto -J_x$ (note that \mathbf{J} is a vector operator). This means that

$$\sum_{n \neq 0} \frac{\langle 0 | J_y | n \rangle \langle n | J_x | 0 \rangle + \langle 0 | J_x | n \rangle \langle n | J_y | 0 \rangle}{E_n - E_0} \stackrel{!}{=} - \sum_{n \neq 0} \frac{\langle 0 | J_x | n \rangle \langle n | J_y | 0 \rangle + \langle 0 | J_y | n \rangle \langle n | J_x | 0 \rangle}{E_n - E_0} \quad (1.72)$$

which implies Eq. (1.71) so that only the *antisymmetric* part of σ_{xy} survives.

Note that this is a quite general argument: If we decompose the 2D conductivity tensor into symmetric and antisymmetric parts, $\sigma = \sigma_s + \sigma_a$, and demand rotational invariance of the tensor, i.e., $\sigma = R\sigma R^T$ for a 2D rotation matrix R , we have $\sigma_s = R\sigma_s R^T$ and $\sigma_a = R\sigma_a R^T$ separately. The only *symmetric* matrix invariant under rotations is proportional to the identity, $\sigma_s = \sigma_{xx} \cdot \mathbb{1}$, so that there cannot be a symmetric contribution to the off-diagonals (that is, the Hall conductivity σ_{xy}). Thus the most general form of a *rotation invariant* conductivity tensor is

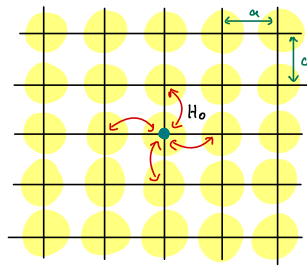
$$\sigma = \begin{pmatrix} \sigma_{xx} & \sigma_{xy} \\ -\sigma_{xy} & \sigma_{xx} \end{pmatrix}. \quad (1.73)$$

1.4.2. The TKNN invariant

Here we want to connect the Hall conductivity [given by the Kubo formula Eq. (1.70)] to the Chern number and thereby explain the quantization of the former. To do so, we consider non-interacting electrons in a two-dimensional periodic potential, so that the momentum space is a torus.

The rationale of the following discussion is similar to the original approach by Thouless *et al.* [17].

- 1 | ◁ Single electron in a periodic potential with Hamiltonian H_0 :



System size: $L_x \times L_y$ & periodic boundaries

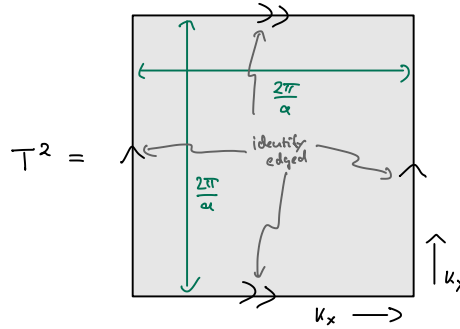
We take the thermodynamic limit $L_x, L_y \rightarrow \infty$ later.

- 2 | ↓ *Bloch theorem*:

- Eigenfunctions: $\Psi_{n\mathbf{k}} = e^{i\mathbf{k}\mathbf{x}} u_{n\mathbf{k}}(\mathbf{x})$
with $u_{n\mathbf{k}}(\mathbf{x} + \mathbf{R}) = u_{n\mathbf{k}}(\mathbf{x})$ for lattice vectors \mathbf{R} and band index $n = 1, 2, \dots$
- Eigenenergies $\varepsilon_n(\mathbf{k})$ continuous in $\mathbf{k} \rightarrow$ “Bands”
- $\Psi_{n\mathbf{k}+\mathbf{K}} = \Psi_{n\mathbf{k}}$ for reciprocal lattice vectors \mathbf{K}

If $\mathbf{R} = a n_x \mathbf{e}_x + a n_y \mathbf{e}_y$ describes a square lattice with lattice constant a , the reciprocal lattice is $\mathbf{K} = m_1 \mathbf{k}_1 + m_2 \mathbf{k}_2$ with $\mathbf{k}_i = \frac{2\pi}{a} \mathbf{e}_i$.

→ Brillouin zone = Torus T^2



Since our system is finite, momenta are discrete. The size of the Brillouin zone is determined by the inverse lattice constant and remains fixed in the following.

3 | < Many-body Fock states with Fermi energy E_F :

! While we can understand the integer quantum Hall effect within the framework of non-interacting fermions, the quantization of the Hall conductivity is a genuine quantum many-body phenomenon. It is crucial that you understand the difference (and relation) between these concepts.

Ground state = $|0\rangle \mapsto |\mathbf{0}\rangle =$ Filled Fermi sea (1.74a)

Excited states = $|n\rangle \mapsto |\mathbf{n}\rangle =$ Fermi sea with particle-hole excitations (1.74b)

Current operator = $J_i \mapsto \mathfrak{J}_i =$ Second-quantized current operator (1.74c)

In the following, **bold states** live in the fermionic Fock space (= many-body states), whereas states in normal font live in the single-particle Hilbert space.

4 | Eq. (1.70) → Hall conductivity of fermionic many-body system:

$$\sigma_{xy} \stackrel{e}{=} \frac{i\hbar}{A} \sum_{\mathbf{n} \neq \mathbf{0}} \frac{\langle \mathbf{0} | \mathfrak{J}_y | \mathbf{n} \rangle \langle \mathbf{n} | \mathfrak{J}_x | \mathbf{0} \rangle - \langle \mathbf{0} | \mathfrak{J}_x | \mathbf{n} \rangle \langle \mathbf{n} | \mathfrak{J}_y | \mathbf{0} \rangle}{(E_{\mathbf{n}} - E_{\mathbf{0}})^2} \quad (1.75)$$

Note that the sum goes over all possible excited many-body states (which are all states except the Fermi sea ground state). However, below we will see that only states with a single particle-hole excitation contribute.

5 | Current operator = Single-particle operator:

$$\mathfrak{J}_i = \sum_{\mathbf{n}\mathbf{k}, \mathbf{m}\mathbf{q}} \langle \Psi_{\mathbf{n}\mathbf{k}} | J_i | \Psi_{\mathbf{m}\mathbf{q}} \rangle c_{\mathbf{n}\mathbf{k}}^\dagger c_{\mathbf{m}\mathbf{q}} \quad (1.76)$$

$c_{\mathbf{n}\mathbf{k}}^\dagger$: Creation operator for fermion in Bloch state $|\Psi_{\mathbf{n}\mathbf{k}}\rangle$

Remember that this recipe produces an operator on Fock space that acts like the single-particle operator J_i within the one-fermion subspace.

6 | Eq. (1.75) → [Here nk' is short for $(nk)' = n'k'$.]

$$\sum_{n \neq 0} \frac{\langle 0 | \mathfrak{J}_y | n \rangle \langle n | \mathfrak{J}_x | 0 \rangle}{(E_n - E_0)^2} = \sum_{nk', mq'} \sum_{nk, mq} \langle \Psi_{nk} | J_y | \Psi_{mq} \rangle \langle \Psi_{nk'} | J_x | \Psi_{mq'} \rangle \quad (1.77)$$

$$\underbrace{\sum_{n \neq 0} \frac{\langle 0 | c_{nk}^\dagger c_{mq} | n \rangle \langle n | c_{nk'}^\dagger c_{mq'} | 0 \rangle}{(E_n - E_0)^2}}_{\substack{\delta_{nk=mq'} \delta_{mq=nk'} \delta_{\varepsilon_m(\mathbf{q}) > E_F} \delta_{\varepsilon_n(\mathbf{k}) < E_F} \\ [\varepsilon_m(\mathbf{q}) - \varepsilon_n(\mathbf{k})]^2}} \stackrel{=}{=} \sum_{\substack{nk, mq \\ \varepsilon_n(\mathbf{k}) < E_F < \varepsilon_m(\mathbf{q})}} \frac{\langle \Psi_{nk} | J_y | \Psi_{mq} \rangle \langle \Psi_{mq} | J_x | \Psi_{nk} \rangle}{[\varepsilon_m(\mathbf{q}) - \varepsilon_n(\mathbf{k})]^2} \quad (1.78)$$

To evaluate the sum $\sum_{n \neq 0}$ over all excited many-body states, convince yourself that you can *w.l.o.g.* replace the denominator by $[\varepsilon_m(\mathbf{q}) - \varepsilon_n(\mathbf{k})]^2$ (which is independent of $n!$). Then $\sum_{n \neq 0} |n\rangle \langle n|$ can be written as $\mathbb{1} - |0\rangle \langle 0|$ and the rest follows.

7 | Assume $\varepsilon_n(\mathbf{k}) \leq E_F$ for all $\mathbf{k} \in T^2$

! This means that the Fermi energy falls into a *band gap*. This is absolutely crucial for what follows. (Note that statements like “ $\varepsilon_n < E_F$ ” are now well-defined since $\varepsilon_n(\mathbf{k}) < E_F$ is true for all momenta and only depends on the band index n .)

→

$$\sigma_{xy} \stackrel{=}{=} \frac{i\hbar}{A} \sum_{\substack{n, m \\ \varepsilon_n < E_F < \varepsilon_m}} \sum_{\mathbf{k}, \mathbf{q} \in T^2} \frac{\begin{cases} \langle \Psi_{n\mathbf{k}} | J_y | \Psi_{m\mathbf{q}} \rangle \langle \Psi_{m\mathbf{q}} | J_x | \Psi_{n\mathbf{k}} \rangle \\ - \langle \Psi_{n\mathbf{k}} | J_x | \Psi_{m\mathbf{q}} \rangle \langle \Psi_{m\mathbf{q}} | J_y | \Psi_{n\mathbf{k}} \rangle \end{cases}}{[\varepsilon_m(\mathbf{q}) - \varepsilon_n(\mathbf{k})]^2} \quad (1.79)$$

8 | As a first simplification, we want to get rid of one of the two momentum summations. To do so, we must show that the current operator cannot change the momentum of a state:

i | Define the single-particle current operator

$$\mathbf{J} := e \frac{i}{\hbar} [H_0, \mathbf{x}] \quad (1.80)$$

This definition is motivated as follows: Physically, a sensible *single particle* current operator must satisfy $\langle \mathbf{J} \rangle = e \frac{d\langle \mathbf{x} \rangle}{dt} = \text{Charge} \times \text{Velocity}$. The \downarrow *Ehrenfest theorem* tells us that $\frac{d\langle \mathbf{x} \rangle}{dt} = \frac{i}{\hbar} \langle [H_0, \mathbf{x}] \rangle$ which immediately suggests the definition (1.80). You can easily check that for a free particle, $H_0 = \frac{p^2}{2m}$, it is $\mathbf{J} = e \frac{p}{m}$ (as it should be).

ii | \leftarrow Translation operator $T_{\mathbf{R}}$ with lattice vector \mathbf{R} :

$$T_{\mathbf{R}} \mathbf{x} T_{\mathbf{R}}^{-1} = \mathbf{x} + \mathbf{R} \quad (1.81a)$$

$$T_{\mathbf{R}} H_0 T_{\mathbf{R}}^{-1} = H_0 \quad (1.81b)$$

$$T_{\mathbf{R}} |\Psi_{n\mathbf{k}}\rangle = e^{i\mathbf{k}\mathbf{R}} |\Psi_{n\mathbf{k}}\rangle \quad (1.81c)$$

- The first equation follows from the definition of the translation operator.
- The commutativity with the Hamiltonian follows from our assumption that the system features a discrete translation invariance (“periodic potential”).

- The energy eigenstates of such a Hamiltonian are Bloch states $|\Psi_{nk}\rangle$ which are also eigenstates of these lattice translations (this is just the statement of ← *Bloch's theorem*).

iii | Consequently

$$T_{\mathbf{R}} \mathbf{J} T_{\mathbf{R}}^{-1} = i \frac{e}{\hbar} [H_0, \mathbf{x} + \mathbf{R}] = i \frac{e}{\hbar} [H_0, \mathbf{x}] = \mathbf{J} \quad (1.82)$$

→ \mathbf{J} cannot change lattice momenta

Formally: $\langle \Psi_{nk} | J_i | \Psi_{mq} \rangle = \langle \Psi_{nk} | J_i | \Psi_{mk} \rangle \delta_{k,q}$

iv | Thus Eq. (1.79) →

$$\sigma_{xy} \stackrel{\circ}{=} \frac{i\hbar}{A} \sum_{\substack{n,m \\ \varepsilon_n < E_F < \varepsilon_m}} \sum_{\mathbf{k} \in T^2} \frac{\begin{cases} \langle \Psi_{nk} | J_y | \Psi_{mk} \rangle \langle \Psi_{mk} | J_x | \Psi_{nk} \rangle \\ - \langle \Psi_{nk} | J_x | \Psi_{mk} \rangle \langle \Psi_{mk} | J_y | \Psi_{nk} \rangle \end{cases}}{[\varepsilon_m(\mathbf{k}) - \varepsilon_n(\mathbf{k})]^2} \quad (1.83)$$

9 | ← Thermodynamic limit (in real space): $L_i \rightarrow \infty$

⇔ Continuum limit (in momentum space): $\Delta k_i \equiv \frac{2\pi}{L_i} \rightarrow 0$

→ The sum over momenta turns into an integral over the Brillouin zone T^2 :

$$\sigma_{xy} \stackrel{\circ}{=} i\hbar \sum_{\substack{n,m \\ \varepsilon_n < E_F < \varepsilon_m}} \int_{T^2} \frac{d^2k}{(2\pi)^2} \frac{\begin{cases} \langle \Psi_{nk} | J_y | \Psi_{mk} \rangle \langle \Psi_{mk} | J_x | \Psi_{nk} \rangle \\ - \langle \Psi_{nk} | J_x | \Psi_{mk} \rangle \langle \Psi_{mk} | J_y | \Psi_{nk} \rangle \end{cases}}{[\varepsilon_m(\mathbf{k}) - \varepsilon_n(\mathbf{k})]^2} \quad (1.84)$$

- The continuum limit is convenient because we can now use tools from calculus to simplify this expression further.
- Here we used the usual approximation of a Riemann sum:

$$\frac{1}{L_i} \sum_{k_i} = \frac{1}{2\pi} \sum_{k_i} \frac{2\pi}{L_i} \xrightarrow{L_i \rightarrow \infty} \int \frac{dk_i}{2\pi} \quad (1.85)$$

Remember that $A = L_x L_y$.

10 | Our next goal is to get rid of the current operators:

i | Use $|\Psi_{nk}\rangle = e^{i\mathbf{k}\mathbf{x}} |u_{nk}\rangle$ (← *Bloch theorem*) and define $\tilde{\mathbf{J}}(\mathbf{k}) := e^{-i\mathbf{k}\mathbf{x}} \mathbf{J} e^{i\mathbf{k}\mathbf{x}}$ so that

$$\langle \Psi_{nk} | J_i | \Psi_{mk} \rangle = \langle u_{nk} | \tilde{J}_i(\mathbf{k}) | u_{mk} \rangle \quad (1.86)$$

;! Note that in $e^{i\mathbf{k}\mathbf{x}}$, \mathbf{x} is the position operator.

ii | Define $\tilde{H}_0(\mathbf{k}) := e^{-i\mathbf{k}\mathbf{x}} H_0 e^{i\mathbf{k}\mathbf{x}}$ so that

$$H_0 |\Psi_{nk}\rangle = \varepsilon_n(\mathbf{k}) |\Psi_{nk}\rangle \Leftrightarrow \tilde{H}_0(\mathbf{k}) |u_{nk}\rangle = \varepsilon_n(\mathbf{k}) |u_{nk}\rangle \quad (1.87)$$

iii | With these preliminaries, we can write:

$$\tilde{J}_i \stackrel{\circ}{=} \frac{e}{\hbar} \tilde{\partial}_i \tilde{H}_0 \quad \text{with} \quad \tilde{\partial}_i := \frac{\partial}{\partial k_i} \quad (1.88)$$

To show this use the definition of $\tilde{H}_0(\mathbf{k})$ and show that $\tilde{\partial}_i \tilde{H}_0 = i[\tilde{H}_0, x]$.

iv | Eqs. (1.84), (1.86) and (1.88) →

$$\sigma_{xy} \doteq i \frac{e^2}{\hbar} \sum_{\substack{n,m \\ \varepsilon_n < E_F < \varepsilon_m}} \int_{T^2} \frac{d^2k}{(2\pi)^2} \left\{ \frac{\langle u_{nk} | \tilde{\partial}_y \tilde{H}_0 | u_{mk} \rangle \langle u_{mk} | \tilde{\partial}_x \tilde{H}_0 | u_{nk} \rangle}{[\varepsilon_m(\mathbf{k}) - \varepsilon_n(\mathbf{k})]^2} \right\} \quad (1.89)$$

11 | Use

$$\langle u_{nk} | \tilde{\partial}_y \tilde{H}_0 | u_{mk} \rangle = \langle u_{nk} | \tilde{\partial}_y (\tilde{H}_0 | u_{mk} \rangle) - \langle u_{nk} | \tilde{H}_0 | \tilde{\partial}_y u_{mk} \rangle \quad (1.90a)$$

$$= [\varepsilon_m(\mathbf{k}) - \varepsilon_n(\mathbf{k})] \langle u_{nk} | \tilde{\partial}_y u_{mk} \rangle \quad (1.90b)$$

$$= [\varepsilon_n(\mathbf{k}) - \varepsilon_m(\mathbf{k})] \langle \tilde{\partial}_y u_{nk} | u_{mk} \rangle \quad (1.90c)$$

The first line is just the product rule, in the second line we used that $\tilde{H}_0 = \tilde{H}_0^\dagger$ and that $\langle u_{nk} | u_{mk} \rangle = 0$ for $n \neq m$ (which is the case in our expression for the Hall conductivity). The last line follows if in the first line the derivative acts on the bra to the left instead on the ket to the right.

→

$$\sigma_{xy} \doteq i \frac{e^2}{\hbar} \sum_{\substack{n,m \\ \varepsilon_n < E_F < \varepsilon_m}} \int_{T^2} \frac{d^2k}{(2\pi)^2} \left\{ \begin{aligned} &\langle \tilde{\partial}_y u_{nk} | u_{mk} \rangle \langle u_{mk} | \tilde{\partial}_x u_{nk} \rangle \\ &- \langle \tilde{\partial}_x u_{nk} | u_{mk} \rangle \langle u_{mk} | \tilde{\partial}_y u_{nk} \rangle \end{aligned} \right\} \quad (1.91)$$

Yay! The denominator is gone ... ☺

12 | Use

$$\sum_m |u_{mk}\rangle \langle u_{mk}| = \mathbb{1} \quad (1.92a)$$

$$\Rightarrow \sum_{m:\varepsilon_m > E_F} |u_{mk}\rangle \langle u_{mk}| = \mathbb{1} - \sum_{m:\varepsilon_m < E_F} |u_{mk}\rangle \langle u_{mk}| \quad (1.92b)$$

These statements are true on the subspace spanned by the Bloch functions $|u_{nk}\rangle$ for fixed \mathbf{k} .

More rigorously, one should replace $\mathbb{1}$ by the projector $P_{\mathbf{k}}$ onto states with lattice momentum \mathbf{k} and do the derivatives in the expression for σ_{xy} properly; the result will be the same, though.

→

$$\sigma_{xy} \doteq i \frac{e^2}{\hbar} \sum_{n:\varepsilon_n < E_F} \int_{T^2} \frac{d^2k}{(2\pi)^2} \left\{ \langle \tilde{\partial}_y u_{nk} | \tilde{\partial}_x u_{nk} \rangle - \langle \tilde{\partial}_x u_{nk} | \tilde{\partial}_y u_{nk} \rangle \right\} \quad (1.93)$$

Only the term with $\mathbb{1}$ survives. The second term vanishes as it replaces the sum over empty bands by a sum over filled bands. But then the sum in the expression for the Hall conductance vanishes identically if one shifts the derivatives to the states with $m\mathbf{k}$ in the first term [using Eq. (1.90)] and substitutes $n \leftrightarrow m$ in the sums (the last step only works because m and n now run over the same range of filled bands).

↓ Lecture 7 [08.05.25]

13 | Finally, we can relate our findings to the geometrical quantities introduced in Section 1.3:

i | Define the Berry connection of band n :

$$\mathcal{A}_i^{[n]}(\mathbf{k}) := -i \langle u_{n\mathbf{k}} | \tilde{\partial}_i u_{n\mathbf{k}} \rangle \quad (1.94)$$

This is a U(1) connection on the Brillouin zone which is the compact 2D manifold T^2 . The parameters are the momenta ($\Gamma = \mathbf{k}$) and the local Hilbert spaces are one dimensional: $\mathcal{V}^{[n]}(\mathbf{k}) = \text{span} \{ |u_{n\mathbf{k}}\rangle \}$; these are the non-degenerate eigenspaces (no band crossings!) of the Hamiltonian family $\tilde{H}_0(\mathbf{k})$ with discrete spectrum $\varepsilon_n(\mathbf{k})$ (fix \mathbf{k} as a parameter!). Thus $n = 1$ and $k = 2$ in the context of our general discussion in Section 1.3; in the present context, n denotes the band index.

ii | → Berry curvature of band n :

$$\begin{aligned} \mathcal{F}_{ij}^{[n]}(\mathbf{k}) &= \tilde{\partial}_j \mathcal{A}_i^{[n]} - \tilde{\partial}_i \mathcal{A}_j^{[n]} \\ &= -i \langle \tilde{\partial}_j u_{n\mathbf{k}} | \tilde{\partial}_i u_{n\mathbf{k}} \rangle + i \langle \tilde{\partial}_i u_{n\mathbf{k}} | \tilde{\partial}_j u_{n\mathbf{k}} \rangle \end{aligned} \quad (1.95)$$

The cross terms cancel.

iii | → Chern number of band n :

$$\begin{aligned} C^{[n]} &= \frac{1}{2\pi} \int_{T^2} \mathcal{F}_{ij} d\sigma^{ij} = -\frac{1}{2\pi} \int_{T^2} \mathcal{F}_{xy} d^2k \\ &= \frac{i}{2\pi} \int_{T^2} \left\{ \langle \tilde{\partial}_y u_{n\mathbf{k}} | \tilde{\partial}_x u_{n\mathbf{k}} \rangle - \langle \tilde{\partial}_x u_{n\mathbf{k}} | \tilde{\partial}_y u_{n\mathbf{k}} \rangle \right\} d^2k \end{aligned} \quad (1.96)$$

The integral is best evaluated with differential forms where $\mathcal{F} = d\mathcal{A}$ is a 2-form and $\mathcal{A} = A_x dk_x + A_y dk_y$ is a 1-form. Then

$$C = \frac{1}{2\pi} \int_{T^2} \mathcal{F} = \frac{1}{2\pi} \int_{T^2} \left(\tilde{\partial}_y A_x dk_y \wedge dk_x + \tilde{\partial}_x A_y dk_x \wedge dk_y \right) \quad (1.97a)$$

$$= -\frac{1}{2\pi} \int_{T^2} \underbrace{\left(\tilde{\partial}_y A_x - \tilde{\partial}_x A_y \right)}_{\mathcal{F}_{xy}} \underbrace{dk_x \wedge dk_y}_{d^2k} \quad (1.97b)$$

where we used $dk_i \wedge dk_j = -dk_j \wedge dk_i$.

14 | Compare Eq. (1.93) with Eq. (1.96) →

! Important: TKNN formula

$$\sigma_{xy} = \frac{e^2}{2\pi\hbar} \sum_{n:\varepsilon_n < E_F} C^{[n]} = \frac{e^2}{h} \nu \quad \text{with} \quad \nu := \sum_{n:\varepsilon_n < E_F} C^{[n]} \in \mathbb{Z} \quad (1.98)$$

- In summary: The Hall conductivity of a system with non-degenerate bands that are either completely filled or completely empty is an integer multiple ν of $e^2/2\pi\hbar = e^2/h$, where ν is the sum of the Chern numbers of the filled bands. This quantization is robust and independent of microscopic details because the Chern numbers are topological invariants that are necessarily integer, as long as they are well-defined (= no gaps close).
- ¡! If the Fermi energy lies *within* a (then partially filled) band, our proof of the quantization of the Hall conductivity breaks down (where?). In this situation, we cannot make any statements about the value of σ_{xy} .
- ¡! You might wonder: Where is the magnetic field? In our derivation of the TKNN formula we didn't use it. But in experiments, the quantized Hall plateaus arise when tuning the magnetic flux through the sample. The answer is that the quantization of the Hall conductivity itself has nothing to do with a magnetic field. The statement is very clear: Whenever the Fermi energy lies within a gap, the Hall conductivity is quantized and given by the sum of Chern numbers of the filled bands. Note that our result is perfectly consistent with these Chern numbers (and thereby the Hall conductivity) being *zero*! In that sense we didn't prove the exact "staircase" shape of the Hall resistance observed in 2DEGs penetrated by a magnetic field. We only showed that *if* the Hall conductivity happens to be non-zero, then it must come in steps. The role of the magnetic field is twofold: First, it opens gaps $\hbar\omega_B$ between the Landau levels, so that the conditions for a quantization of σ_{xy} are met (namely when all Landau levels are either full or empty). Second, and this is both crucial and not obvious, it makes the Landau levels "topological" in that their Chern number is $C^{[n]} = \pm 1$ (the same for all n , the sign depends on conventions and the direction of the perpendicular magnetic field). This then explains the exact structure of the famous Hall resistance plots. One can study the emergence of Landau levels and their Chern numbers in the \uparrow *Hofstadter model* [17, 78] (\Rightarrow Problemset 4). Two different approaches to explicitly compute the Chern numbers of Landau levels are discussed by Fradkin [63, Chapter 12].)
- In our proof, we explicitly used that the many-body ground state is given by a Fermi sea. This description is invalidated by interactions between the fermions (e.g. Coulomb interactions). Similarly, our use of Bloch wave functions is invalidated by disorder in the system. Remarkably, it can be shown that the quantization Eq. (1.98) remains robust under general perturbations (that break translation invariance and/or add interactions) if these perturbations are not too strong [76, 79].
- Another subtlety is that all our calculations refer to *bulk properties* (namely the linear response of the bulk to a homogeneous electric field). This is *not* what one measures in experiments where one attaches point contacts to the *boundary* of a "Hall bar" (which hosts the 2DEG). The conductivity (both longitudinal and transversal) is then determined by the properties of the system boundary and not the bulk. However, due to the \rightarrow *bulk-boundary correspondence*, the topological nature of the bulk directly influences the property of the edge (\rightarrow *below*); in particular, the total Chern number of the bulk (= filled Landau levels) correlates one-to-one with gapless chiral edge modes on the boundary. It is the scattering-free transport in these edge modes that one measures in actual experiments, and the quantized Hall resistance is due to the number of edge modes that contribute (= are partially filled). Formally, this is described by the \uparrow *Landauer-Büttiger formalism* [80].
- This formula was first derived by Thouless, Kohmoto, Nightingale, and Nijs in Ref. [17]; hence the name. It is one of the achievements that earned D. J. Thouless the 2016 Nobel Prize in Physics. Since Thouless got a half-share of the prize, and the Nobel Committee

cited both his description of the KT phase transition and the TKNN result as motivation, one can put a Prize tag on Eq. (1.98): 1/4 of a Nobel Prize. I hope you are duly impressed (you can also be a bit proud of having followed the derivation to this point ☺).

- One can show that, without adding additional symmetry constraints, the TKNN invariant (Chern number) is the *only* quantized topological invariant that can be used to distinguish gapped bands [81].
- Historically, the first convincing (but more heuristic) argument for the quantization of the Hall plateaus was already given by Robert Laughlin in 1981 [82]. However, from this derivation one cannot establish a connection to the Chern number as a topological invariant.

15 | Closing remarks:

The salient feature of the integer quantum Hall effect is that a quantity that describes a macroscopic response of system (the Hall conductivity) is exactly quantized and hence impervious to microscopic disorder. This magic turns into comprehension when we go back [to Eq. (1.70)] and realize that we only showed that the *antisymmetric* part of the conductivity tensor has a topological character (remember that we argued the symmetric part away to evade a divergence in the DC limit). Note that in a conventional conductor (w/o magnetic field) the conductivity tensor is *not* antisymmetric but symmetric. So in general we should start with the decomposition

$$\sigma = \sigma_s + \sigma_a \tag{1.99}$$

with $\sigma_s^T = \sigma_s$ and $\sigma_a^T = -\sigma_a$. W/o magnetic field σ_a vanishes (this is an example of an *Onsager relation* [83]). Strictly speaking, we have only shown that the contribution of this antisymmetric part is topologically quantized. But this contribution is also special in another way. The current \mathbf{J} is the response due to an external electric field: $\mathbf{J} = \sigma \mathbf{E}$. The power that is dissipated in an equilibrium setting (through bumps of the charge carriers with the crystal structure) is then $P = \mathbf{J} \cdot \mathbf{E}$ (if \mathbf{J} is the current *density* this is of course the power *density*); this is known as *Joule's law*. Putting everything together, we find

$$P = \mathbf{E}^T \sigma \mathbf{E} = \mathbf{E}^T \sigma_s \mathbf{E} \tag{1.100}$$

since $\mathbf{E}^T \sigma_a \mathbf{E} = (\mathbf{E}^T \sigma_a \mathbf{E})^T = \mathbf{E}^T \sigma_a^T \mathbf{E} = -\mathbf{E}^T \sigma_a \mathbf{E} = 0$. Thus only the *symmetric* part of the conductivity tensor plays a role for dissipation! But we didn't show that this part is quantized, only the “non-dissipative” contribution σ_a is. So our intuition that a *dissipative* quantity should depend on microscopic details and hence *not* be quantized was right, after all. What we missed is that not everything about the conductivity *tensor* is dissipative; there is also a topological (or geometric) contribution that has nothing to do with microscopic physics. It is this contribution that gives rise to the integer quantum Hall effect.

There is much more to be said about the physics of the integer quantum Hall effect. Since this a course on the broader topic of topological phases, we should not linger too long, though. However, there are three last topics that must be mentioned to prevent misconceptions and embed the IQHE into the Big Picture. For students who want to dig deeper into quantum Hall physics, I can highly recommend the lecture notes by David Tong [64].

1.5. The role of disorder

The above derivation is based on *non-interacting* fermions in a translation invariant potential (= w/o disorder). However, the quantization of the Hall response is more general than that and prevails in the presence of disorder and/or interactions that do not close the spectral gap above the many-body ground state [76, 79].

This statement is based on a more general expression for the Hall conductivity that does not rely on the Brillouin zone (and therefore translation invariance). This approach can also be used to compute the Hall conductivity of the Landau levels of a continuum system on a torus, see Chapter 12.7 of Fradkin's textbook [63].

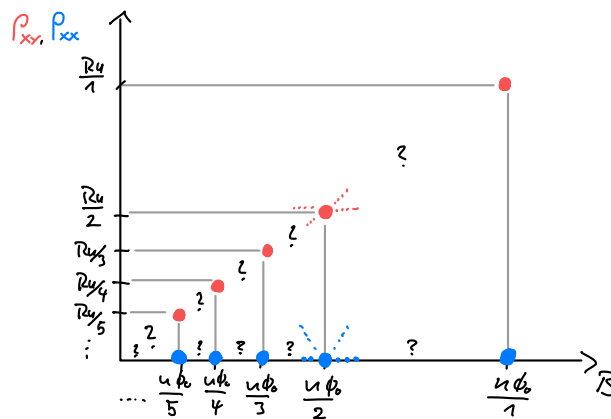
However, even if we take these statements for granted, there is still a problem that is sometimes swept under the rug in superficial discussions of the IQHE:

1 | < System with fixed electron density n (= fixed chemical potential)

Recall Eq. (1.17): Number of states per LL: $N = \frac{AB}{\Phi_0} \stackrel{!}{=} \frac{An}{\nu}$

→ Lowest $\nu \in \mathbb{N}$ LLs *exactly* filled for $B_\nu = \frac{\Phi_0 n}{\nu}$

→ Only for the *discrete* B_ν the Hall response σ_{xy} is topological and thus quantized: (Here we use that $C^{[n]} = \pm 1$ for Landau levels, which we did not derive explicitly.)



- For the longitudinal resistivity ρ_{xx} we used that systems with only completely filled/empty bands are \downarrow *band insulators*, i.e., $\sigma_{xx} = 0 = \sigma_{yy}$ ($\Leftrightarrow \rho_{xx} = 0 = \rho_{yy}$). This can be rigorously shown via a calculation very similar to our derivation in Section 1.4.2, i.e., starting from the Kubo formula.
- Note that $\sigma_{xx} = 0 = \sigma_{yy}$ and $\sigma_{xy} \neq 0$ translates to $\rho_{xx} = 0 = \rho_{yy}$ (!) and $\rho_{xy} = -1/\sigma_{xy}$:

$$\rho = \begin{bmatrix} \rho_{xx} & \rho_{xy} \\ -\rho_{xy} & \rho_{yy} \end{bmatrix} \stackrel{\text{def}}{=} \sigma^{-1} = \begin{bmatrix} 0 & \sigma_{xy} \\ -\sigma_{xy} & 0 \end{bmatrix}^{-1} = \begin{bmatrix} 0 & -1/\sigma_{xy} \\ 1/\sigma_{xy} & 0 \end{bmatrix}. \quad (1.101)$$

This is not true in general, recall Eq. (1.4).

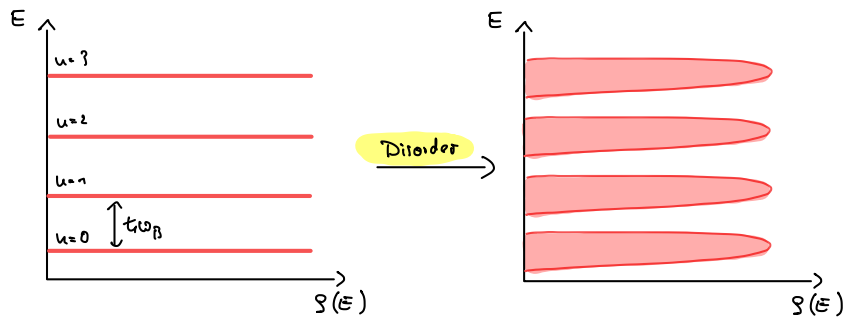
→ This does not explain the observed plateaus!

Recall the experimental data shown previously to motivate our discussion of the IQHE.

The situation is a bit strange: Our hard-earned result (the TKNN formula) explains the quantization of the *height* of the plateaus, but not their *existence* (= finite width).

Solution: Disorder ...

2 | First effect of disorder: LLs are *broadened*: [$\rho(E)$ denotes the ↓ *density of states*]



→ This does *still not* explain the observed plateaus!

The problem stays the same, whether the LLs are perfectly flat or not.

3 | Second effect of disorder:

- (Most) single-electron states are *localized* and *pinned* at local potential peaks/dips

→ Do not contribute to conductivity

This pinning of free electron states due to disorder is known as ↑ *Anderson localization*.

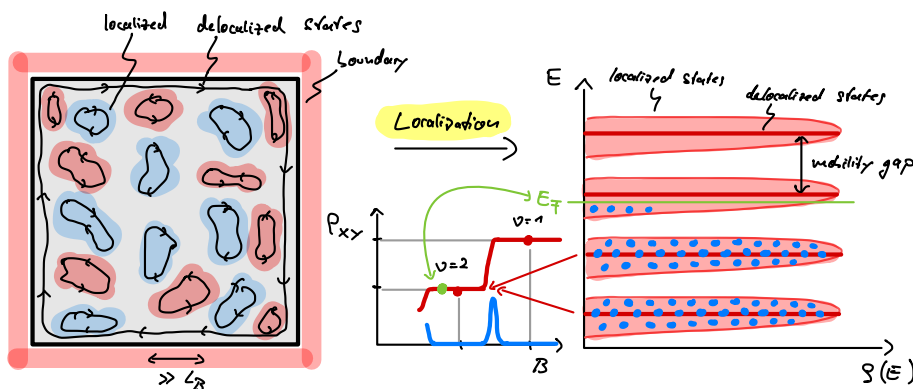
- At least one mode along the edge cannot be localized

→ Contributes to conductivity

The existence of these non-localized “edge states” is a topological consequence of the non-zero Chern number of the LLs: the chirality makes backscattering along the edge impossible and prevents the edge modes from acquiring a gap [note → *below*].

A characterization of “Chern bands” (bands with non-zero Chern number) is therefore that they prevent complete Anderson localization: even with disorder, some states must always remain delocalized.

→ Mobility gap:



→ Filling/depletion of broadened LLs for $B \lesssim B_\nu$ does *not* affect conductivity as long as E_F is in the mobility gap

→ Explains *extended* Hall plateaus around B_ν with quantized height R_K/ν

4 | In a nutshell:

- *Topology* fixes the *height* of the plateaus but
- *disorder* gives them their finite *width* (= makes them visible).

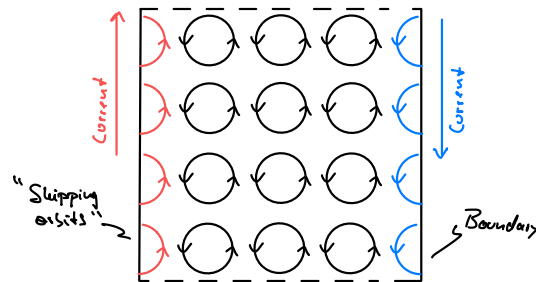
;! This implies that in a (hypothetical) perfectly clean sample, the Hall plateaus cannot be observed.

1.6. Edge states

So far, we focused on the Hall conductivity σ_{xy} , a linear response function of the system; it is a property of the *bulk* and does not depend on the presence or absence of boundaries.

Above we have argued that in systems with boundary, there are delocalized single-particle modes running along the boundary in one direction (determined by the sign of the magnetic field and the sign of the charge carriers). These *edge states* on the 1D “surface” of the 2D system cannot be removed by disorder – they are topologically protected. We will encounter this phenomenon again in our discussion of topological insulators → *later*.

1 | Classical picture:

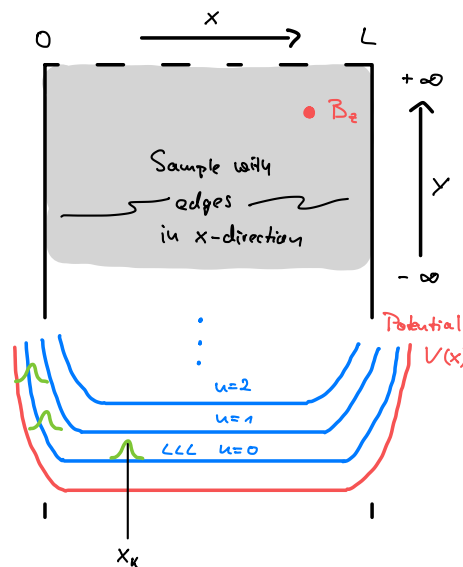


→ *** Skipping orbits* → Chiral currents along edges

2 | Quantum picture:

The following discussion provides a *heuristic* quantum mechanical picture for the emergence of edge states, the quantization of the Hall conductivity, and its robustness against disorder:

i | < Strip geometry:



ii | Hamiltonian in Landau gauge: [recall Eq. (1.14)]

$$H_k = \frac{1}{2m} p_x^2 + \frac{m\omega_B^2}{2} (x + kl_B^2)^2 + V(x) \quad (1.102)$$

$V(x)$: Potential that varies on length scales $\gg l_B$

- iii | LL wavefunctions $\Psi_{n,k}$ [recall Eq. (1.16)] still eigenfunctions (with shifted energies):
 ◁ Lowest Landau Level:

$$\text{Eq. (1.16)} \rightarrow \Psi_{0,k}(x, y) = \mathcal{N} e^{iky} e^{-\frac{(x+kl_B^2)^2}{2l_B^2}} \quad (1.103)$$

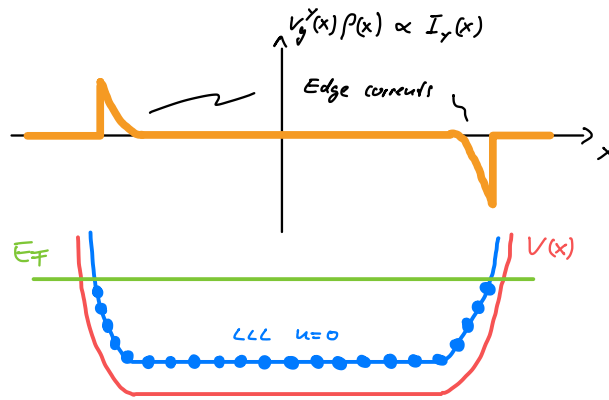
- localized at $X_k = -kl_B^2$ (with y -momentum k)
- Eigenenergy $E_k = \frac{1}{2}\hbar\omega_B + V(X_k)$

- iv | ◁ Group velocity in y -direction: ($l_B = \sqrt{\hbar/eB}$)

$$v_g^y(X) = \frac{1}{\hbar} \frac{\partial E_k}{\partial k} = \frac{1}{\hbar} \frac{\partial E_k}{\partial X_k} \frac{\partial X_k}{\partial k} = -\frac{l_B^2}{\hbar} \frac{\partial V(X)}{\partial X} = -\frac{1}{eB} \frac{\partial V(X)}{\partial X} \quad (1.104)$$

- Current density $I_y(x) = -e v_g^y(x) \rho(x)$

$\rho(x)$: density of occupied states for fixed Fermi energy E_F



Note that the system is gapped with $\hbar\omega_B$ in the bulk but *gapless* on the edges!

- Gapless, chiral edge modes

- The *chirality* of these modes (i.e., the fact that electrons can move only in one direction along the edge) is a consequence of time-reversal symmetry breaking (due to the magnetic field). It makes the charge transport robust against disorder since backscattering is impossible (there are no counterpropagating modes in which to scatter).
- This robustness prevents the generation of a gap on the edge (even in the presence of disorder and/or weak interactions). In the language of field theory, the low-energy physics on the edge is described by a \uparrow *chiral Luttinger liquid*. Due to the missing counterpropagating modes, there are no relevant operators that can open a gap.
- The existence of these edge modes is deeply rooted in topology and a consequence of the non-zero Chern number of the Landau levels. The general statement that topologically non-trivial bulk insulators give rise to gapless modes on their boundary is known as \uparrow *bulk-boundary correspondence* [84–86] and one of the striking features of systems with topological bands.

- v | Consistency check: The current along the strip *vanishes* (at $T = 0$):

$$I_y = \int_{-\infty}^{\infty} I_y(x) dx = -e \int_{-\infty}^{\infty} v_g^y(x) \rho(x) dx \stackrel{1.104}{=} \frac{1}{B} \int_{-\infty}^{\infty} \frac{\partial V(x)}{\partial x} \rho(x) dx \quad (1.105a)$$

$$\stackrel{\circ}{=} \frac{e}{2\pi\hbar} \int_{x_L}^{x_R} \frac{\partial V(x)}{\partial x} dx = \frac{e}{2\pi\hbar} \left[\underbrace{V(x_R)}_{\mu_R} - \underbrace{V(x_L)}_{\mu_L} \right] \stackrel{V \text{ symmetric}}{=} 0 \quad (1.105b)$$

$\mu_i \equiv V(x_i)$: Chemical potential on edge i

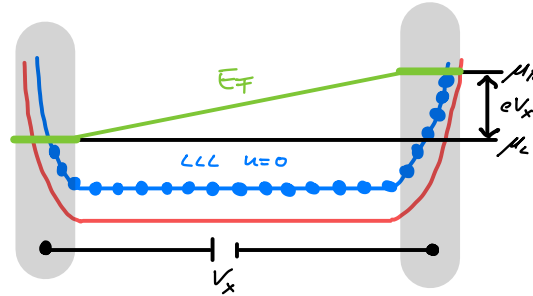
That's good news because there is no voltage applied!

Here we used Eq. (1.17) to show that the electron density of a homogeneous 2DEG with filled lowest Landau level is given by $\rho = N/A = 1/(2\pi l_B^2) = eB/(2\pi\hbar)$ so that $\rho(x) = \frac{eB}{2\pi\hbar} \mathbf{1}_{[x_L, x_R]}(x)$ where $\mathbf{1}_{[x_L, x_R]}(x)$ denotes the indicator function on $[x_L, x_B]$.

vi | < Hall conductivity:

Apply electric field in x -direction: $V(x) \mapsto V(x) + eEx \rightarrow \mu_R - \mu_L = eV_x$

V_x : Hall voltage between left and right boundary



→ Hall current:

$$I_y \stackrel{1.105b}{=} \frac{e}{2\pi\hbar} (\mu_R - \mu_L) = \frac{e^2}{2\pi\hbar} V_x \tag{1.106}$$

→ Hall conductivity per filled LL:

$$\sigma_{xy} = \frac{e^2}{2\pi\hbar} \tag{1.107}$$

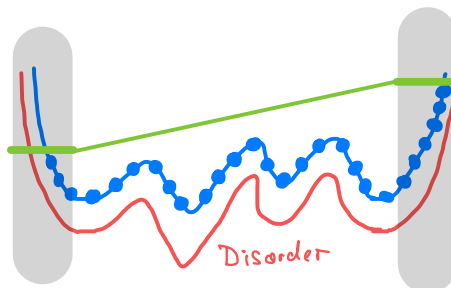
If the ν lowest Landau levels are filled, each contributes Eq. (1.107) to the total conductivity such that

$$\sigma_{xy} = \frac{e^2}{2\pi\hbar} \nu, \tag{1.108}$$

consistent with the TKNN formula Eq. (1.98) and our (unproven) claim that $C^{[n]} = \pm 1$ for Landau levels.

vii | < Disorder:

For weak disorder in the potential $V(x)$ (that does not cross the local Fermi energy), the above calculation of the Hall current remains correct as it only depends on the chemical potential at the left and right boundary, but not the behavior of E_k [or equivalently, $V(x)$] in between:



→ The result for the Hall conductivity Eq. (1.107) is robust to disorder!

3 | Chiral edge modes are special:

i | Let us first cite (the special case of) a no-go theorem with important consequences:

† **Note: Nielsen-Ninomiya-Theorem in 1D**

◁ Non-interacting fermions on a lattice in 1D:

→ Brillouin zone = Circle S^1 (= bands must be periodic!)

→ Equal number of left (ψ_L) and right movers (ψ_R) in low-energy theories of lattice models

This insight was formalized by Nielsen and Ninomiya in 1981 [87, 88] for higher-dimensional (and more important) cases, especially 3 + 1 dimensions. Then the fact that every chiral \uparrow Weyl fermion must have a partner when discretized on a lattice is known as \uparrow fermion doubling problem, which is inherent to lattice formulations of quantum field theories. The no-go theorem prevents lattice discretizations of chiral theories like the weak sector of the standard model. This implies in particular that there is (currently) no way to formulate the Standard Model of particle physics completely and consistently on a lattice! For more details see David Tong’s lecture on gauge theory [89, Chapter 4].

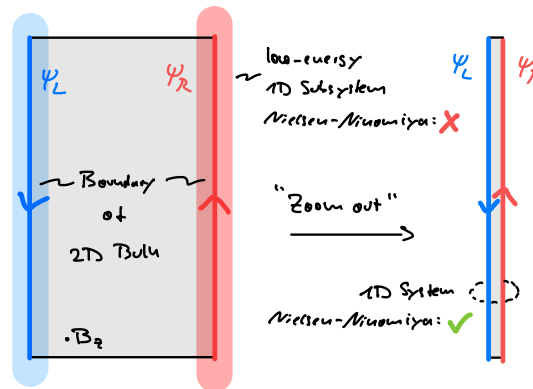
ii | → Chiral 1D modes can only appear on the boundary of a 2D bulk material!

Strictly speaking, the argument above applies only to lattice formulations of the IQHE (e.g. the \uparrow Hofstadter model, \oplus Problemset 4) which, however, feature similar chiral edge modes as the IQHE in its continuum formulation. In the continuum, the proper line of arguments uses the concept of \uparrow gauge anomalies (\uparrow Ref. [64, Chapter 5 & 6]).

This is an observation that goes deep with far-reaching ramifications: Effective low-energy theories that describe the gapless $D - 1$ -dimensional boundaries of gapped D -dimensional systems can have properties that are – under reasonable assumptions – impossible for “true” $D - 1$ -dimensional systems (i.e., systems that are *not* the boundary of some larger system).

iii | Intuitive explanation how to “circumvent” the Nielsen-Ninomiya theorem:

The magnetic field spatially separates left- and right movers:



iv | Comments

- In bands with non-zero Chern number, no single-particle basis exists where *all* wave functions are localized – this is known as a \uparrow *topological obstruction* [90,91]. Localized bases constructed from the Bloch wave functions are called \uparrow *Wannier bases*; a non-zero Chern number therefore forbids the existence of a basis with completely localized Wannier states.

→ Delocalized edge modes

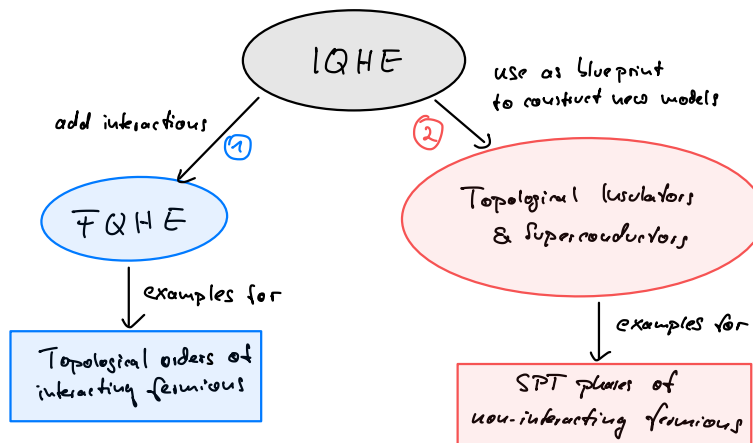
- To proper way to show the existence (and robustness) of the chiral edge modes is to construct a low-energy effective quantum field theory (QFT). This QFT turns out to be a gauge theory known as \uparrow *Chern-Simons (CS) theory* (of the “abelian variety” and with “integer level”). In the presence of a boundary, the gauge invariance of the CS theory *requires* the existence of gapless physical degrees of freedom at the edge of the sample (gauge invariance demands a “chiral Luttinger liquid” on the boundary).

→ Robust edge modes

The neat thing about the QFT approach is that it can be directly generalized to the *fractional* quantum Hall effect (then the CS theory can become “non-abelian” and is of “fractional level”). For details see Ref. [64, Chapter 5 & 6].

1.7. Notes on classification

The IQHE is an important corner stone in the theory of topological phases, both historically and conceptually. Starting from the IQHE, there are (at least) two directions to explore:



(1) Keep the QHE setting but consider fractionally filled Landau levels:

- Interactions become important (flat bands!)
- ↑ Fractional quantum Hall Effect (FQHE)
- States with \leftarrow (non-invertible) topological order with anyonic excitations and fractional charges (depending on the filling)

(2) Leave the QHE setting but stay in the realm of *non-interacting fermions* (on the lattice):

- Construct lattice models with topological bands ...
 - ...w/o magnetic fields (?)
 - ...w/o breaking time reversal symmetry (?)
 - ...w/o particle-number conservation (?)
- → *Topological insulators & superconductors*
[SPT phases of non-interacting fermions & invertible topological orders]

In the following we will pursue **Path 2** which will eventually lead us to the “periodic table of topological insulators and superconductors” in Chapter 6.

Note:

IQH states (= filled Landau levels) are part of the classification of topological phases of non-interacting fermions that we will introduce [92]. However, they are also long-range entangled [35], but this long-range entanglement is of a special “boring” kind in that it does not give rise to fancy anyonic statistics of excitations. In our nomenclature, IQH states are examples of \leftarrow *invertible topological order*. (You can locally disentangle a IQH state by “gluing” a time-inverted copy on top.)

According to another naming scheme [different from the one I introduced], IQH states are “short-range entangled” because they lack anyonic excitations and their \rightarrow *topological entanglement entropy* vanishes

[36, 37]. Because of the time-reversal symmetry breaking and the chiral nature of their edge modes, some call IQH states simply *chiral phases* [93, 94].

It is noteworthy that symmetry *does* play a role for the IQH, namely the $U(1)$ symmetry that describes the *conservation of charge*. It does neither protect the entanglement structure nor the chiral edge states, but it is necessary for the quantization of the Hall response [35, 93, 94]. (Which makes sense: in a material where charge can randomly enter or leave the sample, there is no reason for a conductivity to be quantized.)

2. Topological Bands without Magnetic Fields: The Quantum Anomalous Hall Effect

2.1. Preliminaries

We seek for models with the following properties:

- Lattice model (of non-interacting fermions)
- Band insulator
- Non-zero Chern number
- No magnetic field (!)

The first three conditions are satisfied by the ↑ *Hofstadter model*, a lattice model that captures the IQHE physics. However, the Hofstadter model is a rather complicated multiband model due to the enlarged magnetic unit cell (↪ Problemset 4). This motivates the question:

Are there models without external magnetic field that have Chern bands?

- Chern band = Band with non-zero Chern number
- Note that the sum of Chern numbers of all bands is always zero (↪ Problemset 3). Thus, if the answer to this question is affirmative, the model must have at least two bands. This can be achieved either with an internal degree of freedom (spin) or, alternatively, with sublattice degrees of freedom (i.e., a unit cell with more than one site).

Before we proceed, let us fix the nomenclature:

**** Definition: Chern insulator**

$$\text{Chern insulator}^* (\text{CI}^*) := \left\{ \begin{array}{l} \text{Lattice model} \\ \text{Band insulator} \\ \text{Non-zero Chern number} \end{array} \right. \quad (2.1)$$

Prototype: ↑ Hofstadter model

$$\text{Chern insulator (CI)} := \left\{ \begin{array}{l} \text{Lattice model} \\ \text{Band insulator} \\ \text{Non-zero Chern number} \\ \text{No external magnetic field} \end{array} \right. \quad (2.2)$$

Prototype: → Haldane model

With this definition, the above question can be restated:

Are there Chern insulators?

Before we focus on specific models, let us explore some generic properties of translation invariant models with two bands:

2.1.1. Lattice models with two bands

1 | General setting: (The following is crucial throughout Part I!)

We start with a brief review of Hamiltonians that describe non-interacting fermions in translation invariant lattice models (here with any number of bands in any dimension):

- i | Single-particle (SP) Hilbert space $\mathcal{H} = \text{span} \{ |\Psi_{i\alpha}\rangle \}_{i\alpha}$ with SP Hamiltonian

$$H = \sum_{i\alpha, j\beta} H_{i\alpha, j\beta} |\Psi_{i\alpha}\rangle \langle \Psi_{j\beta}| \quad (2.3)$$

$i = 1 \dots N$: site index

$\alpha = 1 \dots M$: internal degrees of freedom (e.g. multiple sites per unit cell, spin, ...)

- ii | → Many-body (MB) Hilbert space $\hat{\mathcal{H}} = \bigoplus_n \wedge^n(\mathcal{H})$ with MB Hamiltonian

$\hat{\mathcal{H}}$ is the fermionic \downarrow Fock space (the \uparrow exterior algebra of \mathcal{H}); \wedge^n denotes the n th \uparrow exterior power of the single-particle Hilbert space \mathcal{H} .

$$\hat{H} = \sum_{i\alpha, j\beta} c_{i\alpha}^\dagger H_{i\alpha, j\beta} c_{j\beta} \quad (2.4)$$

$c_{i\alpha}^\dagger / c_{i\alpha}$: fermionic creation/annihilation operators for fermion in state $|\Psi_{i\alpha}\rangle$

The fact that this Hamiltonian only includes *quadratic* terms of fermionic operators makes it exactly solvable; one says that \hat{H} describes *quadratic fermions*, *non-interacting fermions*, or *free fermions*.

- iii | Assume Translation symmetry $\overset{\circ}{\rightarrow}$

$$\hat{H} = \sum_{\mathbf{k}; \alpha, \beta} c_{\mathbf{k}\alpha}^\dagger H_{\alpha\beta}(\mathbf{k}) c_{\mathbf{k}\beta} \quad (2.5)$$

with \ast momentum modes

$$c_{\mathbf{k}\alpha} := \frac{1}{\sqrt{N}} \sum_i e^{i\mathbf{x}_i \cdot \mathbf{k}} c_{i\alpha} \quad (2.6)$$

\mathbf{x}_i : position of site i

- iv | So the SP Hamiltonian decomposes as $H = \bigoplus_{\mathbf{k}} H(\mathbf{k})$ with \ast Bloch Hamiltonian $H(\mathbf{k})$ (a Hermitian $M \times M$ -matrix).

Diagonalizing the latter yields

$$H(\mathbf{k}) = \sum_n E_n(\mathbf{k}) |u_{n\mathbf{k}}\rangle \langle u_{n\mathbf{k}}| \quad (2.7)$$

- $|u_{kn}\rangle$: Bloch wavefunction
- $n = 1 \dots M$: band index
- $E_n(\mathbf{k})$: SP spectrum

→ The SP Hilbert space decomposes as $\mathcal{H} = \bigoplus_{\mathbf{k}} \mathcal{H}_{\mathbf{k}}$ with momentum mode space $\mathcal{H}_{\mathbf{k}} = \text{span} \{|u_{n\mathbf{k}}\rangle\}_n$.

2 | We now specialize to models with *two* bands on a 2D lattice ...

◁ Most general two-band Hamiltonian on a 2D lattice:

$$H = \bigoplus_{\mathbf{k} \in T^2} H(\mathbf{k}) \quad \text{with} \quad H(\mathbf{k}) = \varepsilon(\mathbf{k}) \mathbb{1} + \vec{d}(\mathbf{k}) \cdot \vec{\sigma} \quad (2.8)$$

- T^2 : Brillouin zone (BZ) (= Torus)
- σ^α with $\alpha = x, y, z$: Pauli matrices
- $\vec{d}(\mathbf{k}) : T^2 \rightarrow \mathbb{R}^3$: real, vector-valued function on BZ

The two spatial dimensions are responsible for the Brillouin zone being a 2-torus T^2 , the two bands allow us to expand the Hermitian 2×2 -matrix $H(\mathbf{k})$ into Pauli matrices.

3 | Spectrum:

$$E_{\pm}(\mathbf{k}) \doteq \varepsilon(\mathbf{k}) \pm |\vec{d}(\mathbf{k})| \quad (2.9)$$

→ Band insulator iff

$$\min_{\mathbf{k} \in T^2} E_+(\mathbf{k}) > \max_{\mathbf{k} \in T^2} E_-(\mathbf{k}) \quad (2.10)$$

Strictly speaking, this condition *allows* the system to be a band insulator *if* the chemical potential (= Fermi energy E_F) is in the gap (which the above condition guarantees to exist). We assume this situation in the following: $\min_{\mathbf{k} \in T^2} E_+(\mathbf{k}) > E_F > \max_{\mathbf{k} \in T^2} E_-(\mathbf{k})$.

◁ Weaker condition:

$$\forall \mathbf{k} \in T^2 : E_+(\mathbf{k}) - E_-(\mathbf{k}) = 2|\vec{d}(\mathbf{k})| > 0 \quad (2.11)$$

This means that the two bands never touch and/or intersect.

→ Normalization possible:

$$\hat{d}(\mathbf{k}) := \frac{\vec{d}(\mathbf{k})}{|\vec{d}(\mathbf{k})|} \quad \text{such that} \quad \hat{d} : T^2 \rightarrow S^2 \quad (2.12)$$

S^2 : unit sphere in \mathbb{R}^3

4 | Chern number of the lower band:

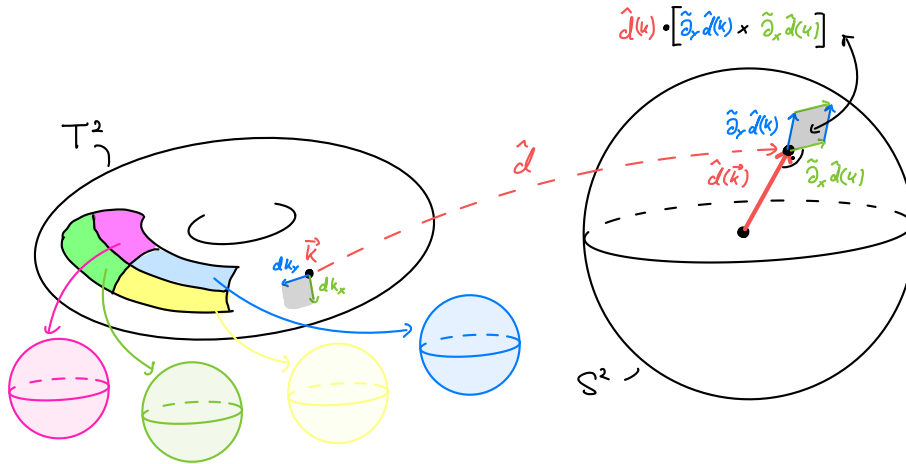
$$C \doteq -\frac{1}{4\pi} \int_{T^2} \underbrace{\hat{d}(\mathbf{k}) \cdot [\tilde{\partial}_x \hat{d}(\mathbf{k}) \times \tilde{\partial}_y \hat{d}(\mathbf{k})]}_{4\pi \mathbb{Z}} d^2k \in \mathbb{Z} \quad (2.13)$$

(Oriented) Jacobian for surface integral
∝ Berry curvature

Derivation: ↻ Problemset 5

5 | Geometric interpretation:

The expression for the Berry curvature is just the ↓ *Jacobian* for the (oriented) surface integral over the sphere S^2 :



i | → C counts how often $\hat{d}(\mathbf{k})$ covers S^2 when sweeping over the Brillouin zone T^2

Note that this can only happen in integer steps since the area element in Eq. (2.13) is *oriented*: “going back” counts negative.

ii | $C = C[\hat{d}] \in \mathbb{Z}$ is a topological invariant

This implies in particular that two different maps \hat{d}_a and \hat{d}_b that can be continuously deformed into each other must have the same winding number C .

Mathematically this follows because Eq. (2.13) is a continuous function of \hat{d} and maps into the integers. It is a well-known fact from topology that such functions are constant on their domain.

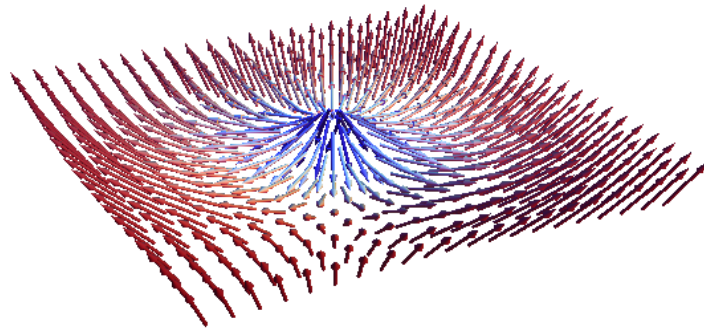
iii | Hamiltonian H_a can be continuously deformed into H_b without closing the gap
 $\Leftrightarrow \hat{d}_a$ can be continuously deformed into \hat{d}_b

Note that when the gap closes, the normalized vector \hat{d} has a *singularity* (= is undefined) somewhere on T^2 so that Eq. (2.13) is undefined as well.

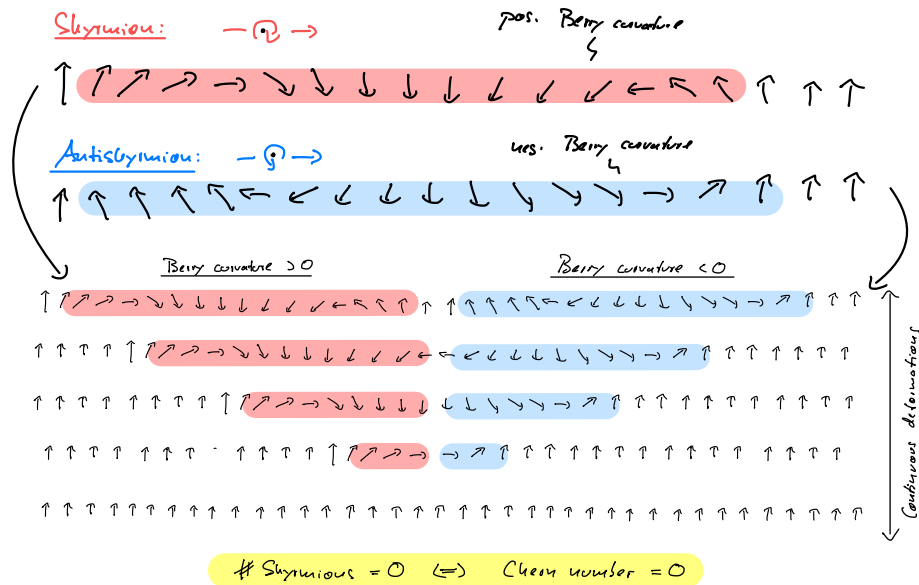
iv | → C labels different topological phases

6 | ‡ Skyrmion interpretation:

i | The region on T^2 where the field $\hat{d}(\mathbf{k})$ “wraps around the sphere” can be quite localized. This creates a local “knot” in the field that can be viewed as an excitation of a specific type of non-linear field theory known as ↑ *non-linear sigma models*. In this (very different) context, these localized excitations are called ↑ *skyrmions* (after TONY SKYRME who introduced them to describe the strong force [95]); they are an example for ↑ *topological solitons*. Here an illustration of a skyrmion that represents a field \hat{d} wrapping once around the sphere:



ii | If the direction how the field sweeps over the sphere is inverted, one ends up with an *anti-skyrmion*. A single skyrmion is a topologically protected field configuration and cannot be removed by continuous deformations of \hat{d} (this is just our argument from above about the topological character of C restated in terms of skyrmions). However, a skyrmion and an antiskyrmion *can* be continuously removed (they “annihilate” each other):



(This is a 1D cut through the 2D surface on which the skyrmion-antiskyrmion pair lives.)

iii | Summary:

- Skyrmions are “twists” of \hat{d} and “live” on the BZ
- Positive (negative) Berry curvature indicates a finite (anti-)skyrmion *density*
- The Chern number is the number of skyrmions minus the number of antiskyrmions

iv | An interesting mathematical tangent:

† **Note: Pontryagin number**

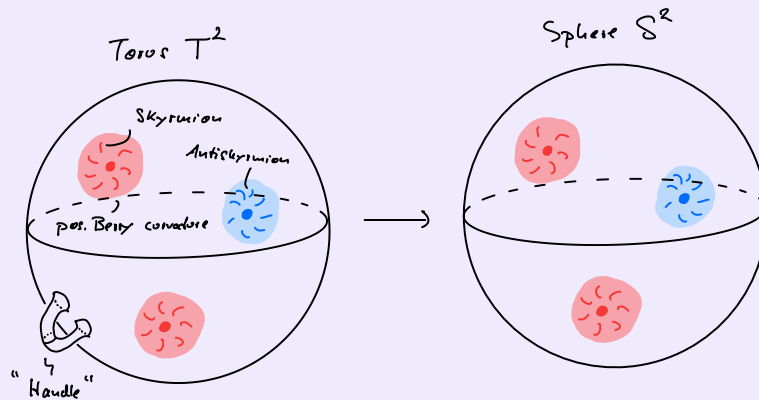
The fact that \hat{d} lives on a torus T^2 (the Brillouin zone) is not important in this situation. Thus it is possible to replace the torus T^2 by a sphere S^2 (which can be seen as the one-point compactified momentum space \mathbb{R}^2 of the continuum). Then

$$\hat{d} : S^2 \rightarrow S^2 \tag{2.14}$$

is a *continuous* function that maps the sphere onto the sphere. Two Hamiltonians H_a and H_b belong to the same phase, if the corresponding functions \hat{d}_a and \hat{d}_b can be “smoothly deformed” into each other.

In topology, such a smooth deformation of one function into another is known as a \uparrow *homotopy*; the set of equivalence classes under homotopy has a group structure and is known as (second) homotopy group of S^2 , write $\pi_2(S^2)$; it is well-known that $\pi_2(S^2) = \mathbb{Z}$. The equivalence classes in $\pi_2(S^2)$ can be labeled by an integer known as \uparrow *Pontryagin number*; it counts how often a map \hat{d} traces out the (target) sphere S^2 when sweeping the (domain) sphere S^2 . In the current situation, this is exactly the Chern number C .

That the torus can be replaced by a sphere is also evident in the skyrmion picture. Since the skyrmions can be localized, they do not care whether they live on a torus or a sphere:



However, note that \hat{d} can have “twists” around the torus that are not reflected in the Chern number (and are not related to skyrmions). These “twists” give rise to \uparrow *weak topological indices* which can have physical effects on the boundary physics in specific directions [57, 96, 97]. Since these effects rely on the domain of \hat{d} to be a torus (= Brillouin zone), they are protected by the translation symmetry of the lattice (this makes them “weak”). Weak topological indices are not important for the models discussed below.

2.1.2. Time-reversal symmetry (TRS)

;! We will introduce time-reversal symmetry as the first of three “generic” symmetries and discuss the restrictions it imposes on the Bloch Hamiltonian $H(\mathbf{k})$. It plays a role for the → *Haldane model* but *not* as protecting symmetry; quite the contrary: it must be *broken* to make the model interesting (recall that the IQHE – which we would like to mimic – is not an SPT phase). However, in upcoming lectures (throughout Part I) we will use this symmetry as a *protecting symmetry* instead, which then leads us to the concept of → *topological insulators* and their classification.

1 | < Single particle with SP Hilbert space \mathcal{H} :

TRS $T : t \mapsto -t$ is a \mathbb{Z}_2 -symmetry (inverting time twice should do nothing!) and should reasonably act as

$$TxT^{-1} \stackrel{!}{=} x \quad \text{but} \quad TpT^{-1} \stackrel{!}{=} -p \quad (2.15)$$

$$\rightarrow Ti\hbar T^{-1} = T[x, p]T^{-1} = -[x, p] = -i\hbar$$

→ T must be antiunitary:

$$T_U = U\mathcal{K} \quad \text{with} \quad \mathcal{K} = \text{Complex conjugation} \quad (2.16)$$

U : unitary operator that determines the *representation* T_U of T on the SP Hilbert space

↑ *Wigner's theorem* [98] states that a *symmetry* (i.e. an operator O that preserves all probability amplitudes, $|\langle O\Psi|O\Phi\rangle|^2 = |\langle\Psi|\Phi\rangle|^2$) acts either as a *unitary* or an *antiunitary* operator on the Hilbert space (⊕ Problemset 1). In combination with $TiT^{-1} = -i$, this fixes T to the generic form T_U above.

→ SP Hamiltonian H is \star *time-reversal symmetric* iff $[H, T_U] = 0$ for a U chosen appropriately to describe the system (→ *below*)

Explicitly the condition for time reversal symmetry reads:

$$HU\mathcal{K} = HT_U = T_UH = U\mathcal{K}H \Leftrightarrow HU = UH^* \Leftrightarrow H = UH^*U^\dagger \quad (2.17)$$

2 | T_U is antiunitary →

$$T_U^2 = UU^* = U(U^T)^{-1} \quad (2.18)$$

T_U is projective representation of \mathbb{Z}_2 →

$$T_U^2 = \lambda\mathbb{1} \quad \text{with} \quad |\lambda| = 1 \quad (2.19)$$

- Being a → *projective representation* of \mathbb{Z}_2 realizes our notion that inverting time twice should bring us back to the same physical state: Because physical states are *rays* (⊕ Problemset 1), this only means that T_U^2 applied to a state vector gives back the same vector *up to a phase*. This phase must be the same for all states since otherwise you could superimpose two states with different phases to construct a state that transforms to a physically distinct state under T_U^2 – in contradiction with our assumption that inverting time twice has no physical consequences.
- Here is an alternative, more generic line of arguments that does not require the assumption that time reversal is a \mathbb{Z}_2 symmetry as input [92]:

Assume that you made the total Hamiltonian block-diagonal by “using up” all its potential unitary symmetries. Then *each block* carries an irreducible representation of the unitary

symmetry group and an “irreducible Hamiltonian” so that the arguments below hold. How T is represented in each block can vary, however the result for T^2 must be the same on all blocks because otherwise T is not a (projective) representation of \mathbb{Z}_2 on the whole SP Hilbert space—and this would contradict our intuition that applying time-reversal twice does nothing.

Now go back to Eq. (2.18) and note that ...

- UU^* is unitary
- $[H, UU^*] = 0 \rightarrow UU^*$ is a symmetry of H

◁ Generic H without any additional unitary symmetries

→ Hamiltonian irreducible

→ $T_U^2 = UU^* = \lambda \mathbb{1}$

(This is an application of ↑ *Schur's lemma* on the irreducible *Hamiltonian*.)

$$\text{Eqs. (2.18) and (2.19)} \Rightarrow U = \lambda U^T \stackrel{\bullet}{\iff} U^T = U\lambda \quad (2.20a)$$

$$\Rightarrow U = \lambda^2 U \quad (2.20b)$$

$$\Rightarrow \lambda = \pm 1 \quad (2.20c)$$

→

$$T_U^2 = \pm \mathbb{1} \quad (2.21)$$

If $T_U^2 = -\mathbb{1}$, T_U is an *antiunitary, projective* representation of \mathbb{Z}_2 .

3 | Examples:

- ◁ Spinless particles: (=no internal degrees of freedom)

$$T_0 := \underbrace{\mathbb{1}}_{U_0} \mathcal{K} \Rightarrow T_0^2 = +\mathbb{1} \quad (2.22)$$

- ◁ Spin- $\frac{1}{2}$ particles with spin operator $\vec{S} = \frac{\hbar}{2} \vec{\sigma}$

Just as time reversal inverts the linear momentum p , it should also invert (internal) angular momentum (= spin):

$$T_U \vec{S} T_U^{-1} \stackrel{!}{=} -\vec{S} \quad (2.23)$$

So we want that $T_U \sigma^i T_U^{-1} \stackrel{!}{=} -\sigma^i$ for all Pauli matrices $i = x, y, z$.

Note that this choice is not arbitrary. For example, it is inconsistent to demand (nonzero) spin to be *invariant* under time-reversal ($T_U S_i T_U^{-1} = S_i$) because then $[S_i, S_j] = i \epsilon_{ijk} S_k$ (which defines spin operators) implies $[S_i, S_j] = -i \epsilon_{ijk} S_k$ (since T_U is still antiunitary) such that $S_k = 0 \not\Leftarrow$.

→ Solution:

$$T_{\frac{1}{2}} := \underbrace{\sigma^y}_{U_{\frac{1}{2}}} \mathcal{K} \Rightarrow T_{\frac{1}{2}}^2 = -\mathbb{1} \quad (2.24)$$

- Note how $T_U \sigma^i T_U^{-1} = -\sigma^i$ is satisfied: for $i = y$ it follows from the complex conjugation \mathcal{K} (antiunitarity), but for $i = x, z$ it follows because σ^x and σ^z are *real* matrices that anticommute with σ^y .
- The statement $T_U^2 = -\mathbb{1}$ is true for all particles with *half-integer* spin (but with other choices for U that depend on the spin, of course).
- Often you will find the choice $T_{\frac{1}{2}} = -i \sigma^y \mathcal{K}$. This follows if one derives $T_{\frac{1}{2}}$ as a spin rotation. Note that you can multiply $T_{\frac{1}{2}}$ with an arbitrary phase without changing its algebraic properties.

4 | Consequence of $T_U^2 = -\mathbb{1}$:

¡! Important: Kramers theorem

Every eigenenergy of a time-reversal invariant Hamiltonian H with $T_U^2 = -\mathbb{1}$ is at least two-fold degenerate.

Proof: ➔ Problemset 5

The theorem was discovered by HANS KRAMERS in 1930 and mathematically studied on general grounds by EUGENE WIGNER in 1932 [99]. It has far-reaching consequences: For instance, the degeneracy of atomic energy levels with half-integer total angular momentum cannot be lifted completely by electric fields alone (which preserve TRS); instead, magnetic fields are needed (which break TRS). → *Later* we will see that Kramers theorem restricts the band structure of time-reversal invariant systems in that it requires crossing bands at so called → *time-reversal invariant momenta* (TRIMs) in the Brillouin zone.

↓ Lecture 9 [15.05.25]

5 | Action of TRS on Fock space:

Now we generalize these *single-particle* concepts to the *many-body* Hilbert space and Hamiltonian:

i | < Representation \mathcal{T}_U of TRS on the fermionic Fock space $\hat{\mathcal{H}}$:

**** Definition: Time-reversal symmetry**

Time-reversal \mathcal{T}_U is antiunitary, $\mathcal{T}_U i \mathcal{T}_U^{-1} := -i$, and acts on fermion modes as

$$\mathcal{T}_U c_{i\alpha} \mathcal{T}_U^{-1} := \sum_{\beta} U_{\alpha\beta}^{\dagger} c_{i\beta} \quad \text{and} \quad \mathcal{T}_U c_{i\alpha}^{\dagger} \mathcal{T}_U^{-1} := \sum_{\beta} \underbrace{(U_{\alpha\beta}^{\dagger})^*}_{U_{\beta\alpha}} c_{i\beta}^{\dagger}. \quad (2.25)$$

Note that we assume that time-reversal only mixes *internal* degrees of freedom (α, β) but not *spatial* ones (i). This restriction complies with our everyday experience and simplifies the following discussion. Furthermore, we assume that TRS acts on every site in the same way (which is reasonable for translational invariant systems).

ii | Let us check that this definition of TRS on $\hat{\mathcal{H}}$ is consistent with our definition on \mathcal{H} above:

$$\mathcal{T}_U \hat{H} \mathcal{T}_U^{-1} = \sum_{i\alpha', j\beta'} c_{i\alpha'}^{\dagger} \sum_{\alpha, \beta} \left[U_{\alpha'\alpha} H_{i\alpha, j\beta}^* U_{\beta\beta'}^{\dagger} \right] c_{j\beta'} \quad (2.26a)$$

$$\stackrel{!}{=} \sum_{i\alpha', j\beta'} c_{i\alpha'}^{\dagger} H_{i\alpha', j\beta'} c_{j\beta'} = \hat{H} \quad (2.26b)$$

→ [use the form Eq. (2.17)]

$$\left[\hat{H}, \mathcal{T}_U \right] = 0 \quad \Leftrightarrow \quad T_U H T_U^{-1} = H$$

with $T_U = \bar{U} \mathcal{K}$ where $\bar{U} := \oplus_i U_i$ with $U_i \equiv U$ (2.27)

This is the form of TRS in the SP Hilbert space that we discussed earlier (where the role of U is now played by \bar{U} since we have single-particle states on each site).

Note that \bar{U} is a unitary $NM \times NM$ -matrix whereas U is a unitary $M \times M$ matrix.

iii | We want to consider *translation invariant* systems →

$$\mathcal{T}_U c_{\mathbf{k}\alpha} \mathcal{T}_U^{-1} \stackrel{2.6}{=} \frac{1}{\sqrt{N}} \sum_i e^{-i\mathbf{x}_i \cdot \mathbf{k}} \sum_{\beta} U_{\alpha\beta}^{\dagger} c_{i\beta} = \sum_{\beta} U_{\alpha\beta}^{\dagger} c_{-\mathbf{k}\beta} \quad (2.28)$$

→ \mathcal{T}_U inverts momenta & mixes internal DOFs

iv | For a time-reversal symmetric many-body Hamiltonian we find:

$$\mathcal{T}_U \hat{H} \mathcal{T}_U^{-1} \stackrel{2.5}{=} \sum_{\mathbf{k}; \alpha', \beta'} c_{-\mathbf{k}\alpha'}^{\dagger} \sum_{\alpha, \beta} \left[U_{\alpha'\alpha} H_{\alpha\beta}^*(\mathbf{k}) U_{\beta\beta'}^{\dagger} \right] c_{-\mathbf{k}\beta'} \quad (2.29a)$$

$$\stackrel{!}{=} \sum_{\mathbf{k}; \alpha', \beta'} c_{-\mathbf{k}\alpha'}^{\dagger} H_{\alpha'\beta'}(-\mathbf{k}) c_{-\mathbf{k}\beta'} = \hat{H} \quad (2.29b)$$

In the last equation we substituted $\mathbf{k} \rightarrow -\mathbf{k}$.

v | Thus we find a constraint on the Bloch Hamiltonians:

$$\boxed{\begin{aligned} [\hat{H}, \mathcal{T}_U] = 0 &\Leftrightarrow \tilde{T}_U H(\mathbf{k}) \tilde{T}_U^{-1} = H(-\mathbf{k}) \\ &\text{with } \tilde{T}_U = U \mathcal{K} \end{aligned}} \quad (2.30)$$

Note that \tilde{T}_U maps between the mode spaces $\mathcal{H}(\mathbf{k})$ and $\mathcal{H}(-\mathbf{k})$ since TRS inverts momenta!

Summary:

Time-reversal invariance can be expressed equivalently as follows:

$$\boxed{\begin{aligned} [\hat{H}, \mathcal{T}_U] = 0 &\Leftrightarrow T_U H T_U^{-1} = H && (2.31a) \\ &\Leftrightarrow \bar{U} H^* \bar{U}^\dagger = H && (2.31b) \\ &\Leftrightarrow \tilde{T}_U H(\mathbf{k}) \tilde{T}_U^{-1} = H(-\mathbf{k}) && (2.31c) \\ &\Leftrightarrow U H^*(\mathbf{k}) U^\dagger = H(-\mathbf{k}) && (2.31d) \end{aligned}}$$

The last two lines are only defined if the system is translation invariant, the first two are generic.

- In words: A (non-interacting) many-body Hamiltonian \hat{H} is time-reversal invariant if its single-particle Hamiltonian H is unitarily equivalent to its complex conjugate.
- Note that often the formal distinction between T_U and \tilde{T}_U is not made in the literature (similarly for \bar{U} and U) and one simply writes T_U (or even just T) for both.
- Conditions like $\bar{U} H^* \bar{U}^\dagger = H$ are sometimes referred to \uparrow *reality conditions* on the Hamiltonian [92]. We will encounter another example when we discuss particle-hole symmetry later in this course.

Furthermore:

$$\boxed{\begin{aligned} T_U^2 = +\mathbb{1} &\Leftrightarrow \tilde{T}_U^2 = +\mathbb{1} &\Leftrightarrow \mathcal{T}_U^2 \stackrel{\circ}{=} +\mathbb{1} && (2.32a) \\ T_U^2 = -\mathbb{1} &\Leftrightarrow \tilde{T}_U^2 = -\mathbb{1} &\Leftrightarrow \mathcal{T}_U^2 \stackrel{\circ}{=} (-\mathbb{1})^{\hat{N}} && (2.32b) \end{aligned}}$$

$\hat{N} := \sum_{i\alpha} c_{i\alpha}^\dagger c_{i\alpha}$: total fermion number operator

$\mathcal{P} := (-1)^{\hat{N}}$ is the fermion *parity operator*.

! Note that for $T_U^2 = -\mathbb{1}$ it is $\mathcal{T}_U^2 = (-\mathbb{1})^{\hat{N}}$ and *not* $\mathcal{T}_U^2 \stackrel{\circ}{=} -\mathbb{1}$, i.e., the representation depends on the *fermion parity sector*. This makes sense: If $T_U^2 = -\mathbb{1}$, the fermions have half-integer spins (\leftarrow above). According the rules of \downarrow *angular momentum addition*, an even (odd) number of such particles have integer (half-integer) *total* angular momentum, consistent with $\mathcal{T}_U^2 = +\mathbb{1}$ (N even) and $\mathcal{T}_U^2 = -\mathbb{1}$ (N odd).

6 | Consequence of TRS for the Spectrum:

$$H(\mathbf{k})|u_{n\mathbf{k}}\rangle = E_n(\mathbf{k})|u_{n\mathbf{k}}\rangle \quad (2.33a)$$

$$\xrightarrow{(2.31d)} H(-\mathbf{k})U|u_{n\mathbf{k}}\rangle^* = E_n(\mathbf{k})U|u_{n\mathbf{k}}\rangle^* \quad (2.33b)$$

→ Eigenstate $U|u_{nk}\rangle^*$ of $H(-\mathbf{k})$ has same energy $E_n(\mathbf{k})$ as eigenstate $|u_{nk}\rangle$ of $H(\mathbf{k})$

→ Inversion-symmetric band structure

This means that for TRI systems, one half of the BZ is determined by the other half via \tilde{T}_U . This motivates the introduction of a so called → *effective Brillouin zone (EBZ)* (essentially “half” the original BZ) which has the topology of a cylinder [100].

7 | Consequence of TRS for the Chern number: [Remember: $H(\mathbf{k}) = \varepsilon(\mathbf{k}) \mathbb{1} + \vec{d}(\mathbf{k}) \cdot \vec{\sigma}$]

- \leftarrow Two bands from pseudo-spin- $\frac{1}{2}$: $\tilde{T}_0 = \mathcal{K}$

“Pseudo-spin- $\frac{1}{2}$ ” refers to degrees of freedom that are not related to angular momentum and therefore remain invariant under time reversal (e.g. sublattice degrees of freedom).

$$H^*(\mathbf{k}) = H(-\mathbf{k}) \quad \stackrel{(2.8)}{\Leftrightarrow} \quad \begin{cases} d_{x,z}(\mathbf{k}) = d_{x,z}(-\mathbf{k}) \\ d_y(\mathbf{k}) = -d_y(-\mathbf{k}) \end{cases} \quad (2.34)$$

Note that Eq. (2.34) implies $|\vec{d}(\mathbf{k})| = |\vec{d}(-\mathbf{k})|$ such that $\hat{d}_{x,z}(\mathbf{k}) = \hat{d}_{x,z}(-\mathbf{k})$ and $\hat{d}_y(\mathbf{k}) = -\hat{d}_y(-\mathbf{k})$ follows also for the *normalized* Bloch vector.

- \leftarrow Two bands from real spin- $\frac{1}{2}$: $\tilde{T}_1 = \sigma^y \mathcal{K}$

$$\sigma^y H^*(\mathbf{k}) \sigma^y = H(-\mathbf{k}) \quad \stackrel{(2.8)}{\Leftrightarrow} \quad \vec{d}(\mathbf{k}) = -\vec{d}(-\mathbf{k}) \quad (2.35)$$

Again it follows also for the *normalized* Bloch vector $\hat{d}(\mathbf{k}) = -\hat{d}(-\mathbf{k})$.

Both cases →

$$C \stackrel{2.13}{=} -\frac{1}{4\pi} \int_{-\pi}^{\pi} dk_x \int_{-\pi}^{\pi} dk_y \epsilon_{ijk} \hat{d}_i(\mathbf{k}) \tilde{\partial}_x \hat{d}_j(\mathbf{k}) \tilde{\partial}_y \hat{d}_k(\mathbf{k}) \stackrel{\circ}{=} 0 \quad (2.36)$$

This follows since $\hat{d}_i(\mathbf{k}) \tilde{\partial}_x \hat{d}_j(\mathbf{k}) \tilde{\partial}_y \hat{d}_k(\mathbf{k})$ is *antisymmetric* for both representations if i, j, k are pairwise distinct (which is enforced by ϵ_{ijk}). →

! Important

Systems with Chern bands must *break* time-reversal symmetry.

This is true in general, i.e., even for models with more than two bands.

- Note that this is completely consistent with the IQHE (or the Hofstadter model) where we found Chern bands and the *magnetic field* breaks TRS.
- This also makes sense from another perspective: Conductivity transforms as $\sigma \mapsto -\sigma$ under time-reversal since $\vec{J} = \sigma \vec{E}$ and $\vec{J} \mapsto -\vec{J}$ but $\vec{E} \mapsto \vec{E}$ (\downarrow *Maxwell equations*). Thus in a *time-reversal invariant* system it must be $\sigma = \sigma_a + \sigma_s = 0$. Note that $\sigma_a \neq 0$ indeed requires a magnetic field (which breaks time-reversal symmetry) and $\sigma_s \neq 0$ requires dissipation (recall the \leftarrow *Drude model*) and breaks time-reversal symmetry because of entropy production.
- This is a restriction (and a hint) for the construction of a Chern insulator.

2.1.3. Dirac fermions

As last preliminary step, we introduce a class of free fermion Hamiltonians *in the continuum* that is very useful to understand topological bands; we will use it as a starting point to construct our first Chern insulator *on the lattice*:

1 | $\triangleleft \downarrow$ Dirac equation in 2D: ($\hbar = 1$)

$$H_D \Psi = \left(\beta m + \sum_{n=1}^2 \alpha_n p_n \right) \Psi = i \partial_t \Psi \quad (2.37)$$

For a motivation/derivation in 3D see my script on \uparrow [Quantum Field Theory](#) [101, Section 3.1].

with

- $\alpha_1, \alpha_2, \beta$: Hermitian matrices
- $\alpha_1^2 = \alpha_2^2 = \beta^2 = \mathbb{1}$
- $\{\alpha_1, \alpha_2\} = \{\beta, \alpha_1\} = \{\beta, \alpha_2\} = 0$

→ Solution: $\alpha_1 = \sigma^x, \alpha_2 = \sigma^y, \beta = \sigma^z$ with 2-dimensional spinor $\Psi = \Psi(t, \mathbf{x})$

In 3D there is a *third* α -matrix and the algebra can only be solved by 4×4 -matrices (\downarrow γ -matrices).

2 | Fourier transform of H_D ($\mathbf{k} \in \mathbb{R}^2$):

Note that the spinor $\Psi(t, \mathbf{x})$ lives on continuous space $\mathbf{x} \in \mathbb{R}^2$, not on a lattice!

$$H_D(\mathbf{k}) = k_x \sigma^x + k_y \sigma^y + m \sigma^z = \vec{d}(\mathbf{k}) \cdot \vec{\sigma} \quad \text{with} \quad \vec{d}(\mathbf{k}) = \begin{pmatrix} k_x \\ k_y \\ m \end{pmatrix} \quad (2.38)$$

Here we used that in Fourier space the momentum operator $p_n = -i \partial_n$ is simply k_n .

Fermions in condensed matter physics that are (approximately) described by a 2-band *Bloch Hamiltonian* of the form Eq. (2.38) are therefore known as \star *Dirac fermions* (this also refers to more general Hamiltonians linear in \mathbf{k} , \rightarrow below).

→ Spectrum:

$$E_{\pm}(\mathbf{k}) \stackrel{2.9}{=} \pm |\vec{d}(\mathbf{k})| = \pm \sqrt{k^2 + m^2} \quad (2.39)$$

→ Gapped if $m \neq 0$

This is where the name “mass gap” comes from.

3 | Time-reversal symmetry:

- $\tilde{T}_0 = \mathcal{K} \rightarrow d_x(\mathbf{k}) \stackrel{!}{=} d_x(-\mathbf{k}) \rightarrow H_D$ not TRI!
- $\tilde{T}_{\frac{1}{2}} = \sigma^y \mathcal{K} \rightarrow d_z(\mathbf{k}) \stackrel{!}{=} -d_z(-\mathbf{k}) \rightarrow H_D$ not TRI for $m \neq 0$!

→ H_D is only TRI for $m = 0$, but there the gap closes anyway!

→ Non-zero Chern number *possible* ...

4 | Berry curvature: (of the lower band)

$$\mathcal{F}_{xy}(\mathbf{k}) \stackrel{\circ}{=} \frac{m}{2(k^2 + m^2)^{3/2}} \quad (2.40)$$

Proof: → Problemset 5

Use the form Eq. (2.13) to show this and remember that here momentum space is not a torus (Brillouin zone) but \mathbb{R}^2 (→ next).

5 | “Chern number”: (→ Problemset 5)

$$C \stackrel{2.13}{=} -\frac{1}{2\pi} \int_{\mathbb{R}^2} \mathcal{F}_{xy}(\mathbf{k}) d^2k = -\int_0^\infty \frac{mk}{2(k^2 + m^2)^{3/2}} dk \stackrel{\circ}{=} -\frac{\text{sign}(m)}{2} \quad (2.41)$$

Why $C \notin \mathbb{Z}$?

The quantization of C is based on Stokes theorem (← Section 1.3.1) which is only valid for integrations over compact manifolds (sphere, torus). Here, however, we integrate over the non-compact \mathbb{R}^2 instead, so we cannot expect C to be quantized.

Remember the geometric interpretation of the Chern number for two-band models as the number of times the sphere S^2 is covered by the Bloch vector when sweeping over momentum space (← Section 2.1.1). When you are on a non-compact space like \mathbb{R}^2 , you can start at one point where the Bloch vector points, say, at the north pole of S^2 . Then you let the vector continuously move towards the equator of S^2 for $|\mathbf{k}| \rightarrow \infty$ where the direction on S^2 is determined by the direction of \mathbf{k} in \mathbb{R}^2 . This produces a continuous function $\hat{d}(\mathbf{k})$ that wraps S^2 only “half.” Convince yourself that this construction necessarily fails on a compact momentum space like S^2 or T^2 .

Eq. (2.41) → Change from $m < 0$ to $m > 0 \Rightarrow$ Change of Chern number $\Delta C = -1$

6 | < 2-Band lattice model $H_\Gamma(\mathbf{k}) = \varepsilon_\Gamma(\mathbf{k})\mathbb{1} + \vec{d}_\Gamma(\mathbf{k}) \cdot \vec{\sigma}$

Γ : parameters of the model

We say that $\mathbf{K} \in T^2$ is a $\ast\ast$ Dirac point if

$$H_\Gamma(\mathbf{K} + \mathbf{k}) = v_F [k_x \sigma^x + k_y \sigma^y + v_F m_\Gamma \sigma^z] + \mathcal{O}(k^2) \quad (2.42)$$

$m_\Gamma = 0 \rightarrow$ Band structure at \mathbf{K} : $E_\pm(\mathbf{K} + \mathbf{k}) = \pm v_F |\mathbf{k}| \rightarrow \ast\ast$ Dirac cone

v_F : Fermi velocity (corresponds to the speed of light c in the Dirac equation)

In the following we set always $|v_F| = 1$.

Dirac points are interesting because they harbour “half a (anti-)skyrmion” (depending on the sign of m_Γ). When the sign of m_Γ changes at a gap closing (by varying Γ), this can change the (quantized) Chern number of the bands by ± 1 (as discussed ← above).

2.2. The Qi-Wu-Zhang Model

Historically, the Haldane model (see → *below*) was the first Chern insulator. However, it is not the *simplest* one (at least its momentum space representation is rather complex due to the honeycomb lattice). Later, QI, WU and ZHANG introduced a simpler model on the square lattice [102] which we will discuss first. “Simpler” refers here to its representation in momentum space – the real-space representation of the QWZ model is rather unintuitive.

1 | Idea: “Regularize” Dirac Hamiltonian on a lattice →

$$\langle H_{\text{QWZ}}(\mathbf{k}) = \vec{d}(\mathbf{k}) \cdot \vec{\sigma} \text{ with}$$

$$d_x := \sin(k_x) = k_x + \mathcal{O}(k^2) \tag{2.43a}$$

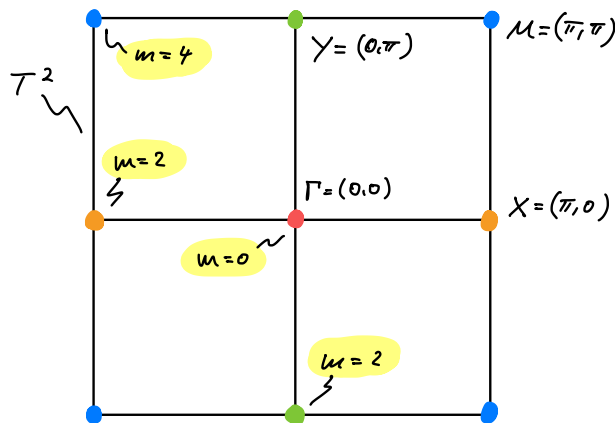
$$d_y := \sin(k_y) = k_y + \mathcal{O}(k^2) \tag{2.43b}$$

$$d_z := -m + 2 - \cos(k_x) - \cos(k_y) = -m + \mathcal{O}(k^2) \tag{2.43c}$$

$m \in \mathbb{R}$: only parameter of the theory

- The inverted sign of m is convention and motivated by the results (→ *below*).
- The two bands are interpreted as spin- $\frac{1}{2}$ degrees of freedom of fermions hopping on a square lattice (→ *below*).

2 | Spectrum: $E_{\pm}(\mathbf{k}) = \pm |\vec{d}(\mathbf{k})| \neq 0$ for all $\mathbf{k} \in T^2 \setminus \{\Gamma, X, Y, M\}$ with



In the sketch we indicate for which parameter m the gap *closes* at which point in the BZ. This follows directly by inspection of d_z in Eq. (2.43c).

↓ Lecture 10 [16.05.25]

3 | Phases:

With our knowledge from Section 2.1.3 we can now classify the four gapped phases separated by phase transitions at $m = 0, 2, 4$:

- $m < 0$:

Remember that neither the quantum phase nor the Chern number changes as long as the gap does not close. Hence we can choose a limit in the phase for $m < 0$ that makes the computation of the Chern number particularly simple:

$$\langle m \rightarrow -\infty \rightarrow \vec{d}(\mathbf{k}) \approx -m\vec{e}_z \rightarrow C(m < 0) = 0 \rightarrow \text{Trivial band insulator}$$

Recall that C counts the skyrmions in the BZ, i.e., how often $\hat{d}(\mathbf{k}) = \vec{d}(\mathbf{k})/|\vec{d}(\mathbf{k})|$ “wraps” around the sphere S^2 . But if \vec{d} is pinned to the north pole of S^2 , it cannot “wrap” anything.

- $m > 4$:

$$\langle m \rightarrow +\infty \rightarrow \vec{d}(\mathbf{k}) \approx -m\vec{e}_z \rightarrow C(m > 0) = 0 \rightarrow \text{Trivial band insulator}$$

The argument is the same as for $m < 0$.

- $0 < m < 2$:

↖ Transition from $m < 0$ to $m > 0$ → Gap closing at Γ :

$$H_{\text{QWZ}}(\Gamma + \mathbf{k}) = k_x\sigma^x + k_y\sigma^y - m\sigma^z + \mathcal{O}(k^2) \quad (2.44)$$

Eq. (2.41) →

$$C(0 < m < 2) = C(m < 0) + \Delta C(m < 0 \rightarrow m > 0) \quad (2.45a)$$

$$= 0 - \left[\frac{\text{sign}(-m)|_{m>0}}{2} - \frac{\text{sign}(-m)|_{m<0}}{2} \right] \quad (2.45b)$$

$$= +1 \quad (2.45c)$$

→ Topological phase (I)

- $2 < m < 4$:

↖ Transition from $m > 4$ to $m < 4$ → Gap closing at M :

$$H_{\text{QWZ}}(M + \mathbf{k}) = -k_x\sigma^x - k_y\sigma^y + (4 - m)\sigma^z + \mathcal{O}(k^2) \quad (2.46)$$

The negative signs of the momenta do not affect the result for the Chern number. You show this on ↻ Problemset 5, see also Eq. (2.60) in Section 2.3 later.

Eq. (2.41) →

$$C(2 < m < 4) = C(m > 4) + \Delta C(m > 4 \rightarrow m < 4) \quad (2.47a)$$

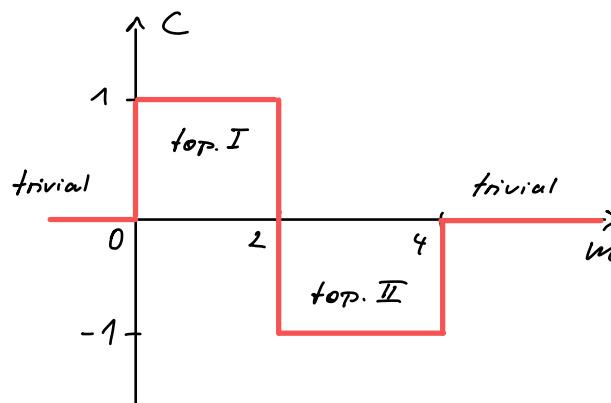
$$= 0 - \left[\frac{\text{sign}(4 - m)|_{m<4}}{2} - \frac{\text{sign}(4 - m)|_{m>4}}{2} \right] \quad (2.47b)$$

$$= -1 \quad (2.47c)$$

→ Topological phase (II) ≠ Topological phase (I)

In summary, this leads us to the ...

Phase diagram:



- The two trivial phases for $m < 0$ and $m > 4$ are the *same* trivial quantum phase, i.e., they can be connected by continuously deforming the Hamiltonian without closing the gap. To do this, start from the limit $m \ll 0$ where \vec{d} points to the north pole and then rotate this vector [more precisely: this (almost constant) function] continuously to the south pole (without changing its length). Then you end up in the phase for $m \gg 4$ while the gap on the path was always on the order of $|\vec{d}|$ (i.e., very large).
- By contrast, the two topological phases I and II are *different* quantum phases that cannot be connected by smooth deformations of the Hamiltonian without closing the gap. This follows from the discreteness of the Chern number and the definition of the latter in terms of the normalized Bloch vector $\hat{d}(\mathbf{k})$.
- Note that we can compute $C(2 < m < 4)$ alternatively via the transition from $m < 2$ to $m > 2$. At this transition there are *two* Dirac points (X and Y), each of which contributes a change of the Chern number by -1 which explains the jump from $C(0 < m < 2) = +1$ to $C(2 < m < 4) = -1$.
- It is recommended to plot $\vec{d}(\mathbf{k})$ on the BZ as a vector field and observe the changes for $m < 0$ to $m > 4$ (in Mathematica you can use the Manipulate function to visualize the changes). Try to count the skyrmions, i.e., how often $\vec{d}(\mathbf{k})$ “wraps” around the sphere (and in which direction).

Here is an animation (courtesy of Tobias Maier) of the Berry curvature on the Brillouin zone where m ramps from $m < 0$ to $m > 4$ and the Chern number (integral of the Berry curvature) is shown on the top:

↪ **Animation of the Berry curvature (GIF)**

The wrapping of the Bloch vector can be seen if, instead of the Berry curvature, the z -component $d_z(\mathbf{k})$ is plotted:

↪ **Animation of d_z (GIF)**

Note how (in the topological phases $0 < m < 4$) d_z goes from the north pole (red) to the south pole (blue), thereby wrapping the sphere S^2 once when traversing the Brillouin torus.

4 | Real-space Hamiltonian:

The real-space Hamiltonian of the QWZ model is defined on a square lattice with spin- $\frac{1}{2}$ fermions on the sites (the spin DOF is responsible for the two bands):

i | SP Hilbert space spanned by

$$|\Psi_{i\alpha}\rangle \rightarrow \underbrace{|x, y\rangle}_{\text{external}} \otimes \underbrace{|\sigma\rangle}_{\text{internal}} \tag{2.48}$$

$x = 1, \dots, N_x$: x -position

$y = 1, \dots, N_y$: y -position

$\sigma = \pm 1$: spin

The Pauli algebra is then represented as follows:

$$\sigma^x = |+1\rangle\langle-1| + |-1\rangle\langle+1| \tag{2.49a}$$

$$\sigma^y = i|-1\rangle\langle+1| - i|+1\rangle\langle-1| \tag{2.49b}$$

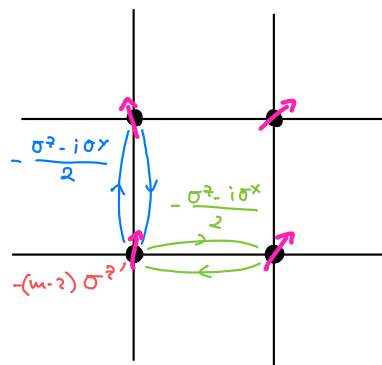
$$\sigma^z = |+1\rangle\langle+1| - |-1\rangle\langle-1| \tag{2.49c}$$

ii | SP Hamiltonian:

$$\begin{aligned} H_{\text{QWZ}} \stackrel{\circ}{=} & - \sum_{x,y} \left[|x+1, y\rangle\langle x, y| \otimes \frac{\sigma^z - i\sigma^x}{2} + \text{h.c.} \right] \\ & - \sum_{x,y} \left[|x, y+1\rangle\langle x, y| \otimes \frac{\sigma^z - i\sigma^y}{2} + \text{h.c.} \right] \\ & - (m-2) \sum_{x,y} |x, y\rangle\langle x, y| \otimes \sigma^z \end{aligned} \tag{2.50}$$

- The kinetic terms of the Hamiltonian (hopping in x - and y -direction) couple the spatial (“orbital”) motion with the internal (“spin”) degrees of freedom. This is an example of \downarrow *spin-orbit coupling* in a lattice model.
- Fourier transform H_{QWZ} in both spatial directions and show that the Bloch Hamiltonian is $H_{\text{QWZ}}(\mathbf{k})$ as defined above.

Pictorially:



iii | Note that there is no magnetic field involved and therefore no magnetic unit cell necessary.

→ This makes the QWZ model our first Chern insulator! ☺

(For the parameters $0 < m < 2$ or $2 < m < 4$, otherwise it is a trivial band insulator.)

Strictly speaking, we should use the SP Hamiltonian (2.50) to construct via Eq. (2.4) the corresponding second quantized MB Hamiltonian \hat{H}_{QWZ} that acts on fermionic Fock space.

The topological phase is then realized by the *many-body ground state* of \hat{H}_{QWZ} for $0 < m < 2$ or $2 < m < 4$. This ground state is the Fermi sea obtained by filling the lower of the two bands (both of which are Chern bands; recall that the sum of all Chern numbers always vanishes, ☺ Problemset 3).

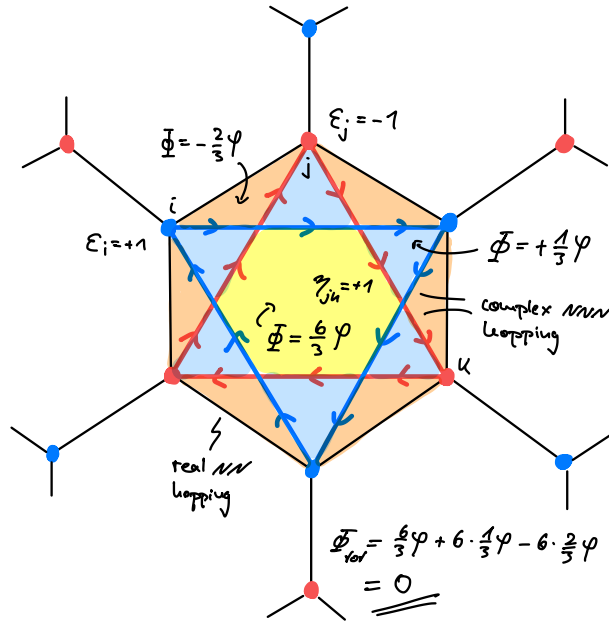
2.3. The Haldane Model

- Historically, the Haldane model (HM) on the honeycomb lattice was the first model that realized the phenomenology of the IQHE without (external) magnetic fields (and therefore without Landau levels) [19]; this phenomenon is nowadays referred to as *quantum anomalous Hall effect (QAHE)*.
- Hence the Haldane model is also regarded as the prototype of a \leftarrow *Chern insulator*. However, some also refer to the \leftarrow *Hofstadter model* as a Chern insulator* [35].
- Regarding classification (\leftarrow Section 0.6), the Haldane model belongs to the same \leftarrow *invertible topological order* as the IQHE (\leftarrow Chapter 1): it features chiral edge modes but no anyonic excitations and is not protected by any symmetry (only quantization of the Hall response requires charge conservation).
- HALDANE discussed this model in his 2016 Nobel Lecture [103].

1 | Rationale of the following construction:

1. Start with the Hamiltonian of \downarrow *graphene*:
→ 2 Dirac cones in the BZ (but not gapped!)
2. Add a staggered potential (parameter m) to break the \rightarrow *sublattice symmetry (SLS)* (\rightarrow ??):
→ Gap opens at Dirac points but Chern number is zero since TRS is not broken.
→ Dead end! ☹
3. Add instead a complex next-nearest neighbor (NNN) hopping (strength t and phase φ) to break \leftarrow *time-reversal symmetry*:
→ Gap opens at Dirac points *and* Chern number is non-zero.
→ Success! ☺
4. Map out the phase diagram in the m/t - φ plane.

2 | Real-space MB Hamiltonian on the honeycomb lattice:



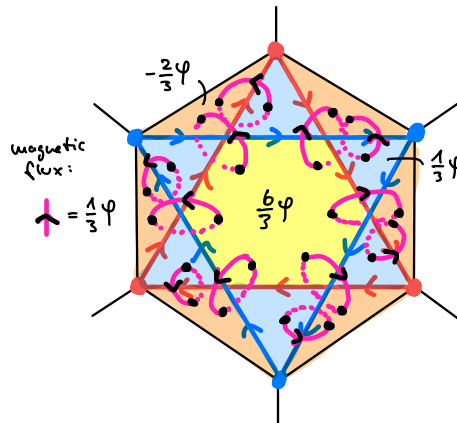
$$\hat{H}_H = \underbrace{\sum_{\langle i,j \rangle} c_i^\dagger c_j}_{\text{Graphene}} + m \underbrace{\sum_i \epsilon_i c_i^\dagger c_i}_{\text{Staggered potential}} + t \underbrace{\sum_{\langle\langle i,j \rangle\rangle} e^{i\eta_{ij}\varphi} c_i^\dagger c_j}_{\text{Complex NNN hopping}} \quad (2.51)$$

- $\langle i, j \rangle$: Nearest-neighbours (NN)
- $\langle\langle i, j \rangle\rangle$: Next-Nearest-neighbours (NNN)
- m : Strength of the staggered potential
- t : Strength of the complex NNN hopping
- φ : Phase of the complex NNN hopping
- $\epsilon_i = \pm 1$: Sublattice-dependent sign (see sketch above)
- $\eta_{ij} = \pm 1$ and $\eta_{ij} = -\eta_{ji}$: Direction-dependent sign
It is $\eta_{ij} = +1$ ($\eta_{ij} = -1$) if the arrow points from i to j (j to i) in the sketch above.

Notes:

- This is a two-band model because of the two sites in each unit cell of the honeycomb lattice, i.e., the fermions are *spinless*. (This is in contrast to the QWZ model where the two bands described internal spin degrees of freedom.)
- Despite the complex hopping, there is no *net* magnetic flux through the plaquettes of the honeycomb model, $\Phi_{\text{tot}} = 0$, hence no magnetic unit cell is needed (cf. the *Hofstadter model*).

- You can think of the complex hoppings arising from a *local* magnetic field “curled up” in each plaquette (maybe due to local magnetic moments in the material):



Note that other equivalent gauges (= distribution of complex hopping phases) are possible. For instance, one can “concentrate” the accumulated phase on the central third of the NNN hopping trajectories so that the outer (orange) triangles do not carry any flux and the blue triangles cancel the flux through the yellow hexagon.

- The staggered potential breaks → *sublattice symmetry* (SLS, Section 4.1) but not ← *time-reversal symmetry* (TRS, Section 2.1.2), whereas the complex NNN hopping breaks SLS *and* TRS. Breaking SLS *and/or* TRS is sufficient to open a gap at the Dirac points, but only breaking of TRS can result in bands with non-zero Chern number.

3 | Momentum space representation of H_H :

We want to understand the physics of Eq. (2.51) in momentum space:

i | Brillouin zone:

Honeycomb lattice = Hexagonal/Triangular lattice + 2-atom basis

- Hexagonal lattice → Brillouin zone
- 2-atom basis → 2 bands

Basis vectors of the Hexagonal lattice:

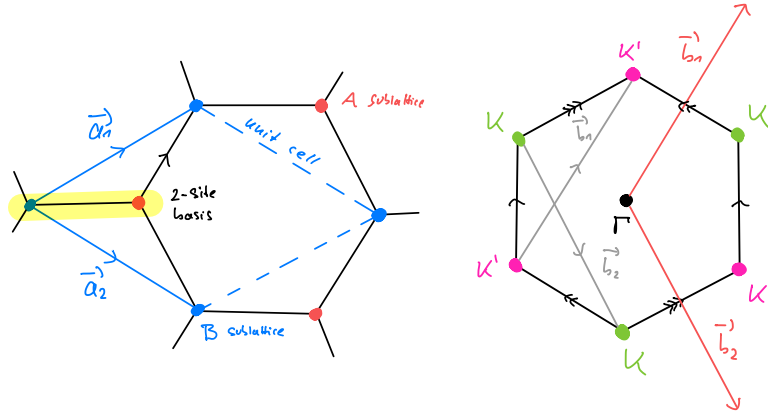
$$\mathbf{a}_1 = \frac{1}{2} (\sqrt{3}, 1)^T \quad \text{and} \quad \mathbf{a}_2 = \frac{1}{2} (\sqrt{3}, -1)^T \quad (2.52)$$

→ Reciprocal lattice (= Hexagonal lattice):

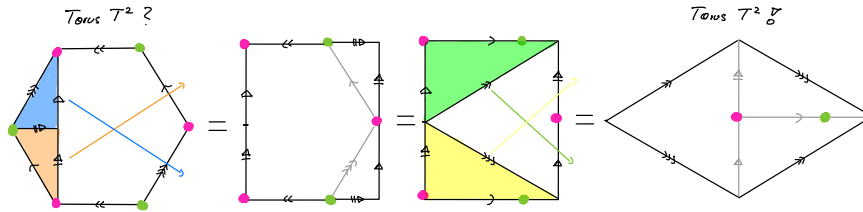
$$\mathbf{b}_1 = 2\pi \left(\frac{1}{\sqrt{3}}, 1 \right)^T \quad \text{and} \quad \mathbf{b}_2 = 2\pi \left(\frac{1}{\sqrt{3}}, -1 \right)^T \quad (2.53)$$

The ↓ *reciprocal lattice* is defined by vectors \mathbf{b} that satisfy $\mathbf{b} \cdot \mathbf{a} \in 2\pi\mathbb{Z}$ for $\mathbf{a} \in \mathbb{Z}\mathbf{a}_1 + \mathbb{Z}\mathbf{a}_2$ some lattice vector of the original lattice. The vectors \mathbf{b}_i above are a basis of this reciprocal lattice.

→ Brillouin zone = Wigner-Seitz cell of the reciprocal lattice:
 (= rotated Honeycomb plaquette)



Note that the BZ obtained from the Wigner-Seitz cell is a torus T^2 even though this is not obvious from its shape (the BZ of every 2D periodic system is a torus as it is just the parallelogram spanned by the reciprocal basis b_i with opposite edges identified):



(Edges with the same arrow type are identified along the direction indicated by the arrow.)

The last diagram is known as a fundamental polygon of the torus.

ii | Bloch Hamiltonian:

The two sublattice degrees of freedom per unit cell lead to a 2×2 Bloch Hamiltonian

$$H_H(\mathbf{k}) = \varepsilon(\mathbf{k})\mathbb{1} + \vec{d}(\mathbf{k}) \cdot \vec{\sigma} \text{ with}$$

$$d_x \doteq \cos(\mathbf{k}a_1) + \cos(\mathbf{k}a_2) + 1 \tag{2.54a}$$

$$d_y \doteq \sin(\mathbf{k}a_1) + \sin(\mathbf{k}a_2) \tag{2.54b}$$

$$d_z \doteq m + 2t \sin(\varphi) [\sin(\mathbf{k}a_1) - \sin(\mathbf{k}a_2) - \sin(\mathbf{k}(a_1 - a_2))] \tag{2.54c}$$

$$\varepsilon(\mathbf{k}) \doteq 2t \cos(\varphi) [\cos(\mathbf{k}a_1) + \cos(\mathbf{k}a_2) + \cos(\mathbf{k}(a_1 - a_2))] \tag{2.54d}$$

As $\varepsilon(\mathbf{k})$ has no effect on the gap and the Chern number, we set it the following to zero.

The above Bloch Hamiltonian follows straightforwardly from the Hamiltonian Eq. (2.51) together with the sketches above (for the sign conventions) and the Fourier transform

$$c_{x,r} = \frac{1}{\sqrt{L_1 L_2}} \sum_{\mathbf{k} \in T^2} e^{-i\mathbf{k}r} \tilde{c}_{x,\mathbf{k}} \quad \text{and} \quad \tilde{c}_{x,\mathbf{k}} = \frac{1}{\sqrt{L_1 L_2}} \sum_{r \in \mathcal{L}} e^{i\mathbf{k}r} c_{x,r} \tag{2.55}$$

of the fermion modes on the sublattices $x = A, B$ with $\mathcal{L} = a_1\mathbb{Z}_{L_1} + a_2\mathbb{Z}_{L_2}$ the (periodic) lattice and T^2 the Brillouin zone. It is then

$$\hat{H}_H = \sum_{\mathbf{k} \in T^2} \Psi_{\mathbf{k}}^\dagger H_H(\mathbf{k}) \Psi_{\mathbf{k}} \tag{2.56}$$

with $\Psi_{\mathbf{k}} = (\tilde{c}_{A,\mathbf{k}}, \tilde{c}_{B,\mathbf{k}})^T$.

iii | Gap can only close at the corners of the BZ (check this for $m = 0$ and $t = 0$):

$$\mathbf{K} \doteq \frac{2\pi}{3} (\sqrt{3}, 1) \quad \text{and} \quad \mathbf{K}' \doteq \frac{2\pi}{3} (\sqrt{3}, -1) \quad (2.57)$$

For $m = 0$ and $t = 0$ the Hamiltonian Eq. (2.51) describes the \downarrow *semimetal* \downarrow *Graphene* with two Dirac cones where the two bands touch.

iv | → Dirac Hamiltonians: (Here i, j run only over 1, 2: σ^x and σ^y)

$$H_H(\mathbf{K} + \mathbf{k}) \doteq k_i h_{ij} \sigma^j + \overbrace{[m - 3\sqrt{3}t \sin(\varphi)]}^{h_z} \sigma^z + \mathcal{O}(k^2) \quad (2.58a)$$

$$\text{with } h = \frac{\sqrt{3}}{2} \begin{bmatrix} 0 & -1 \\ 1 & 0 \end{bmatrix}$$

$$H_H(\mathbf{K}' + \mathbf{k}) \doteq k_i h'_{ij} \sigma^j + \overbrace{[m + 3\sqrt{3}t \sin(\varphi)]}^{h'_z} \sigma^z + \mathcal{O}(k^2) \quad (2.58b)$$

$$\text{with } h' = \frac{\sqrt{3}}{2} \begin{bmatrix} 0 & -1 \\ -1 & 0 \end{bmatrix}$$

We will use these two Dirac Hamiltonians to derive conditions when the gap closes (= a phase transition occurs) and to compute the Chern numbers of the bands using the tricks developed in Section 2.1.3.

4 | Gap closings:

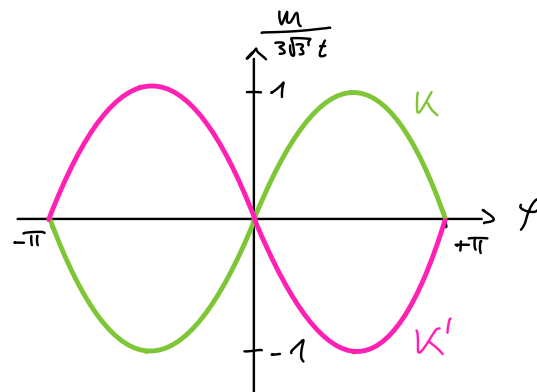
We start by identifying the parameters where the gap closes to pin down the phase transitions:

$$@\mathbf{K} : h_z \stackrel{!}{=} 0 \Leftrightarrow \frac{m}{3\sqrt{3}t} = +\sin(\varphi) \quad (2.59a)$$

$$@\mathbf{K}' : h'_z \stackrel{!}{=} 0 \Leftrightarrow \frac{m}{3\sqrt{3}t} = -\sin(\varphi) \quad (2.59b)$$

→ Preliminary phase diagram:

Eq. (2.59) suggests to use the ratio $\frac{m}{3\sqrt{3}t}$ of staggering strength m and NNN hopping strength t as an independent parameter:



There are 4 different parameter regimes that are separated by lines where the gap closes (note that the two points $\varphi = \pm\pi$ are identified). To identify the phases, we have to compute the Chern number (of the lower band) in all 4 areas ...

- 5 | To do this, we need the following generalized expression for the Chern number of a Dirac Hamiltonian (cf. Section 2.1.3 and our analysis of the QWZ model in Section 2.2):

$$H(\mathbf{k}) = \sum_{i,j=1}^2 k_i h_{ij} \sigma^j + h_z \sigma^z \Rightarrow C = -\frac{\text{sign}(h_z) \text{sign}(\det h)}{2} \quad (2.60)$$

Proof: → Problemset 5

Eqs. (2.58) and (2.60) →

$$C_{\mathbf{K}} = -\frac{1}{2} \text{sign}[m - 3\sqrt{3}t \sin(\varphi)], \quad (2.61a)$$

$$C_{\mathbf{K}'} = +\frac{1}{2} \text{sign}[m + 3\sqrt{3}t \sin(\varphi)]. \quad (2.61b)$$

The different sign for $C_{\mathbf{K}'}$ is due to $\det h' = -1$.

With these preparations we can finally characterize the four gapped phases ...

6 | Phases:

We use the same approach as for the QWZ model in Section 2.2.

- $m \rightarrow +\infty$:

$$\vec{d}(\mathbf{k}) \stackrel{2.54}{\approx} m \vec{e}_z \rightarrow \text{Trivial phase with } C = 0 \quad (2.62)$$

- $m \rightarrow -\infty$:

$$\vec{d}(\mathbf{k}) \stackrel{2.54}{\approx} m \vec{e}_z \rightarrow \text{Trivial phase with } C = 0 \quad (2.63)$$

- $0 < \varphi < \pi$ and change parameters as follows:

$$\underbrace{m > 3\sqrt{3}t \sin(\varphi)}_A \mapsto \underbrace{m < 3\sqrt{3}t \sin(\varphi)}_B \quad (2.64)$$

This means we cross a phase boundary where the gap closes at $\mathbf{K} \rightarrow$

$$C = 0 + C_{\mathbf{K}}(B) - C_{\mathbf{K}}(A) \stackrel{2.61a}{=} [-1/2 \cdot (-1)] - [-1/2 \cdot (+1)] = +1 \quad (2.65)$$

→ Topological phase (I)

- $-\pi < \varphi < 0$ and change parameters as follows: [note that $\sin(\varphi) < 0$]

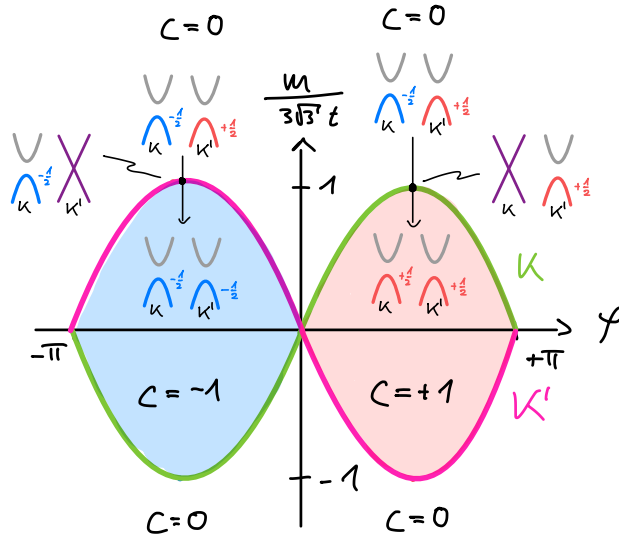
$$\underbrace{m > -3\sqrt{3}t \sin(\varphi)}_A \mapsto \underbrace{m < -3\sqrt{3}t \sin(\varphi)}_B \quad (2.66)$$

This means we cross a phase boundary where the gap closes at $\mathbf{K}' \rightarrow$

$$C = 0 + C_{\mathbf{K}'}(B) - C_{\mathbf{K}'}(A) \stackrel{2.61b}{=} [+1/2 \cdot (-1)] - [+1/2 \cdot (+1)] = -1 \quad (2.67)$$

→ Topological phase (II)

→ Phase diagram:



Thus in total there are *three* different phases, one trivial ($C = 0$) and two topological ($C = \pm 1$). Note that just as for the QWZ model, the two trivial regions with $C = 0$ are continuously connected without closing the gap, i.e., they are *the same phase*.

→ 2 × Topological phases + Trivial phase

7 | Time-reversal symmetry:

Finally, let us check when the model becomes time-reversal symmetric.

$\langle \tilde{T}_0 = \mathcal{K}$ & Eq. (2.34) (assume $t \neq 0$) →

$$d_x(\mathbf{k}) \stackrel{?}{=} d_x(-\mathbf{k}) \quad \checkmark \tag{2.68a}$$

$$d_y(\mathbf{k}) \stackrel{?}{=} -d_y(-\mathbf{k}) \quad \checkmark \tag{2.68b}$$

$$d_z(\mathbf{k}) \stackrel{?}{=} d_z(-\mathbf{k}) \quad \checkmark \text{ for } \varphi = 0, \pi \pmod{2\pi} \quad \times \text{ otherwise} \tag{2.68c}$$

The spin- $\frac{1}{2}$ TRS representation $\tilde{T}_{\frac{1}{2}} = \sigma^y \mathcal{K}$ is always broken, irrespective of the parameter φ .

→ $C = 0$ for $\varphi = 0, \pi \pmod{2\pi}$ (i.e., for real NNN hopping)

! Note that when TRS is broken for $\varphi \neq 0, \pi \pmod{2\pi}$, it is only *possible* that $C \neq 0$; the phase diagram above demonstrate that TRS breaking *not* sufficient.

2.4. ‡ Experiments

- In 2010 it was predicted that the QAHE could be observed in certain solid state systems [104], namely magnetic → *topological insulators*.
- These predictions were experimentally confirmed in 2013 [105] and further explored in the following years [106, 107].
- The Haldane model on the honeycomb lattice was artificially realized in a quantum simulator based on ultracold fermions in 2014 [108].
- Much later, in 2023, a quantum simulation with ultracold fermions of the Qi-Wu-Zhang model was reported [109].

3. Topological Bands with Time-Reversal Symmetry: The Topological Insulator

This section is based on various sources. A detailed account can be found in Bernevig's textbook [1]. However, also the original papers by KANE and MELE [110, 111] and FU and KANE [97, 112] are accessible and worthwhile to read. The concept of vector bundles is discussed by CARPENTIER [113, 114] from a physicist's perspective; a more mathematical account is given by WEHEFRITZ-KAUFMANN [115]. The mathematical foundations underlying topological band theory (in particular the concepts of vector bundles and their characterization) are covered in the textbooks by NASH and SEN [116] and NAKAHARA [12].

We seek for models with the following properties:

- Lattice model
- Band insulator
- Time-reversal symmetric (!)
- Topological band structure (!)

;! We do not call for *Chern bands* as we know that this is impossible without breaking time-reversal symmetry. So we need to look for another topological invariant ...

Before we proceed, let us fix the nomenclature:

✱ Definition: Topological insulator

$$\text{Topological insulator (TI)} := \begin{cases} \text{Lattice model} \\ \text{Band insulator} \\ \text{Topological band structure} \\ \text{Time-reversal symmetric} \end{cases} \quad (3.1)$$

Prototype: Kane-Mele model

With this definition, the question we want to answer is:

Are there topological insulators?

The term “topological insulator” is not used consistently in the literature. In particular, the above definition is only one of at least three:

- Sometimes “TI” refers specifically to the Kane-Mele model. This is usually the case when people talk about *the* topological insulator.

- Sometimes “TI” is used to denote the class of gapped free fermion theories with time-reversal symmetry, particle number conservation (to distinguish them from superconductors, → *later*) and topological bands. This is essentially our definition above.
- Sometimes “TI” refers to arbitrary band insulators with topological bands (then including also Chern insulators). This is how the term is used when referring to the class of *topological insulators & superconductors*. I.e., there the term “insulator” distinguishes models from “superconductors” (which violate particle number conservation) without referring to time-reversal symmetry.

So be aware of this when you study other sources.

3.1. Construction of the Kane-Mele model

1 | Starting point: ← Low-energy theory of ← *graphene*:

Recall that this is just the ← *Haldane model* for $m = 0 = t$ [Eq. (2.58)]:

$$H(\mathbf{K} + \mathbf{k}) = -\frac{\sqrt{3}}{2}(k_x\sigma^y - k_y\sigma^x) \quad (3.2a)$$

$$H(\mathbf{K}' + \mathbf{k}) = -\frac{\sqrt{3}}{2}(k_x\sigma^y + k_y\sigma^x) \quad (3.2b)$$

To translate into the conventions used in the original papers, we rotate in momentum space by $\pi/2$ so that $k_x \mapsto k_y$ and $k_y \mapsto -k_x$:

$$H(\mathbf{k}) := H(\mathbf{K} + \mathbf{k}) = -\frac{\sqrt{3}}{2}(k_x\sigma^x + k_y\sigma^y) \quad (3.3a)$$

$$H'(\mathbf{k}) := H(\mathbf{K}' + \mathbf{k}) = -\frac{\sqrt{3}}{2}(-k_x\sigma^x + k_y\sigma^y) \quad (3.3b)$$

2 | The low-energy physics is determined by momentum modes in the vicinity of \mathbf{K} and \mathbf{K}' . We can therefore combine the two Bloch Hamiltonians by a direct sum (corresponding to the direct sum of low-energy single-particle momentum modes): →

$$\tilde{H}_0(\mathbf{k}) := H(\mathbf{k}) \oplus H'(\mathbf{k}) \quad (3.4a)$$

$$= v_F \begin{pmatrix} k_x\sigma^x + k_y\sigma^y & 0 \\ 0 & -k_x\sigma^x + k_y\sigma^y \end{pmatrix} \quad (3.4b)$$

$$= v_F(\sigma^x \otimes \tau^z k_x + \sigma^y \otimes \mathbb{1} k_y) \quad (3.4c)$$

$$\equiv v_F(\sigma^x \tau^z k_x + \sigma^y k_y) \quad (3.4d)$$

- σ^i : band DOF (mixes modes of upper/lower bands)
- τ^i : valley DOF (mixes modes between valleys \mathbf{K}/\mathbf{K}')
- $v_F = -\sqrt{3}/2$: Fermi velocity

3 | Time-reversal:

Note that under time-reversal we have $\mathbf{K} + \mathbf{k} \mapsto -\mathbf{K} - \mathbf{k} = \mathbf{K}' - \mathbf{k}$ so that in the low-energy description time-reversal flips the valley DOF; this can be achieved by τ^x :

$$\tilde{T}_0 := \mathbb{1}_\sigma \otimes \tau^x \mathcal{K} \quad \text{with} \quad \tilde{T}_0^2 = +\mathbb{1} \quad (3.5)$$

$$\rightarrow \tilde{T}_0 \tilde{H}_0(\mathbf{k}) \tilde{T}_0^{-1} = \tilde{H}_0(-\mathbf{k})$$

The time-reversal operator of spinless graphene is simply $T_0 = \mathcal{K}$ (all terms in the Hamiltonian are real). The τ^x in Eq. (3.5) is a consequence of our low-energy description at the two Dirac points.

4 | Add Spin- $\frac{1}{2}$: Pauli matrices μ^i with $i = x, y, z$

This gives us more possibilities to add gap-opening terms to \tilde{H}_0 . It is also physically motivated: electrons *do have* spin!

$$\tilde{H}_{\frac{1}{2}}(\mathbf{k}) := v_F (\sigma^x \otimes \mathbb{1}_\mu \otimes \tau^z k_x + \sigma^y \otimes \mathbb{1}_\mu \otimes \mathbb{1}_\tau k_y) \quad (3.6a)$$

$$\equiv v_F (\sigma^x \tau^z k_x + \sigma^y k_y) \quad (3.6b)$$

→ Bloch space $\mathcal{H}(\mathbf{k}) \simeq \mathbb{C}^2 \otimes \mathbb{C}^2 \otimes \mathbb{C}^2 \simeq \mathbb{C}^8$

→ Time-reversal:

$$\tilde{T}_{\frac{1}{2}} := \mathbb{1}_\sigma \otimes \mu^y \otimes \tau^x \mathcal{K} \quad \text{with} \quad \tilde{T}_{\frac{1}{2}}^2 = -\mathbb{1} \quad (3.7)$$

$$\rightarrow \tilde{T}_{\frac{1}{2}} \tilde{H}_{\frac{1}{2}}(\mathbf{k}) \tilde{T}_{\frac{1}{2}}^{-1} = \tilde{H}_{\frac{1}{2}}(-\mathbf{k})$$

Note that this model is perfectly spin-degenerate: we “copied” the 4-band model \tilde{H}_0 to represent spin *up* and *down*, but didn’t add any coupling between the two copies yet!

5 | Goal: Open topological gap by adding terms to $\tilde{H}_{\frac{1}{2}}(\mathbf{k})$:

At this point it is unclear what we mean by a “topological gap” (→ *below*).

The rationale is to use the linearized Bloch Hamiltonian for this construction because it is simpler. We can then later reconstruct a *lattice* model from the low-energy (= small momentum) Hamiltonian as we did for the QWZ model. The 8 bands of $\tilde{H}_{\frac{1}{2}}$ will therefore reduce again to 4 bands since the valley Hilbert space \mathbb{C}^2 does not exist for a true lattice model.

i | Observation I: Must contain σ^z !

Because otherwise we only shift the position of the Dirac points:

$$\tilde{H}(\mathbf{k}) = v_F [\sigma^x \tau^z k_x + \sigma^y k_y] + v_F (\delta_x \sigma^x \tau^z + \delta_y \sigma^y) \quad (3.8a)$$

$$= v_F [\sigma^x \tau^z (k_x + \delta_x) + \sigma^y (k_y + \delta_y)] \quad (3.8b)$$

$$= H(\underbrace{\mathbf{K} + \delta}_{\mathbf{K}_\delta} + \mathbf{k}) \oplus H(\underbrace{\mathbf{K}' + \delta}_{\mathbf{K}'_\delta} + \mathbf{k}) \quad (3.8c)$$

with $\delta = (\delta_x, \delta_y)^T$. You can think of δ_x and δ_y as operators (products of Pauli matrices) that do not contain any σ^i matrices. Then Eq. (3.8a) is the most general modification *without* using σ^z . The argument that the cones are shifted but not gapped then applies within the eigenspaces of the operators δ_x and δ_y .

ii | We know already the Trivial mass term: [cf. Eq. (2.58) for $t = 0$]

$$\delta \tilde{H}_m(\mathbf{k}) = m \sigma^z \quad (3.9)$$

→

✓ Time-reversal invariant [since $\tilde{T}_{\frac{1}{2}} \delta \tilde{H}_m(\mathbf{k}) \tilde{T}_{\frac{1}{2}}^{-1} = \delta \tilde{H}_m(-\mathbf{k})$]

✓ Opens a gap of $2m$

✗ *But*: Bands are topologically trivial ☹

They are “topologically trivial” because their Chern number vanishes. However, below we will derive a new topological invariant distinct from the Chern number, so that this statement seems short-sighted. The true argument is therefore that for $m \rightarrow \infty$ the

system is clearly a trivial band insulator where one sublattice is empty and the other completely filled; this phase is “trivial” in the original sense of being a product state. Then, no matter which topological invariant we cook up, to comply with our physically motivated notion of “trivial”, it *must* vanish in the gapped phase dominated by $\delta\tilde{H}_m$.

→ So we should look for other gap opening terms ...

iii | We also know the Haldane mass term:

$$\text{Eq. (2.58)} \quad \xrightarrow[m=0]{\varphi=-\pi/2} \quad \delta\tilde{H}_H(\mathbf{k}) = \tau^z \sigma^z 3\sqrt{3}t \quad (3.10)$$

Because of the valley encoding, we can now combine both Hamiltonians in Eq. (2.58) into a single expression with τ^z .

→ $\tilde{H}_H := \tilde{H}_{\frac{1}{2}} + \delta\tilde{H}_m + \delta\tilde{H}_H =$ two independent copies of the Haldane model (one for spin *up*, one for spin *down*)

→ Not TRI:

$$\tilde{T}_{\frac{1}{2}} \delta\tilde{H}_H(\mathbf{k}) \tilde{T}_{\frac{1}{2}}^{-1} \neq \delta\tilde{H}_H(-\mathbf{k}) \quad \ominus \quad (3.11)$$

Of course you do not have to check this. Since the two copies of the Haldane model are independent, we can consider them separately. But each allows for bands with non-zero Chern numbers (this was the point!). But then the model must *break* TRS because we know that this is a necessary condition for non-zero Chern numbers in the first place (← Section 2.1.2).

iv | Observation II: Must contain spin-coupling that *anticommutes* with $\tilde{T}_{\frac{1}{2}}$!

→

$$\delta\tilde{H}_{\text{KM}}(\mathbf{k}) := \lambda_{\text{SO}} \sigma^z \otimes \mathbb{1}_{\mu} \otimes \tau^z \quad \propto \delta\tilde{H}_H \quad \rightarrow \text{Not TRI} \quad \times \quad (3.12a)$$

$$\delta\tilde{H}_{\text{KM}}(\mathbf{k}) := \lambda_{\text{SO}} \sigma^z \otimes \mu^{\{x,y,z\}} \otimes \mathbb{1}_{\tau} \quad \rightarrow \text{Not TRI} \quad \times \quad (3.12b)$$

$$\delta\tilde{H}_{\text{KM}}(\mathbf{k}) := \lambda_{\text{SO}} \sigma^z \otimes \mu^{\{x,y,z\}} \otimes \tau^z \quad \rightarrow \text{TRI} \quad \checkmark \quad (3.12c)$$

→ **** Kane-Mele mass term**

- Couples “orbital” DOFs (τ^z) with spin DOFs (μ^z)
→ Discrete version of \downarrow *Spin-orbit coupling (SO)*
- $\delta\tilde{H}_{\text{KM}}(\mathbf{k})$ is just Haldane’s TRS breaking term $\tau^z \sigma^z 3\sqrt{3}t \sin(\varphi)$ augmented by spin-orbit coupling to “recover” time-reversal symmetry.
- The choice of μ^z is arbitrary since all μ^i anticommute with $\tilde{T}_{\frac{1}{2}}$. It is just conventional to think in the z -basis for spin (i.e., spin “up” and “down” now have conjugate imaginary hopping phases). Note also that on its own, μ^z is interchangeable with the other Pauli matrices by permutations (or spin rotations) without changing the spin-algebra.

6 | Kane-Mele model:

Low-energy description:

$$\tilde{H}'_{\text{KM}}(\mathbf{k}) := \tilde{H}_{\frac{1}{2}}(\mathbf{k}) + \delta\tilde{H}_m(\mathbf{k}) + \delta\tilde{H}_{\text{KM}}(\mathbf{k}) \quad (3.13)$$

→ Reconstruction of the Full lattice model:

$$\hat{H}'_{\text{KM}} = \underbrace{\sum_{\langle i,j \rangle, \alpha} c_{i\alpha}^\dagger c_{j\alpha}}_{\text{Spinful graphene}} \underbrace{+ m \sum_{i, \alpha} \epsilon_i c_{i\alpha}^\dagger c_{i\alpha}}_{\text{Staggered potential}} \underbrace{+ \lambda_{\text{SO}} \sum_{\langle\langle i,j \rangle\rangle, \alpha, \beta} i \eta_{ji} c_{i\alpha}^\dagger \mu_{\alpha\beta}^z c_{j\beta}}_{\text{Complex NNN hopping with SO coupling}} \quad (3.14)$$

$c_{i\alpha}^\dagger$: Creates fermion with spin $\alpha \in \{\uparrow, \downarrow\}$ on site i

- Note that the phase in the Kane-Mele term is the phase $e^{i\eta_{ij}\varphi}$ of the Haldane term for $\varphi = -\pi/2$.
- If you don't believe this, you can retrace our path to derive the Dirac Hamiltonian for the Haldane model again for the Kane-Mele model to derive $\tilde{H}'_{\text{KM}}(\mathbf{k})$ in Eq. (3.13) from Eq. (3.14).
- The model (3.14) (together with the Rashba term → below) was introduced by C. L. KANE and E. J. MELE in 2005 [110, 111] under the name *Quantum spin Hall effect* as a time-symmetric generalization of Haldane's *Chern insulator* discussed in Chapter 2 (the designation "Quantum spin Hall effect" is a bit misleading and subtle, see comments at the end of Section 3.4).

7 | Observation III: \hat{H}'_{KM} does *not* mix spin:

$$\left[\hat{H}'_{\text{KM}}, N_\alpha \right] = 0 \quad \text{with} \quad N_\alpha := \sum_i c_{i\alpha}^\dagger c_{i\alpha} \quad (3.15)$$

→ \hat{H}'_{KM} = two *decoupled* copies of the Haldane model with opposite complex phases

Note that this rather trivial construction already fixed the breaking of time-reversal symmetry because the two copies map onto each other under time reversal. However ...

→ Not generic

Mixing of up and down spins can happen, e.g., by applying an electric field perpendicular to the plane. The conservation of spin should not be necessary for the system to be time-reversal symmetric. That is, the model H'_{KM} is a bit too symmetric ...

→ Add term that *breaks* the unitary symmetry generated by N_α (but preserves TRS)

8 | Rashba term:

There is indeed another SO coupling term that does not break TRS known as

✱ *Rashba spin-orbit coupling*:

$$\delta \tilde{H}_{\text{R}}(\mathbf{k}) := \lambda_{\text{R}} \left[\sigma^x \mu^y \tau^z - \sigma^y \mu^x \right] \quad (3.16)$$

→ $\tilde{T}_{\frac{1}{2}} \delta \tilde{H}_{\text{R}}(\mathbf{k}) \tilde{T}_{\frac{1}{2}}^{-1} = \delta \tilde{H}_{\text{R}}(-\mathbf{k})$

- Does not open a gap (missing σ^z) ...
- ... but *modifies* the gap generated by the Kane-Mele term.
- *Breaks* spin conservation (the \uparrow and \downarrow sectors no longer decouple)

This type of SO coupling in 2D systems was first studied by Y. A. BYCHKOV and E. I. RASHBA in 1984 [117], i.e., long before the discovery of the Kane-Mele model.

→ We make the KM model more generic by adding the Rashba term:

$$\hat{H}_{\text{KM}} := \hat{H}'_{\text{KM}} + \underbrace{\lambda_R \sum_{\langle i,j \rangle, \alpha, \beta} c_{i\alpha}^\dagger R_{ij}^{\alpha\beta} c_{j\beta}}_{\text{NN hopping with Rashba SO coupling}} \stackrel{\triangleq}{=} \delta \tilde{H}_R(\mathbf{k}) \quad (3.17)$$

with

$$R_{ij}^{\alpha\beta} \stackrel{\triangleq}{=} i \left[(\vec{\mu} \times \vec{d}_{ij}) \cdot \hat{e}_z \right]_{\alpha\beta} \quad (3.18)$$

\vec{d}_{ij} : vector from site i to site j (in the x - y -plane)

$\vec{\mu} = (\mu^x, \mu^y, \mu^z)$: vector of spin matrices

\hat{e}_z : unit vector in z -direction

- Note that $(\vec{\mu} \times \vec{d}_{ij})_z = \mu^x d_{ij}^y - \mu^y d_{ij}^x$ is a Hermitian 2×2 matrix.
- Because of the μ^x and μ^y in the Rashba term, it is now $[\hat{H}_{\text{KM}}, N_\alpha] \neq 0$ so that \hat{H}_{KM} can no longer be interpreted as a sum of two independent Haldane models.
- The direction-dependent phase and spin-coupling of the *Kane-Mele term* can be encoded in a similar form (for the fixed hopping phase $\varphi = -\pi/2$):

$$H_{ij}^{\alpha\beta} := e^{\eta_{ij} i \varphi} \mu_{\alpha\beta}^z = -i \eta_{ij} \mu_{\alpha\beta}^z \stackrel{\triangleq}{=} i 2\sqrt{3} \left[(\vec{d}_{ik} \times \vec{d}_{kj}) \cdot \vec{\mu} \right]_{\alpha\beta} \quad (3.19)$$

where k denotes the site that is *skipped* when jumping from i to the next-nearest neighbour j .

- You can think of the Rashba term being induced by an *electric* field perpendicular to the 2D system. Then electrons hopping from one site to another experience an *in-plane magnetic field* (remember your course on \downarrow *electrodynamics*) which couples to the magnetic moment induced by the spin via μ^x - and μ^y -components. The direction of the magnetic field depends on the direction the electron hops, which explains the directional dependence in Eq. (3.18).

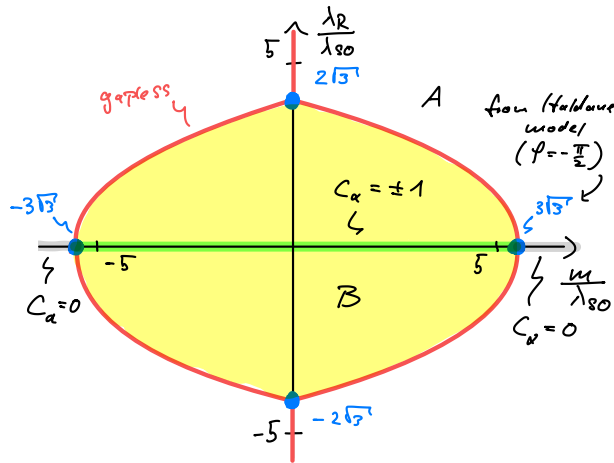
3.2. Phase diagram

We are now ready to sketch the phase diagram of \hat{H}_{KM} by identifying the *gapped phases* in parameter space and the *gapless phase transitions* that separate them:

1 | Gap closings:

We have three parameters (in units of the graphene hopping strength). For simplicity, we fix the Kane-Mele term λ_{SO} and plot the gap closings in the λ_R - m -plane:

$$\ll 0 < \lambda_{SO} = \text{const} \ll 1:$$



- The gapless values on the m -axis follow directly from our discussion of the Haldane model with $\varphi = -\pi/2$.
- Note that there are two gapless lines emanating from region B along the λ_R -axis. These divide region A , which must be the trivial phase (because it contains the limit $m \rightarrow \pm\infty$ in which the system is clearly in a product state). As before, one can connect these two halves of region A without crossing the gapless line on the γ_R -axis by extending the Hamiltonian appropriately, i.e., there is only *one* (trivial) phase A .
- To derive the full plot, you must Fourier transform \hat{H}_{KM} on a periodic lattice to derive the 4×4 -Bloch Hamiltonian,

$$\tilde{H}_{KM}(\mathbf{k}) = \sum_{i=1}^5 d_i(\mathbf{k})\Gamma_i + \sum_{i<j=1}^5 d_{ij}(\mathbf{k})\Gamma_{ij} \tag{3.20}$$

which is generated by (at most) 15 terms which take the place of the three-component Bloch vector $\vec{d}(\mathbf{k})$ for models with two bands. Recall that $n \times n$ Hamiltonians (with vanishing trace) generate unitaries in the group $SU(n)$ which has $n^2 - 1$ generators; e.g., 3 Pauli matrices for $n = 2$ or 15 Γ -matrices for $n = 4$. The generators for $n = 4$ satisfy $\{\Gamma_i, \Gamma_j\} = 2\delta_{ij}$ and $\Gamma_{ij} = 1/2i [\Gamma_i, \Gamma_j]$ with $i, j \in \{1, \dots, 5\}$. See [111] for the expressions for d_i and d_{ij} .

2 | $\ll \lambda_R = 0$ (m -axis in the above plot)

- Spin-sectors decouple
- Chern number C_α of spin-polarized sub-bands well-defined →

$$I^* := \frac{C_\uparrow - C_\downarrow}{2} \text{ mod } 2 = \begin{cases} 1 & \text{topological phase of Haldane model(s)} \\ 0 & \text{trivial phase of Haldane model(s)} \end{cases} \tag{3.21}$$

Note that the *sum* $C_\uparrow + C_\downarrow = 0$ of the filled bands is zero everywhere because of TRS!

- Suggests that Phase B is in some sense topological. (Phase A is a trivial insulator.)
- Not characterized by I^* since I^* requires spin-conservation, whereas the phase is stable against perturbations that violate spin-conservation (like the Rashba term).
- What characterizes Phase B?

3.3. Vorticity of the Pfaffian and the \mathbb{Z}_2 -Index

So what is the label that distinguishes the two phases of the Kane-Mele model?

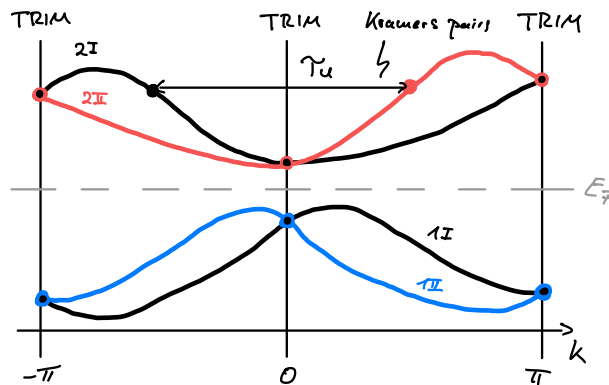
We need a *new topological index* that replaces the Chern number ...

3 | \triangleleft TRI system with $\tilde{T}_U^2 = -1 \rightarrow$ Band crossings at TRIMs

TRIM \equiv $\star\star$ Time-reversal invariant momentum

$$K^* \in T^2 : \text{TRIM} \Leftrightarrow -K^* = K^* + G, \quad G : \text{reciprocal lattice vector} \quad (3.22)$$

\rightarrow Generic bandstructure of TRI System in 1D with $\tilde{T}_U^2 = -1$:

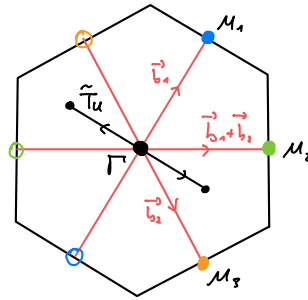


\triangleleft Gapped system \rightarrow Even number $2n$ of filled bands

- Note that time-reversal symmetry (irrespective of $T_U^2 = \pm 1$) implies the $k \leftrightarrow -k$ symmetry of the spectrum [\leftarrow Eq. (2.33)]. However, this does *not* imply a degeneracy at the TRIMs! (Think of free fermions on a lattice.)
- If $T_U^2 = -1 \Leftrightarrow \tilde{T}_U^2 = -1$, \leftarrow Kramers theorem (\leftarrow Section 2.1.2, \rightarrow Problemset 6) applies to the single-particle Hamiltonian, $T_U H T_U^{-1} = H$, and demands a two-fold degeneracy for every eigenenergy. At the TRIMs, this necessitates a crossing band; hence all bands come in pairs!
- For the Bloch Hamiltonians $H(k)$, Kramers theorem does *not* apply in general, since TRI requires $\tilde{T}_U H(k) \tilde{T}_U^{-1} = H(-k)$ which is *not* a symmetry of $H(k)$. Only at the TRIMs we have $\tilde{T}_U H(K^*) \tilde{T}_U^{-1} = H(-K^*) = H(K^* + G) = H(K^*)$ so that Kramers theorem implies a two-fold degeneracy *in the Bloch space* of a TRIM K^* . This is another perspective on the band crossings at the TRIMs.
- Note that the Kramers pairs of bands (I and II) *can* be degenerate everywhere in the BZ (for the Kane-Mele model they are perfectly degenerate for $\lambda_R = 0 = m$). TRI only requires this degeneracy at the TRIMs but does not exclude it elsewhere.

In particular, there are ...

Four TRIMs for the hexagonal lattice:



4 | \leftarrow Matrix of \tilde{T}_U on occupied Bloch space $\mathcal{H}_k^{\text{filled}} := \text{span} \{|u_i(\mathbf{k})\rangle\}_{i=1\dots 2n}$

Here, i, j run over the occupied bands. For the 4-band Kane-Mele model, this means $i, j \in \{1, 2\}$ which correspond to the filled lower bands of the spin-up and -down copy of the Haldane model (for $\lambda_R = 0$).

$$M_{ij}(\mathbf{k}) := \langle u_i(\mathbf{k}) | \tilde{T}_U | u_j(\mathbf{k}) \rangle \tag{3.23a}$$

$$= \langle u_i(\mathbf{k}) | U u_j^*(\mathbf{k}) \rangle \tag{3.23b}$$

$$= -\langle U^* u_i(\mathbf{k}) | u_j^*(\mathbf{k}) \rangle \tag{3.23c}$$

$$= -\langle u_j(\mathbf{k}) | U u_i^*(\mathbf{k}) \rangle \tag{3.23d}$$

$$= -\langle u_j(\mathbf{k}) | \tilde{T}_U | u_i(\mathbf{k}) \rangle \tag{3.23e}$$

$$\stackrel{\circ}{=} -M_{ij}^T(\mathbf{k}) \tag{3.23f}$$

Here we used $U^\dagger = (U^*)^T$ and $U^T = -U$ since $\tilde{T}_U^2 = \tilde{T}_{\frac{1}{2}}^2 = -\mathbb{1}$ with $\tilde{T}_{\frac{1}{2}} = \mathbb{1}_\sigma \otimes \mu^y \mathcal{K}$.

- The matrix $M(\mathbf{k})$ is Gauge-dependent (= depends on chosen basis of $\mathcal{H}_k^{\text{filled}}$)
- For every $\mathbf{k} \in T^2$, $M(\mathbf{k})$ is a Skew-symmetric matrix of even dimensions (Remember that TRI demands an even number of filled bands.)

↓ Lecture 12 [23.05.25]

5 | → < Pfaffian:

Definition: For M a skew-symmetric $2n \times 2n$ -matrix, the Pfaffian is defined as

$$\text{Pf}[M] := \frac{1}{2^n n!} \sum_{\sigma \in S_{2n}} (-1)^\sigma \prod_{i=1}^n M_{\sigma(2i-1), \sigma(2i)} \quad (3.24)$$

Cf. the ↓ *Leibniz formula* for determinants:

$$\det(M) = \sum_{\sigma \in S_{2n}} (-1)^\sigma \prod_{i=1}^{2n} M_{i\sigma(i)} \quad (3.25)$$

→ It follows:

- $(\text{Pf}[M])^2 = \det(M)$, i.e., the Pfaffian contains the same information as the determinant (but with an additional sign that is lost when considering the determinant).
- $\text{Pf}[BAB^T] = \det(B) \text{Pf}[A]$ for an arbitrary $2n \times 2n$ -matrix B
- For skew-symmetric matrices of even dimension, the Pfaffian is a “more natural” object than the determinant (it contains at least as much information!).

This motivates the definition of the following function:

$$P : T^2 \rightarrow \mathbb{C} \quad P(\mathbf{k}) := \text{Pf}[M(\mathbf{k})] \quad (3.26)$$

Kane-Mele model: $P(\mathbf{k}) = M_{12}(\mathbf{k}) = \langle u_1(\mathbf{k}) | \tilde{T}_U | u_2(\mathbf{k}) \rangle$

→ $P(\mathbf{k})$ is a complex-valued function on the BZ that depends (continuously) on the Hamiltonian.

The idea is now to identify topologically robust properties of this function to distinguish the two phases of the Kane-Mele model ...

6 | Properties of $P(\mathbf{k})$:

Next, we carefully study the properties of $P(\mathbf{k})$ to lay the foundations for a new topological index defined → *below*:

i | Not gauge invariant: $\leftarrow U \in \text{U}(2n)$ and $|u'_i(\mathbf{k})\rangle := U_{ij} |u_j(\mathbf{k})\rangle$

This gauge transformation mixes the $2n$ filled bands!

w.l.o.g. $U = e^{i\phi} \tilde{U}$ with $\tilde{U} \in \text{SU}(2n) \rightarrow$

$$P'(\mathbf{k}) = \text{Pf} \left[\left(\langle u'_i(\mathbf{k}) | \tilde{T}_U | u'_j(\mathbf{k}) \rangle \right)_{ij} \right] \quad (3.27a)$$

$$= \text{Pf} \left[\left(U_{ii'}^* \langle u_{i'}(\mathbf{k}) | \tilde{T}_U | u_{j'}(\mathbf{k}) \rangle U_{jj'}^* \right)_{ij} \right] \quad (3.27b)$$

$$= \text{Pf} \left[U^* \left(\langle u_{i'}(\mathbf{k}) | \tilde{T}_U | u_{j'}(\mathbf{k}) \rangle \right)_{i'j'} (U^*)^T \right] \quad (3.27c)$$

$$= \det(U^*) P(\mathbf{k}) \quad (3.27d)$$

$$= e^{-i2n\phi} P(\mathbf{k}) \quad (3.27e)$$

Here we used that $\det(\tilde{U}) = 1$.

→ $|P(\mathbf{k})|$ is gauge invariant

Note: We can consider even unitary transformations *between* filled bands (for a fixed \mathbf{k}) although these states are not energetically degenerate (strictly speaking, they do not even have to be energy eigenstates to begin with, → *below*) because such transformations do *not* alter the many-body ground state (namely the Fermi sea or the Slater determinant):

$$|\Psi'_0\rangle = \prod_{\mathbf{k}} \prod_i c_{\mathbf{k},i}^\dagger |0\rangle = \prod_{\mathbf{k}} \prod_i U_{ij} c_{\mathbf{k},j}^\dagger |0\rangle \quad (3.28a)$$

$$\doteq \prod_{\mathbf{k}} \det(U) \prod_i c_{\mathbf{k},i}^\dagger |0\rangle = e^{i\chi} \prod_{\mathbf{k}} \prod_i c_{\mathbf{k},i}^\dagger |0\rangle = e^{i\chi} |\Psi_0\rangle. \quad (3.28b)$$

Here, $c_{\mathbf{k},i}^\dagger$ creates a fermion in mode $|u_i(\mathbf{k})\rangle$ and $e^{i\chi}$ is some *global* (and therefore unphysical) phase determined by (powers of) $\det(U)$. The determinant arises due to the anticommutation relations $\{c_{\mathbf{k},i}^\dagger, c_{\mathbf{k},j}^\dagger\} = 0$; have a look at the concepts of \uparrow *alternating multilinear forms* and the \uparrow *exterior algebra* if so don't believe this (or prove it by hand).

ii | Time-reversal symmetry (TRS/TRI)

→ Chern numbers of “valence bundle” $\mathcal{H}_{\mathbf{k}}^{\text{filled}} = \text{span}\{|u_i(\mathbf{k})\rangle\}_{i=1\dots 2n}$ vanish

→ $\mathcal{H}_{\mathbf{k}}^{\text{filled}} = \uparrow$ *Trivial vector bundle*

→ \exists Continuous basis $\{|e_i(\mathbf{k})\rangle\}_{i=1\dots 2n}$ of $\mathcal{H}_{\mathbf{k}}^{\text{filled}}$ on T^2

It is $|e_i(\mathbf{k})\rangle = U_{ij}(\mathbf{k})|u_j(\mathbf{k})\rangle$ a (potentially discontinuous) gauge transformation.

Remember that we showed in Section 1.3.1 (for the special case of a single band) that a non-zero Chern number implies that a globally continuous Bloch basis does *not* exist. Here we use the inverse claim (without proof).

→ $P(\mathbf{k})$ continuous on T^2 if defined by $\{|e_i(\mathbf{k})\rangle\}_{i=1\dots 2n}$

This follows from the fact that the Chern number(s) of the filled Bands (mathematically speaking, the filled \uparrow *Bloch bundle* or \uparrow *valence bundle*) vanish. Thus there is no obstruction in choosing a globally defined, continuous basis $\{|e_i(\mathbf{k})\rangle\}_{i=1\dots 2n}$ of the filled band fiber $\mathcal{H}_{\mathbf{k}}^{\text{filled}}$ at every \mathbf{k} . Mathematically, this means that the Bloch bundle of filled bands can be \uparrow *trivialized*. Because there is a continuous basis choice $\{|e_i(\mathbf{k})\rangle\}_{i=1\dots 2n}$ for the filled bands, the matrix of \tilde{T}_U , and subsequently the Pfaffian $P(\mathbf{k})$, are continuous on T^2 if defined with this basis choice.

Note that in general the continuous basis $\{|e_i(\mathbf{k})\rangle\}_{i=1\dots 2n}$ is *not* necessarily an eigenbasis of the Bloch Hamiltonian! This is why we changed the notation from $u_i(\mathbf{k})$ to $e_i(\mathbf{k})$; in the following, $\{|e_i(\mathbf{k})\rangle\}_{i=1\dots 2n}$ always denotes a globally continuous basis whereas $\{|u_i(\mathbf{k})\rangle\}_{i=1\dots 2n}$ is a (potentially discontinuous) *eigenbasis* of the Bloch Hamiltonian.

iii | \leftarrow Two special subspaces of Bloch states:

- $\mathcal{H}_{\mathbf{k}}^{\text{filled}}$ is $\ast\ast$ *even* $:\Leftrightarrow \tilde{T}_U \mathcal{H}_{\mathbf{k}}^{\text{filled}} = \mathcal{H}_{\mathbf{k}}^{\text{filled}}$

This means that $\tilde{T}_U |u_i(\mathbf{k})\rangle = M_{ij} |u_j(\mathbf{k})\rangle$ with a *unitary* matrix $M \neq 0$.

$$\rightarrow |P(\mathbf{k})| = |\text{Pf}[M(\mathbf{k})]| = \sqrt{|\det M(\mathbf{k})|} = 1$$

To show that $M(\mathbf{k})$ is unitary, evaluate $(M^\dagger M)_{ij}$ using the definition in Eq. (3.23) and use that the projector $P_{\mathcal{H}_{\mathbf{k}}^{\text{filled}}} = \sum_{k=1}^{2n} |u_k(\mathbf{k})\rangle \langle u_k(\mathbf{k})|$ acts as the identity on $\tilde{T}_U |u_j(\mathbf{k})\rangle$ since $\tilde{T}_U \mathcal{H}_{\mathbf{k}}^{\text{filled}} = \mathcal{H}_{\mathbf{k}}^{\text{filled}}$ by assumption. Remember that $\tilde{T}_U = U \mathcal{K}$ with $U^\dagger U = \mathbb{1}$ and use that $\langle u_i^\ast(\mathbf{k}) | u_j^\ast(\mathbf{k}) \rangle = \langle u_j(\mathbf{k}) | u_i(\mathbf{k}) \rangle = \delta_{ij}$.

- $\mathcal{H}_{\mathbf{k}}^{\text{filled}}$ is $\ast\ast$ *odd* $:\Leftrightarrow \tilde{T}_U \mathcal{H}_{\mathbf{k}}^{\text{filled}} \perp \mathcal{H}_{\mathbf{k}}^{\text{filled}}$

This means that $\langle u_j(\mathbf{k}) | \tilde{T}_U |u_i(\mathbf{k})\rangle = 0 = M_{ij}$. Remember that i runs only over *filled* bands whereas \tilde{T}_U can mix the *whole* fiber $\mathcal{H}_{\mathbf{k}} = \mathcal{H}_{\mathbf{k}}^{\text{filled}} \oplus \mathcal{H}_{\mathbf{k}}^{\text{empty}}$.

- ¡ Let $|u_i(\mathbf{k})\rangle$ be an eigenstate of $H(\mathbf{k})$ in $\mathcal{H}_{\mathbf{k}}^{\text{filled}}$ and think of it as a vector in $\mathbb{C}^N \simeq \mathcal{H}_{\mathbf{k}} = \mathcal{H}_{\mathbf{k}}^{\text{filled}} \oplus \mathcal{H}_{\mathbf{k}}^{\text{empty}}$, where N is the total number of bands. Then time-reversal symmetry implies that $\tilde{T}_U |u_i(\mathbf{k})\rangle$ is an eigenvector with the same eigenvalue of $H(-\mathbf{k})$ [recall Eq. (2.33)]. But this is not necessarily the same matrix as $H(\mathbf{k})$ (except for \mathbf{k} a TRIM)! Hence $\tilde{T}_U |u_i(\mathbf{k})\rangle$ can be in the linear subspace $\mathcal{H}_{\mathbf{k}}^{\text{empty}}$ that corresponds to the conduction band at \mathbf{k} , and therefore orthogonal to all vectors in $\mathcal{H}_{\mathbf{k}}^{\text{filled}}$.

- Strictly speaking, here we compare vectors in different “fibers” $\mathcal{H}_{\mathbf{k}}^{\text{filled}}$ and $\mathcal{H}_{-\mathbf{k}}^{\text{filled}}$. To do so, we (silently) assume a \uparrow trivialization $T^2 \times \mathbb{C}^N$ of the complete \uparrow Bloch bundle with $\mathcal{H}_{\mathbf{k}} = \mathcal{H}_{\mathbf{k}}^{\text{filled}} \oplus \mathcal{H}_{\mathbf{k}}^{\text{empty}} \simeq \mathbb{C}^N$ (\uparrow Refs. [113,114] for more details).

$$\rightarrow |P(\mathbf{k})| = |\text{Pf}[M(\mathbf{k})]| = 0$$

These are two special cases; $\mathcal{H}_{\mathbf{k}}^{\text{filled}}$ can also be neither even nor odd!

iv | Observation: \mathbf{K}^* TRIM $\rightarrow \mathcal{H}_{\mathbf{K}^*}^{\text{filled}}$ is even since

$$|u_i(\mathbf{K}^*)\rangle \in \mathcal{H}_{\mathbf{K}^*}^{\text{filled}} \xrightarrow{\tilde{T}_U H(\mathbf{K}^*) \tilde{T}_U^{-1} = H(\mathbf{K}^*)} \tilde{T}_U |u_i(\mathbf{K}^*)\rangle \in \mathcal{H}_{\mathbf{K}^*}^{\text{filled}} \quad (3.29)$$

$[\tilde{T}_U, H(\mathbf{K}^*)] = 0$ means that \tilde{T}_U can only mix states with the same eigenenergy. In particular, a mixing between valence and conduction bands cannot occur, so that $\tilde{T}_U |u_i(\mathbf{K}^*)\rangle \in \mathcal{H}_{\mathbf{K}^*}^{\text{filled}}$ if $|u_i(\mathbf{K}^*)\rangle \in \mathcal{H}_{\mathbf{K}^*}^{\text{filled}}$. Note that this argument breaks down at a gapless point!

$$\rightarrow |P(\mathbf{K}^*)| = 1 \text{ at all TRIMs } \mathbf{K}^*$$

v | Effective Brillouin Zones:

Remember:

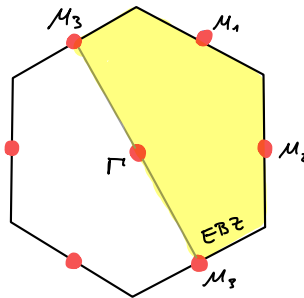
$$\text{TRI} \Leftrightarrow \tilde{T}_U H(\mathbf{k}) \tilde{T}_U^{-1} = H(-\mathbf{k}) \quad (3.30)$$

\rightarrow Defining $H(\mathbf{k})$ on half the BZ is sufficient!

The other half can then be reconstructed via Eq. (3.30).

\rightarrow Define an $\ast\ast$ Effective Brillouin Zone (EBZ) as any subset of T^2 that does not contain both \mathbf{k} and $-\mathbf{k}$ (except for the boundaries which connect pairs of TRIMs).

Example on the hexagonal lattice:



- The EBZ has the topology of a cylinder (and not a torus).
- Note that the choice of an EBZ is not unique [113].
- The concept of an EBZ was originally introduced by MOORE and BALENTS in 2007 [100]. See also Ref. [113] for an accessible introduction.

The concept of an EBZ will become important \rightarrow below.

vi | Consequences for $P(\mathbf{k})$ from TRI:

(Remember the TRI band structure with Kramers pairs above!)

$$\tilde{T}_U H(\mathbf{k}) \tilde{T}_U^{-1} = H(-\mathbf{k}) \Rightarrow \tilde{T}_U \mathcal{H}_{\mathbf{k}}^{\text{filled}} = \mathcal{H}_{-\mathbf{k}}^{\text{filled}} \quad (3.31a)$$

$$\Rightarrow |e_i(-\mathbf{k})\rangle = w_{ij}^*(\mathbf{k}) \tilde{T}_U |e_j(\mathbf{k})\rangle \quad (3.31b)$$

$w_{ij}(\mathbf{k}) := \langle e_i(-\mathbf{k}) | \tilde{T}_U | e_j(\mathbf{k}) \rangle$: unitary $\star\star$ Sewing matrix

$|e_i(\mathbf{k})\rangle$ denotes the globally continuous basis of the valence bundle $\mathcal{H}_{\mathbf{k}}^{\text{filled}}$ defined \leftarrow above.

The sewing matrix was originally introduced by FU and KANE in 2006 [112]. See also FRUCHART and CARPENTIER [113] and \rightarrow Problemset 7.

\rightarrow With this we can evaluate the Pfaffian at $-\mathbf{k}$:

$$P(-\mathbf{k}) = \text{Pf}[M(-\mathbf{k})] \quad (3.32a)$$

$$= \text{Pf} \left[\left(\langle e_i(-\mathbf{k}) | \tilde{T}_U | e_j(-\mathbf{k}) \rangle \right)_{ij} \right] \quad (3.32b)$$

$$= \text{Pf} \left[\left(w_{ii'}(\mathbf{k}) \langle \tilde{T}_U e_{i'}(\mathbf{k}) | \tilde{T}_U | \tilde{T}_U e_{j'}(\mathbf{k}) \rangle w_{jj'}(\mathbf{k}) \right)_{ij} \right] \quad (3.32c)$$

$$= (-1)^n \text{Pf} \left[\left(w_{jj'}(\mathbf{k}) \langle e_{j'}(\mathbf{k}) | \tilde{T}_U | e_{i'}(\mathbf{k}) \rangle^* w_{ii'}(\mathbf{k}) \right)_{ij} \right] \quad (3.32d)$$

$$\stackrel{\circ}{=} (-1)^n \text{Pf} \left[w(\mathbf{k}) M^*(\mathbf{k}) w^T(\mathbf{k}) \right] \quad (3.32e)$$

$$= (-1)^n \det[w(\mathbf{k})] [P(\mathbf{k})]^* \quad (3.32f)$$

Here we used $\tilde{T}_U^2 = -1$, $\text{Pf}[\lambda A] = \lambda^n \text{Pf}[A]$ and that \tilde{T}_U is antiunitary.

\rightarrow Two conclusions:

- $P(\mathbf{k}') = 0 \Leftrightarrow P(-\mathbf{k}') = 0$

Note that $w^\dagger(\mathbf{k})w(\mathbf{k}) = \mathbb{1}$ so that $\det[w(\mathbf{k})] \neq 0$ for all $\mathbf{k} \in T^2$.

- The $\star\star$ vorticities ν around \mathbf{k}' and $-\mathbf{k}'$ have opposite signs:

$$\nu[\mathbf{k}'] := \frac{1}{2\pi i} \oint_{\partial \mathbf{k}'} \nabla \log[P(\mathbf{k})] \cdot d\mathbf{k} = -\nu[-\mathbf{k}'] \in \mathbb{Z} \quad (3.33)$$

$\partial \mathbf{k}'$: loop around \mathbf{k}'

- The vorticity $\nu[\mathbf{k}']$ measures the *complex phase* accumulated when travelling around the zero of $P(\mathbf{k})$ at \mathbf{k}' . Since $P(\mathbf{k})$ is continuous, this can only be integer multiples of 2π .
- Since $w(\mathbf{k})$ is continuous and unitary, the vorticity of $\det[w(\mathbf{k})] \neq 0$ must vanish everywhere, so that the vorticity of the expression in Eq. (3.32f) is completely determined by $[P(\mathbf{k})]^*$ [which has the negative vorticity of $P(\mathbf{k})$].
- Let $P(\mathbf{k}) = |P(\mathbf{k})| e^{i \arg P(\mathbf{k})}$ so that $\log[P(\mathbf{k})] = \ln |P(\mathbf{k})| + i \arg P(\mathbf{k})$.

Then we have

$$\frac{1}{2\pi i} \oint_{\partial \mathbf{k}'} \nabla \log[P(\mathbf{k})] \cdot d\mathbf{k} \quad (3.34a)$$

$$= \underbrace{\frac{1}{2\pi i} \oint_{\partial \mathbf{k}'} \nabla \ln |P(\mathbf{k})| \cdot d\mathbf{k}}_{=0} + \underbrace{\frac{1}{2\pi} \oint_{\partial \mathbf{k}'} \nabla \arg P(\mathbf{k}) \cdot d\mathbf{k}}_{\in 2\pi \mathbb{Z}} \quad (3.34b)$$

where we used that $|P(\mathbf{k})| \neq 0$ is continuous everywhere along the contour $\partial k'$; in particular, the argument $\arg P(\mathbf{k})$ can only change by multiples of 2π . This shows that the expression (3.33) measures the phase winding of $P(\mathbf{k})$ along the contour $\partial k'$, i.e., its *vorticity*.

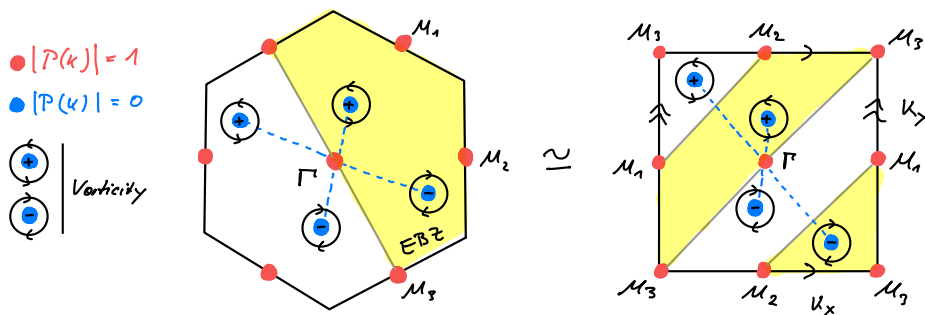
→ Phase vortices of $P(\mathbf{k})$ on the BZ T^2 come in pairs of opposite vorticity

vii | Observation: Zeros of $P(\mathbf{k})$ with $v[\mathbf{k}'] \neq 0$ are topologically stable

This is intuitively clear: If one makes the function non-zero at the vortex, it becomes discontinuous at this point due to the winding phase. Furthermore, the winding phase cannot be smoothly removed without discontinuous deformations of the function as well.

7 | If we combine all the above facts, we arrive at the following ...

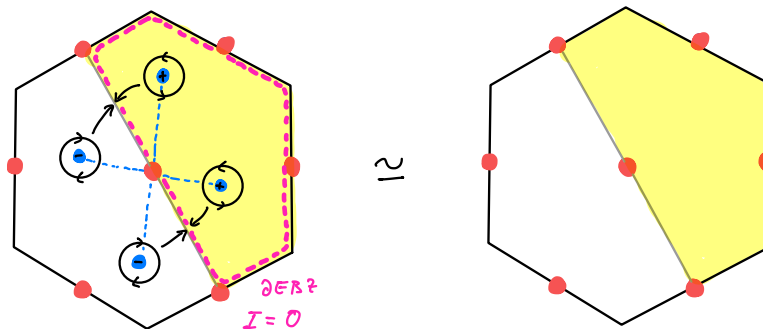
→ Generic picture:



- Without additional symmetries, the zeros of $|P(\mathbf{k})|$ occur at *points* in the BZ. This is true for the Kane-Mele model if $m \neq 0$.
- With additional symmetries, the zeros can form *lines* that avoid the TRIMs. In the Kane-Mele model, this happens for $m = 0$, ↑ Ref. [111] and → below.
- Zeros with vanishing vorticity are not stable and therefore not “generic” but “fine-tuned.”
- On the TRIMs, $|P(\mathbf{k})|$ is pinned to 1, so that zeros (vortices) *cannot* occupy these positions.
- In the following, we focus on the least symmetric (and therefore most generic) case with point-like zeros. Without loss of generality, we assume a vorticity of ± 1 per vortex (a vortex with vorticity $|\nu| > 1$ can be continuously split into $|\nu|$ vortices of vorticity ± 1). Furthermore, we assume that all vortices in the EBZ have the same vorticity (vortices of opposite vorticity in the EBZ can be pairwise annihilated).

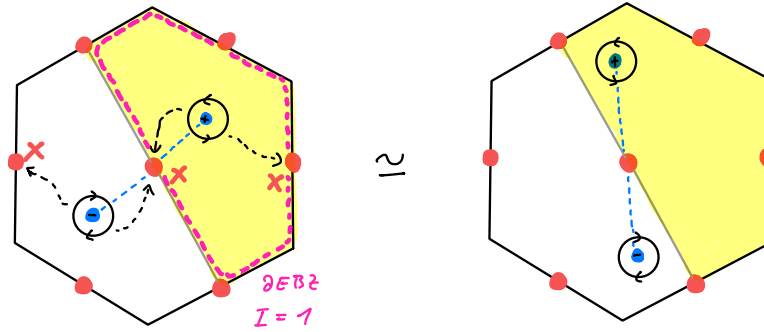
8 | Two situations:

- < Even number of vortices in EBZ:



→ All vortices can be continuously removed

- < Odd number of vortices in EBZ:



- To remove the last vortex pair, the partners must meet at one of the TRIMs.
 - But this is *impossible* because of TRS which demands $|P(\mathbf{K}^*)| = 1$ [← Eq. (3.29)].
- A single pair of vortices cannot be continuously removed
- The two situations are Topologically distinct (as long as TRS is not broken)
- Odd number of vortices = Topological phase protected by time-reversal symmetry

This is our first example of a true ← *symmetry-protected topological (SPT) phase*.

- 9 | This distinction is quantified by the \mathbb{Z}_2 Topological/Pfaffian \mathbb{Z}_2 index ...

$$I := \frac{1}{2\pi i} \oint_{\partial\text{EBZ}} \nabla \log[P(\mathbf{k})] \cdot d\mathbf{k} \pmod{2} = \frac{1}{2\pi i} \oint_{\partial\text{EBZ}} d \log[P(\mathbf{k})] \pmod{2} \quad (3.35)$$

∂EBZ : Closed path that encircles an EBZ

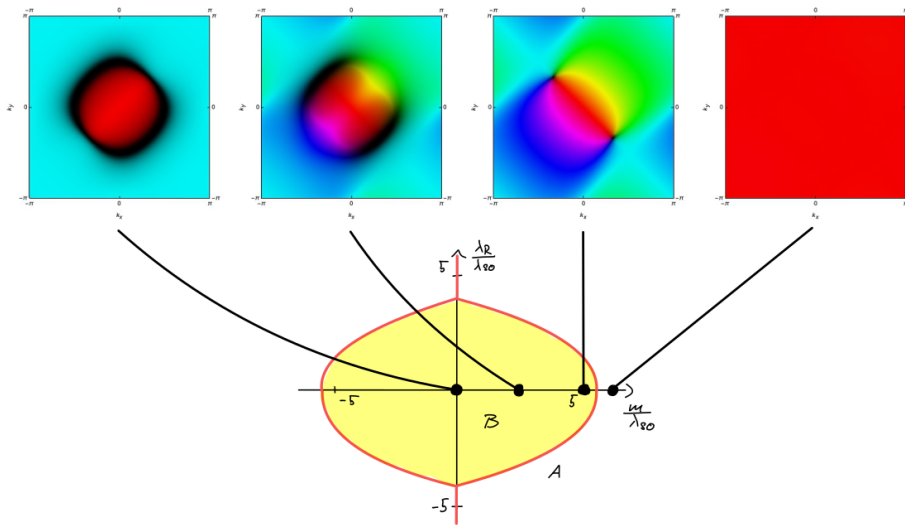
... which measures the parity of the total vorticity in half the Brillouin zone.

- The choice of a EZB is constrained by the vortices. It should be chosen such that the vortices stay away from the boundary ∂EBZ . For example, see Ref. [111, Fig. 2].
- $I \in \mathbb{Z}_2$ is gauge invariant because a gauge transformation that is continuous everywhere cannot change the vorticity of $P(\mathbf{k})$ [← Eq. (3.27)].
- There is an alternative way to compute the topological \mathbb{Z}_2 index I by evaluating the ← *sewing matrix* $w(\mathbf{k})$ at the TRIMs:

$$(-1)^I \stackrel{*}{=} \prod_{\mathbf{K}^* \text{ TRIM}} \frac{\text{Pf}[w(\mathbf{K}^*)]}{\sqrt{\det w(\mathbf{K}^*)}}. \quad (3.36)$$

This assumes that the sewing matrix $w_{ij}(\mathbf{k}) = \langle e_i(-\mathbf{k}) | \tilde{T}_U | e_j(\mathbf{k}) \rangle$ is calculated from a globally continuous basis $|e_i(\mathbf{k})\rangle$. You show the equivalence of Eq. (3.35) and Eq. (3.36) on ↻ Problemset 7. This alternative form of the \mathbb{Z}_2 index is important because it naturally generalizes to three dimensions and paves the way to ↑ *3D topological insulators* and ↑ *weak topological insulators* [96].

10 | Example: Kane-Mele model:



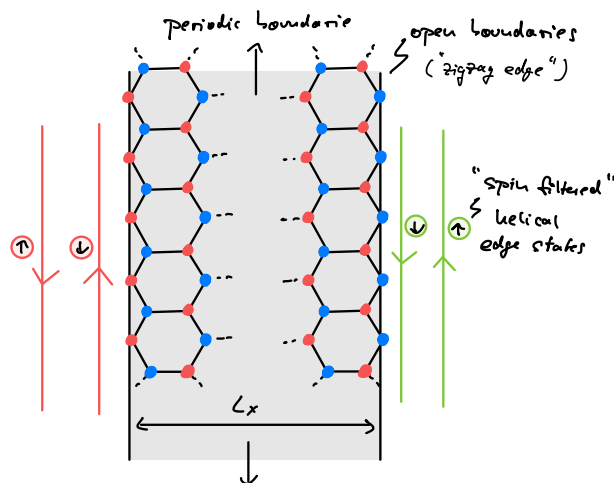
- In the color plots, the BZ is deformed to a square. The color denotes the phase (red = +1, turquoise = -1) and the lightness the absolute value (black = 0) of the Pfaffian computed from a family of global sections of the valence bundle.
- Note that in the topological phase (for $m \neq 0$) there is a single vortex in each EBZ and the phase winds once around each vortex so that $I = 1$. For this result, it is crucial that the Pfaffian is computed from a *globally continuous basis* $\{|e_i(\mathbf{k})\}_{i=1\dots 2n}$ (= a family of global sections of the valence bundle that form a basis at every point), otherwise the vorticity can be changed by integers (even if the Pfaffian is continuous!) and I cannot distinguish the phases. Note that these global sections are typically not eigenstates of the Bloch Hamiltonian; their existence, however, is guaranteed by time-reversal symmetry (because then all Chern numbers of the rank-2 valence bundle vanish).
- Here you can download the Mathematica notebook that I used to create the plots above:
 - ➡ [Download Mathematica notebook](#)
- The enhanced symmetry for $m = 0$ make the zeros form a line that circles the central TRIM (and therefore cannot be contracted without breaking TRS). In this situation, the Pfaffian can be gauged real (as already mentioned by Kane and Mele [111]). Continuously breaking the “ring of zeros” is only possible if a pair of vortices is introduced that makes the phase wind around the two islands of zeros that result from such a procedure.

3.4. Edge modes

A particularly intriguing feature of phases with topological bands is the emergence of robust *edge modes* (the analogs of the chiral edge modes we encountered in quantum Hall systems, ← Section 1.6):

11 | $\langle \hat{H}_{KM}$ on a cylinder:

The system is therefore periodic in *y*-direction but has *boundaries* in *x*-direction.



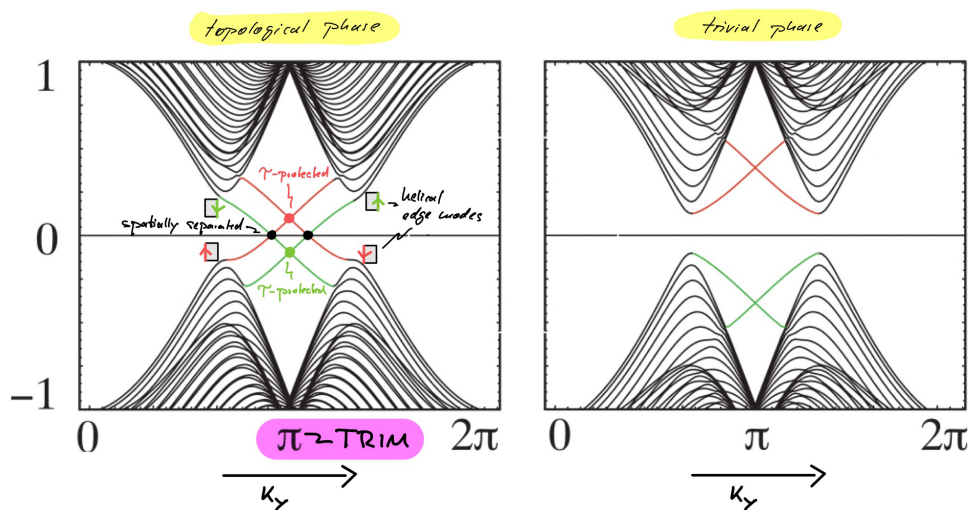
The type of boundary (“zigzag” vs. “armchair”) has no effect on the existence of the edge states but the spectrum below looks different for armchair boundaries.

→ Interpret strip as a 1D system with large, L_x -dependent unit cell

→ Fourier transform \hat{H}_{KM} only in *y*-direction

→ 1D spectrum with $\mathcal{O}(L_x)$ bands labeled by *y*-momentum k_y

12 | Numerics → Edge modes:



This figure is taken from KANE and MELE’s original work [111].

- Topological phase → Gapless edge modes
 - Robust (= no backscattering / gap opening) to TRS perturbations
 - The four band crossings of the edge modes are protected for two different reasons:
 - * Black crossings: The crossing modes are localized on *opposite* edges of the strip. Gapping them out is therefore exponentially suppressed with the width L_x of the strip (gapped bulk!).
 - * Colored crossings: The crossing modes live on the *same* edge of the sample (with opposite group velocity). Gapping them out is forbidden by *time-reversal symmetry* as these crossings happen at a TRIM ($k_y = \pi$) and are enforced by Kramers degeneracy. This is why the Kane-Mele topological insulator is an SPT phase: Disorder that *breaks* TRS can hybridize these edge modes and destroy the topological phase.
 - On each edge there is a right-propagating mode for one spin polarization and a left-propagating mode for the opposite spin polarization (for $\lambda_R = 0$, if spin is conserved).
In the original plots above, it is actually $\lambda_R = 0.05 \neq 0$ so that spin conservation is broken. The breaking of spin-conservation is responsible for the \downarrow *avoided crossings* that fuse the edge modes into the bulk bands (for $\lambda_R = 0$ the edge modes would *cross* the bulk modes, \ominus Problemset 6).
 - The edge modes are *helical* (not *chiral*) since the product of spin and momentum is constant on each edge.
- Trivial phase → No gapless edge modes

Details: \ominus Problemset 6

Notes:

- The two “stalactite-stalagmite” pairs in the above spectrum correspond to the 1D projections of the two (gapped) Dirac cones around \mathbf{K} and \mathbf{K}' . The tips of these bulk bands are connected by the edge modes.
- For $\lambda_R = 0$ you can extract the edge modes of the \leftarrow *Haldane Chern insulator* by just looking at one of the two spin sectors (up or down, which determines the sign of the complex NNN hopping phase). Thus in the topological phase, the Haldane model supports *one* (then *chiral* [since spin does not exist]) edge mode on each boundary.

13 | Final Note on symmetries and names:

- As discussed, the KM model \hat{H}_{KM} without Rashba SO coupling ($\lambda_R = 0$) can be thought of as two uncoupled, time-reversed copies of Haldane’s Chern insulator. As such, the model features a particle conservation symmetry in each of the two spin sectors, i.e., its total symmetry is $U(1)_\uparrow \times U(1)_\downarrow$. By defining *charge* $n_c = n_\uparrow + n_\downarrow$ and *spin* $n_s = n_\uparrow - n_\downarrow$, one can reinterpret this symmetry as $U(1)_{\text{charge}} \times U(1)_{\text{spin}}$, where total charge (particle) conservation $U(1)_{\text{charge}}$ and total spin conservation $U(1)_{\text{spin}}$ hold separately. One can then introduce the usual charge current $\mathbf{J}_c = \mathbf{J}_\uparrow + \mathbf{J}_\downarrow$ and the $\ast\ast$ *spin current* $\mathbf{J}_s = (\hbar/2e) (\mathbf{J}_\uparrow - \mathbf{J}_\downarrow)$ and ask for the linear response of these quantities when an electric field is applied. This response is quantified by the usual charge Hall conductivity σ_{xy}^c (previously σ_{xy}) and its analogue, the $\ast\ast$ *spin Hall conductivity* σ_{xy}^s . Because the ground state of \hat{H}_{KM} is given by two filled Chern bands with opposite Chern numbers $C = \pm 1$, the charge Hall conductivity vanishes identically: $\sigma_{xy}^c = 0$ (this follows from our general discussion in Section 1.4.2). By contrast, the spin Hall conductivity is non-zero and quantized at $\sigma_{xy}^s = e/2\pi = 2 \times (\hbar/2e) \times e^2/h$

(because there are two counterpropagating edge modes with opposite spin, coming from the two Chern bands with opposite Chern number). The phenomenon of a quantized spin Hall conductivity (and vanishing charge Hall conductivity) is called *quantum spin Hall effect (QSHE)* and characterized by the combined symmetry $U(1)_{\text{charge}} \times U(1)_{\text{spin}}$.

- It was a remarkable insight by Kane and Mele [111] that the two phases of the “Quantum Spin Hall effect in Graphene” [110] remained topologically distinct (via the Pfaffian index) *even without spin conservation* ($\lambda_R \neq 0$) – time-reversal symmetry is sufficient! This phase, protected by charge conservation $U(1)_{\text{charge}}$ and time-reversal symmetry \mathbb{Z}_2^T [recall that $\tilde{T}_U^2 = -1$ is equivalent to $\mathcal{T}_U^2 = (-1)^{\hat{N}_c}$, Section 2.1.2], and characterized by the Pfaffian \mathbb{Z}_2 index, is the *topological insulator (TI)* phase. Since spin conservation $U(1)_{\text{spin}}$ is generally broken in this phase, it is *not* characterized by a quantized spin Hall conductivity (= quantum spin Hall effect). One can indeed check that adding either TRS breaking terms *or* superconducting terms to the KM Hamiltonian \hat{H}_{KM} on a cylinder *gaps out* the edge modes, indicating that the topological insulator is protected by TRS *and* charge conservation symmetry [94].

Thus, the *topological insulator (TI)* and the *quantum spin Hall (QSH) phase* are *different* symmetry-protected topological phases, and the KM model happens to realize both for $\lambda_R = 0$ [35]. [Remember (Section 0.5) that the classification of SPT phases depends on our choice of protecting symmetry!]

In the context of this (modern) terminology, the title of Kane and Mele’s original paper “ \mathbb{Z}_2 Topological Order and the Quantum Spin Hall Effect” [111] is confusing for two reasons: First, the paper is mostly about the topological insulator phase – and not the quantum spin Hall effect. The authors even point this out explicitly: “*The QSH phase is not generally characterized by a quantized spin Hall conductivity.*” In addition, their notion of “topological order” does not match the modern terminology of “long-range entanglement.” That is, Kane and Mele’s topological insulator is the paradigmatic example of a *topological phase* that is *not* topologically ordered but *symmetry protected*.

3.5. ‡ Experiments

- The possibility to observe the quantum spin Hall effect (via a quantized \leftarrow *spin Hall conductance* that requires spin conservation, i.e., $\lambda_R = 0$) was predicted by BERNEVIG *et al.* in 2006 [118] and experimentally confirmed by KÖNIG *et al.* in 2007 [119] in so called \uparrow HgTe *quantum wells* (HgTe = Mercury-Telluride).
- The alloy $\text{Bi}_{1-x}\text{Sb}_x$ (BiSb = Bismuth-Antimony) was predicted to be a (strong) topological insulator (in three dimensions) by FU and KANE in 2007 [97] which was experimentally confirmed by HSIEH *et al.* in 2008 [120].
- Following these first discoveries, many more materials were identified as topological insulators. For an extensive review including experimental results (before 2011) see QI and ZHANG [121].

Closing remarks for Chapters 1 to 3

We have now discussed two topological indices to label topological phases in two dimensions:

- The (first) *Chern number* classifies two-dimensional chiral topological phases (IQHE, QWZ model, Haldane model); we discussed these models in Chapters 1 and 2.
 - The Chern number *cannot* be generalized to three dimensions! (There are generalizations to *even* dimensions, though [122].)
 - For non-zero Chern numbers, time-reversal symmetry must be *broken*.
 - Phases of non-interacting fermions in bands with non-zero Chern numbers are examples of the \leftarrow *invertible topological orders* introduced in Section 0.5 [35].
- The \mathbb{Z}_2 *Pfaffian index* classifies symmetry-protected topological (SPT) phases in two dimensions (Kane-Mele topological insulator); we discussed this model in Chapter 3.
 - The Pfaffian index *can* be generalized to three dimensions and allows for the characterization of three-dimensional topological insulators [96, 100, 123].
 - For the Pfaffian index to be well-defined, time-reversal symmetry must be *preserved*.
 - The Kane-Mele topological insulator is a \leftarrow *short-range entangled* phase protected by time-reversal symmetry (and particle number/charge conservation) [35].

We now turn to topological phases of non-interacting fermions in *one* dimension ...

4. Topological Insulators in 1D: The Su-Schrieffer-Heeger Chain

After our study of two-dimensional systems with topological band structures in Chapters 1 to 3, we now turn to *one-dimensional* systems (still with non-interacting fermions). We will introduce the paradigmatic Su-Schrieffer-Heeger chain and identify a new topological invariant to characterize its quantum phases. However, as a preliminary step, we must introduce a new symmetry (beyond time-reversal symmetry) called *sublattice symmetry* ...

4.1. Preliminaries: Sublattice symmetry

1 | Reminder: (Symmetries we already know.)

In the following, \hat{H} denotes a non-interacting many-body Hamiltonian on (fermionic) Fock space and H its single-particle counterpart.

- *Unitary symmetry* \mathcal{U} :

$$\mathcal{U}i\mathcal{U}^{-1} = +i \quad \text{and} \quad \mathcal{U}c_i\mathcal{U}^{-1} = \sum_j U_{ij}^\dagger c_j \quad (4.1a)$$

$$[\hat{H}, \mathcal{U}] = 0 \quad \Leftrightarrow \quad UHU^\dagger = H \quad \Leftrightarrow \quad [H, U] = 0 \quad (4.1b)$$

- *Time-reversal symmetry* \mathcal{T}_U : [\leftarrow Section 2.1.2]

$$\mathcal{T}_U i \mathcal{T}_U^{-1} = -i \quad \text{and} \quad \mathcal{T}_U c_i \mathcal{T}_U^{-1} = \sum_j U_{ij}^\dagger c_j \quad (4.2a)$$

$$[\hat{H}, \mathcal{T}_U] = 0 \quad \Leftrightarrow \quad UH^*U^\dagger \doteq H \quad \Leftrightarrow \quad [H, \underbrace{U\mathcal{K}}_{\mathcal{T}_U}] = 0 \quad (4.2b)$$

Note that both U and $U\mathcal{K}$ are valid *symmetries* on the single-particle Hilbert space (i.e., they commute with the Hamiltonian H), in accordance with *Wigner's theorem* (\rightarrow Problemset 1).

2 | Other symmetry types (?):

Having the (classes of) symmetries Eqs. (4.1) and (4.2) in mind, are there other types of symmetries that one can realize on a fermionic Fock space?

- \triangleleft *Unitary like* \mathcal{U} but with $c_i \leftrightarrow c_i^\dagger$:

$$\mathcal{C}_U i \mathcal{C}_U^{-1} = +i \quad \text{and} \quad \mathcal{C}_U c_i \mathcal{C}_U^{-1} = \sum_j U_{ij}^{*\dagger} c_j^\dagger \quad (4.3a)$$

$$[\hat{H}, \mathcal{C}_U] = 0 \quad \Leftrightarrow \quad UH^*U^\dagger \doteq -H \quad \Leftrightarrow \quad \{H, \underbrace{U\mathcal{K}}_{\mathcal{C}_U}\} = 0 \quad (4.3b)$$

! Note that H anticommutes with C_U : $\{\bullet, \bullet\} = 0$
(The complex conjugate in U_{ij}^* is conventional and not crucial.)

→ \mathcal{C}_U : \mathbb{Z}_2 Particle-hole symmetry (PHS)

→ Future lectures on topological superconductors

- \triangleleft Antiunitary like \mathcal{T}_U but with $c_i \leftrightarrow c_i^\dagger$:

$$\mathcal{S}_U i \mathcal{S}_U^{-1} = -i \quad \text{and} \quad \mathcal{S}_U c_i \mathcal{S}_U^{-1} = \sum_j U_{ij}^{*\dagger} c_j^\dagger \quad (4.4a)$$

$$[\hat{H}, \mathcal{S}_U] = 0 \quad \Leftrightarrow \quad U H U^\dagger \doteq -H \quad \Leftrightarrow \quad \left\{ H, \underbrace{U}_{\mathcal{S}_U} \right\} = 0 \quad (4.4b)$$

! Note that H anticommutes with S_U ($\{\bullet, \bullet\} = 0$) but also that there is *no* complex conjugation on the single-particle level, i.e., $S_U = U$ is a *unitary* operator. (The complex conjugate in U_{ij}^* is again conventional and not crucial.)

→ \mathcal{S}_U : \mathbb{Z}_2 Chiral- or Sublattice symmetry (SLS)

Here we stick to the term “sublattice symmetry” (SLS).

But why should we call \mathcal{S}_U “sublattice symmetry” in the first place?

→ Next point below ...

Note: The same arguments used for time-reversal symmetry (\leftarrow Section 2.1.2) lead to

$$\{H, U\} = 0 \quad \Rightarrow \quad [H, U^2] = 0 \quad \xrightarrow{H \text{ generic}} \quad U^2 = e^{i\varphi} \mathbb{1} \quad (4.5)$$

→ Redefine $\tilde{U} = e^{-i\varphi/2} U \rightarrow \tilde{U}^2 = +\mathbb{1} \rightarrow \text{w.l.o.g. } U^2 = +\mathbb{1}$

→ In contrast to time-reversal, there are not two “types” of sublattice symmetry!

(This difference is due to the missing antiunitarity on the single-particle level.)

! Whereas \mathcal{U} and \mathcal{T}_U can be interpreted as symmetries both on Fock space and on the single-particle Hilbert space, particle-hole symmetry \mathcal{C}_U and sublattice symmetry \mathcal{S}_U are only symmetries on Fock space; on the single-particle Hilbert space they act as unitary and antiunitary \uparrow *pseudosymmetries*, respectively (i.e., they anticommute with the single-particle Hamiltonian).

This should be not surprising since both include an exchange of particles with holes, so that they mix sectors of different particle numbers. Such an operation is intrinsic to the many-particle description in Fock space and cannot be sensibly defined (or interpreted) as a symmetry in a (first quantized) single-particle description.

3 | Why “sublattice symmetry”?

- i | \triangleleft SP Hamiltonian H with $U H U^\dagger = -H$

→ Spectrum $\sigma(H) = \sigma(-H)$

→ Spectrum symmetric about $E = 0$

By contrast, TRS implied a symmetric spectrum about the energy axis: $E(k) = E(-k)$.

- ii | Assume H is $2L \times 2L$ -matrix →

$$\exists \text{ Unitary } M : M H M^\dagger = \begin{pmatrix} D & 0 \\ 0 & -D \end{pmatrix} \quad \text{with diagonal matrix } D. \quad (4.6)$$

→

$$(QM)H(QM)^\dagger = \begin{pmatrix} 0 & D \\ D & 0 \end{pmatrix} \quad \text{with} \quad Q = \frac{1}{\sqrt{2}} \begin{pmatrix} \mathbb{1} & \mathbb{1} \\ \mathbb{1} & -\mathbb{1} \end{pmatrix} \quad (4.7)$$

To see this, remember that a Hadamard gate H transforms a σ^z Pauli matrix into a σ^x Pauli matrix under conjugation.

Note that QM is just a unitary basis transformation in the SP Hilbert space.

- iii | This means that for a sublattice symmetric system, there exists a unitary transformation of modes $\tilde{c}_i = \sum_j \tilde{U}_{ij} c_j$ such that

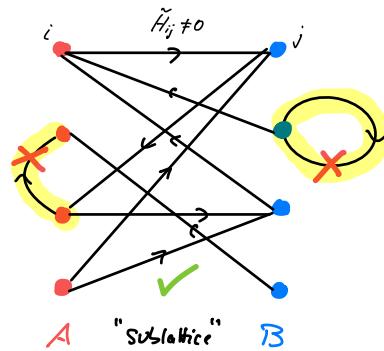
$$\hat{H} = \sum_{i,j} c_i^\dagger H_{ij} c_j \stackrel{\text{SLS}}{\underset{\text{w.l.o.g.}}{=}} \sum_{i,j} \tilde{c}_i^\dagger \tilde{H}_{ij} \tilde{c}_j \quad (4.8)$$

with block-off-diagonal SP Hamiltonian

$$\tilde{H} = \begin{pmatrix} 0 & h & \text{Hopping } A \mapsto B \\ h^\dagger & 0 & \text{Hopping } B \mapsto A \end{pmatrix} \quad (4.9)$$

The two subsets of modes A and B are referred to as “sublattices” even if a spatial lattice structure is missing.

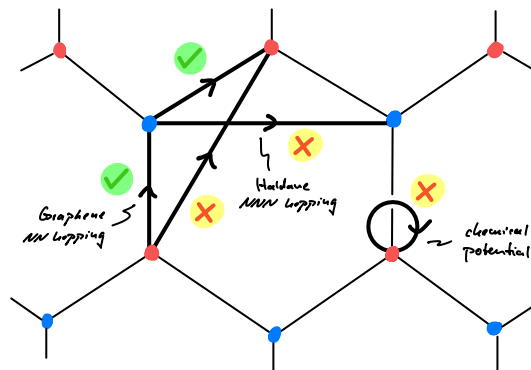
- iv | \tilde{H} couples only modes *between* the two “sublattices” A and B :



Often this sublattice structure is already visible in the real-space basis, i.e., a transformation to \tilde{H} is not even necessary (SSH chain → below).

If one interprets \tilde{H} as a (complex valued) adjacency matrix of a graph, the “sublattice symmetry” would be called ↑ *bipartiteness*. And indeed, it is well-known that a graph is bipartite if and only if the spectrum of its adjacency matrix is symmetric [124, Chapter 6.5].

- v | Example: Graphene

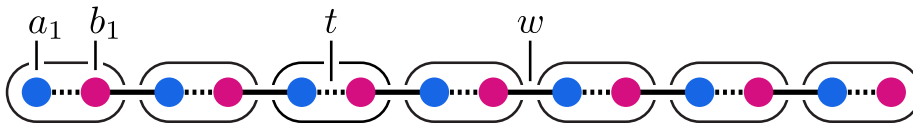


Note that a chemical potential $\mu \sum_i c_i^\dagger c_i$ can be interpreted as a hopping from site i to the same site; therefore it violates SLS.

4.2. The Su-Schrieffer-Heeger chain

- The *Su-Schrieffer-Heeger (SSH) chain* is a model of non-interacting, spinless fermions in one dimension that has been introduced by SU, SCHRIEFFER and HEEGER in 1979 [125] to describe soliton formation in polyacetylene (a linear chain of carbon atoms with alternating single and double bonds and one hydrogen atom bound to each carbon atom).
- In the context of topological phases, the model has become the example of choice to illustrate topological invariants and the emergence of robust edge modes [2] (which is why we study it).
- A detailed exposition of the SSH chain is given in the textbook by ASBOTH [2] but may also be found in almost any other textbook on topological insulators. There is also an introduction in my PhD thesis [126] (on which this section is based) with a quite detailed discussion of edge states in the appendices of Chapter 3.

1 | < 1D lattice with $2L$ sites grouped into L unit cells:



a_i, b_i : spinless fermion modes ($i = 1, \dots, L$)

We can now define the \star SSH chain Hamiltonian:

$$\hat{H}_{\text{SSH}} = t \underbrace{\sum_{i=1}^L (a_i^\dagger b_i + b_i^\dagger a_i)}_{\text{Intra-site hopping}} + w \underbrace{\sum_{i=1}^{L'} (b_i^\dagger a_{i+1} + a_{i+1}^\dagger b_i)}_{\text{Inter-site hopping}} \quad (4.10)$$

- $t, w \in \mathbb{R}$: alternating hopping amplitudes
- $L' = L - 1$ for OBC and $L' = L$ for PBC

We will use both boundary types: Open boundaries (OBC) to study edge modes, and periodic boundaries (PBC) allow for Fourier transformation and definition of a topological index.

2 | Symmetries:

The SSH Hamiltonian (4.10) has several symmetries, not all crucial for the following discussion:

- Particle-number conservation/symmetry (PNS)
This is an intrinsic symmetry of the class of quadratic fermion models without superconductivity; we cannot break it without leaving this class.
- Translation symmetry (TS)
Translation symmetry is typically broken in real samples due to disorder.
- Sublattice symmetry (SLS):

$$\mathcal{S}i\mathcal{S}^{-1} := -i \quad \text{and} \quad \mathcal{S}a_i\mathcal{S}^{-1} := a_i^\dagger \quad \text{and} \quad \mathcal{S}b_i\mathcal{S}^{-1} := -b_i^\dagger \quad (4.11)$$

$$\rightarrow [\hat{H}_{\text{SSH}}, \mathcal{S}] \doteq 0$$

Note that the minus sign $b_i \mapsto -b_i^\dagger$ is crucial for the commutation with the Hamiltonian!

The above definition is realized by the operator

$$\mathcal{S} \doteq \prod_i (a_i^\dagger - a_i)(b_i^\dagger + b_i) \circ \mathcal{K} \quad (4.12)$$

Use $\{a_i, a_i^\dagger\} = 1$ and $a_i^2 = 0 = (a_i^\dagger)^2$ (and the same for b_i) to show this.

- Time-reversal symmetry (TRS):

$$\mathcal{T}i\mathcal{T}^{-1} := -i \quad \text{and} \quad \mathcal{T}a_i\mathcal{T}^{-1} := a_i \quad \text{and} \quad \mathcal{T}b_i\mathcal{T}^{-1} := b_i \quad (4.13)$$

$$\rightarrow [\hat{H}_{\text{SSH}}, \mathcal{T}] \doteq 0$$

- Particle-hole symmetry (PHS):

$$\mathcal{C}i\mathcal{C}^{-1} := i \quad \text{and} \quad \mathcal{C}a_i\mathcal{C}^{-1} := a_i^\dagger \quad \text{and} \quad \mathcal{C}b_i\mathcal{C}^{-1} := -b_i^\dagger \quad (4.14)$$

$$\rightarrow [\hat{H}_{\text{SSH}}, \mathcal{C}] \doteq 0$$

Are all these symmetries of the same importance to characterize the SSH chain?

3 | < “Generic” SSH chain:

$$\hat{H}'_{\text{SSH}} = \sum_{i=1}^L (t_i a_i^\dagger b_i + t_i^* b_i^\dagger a_i) + \sum_{i=1}^{L'} (w_i b_i^\dagger a_{i+1} + w_i^* a_{i+1}^\dagger b_i) \quad (4.15)$$

$t_i, w_i \in \mathbb{C}$: site-dependent & complex hopping amplitudes

$\overset{\circ}{\rightarrow}$ Preserved symmetries: PN & SLS

(Check that the complex hoppings destroy both TRS and PHS but not SLS.)

\rightarrow *Sublattice symmetry* is the natural symmetry of the SSH chain.

! For the analytical analysis below, we will still assume *translation invariance* so that we can Fourier transform the Hamiltonian. However, if one studies the model numerically, one can add translation-symmetry breaking perturbations to the Hamiltonian and verify that the features (in particular: the quantum phases) of the SSH chain are robust to SLS-symmetric disorder (\rightarrow *discussion of edge modes below*).

↓ Lecture 14 [05.06.25]

4.3. Diagonalization

As a first step, we diagonalize the SSH Hamiltonian (quadratic fermions!) to obtain the spectrum and sketch the quantum phase diagram. To this end, we return to real & uniform hopping strengths t and w :

4 | \hat{H}_{SSH} with PBC and Fourier transform

$$\tilde{x}_k = \frac{1}{\sqrt{L}} \sum_{n=1}^L e^{-ikn} x_n, \quad x = a, b \tag{4.16}$$

→

$$\hat{H}_{SSH} = \sum_{k \in \text{BZ}} \begin{pmatrix} \tilde{a}_k^\dagger & \tilde{b}_k^\dagger \end{pmatrix} \cdot \underbrace{\begin{pmatrix} 0 & t + we^{-ik} \\ t + we^{ik} & 0 \end{pmatrix}}_{H(k)} \cdot \begin{pmatrix} \tilde{a}_k \\ \tilde{b}_k \end{pmatrix} \tag{4.17}$$

BZ: Brillouin zone = (discrete) Circle S^1

Here BZ = $\{\frac{2\pi}{L} \nu \mid \nu = 0, \dots, L-1\}$.

5 | Bloch Hamiltonian:

$$H(k) = (t + w \cos k) \sigma^x + w \sin k \sigma^y \equiv \vec{d}(k) \cdot \vec{\sigma} \tag{4.18}$$

with Bloch vector

$$\vec{d}(k) = \begin{pmatrix} t + w \cos k \\ w \sin k \\ 0 \end{pmatrix} \tag{4.19}$$

6 | Band structure:

Recall our discussion of general two-band models in Section 2.1.1.

$$E_{\pm}(k) = \pm |\vec{d}(k)| = \pm \sqrt{t^2 + w^2 + 2tw \cos k} \tag{4.20}$$

There are two bands due to the two fermionic modes a_i and b_i per unit cell i .

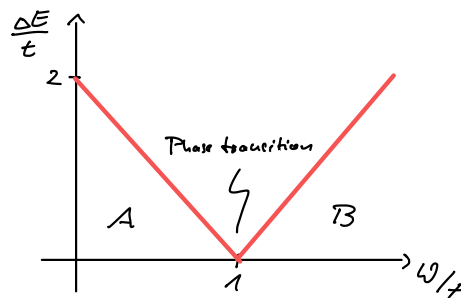
The \pm (without a constant energy offset) is a consequence of SLS (as discussed above).

7 | → Phase diagram:

Bandgap: $\Delta E = \min_k |E_+(k) - E_-(k)| \stackrel{\circ}{=} 2||t| - |w||$ (this is valid for $t, w \in \mathbb{R}$)

$\triangleleft t, w > 0 \rightarrow$ Gapless point for $w = t$, gapped insulator for $w \leq t$:

(The restriction $t, w > 0$ is not important as chains with different signs are unitarily equivalent.)



→ Unique ground state in A and B (→ no symmetry breaking)

→ How to distinguish/label the two gapped phases A and B?

We cannot use the Chern number because the Brillouin zone is S^1 in one dimensional systems (and not a torus T^2). The Chern number, however, is only defined on a two-dimensional manifold!

→ Idea:

Can we use SLS to define a new topological invariant?

Just like we used TRS to define the Pfaffian invariant to label the phases of the Kane-Mele model ...

4.4. A new topological invariant

8 | **Observation:** PNS does *not constrain* $H(k)$

For any $H(k)$ the many-body Hamiltonian (4.17) conserves particle number by construction.

→ \triangleleft SLS:

$$\left[\hat{H}_{\text{SSH}}, \mathcal{S} \right] = 0 \quad \stackrel{4.4}{\Leftrightarrow} \quad U^\dagger H U = -H \quad \stackrel{4.11}{\Leftrightarrow} \quad \sigma^z H(k) \sigma^z \stackrel{\circ}{=} -H(k) \quad (4.21)$$

The last condition follows along the same lines as for time-reversal symmetry [Eq. (2.29b)] with the unitary U defined by Eq. (4.11).

9 | Eqs. (2.8) and (4.21) → **Constrained Bloch vector:**

$$d_z(k) \stackrel{\text{SLS}}{=} 0 \quad \forall k \in \text{BZ} \quad (4.22)$$

→ $\vec{d}(k)$ cannot leave the x - y -plane

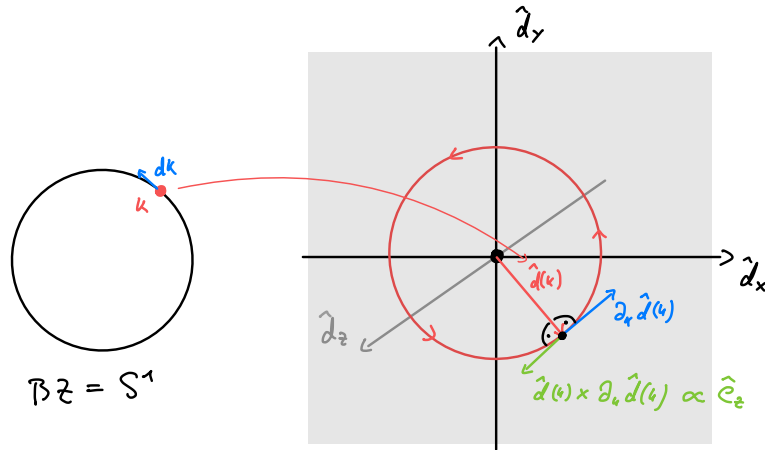
10 | \triangleleft Gapped phase → Normalization possible:

$$\hat{d}(k) = \frac{\vec{d}(k)}{|\vec{d}(k)|} \quad (4.23)$$

11 | → Winding number around the origin in the x - y -plane is well defined:

$$v[\hat{d}] := \frac{1}{2\pi} \int_{\text{BZ}} \hat{e}_z \cdot \left[\hat{d}(k) \times \partial_k \hat{d}(k) \right] dk \in \mathbb{Z} \quad (4.24)$$

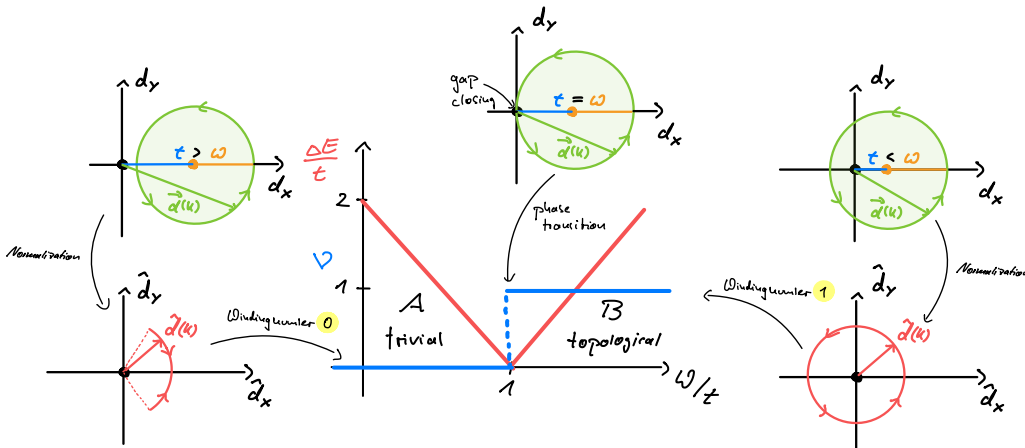
;! It is crucial that \hat{d} is pinned to the x - y -plane by SLS for this to be an integer.



12 | The winding number ν distinguishes the Two phases:

[This follows directly from the form of the Bloch vector Eq. (4.19).]

$$\nu = \begin{cases} 0 & \text{for } t > w \text{ (Phase A)} \\ 1 & \text{for } t < w \text{ (Phase B)} \end{cases} \quad (4.25)$$



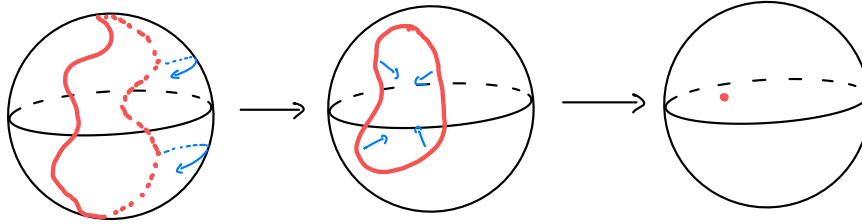
The phase A is trivial because it can be connected to the limit $t \neq 0$ and $w = 0$ without closing the gap. For these parameters, the different sites (each with two fermion modes a_i and b_i) do not couple at all and the ground state is a trivial product state.

13 | ‡ Some comments:

- Homotopy:

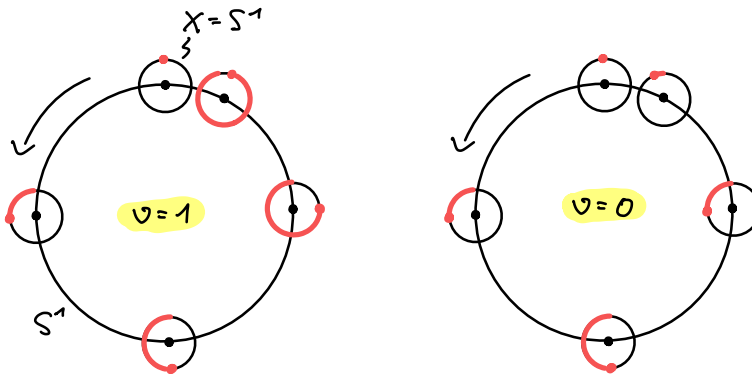
We can embed this new topological invariant and the Chern number into a bigger picture if we invoke the concept of *homotopy groups* from topology. Simply speaking, the homotopy group $\pi_p(X)$ for $p = 0, 1, 2, \dots$ and a topological space X consists of equivalence classes of continuous maps from the p -dimensional sphere S^p into X , where two maps are considered equivalent if they can be transformed into each other continuously (if the space X has a dedicated “base point” one can glue two such maps together and obtains a group structure on these equivalence classes).

The maps we are interested in are the Bloch vectors $\hat{d}(k)$ that map the Brillouin zone onto the sphere $X = S^2$. In 1D, the BZ is S^1 so that we are interested in the homotopy group $\pi_1(S^2) = 0$ which is trivial because every circle (S^1) that you draw onto the sphere ($X = S^2$) can be continuously contracted to a point (which represents the constant map):



This is why there is *no* analog of the Chern number in 1D. By contrast, in 2D the BZ is a torus T^2 which we can simplify to the sphere S^2 in the continuum limit (thereby ignoring weak topological indices), so that we are interested in the homotopy group $\pi_2(S^2) = \mathbb{Z}$. Now there are different homotopy classes (corresponding to different topological phases) that are labeled by an integer – the Chern number – and distinguished by how often they wrap the target sphere when tracing over the domain sphere (which is hard to visualize, ← Section 2.1.1).

However, if we are in 1D *and* a symmetry like SLS restricts the Bloch vector to a 2D cut of S^2 , namely a circle S^1 , then we are interested in the homotopy group $\pi_1(S^1) = \mathbb{Z}$. The different homotopy classes consist of maps from the circle onto the circle that have different winding numbers, and therefore cannot be continuously deformed into each other:



The label in this situation is the topological index ν defined above.

- Zak phase:

We introduced the topological index ν as a winding number of the Bloch vector. When we discussed the Chern number, we arrived at it via the Berry curvature, and only later showed that in systems with two bands it can be interpreted as a winding number of the Bloch vector. This begs the question whether there is a similar expression in terms of Bloch *states* (instead of the Bloch vector) to distinguish the two phases of the SSH chain?

The answer is “yes” and known as the *Zak phase* [127]:

$$\varphi_{\text{Zak}} = \int_{S^1} i \langle u(k) | \partial_k u(k) \rangle dk \tag{4.26}$$

where $|u(k)\rangle$ are the Bloch states of the lower (filled) band. The Zak phase is the Berry *phase* collected when traversing the 1D BZ (note that there is no Berry *curvature* in 1D).

Remember that the Berry phase is a gauge dependent quantity and can change by multiples of 2π under continuous gauge transformations. The two phases of the SSH chain are then distinguished by the *difference* of their Zak phases:

$$\Delta\varphi_{\text{Zak}} = (\varphi_{\text{Zak}}^{\text{topological}} - \varphi_{\text{Zak}}^{\text{trivial}}) \bmod 2\pi = \pi \tag{4.27}$$

Proof: ➔ Problemset 7

This quantity has already been measured in experiments with cold atoms in optical lattices [128].

- Polarization:

Remember that in momentum space the *position operator* has the form $\hat{x} = i\partial_k$. The expression (4.26) for the Zak phase then looks very much like the expectation value of the position operator in the many-body ground state (= all states in the lower band filled). Indeed, the quantity $\frac{\varphi_{\text{Zak}}}{2\pi}$ is known as ↑ *polarization* and quantifies the polarization of charge within a unit cell. The difference $\Delta\varphi_{\text{Zak}} = \pi$ between the two phases then translates to a difference in polarization by $\frac{1}{2}$ (in units of the lattice constant). And if you have a look at the distribution of hopping strengths within and between unit cells for the two cases $t > w$ and $t < w$, it is immediately clear that the electron in a unit cell will be localized either in its center (for $t > w$) or between two adjacent unit cells (for $t < w$), producing the difference of $\frac{1}{2}$ in polarization. See [2, Section 3.2.3] for more details.

4.5. Breaking the symmetry

The topological phase of the SSH chain is – supposedly – a symmetry-protected topological (SPT) phase that is protected by sublattice symmetry. According to our discussion in Section 0.5 we should therefore be able to transform the Hamiltonian without closing the gap into a trivial band insulator *if we break SLS*.

Let us check this explicitly ...

14 | Add a staggered chemical potential:

$$\hat{H}'_{\text{SSH}} = \hat{H}_{\text{SSH}} + \underbrace{\mu \sum_{i=1}^L (a_i^\dagger a_i - b_i^\dagger b_i)}_{\hat{H}_\mu} \quad (4.28)$$

Important: $[\hat{H}_\mu, \mathcal{S}] \neq 0$

To see this, remember the interpretation of SLS as bipartiteness of the coupling graph.

15 | → New Bloch vector:

$$\vec{d}(k) = \begin{pmatrix} t + w \cos k \\ w \sin k \\ \mu \end{pmatrix} \quad (4.29)$$

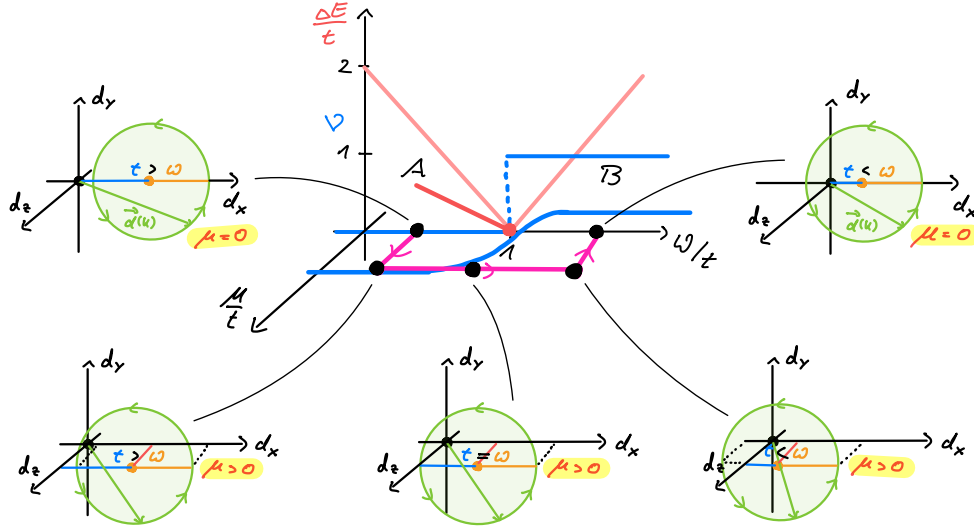
→ Spectrum:

$$\pm E_\pm(k) = |\vec{d}(k)| = \sqrt{\mu^2 + t^2 + w^2 + 2tw \cos k} \geq |\mu| \quad (4.30)$$

→ Gapped for *all* w, t (in particular $w = t$) if $\mu \neq 0$

Note that the spectrum becomes flat for $t \cdot w = 0$ and the many-body ground state of \hat{H}'_{SSH} for $t > 0$ and $w = 0$ is a simple product state at half-filling with one delocalized fermion per unit cell; we label this state as “trivial.” For $t = 0$ and $w > 0$ the bands are again flat and the many-body ground state can be read off the Hamiltonian: now the fermions are delocalized between two modes of *adjacent* unit cells. The family of Hamiltonians \hat{H}'_{SSH} connects these two representatives adiabatically, i.e., without crossing a phase transition (→ *next point*).

16 | Connect phases without closing the gap:



- Note that the winding number (4.24) is not quantized for $\mu \neq 0$ (= no longer an integer).
- This situation is typical for SPT phases.
- This also demonstrates that the topological phase of the SSH chain is *not* topologically ordered (= long-range entangled).

4.6. Edge modes

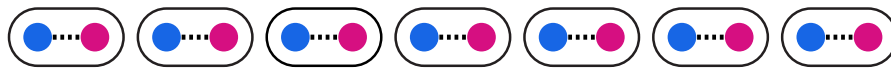
We now cut the SSH chain open to study one of the characteristic features of topological phases, namely the emergence of robust *edge modes* on boundaries:

Remember the inter quantum Hall states (Chapter 1), Chern insulators (Chapter 2), and topological insulators (Chapter 3) all feature robust edge modes on 1D boundaries of 2D samples. By contrast, here we consider a 1D system with 0D boundaries (points).

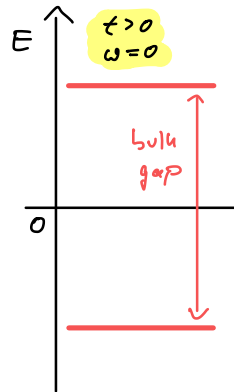
17 | < Open chain of length L :

For a qualitative understanding, we consider the \uparrow *renormalization fixpoints* in each of the two phases (characterized by a vanishing correlation length):

- Trivial phase (A) for $t > 0$ and $w = 0$:

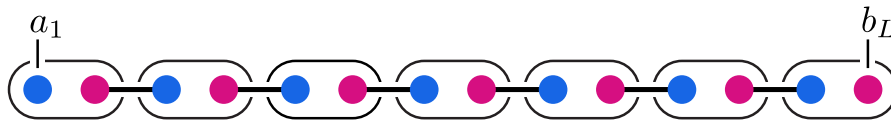


→ SP Spectrum:



Note that due to the OBC, momentum is no longer a good quantum number, the x -axis is therefore of no relevance.

- Topological phase (B) for $t = 0$ and $w > 0$:



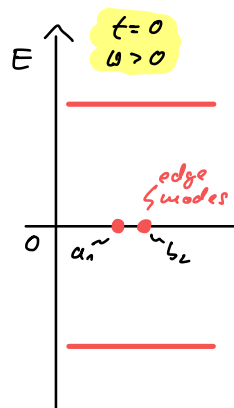
→ * Edge modes $\tilde{a}_l = a_1$ and $\tilde{b}_r = b_L$ commute with \hat{H}_{SSH}

To see this, note that a_1 and b_L no longer show up in \hat{H}_{SSH} .

→ 4-fold degenerate ground state space

The four ground states $|n_l, n_r\rangle$ are labeled by the occupancy $n_l = 0, 1$ and $n_r = 0, 1$ of the edge modes \tilde{a}_l and \tilde{b}_r , i.e., $\tilde{a}_l^\dagger \tilde{a}_l |n_l, n_r\rangle = n_l |n_l, n_r\rangle$ etc.

→ SP Spectrum:



Remember that the phase is still *gapped*, despite the edge modes within the gap.

- 18 | Edge modes persist for $t > 0$ as long as $t < w$ (= in the topological phase):

$$\tilde{a}_l \approx \mathcal{N} \sum_{i=1}^L \left(-\frac{t}{w}\right)^{i-1} a_i \quad \text{and} \quad \tilde{b}_r \approx \mathcal{N} \sum_{i=1}^L \left(-\frac{t}{w}\right)^{i-1} b_{L-i+1} \quad (4.31)$$

The normalization \mathcal{N} depends on t , w and L .

→ Exponentially localized on edges

To show that these are fermionic edge modes in the thermodynamic limit, you must first verify that they indeed describe two fermions,

$$\{\tilde{a}_l, \tilde{a}_l\} = 0, \quad \{\tilde{a}_l, \tilde{a}_l^\dagger\} = 1, \quad \{\tilde{a}_l^{(\dagger)}, \tilde{b}_r^{(\dagger)}\} = 0 \tag{4.32a}$$

$$\{\tilde{b}_r, \tilde{b}_r\} = 0, \quad \{\tilde{b}_r, \tilde{b}_r^\dagger\} = 1. \tag{4.32b}$$

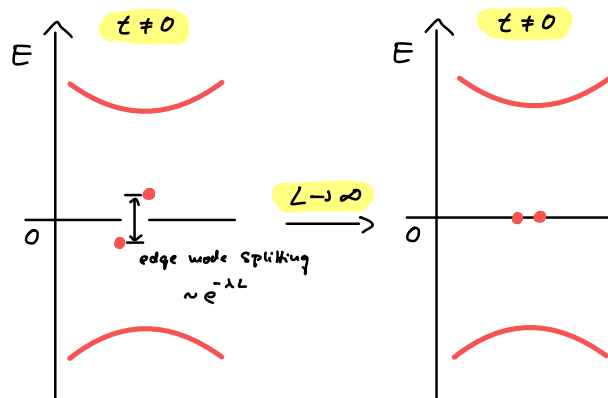
Now you know that \tilde{a}_l and \tilde{b}_r are proper fermionic modes. They are *edge* modes because their mode weight is exponentially localized on the two edges of the chain. To show that they are edge modes of the SSH chain, you must show that they commute with the Hamiltonian (up to corrections that vanish exponentially in the system size):

$$[\tilde{a}_l, \hat{H}_{SSH}] = \mathcal{O}\left(\left(\frac{t}{w}\right)^L\right) \quad \text{and} \quad [\tilde{b}_r, \hat{H}_{SSH}] = \mathcal{O}\left(\left(\frac{t}{w}\right)^L\right). \tag{4.33}$$

This proves the four-fold degeneracy of the ground state space for $L \rightarrow \infty$ in the topological phase $t < w$, even away from the fixpoint $t = 0$. Note that this argument fails in the trivial phase for $t > w$!

Details: → Problemset 7

→ Finite-size scaling of SP spectrum:



Because of the finite extend of the edge modes, there is an exponentially suppressed amplitude for a fermion located on one edge to tunnel across the chain to the other edge. The true eigenstates are therefore non-degenerate symmetric and antisymmetric superpositions of exponentially localized modes on the two boundaries. This splitting vanishes exponentially fast with the system size L . The *edge mode splitting* away from the fixpoint with $t = 0$ is therefore a *finite-size effect*.

You have observed a similar effect for the edge modes of the Kane-Mele model (Section 3.4) when studying narrow strips with open boundaries on → Problemset 6: There, two of the four crossings of edge modes gapped out when the distance between the two open boundaries was small (the other two crossings were protected by time-reversal symmetry).

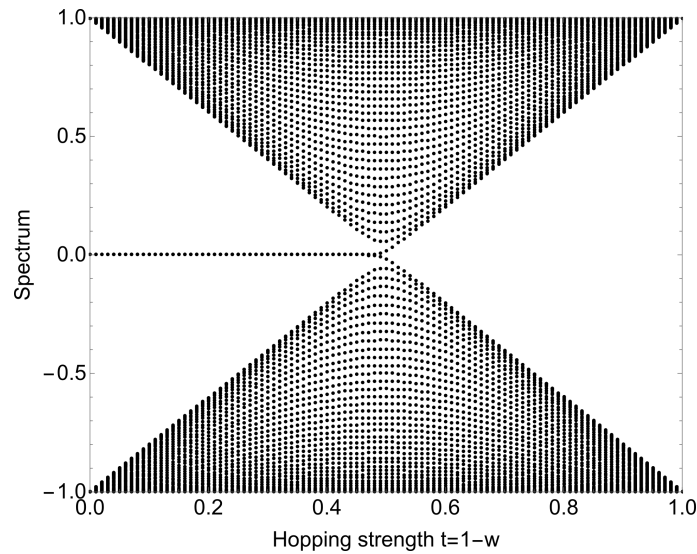
19 | Disorder:

The topological origin of the edge modes makes their existence & degeneracy robust against SLS-preserving disorder:

See three plots → below. (Use beamer to show plots.)

- < No disorder:

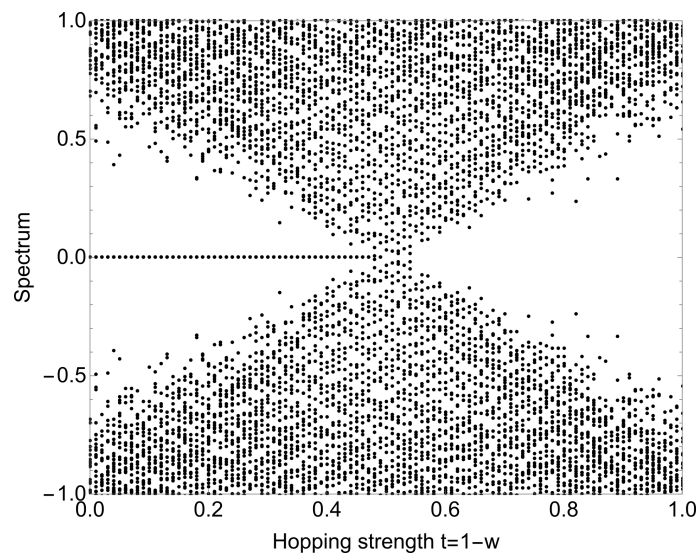
Plot SP spectrum of Eq. (4.10) for $w = 1 - t$ and $t \in [0, 1]$ for a chain of length $L = 40$:



→ Degenerate zero-energy edge modes appear for $t < 0.5$ (= in the topological phase)

- < SLS-preserving disorder:

Plot SP spectrum with $t \mapsto t_i$ and $w \mapsto w_i$ site dependent [Eq. (4.15)]. Choose normal distributed couplings with $\langle t_i \rangle = t$, $\langle w_i \rangle = w$ and $w = 1 - t$ for $t \in [0, 1]$, with variance of 20% of the mean:



! Every spectrum (= points in a column) is computed from a *different* random configuration of couplings for a prescribed mean.

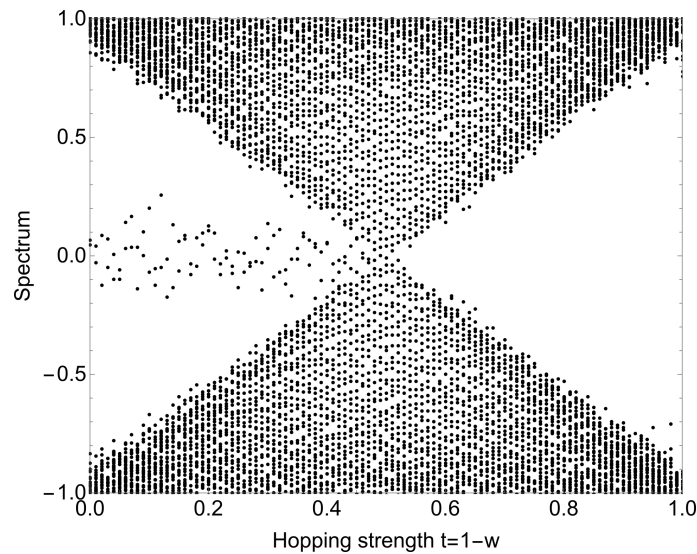
→ Bulk spectrum is scrambled but Edge modes remain degenerate and are not influenced by the disorder in the topological phase.

Whereas the behaviour of the bulk spectrum is generic, the degeneracy of the edge modes is highly atypical and a consequence of the topological nature of the phase (and of course SLS). It is this remarkable behaviour of edge modes that is often referred to as “topologically robust ground state degeneracy” in the context of SPT phases.

- < SLS-breaking disorder:

Let t and w be again uniform but add a *site-dependent chemical potential* $\mu_i^a a_i^\dagger a_i + \mu_i^b b_i^\dagger b_i$ to

the Hamiltonian (4.10) (this breaks SLS!). We choose μ_i^x normal distributed around zero with variance of 0.1 (remember that $w + t = 1$):



The complete spectrum (including the edge modes) is now generic as
→ All degeneracies are lifted!

This demonstrates the symmetry-protection of the ground-/edge-state degeneracy.

20 | Comments:

- These results finally explain (at least partially) how the classical “experiment” in Section 0.1 (where we tried to transfer energy with a chain of coupled, classical pendulums) was motivated. Our findings above explain where the (classical) edge modes come from, and why they are robust against particular types of disorder. Recall that the energy transfer between pendulums on the boundary was perfect for disorder in the springs; this corresponds to SLS-preserving disorder in the hopping amplitudes t and w of the SSH chain. Conversely, disorder in the eigenfrequencies (= lengths) of the pendulums maps to SLS-breaking chemical potentials. (In this situation, the energy transfer was imperfect since the two edge-modes were no longer in resonance.) What remains unclear is how exactly our results for many-body *quantum systems* (described by a Hamiltonian and the Schrödinger equation) translate to *classical systems* (described by Newtonian equations of motion); we study this → later in ??.
- Our study of edge modes suggests that these modes exist throughout the topological phase of the SSH chain. Note that our characterization in terms of the winding number (4.24) relies on *translation invariance* (since we make use of the Bloch Hamiltonian) – but this symmetry is explicitly broken in the scenario with SLS-preserving disorder above. The survival of the degenerate edge modes shows that the topological phase is *not* protected by translation symmetry – it is our characterization in terms of the winding number that makes use of this “auxiliary symmetry.” The fact that the topological nature of the bulk influences the physics on the boundary is known as ↑ *bulk-boundary correspondence*. We encountered other examples previously; for instance, the robust boundary modes of quantum Hall states (Section 1.6) reflect the non-zero Chern number of Landau levels (which describe the bulk).
- You show on ↻ Problemset 7 analytically that edge modes of the form (4.31) persist even in the presence of SLS-preserving disorder (which explains the numerical results above).

4.7. ‡ Experiments

- The *single-particle* physics of the SSH chain has been reproduced experimentally on various platforms [128–131]. Realizing the fermionic *many-body* ground state of \hat{H}_{SSH} is experimentally much more challenging (at least I am not aware of any experiments).
- The topological edge physics of the SSH chain can be applied to the problems of state transfer in quantum chains. We studied this concept theoretically in Ref. [20]; this is the paper that the classical motivation in Section 0.1 is based on. Experiments of this concept have been reported as well [132, 133].
- In 2019, we explored the single-particle physics of the SSH chain experimentally with a quantum simulator based on Rydberg atoms that interact via dipolar interactions [134]. In this experiment, we were interested in an SSH chain filled with *hardcore bosons* instead of fermions (↪ Problemset 1). While the single-particle physics (including edge states) is the same for both particle types, the many-body ground state and the symmetry classification is very different. We study the effect of interactions on topological phases in one-dimension in → Part II.

5. Topological superconductors in 1D: The Majorana Chain

5.1. Preliminaries: Particle-hole symmetry and mean-field superconductors

Before we can discuss the Majorana chain – the paradigmatic model of a *topological superconductor* – we first review a few important concepts needed for its description:

- Remember (← Section 4.1):

Particle-hole symmetry (PHS) \mathcal{C}_U :

The naming should be evident:

\mathcal{C}_U exchanges particles with holes ($c_i \leftrightarrow c_i^\dagger$) up to a unitary transformation U .

$$\mathcal{C}_U i \mathcal{C}_U^{-1} = +i \quad \text{and} \quad \mathcal{C}_U c_i \mathcal{C}_U^{-1} = \sum_j U_{ij}^{*\dagger} c_j^\dagger \quad (5.1a)$$

$$[\hat{H}, \mathcal{C}_U] = 0 \quad \Leftrightarrow \quad U H^* U^\dagger = -H \quad \Leftrightarrow \quad \{H, \underbrace{U \mathcal{K}}_{\mathcal{C}_U}\} = 0 \quad (5.1b)$$

(The complex conjugate at the U is convention and not crucial.)

→

- Unitary symmetry on MB Hamiltonian
- Antiunitary pseudosymmetry on SP Hamiltonian

As a pseudosymmetry, $\mathcal{C}_U = U \mathcal{K}$ anticommutes with the SP Hamiltonian.

Of course, this symmetry will be crucial to define a *new topological invariant*.

- Remember (↓ your lecture on solid state physics):

BCS theory of superconductivity:

Until now, we only considered (topological) *insulators*, i.e., quadratic fermion theories with *particle number conservation*. By contrast, the Majorana chain is a (topological) *superconductor*, where only *fermion parity* survives as symmetry. Let us briefly review how these particle-number violating terms emerge from a microscopic theory:

- 1 | < ** BCS Hamiltonian: (BCS = BARDEEN-COOPER-SCHRIEFFER)

$$\hat{H}_{\text{BCS}} = \underbrace{\sum_{\mathbf{k}, \sigma} (\varepsilon_{\mathbf{k}} - \mu) c_{\mathbf{k}\sigma}^\dagger c_{\mathbf{k}\sigma}}_{\text{Free fermions}} + \underbrace{\sum_{\mathbf{k}, \mathbf{k}'} V_{\mathbf{k}\mathbf{k}'} c_{\mathbf{k}\uparrow}^\dagger c_{-\mathbf{k}\downarrow}^\dagger c_{-\mathbf{k}'\downarrow} c_{\mathbf{k}'\uparrow}}_{\text{Pairing term (interaction)}} \quad (5.2)$$

$\sigma \in \{\uparrow, \downarrow\}$: fermion spin

μ : chemical potential

$\varepsilon_{\mathbf{k}}$: free fermion dispersion

$V_{\mathbf{k}\mathbf{k}'}$: pairing potential

- *Rationale*: Superconductivity is a condensation mechanism that is triggered by attractive interactions $V_{\mathbf{k}\mathbf{k}'}$ (mediated by phonons) between fermions. The formation of bosonic \downarrow Cooper pairs then lowers the energy, the Cooper pairs condense and form the superconducting condensate.
- Note that Eq. (5.2) is a theory of interacting fermions with particle-number conservation. The symmetry group $U(1)$ is generated by the total particle number operator $N = \sum_{\mathbf{k},\sigma} c_{\mathbf{k}\sigma}^\dagger c_{\mathbf{k}\sigma}$ with $[\hat{H}_{\text{BCS}}, N] = 0$. Due to the interactions, Eq. (5.2) cannot be diagonalized exactly.

2 | The BCS Hamiltonian is interacting (= not quadratic) and therefore hard to study.

→ \downarrow Mean-field theory:

$$c_{\mathbf{k}\uparrow}^\dagger c_{-\mathbf{k}\downarrow}^\dagger = X_{\mathbf{k}}^* + (c_{\mathbf{k}\uparrow}^\dagger c_{-\mathbf{k}\downarrow}^\dagger - X_{\mathbf{k}}^*) \quad \text{with} \quad X_{\mathbf{k}}^* = \langle c_{\mathbf{k}\uparrow}^\dagger c_{-\mathbf{k}\downarrow}^\dagger \rangle \quad (5.3a)$$

$$c_{-\mathbf{k}'\downarrow} c_{\mathbf{k}'\uparrow} = \underbrace{X_{\mathbf{k}'}}_{\text{Mean}} + \underbrace{(c_{-\mathbf{k}'\downarrow} c_{\mathbf{k}'\uparrow} - X_{\mathbf{k}'})}_{\text{Small fluctuations } \delta X_{\mathbf{k}'}} \quad \text{with} \quad X_{\mathbf{k}} = \langle c_{-\mathbf{k}'\downarrow} c_{\mathbf{k}'\uparrow} \rangle \quad (5.3b)$$

* Cooper pair condensation $\Leftrightarrow X_{\mathbf{k}'} \neq 0$ and $\delta X_{\mathbf{k}'}$ small

[The approximation $c_{\mathbf{k}\uparrow}^\dagger c_{-\mathbf{k}\downarrow}^\dagger = X_{\mathbf{k}}^* \times \mathbb{1} + \delta X_{\mathbf{k}}$ means that we expect the ground state to be (approximately) invariant under the application of $c_{\mathbf{k}\uparrow}^\dagger c_{-\mathbf{k}\downarrow}^\dagger$ (and similarly $c_{-\mathbf{k}\downarrow} c_{\mathbf{k}\uparrow}$). This can only be true if the ground state is a superposition of states with all possible numbers of fermions (with the same parity). Such a superposition is usually called a * condensate.]

→ Drop terms of order $\mathcal{O}(\delta X_{\mathbf{k}'}^2)$ (and a constant offset):

$$\hat{H}_{\text{BCS}}^{\text{mf}} \stackrel{\circ}{=} \underbrace{\sum_{\mathbf{k},\sigma} (\varepsilon_{\mathbf{k}} - \mu) c_{\mathbf{k}\sigma}^\dagger c_{\mathbf{k}\sigma}}_{\text{Free fermions}} + \sum_{\mathbf{k}} \underbrace{\left[\Delta_{\mathbf{k}} c_{\mathbf{k}\uparrow}^\dagger c_{-\mathbf{k}\downarrow}^\dagger + \Delta_{\mathbf{k}}^* c_{-\mathbf{k}\downarrow} c_{\mathbf{k}\uparrow} \right]}_{\text{Quadratic pairing terms}} \quad (5.4)$$

with order parameter

$$\Delta_{\mathbf{k}} = \sum_{\mathbf{k}'} V_{\mathbf{k}\mathbf{k}'} X_{\mathbf{k}'} \in \mathbb{C} \quad (5.5)$$

Since here Cooper pairs are formed by fermions with total spin zero [$X_{\mathbf{k}} = \langle c_{-\mathbf{k}'\downarrow} c_{\mathbf{k}'\uparrow} \rangle$] this is called \downarrow s-wave superconductivity.

- ¡! $\hat{H}_{\text{BCS}}^{\text{mf}}$ is no longer particle-number conserving; only the fermion parity $\mathcal{P} = (-1)^N$ is conserved: $[\hat{H}_{\text{BCS}}^{\text{mf}}, \mathcal{P}] = 0$.
- The \mathbb{Z}_2 group generated by \mathcal{P} is a subgroup of $U(1)$ generated by N , hence this is an example of \leftarrow spontaneous symmetry breaking (Section 0.4), where the superconducting condensate breaks (global) particle-number conservation and only fermion parity survives. The Hamiltonian $\hat{H}_{\text{BCS}}^{\text{mf}}$ makes only sense as an effective mean-field description that excludes the superconducting condensate from/into which pairs of electrons can be transferred.

[As mentioned in Section 0.5, the correct classification of the superconducting phase is subtle [35]. When the fermions are charged and coupled to a *dynamical* gauge field, the transition is not described by SSB but a topological phase transition [39, 40]. When the fermions couple to a *static* (= background) gauge field, the transition is described by spontaneous breaking of the *global* U(1) symmetry. It is not correct (as one sometimes hears) that the (local) *gauge* symmetry is broken spontaneously [135–138].]

- The benefit of the mean-field description $\hat{H}_{\text{BCS}}^{\text{mf}}$ of superconductivity is that the Hamiltonian is *quadratic* in fermions and therefore fits our current class of models (“non-interacting fermions”).

In this section, we consider quadratic fermion Hamiltonians of the form (5.4) (i.e., with superconducting pairing terms). We treat these models as *fundamental*, and ignore that they actually arise from microscopic, interacting, particle-number conserving theories via spontaneous symmetry breaking!

5.2. The Majorana chain

A detailed exposition of the Majorana chain is given in the textbook by Bernevig [1] but may also be found in almost any other textbook that covers topological superconductors. Furthermore, the original paper by KITAEV is worthwhile to read [139]. There is also an introduction in my PhD thesis [126] (on which this section is based) and a more detailed account in my Master thesis [140].

- 1 | < 1D superconductor of spinless fermions c_i (= *p*-wave pairing):

$$\hat{H}_{\text{MC}} := - \sum_{i=1}^{L'} \left(w c_i^\dagger c_{i+1} - \Delta c_i c_{i+1} + \text{h.c.} \right) - \sum_{i=1}^L \mu \left(c_i^\dagger c_i - \frac{1}{2} \right) \quad (5.6)$$

$w \in \mathbb{R}$: tunneling amplitude

$\Delta = e^{i\theta} |\Delta| \in \mathbb{C}$: superconducting gap (θ is the phase of the condensate)

$\mu \in \mathbb{R}$: chemical potential

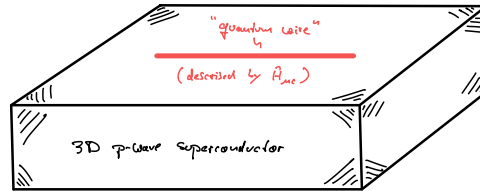
$L' = L$ (PBC) or $L' = L - 1$ (OBC)

- This is the mean-field theory (in real space!) of a “triplet superconductor” with *p*-wave pairing, i.e., Cooper pairs consist of *spin-polarized* (and therefore effectively *spinless*) electrons with total angular momentum of one.

Of course there are no true “spinless fermions” because of the \uparrow *spin-statistics theorem*. However, imagine you apply a strong magnetic field such that only fermions in spin-polarized modes $c_{i\uparrow}$ are relevant for the low-energy physics (in particular: ground state). If only operators like $c_{i\uparrow}$ show up in the (low-energy) Hamiltonian, one can drop the spin-index \uparrow altogether: $c_{i\uparrow} \mapsto c_i$. This is what we mean by “spinless fermions.”

- \ddagger We are interested in topological phase transitions *between* different superconducting phases – and not in the superconducting phase transition itself (which is, as mentioned above, described by spontaneous symmetry breaking). Therefore we do not determine the gap Δ self-consistently (as done in BCS theory) but simply take it as a non-zero, translation invariant parameter of the theory.

- With a unitary transformation $c_i = e^{-i\theta/2} c'_i$ one can remove the superconducting phase, so that *w.l.o.g.* $\Delta = |\Delta|$ is real. Note that since the system is one-dimensional, there cannot be vortices in the superconducting condensate (= flux tubes).
- In one dimension, the \uparrow *Mermin-Wagner theorem* forbids the spontaneous breaking of the continuous $U(1)$ symmetry (particle-number conservation) that is responsible for the superconducting phase. (Instead one finds a disordered phase known as a \uparrow *Luttinger liquid* with correlations that decay algebraically.) Thus one should think of the superconducting terms in \hat{H}_{MC} as being induced by the \uparrow *proximity effect* of an attached *three dimensional bulk superconductor*:



This is also (roughly) the setting used to study the Majorana chain in experiments [141] (although there have been setbacks [142]).

2 | \leftarrow PBC \rightarrow Fourier transform:

$$\tilde{c}_k = \frac{1}{\sqrt{L}} \sum_{n=1}^L e^{-ikn} c_n \quad \Leftrightarrow \quad c_n = \frac{1}{\sqrt{L}} \sum_{k \in \text{BZ}} e^{ikn} \tilde{c}_k \quad (5.7)$$

with $k = \frac{2\pi}{L}m$ for $m = 0, \dots, L-1$.

$\xrightarrow{\circ}$ (up to a constant)

$$\hat{H}_{MC} = - \sum_{k \in \text{BZ}} \left[(2w \cos k + \mu) \tilde{c}_k^\dagger \tilde{c}_k + i \Delta \sin(k) \tilde{c}_k \tilde{c}_{-k} - i \Delta \sin(k) \tilde{c}_{-k}^\dagger \tilde{c}_k^\dagger \right] \quad (5.8)$$

Note that because of the pairing terms, this Hamiltonian is not yet diagonal (despite there being only a single mode per unit cell and no spin involved). To diagonalize it, we can use a trick:

3 | Bogoliubov-de Gennes Hamiltonian:

We expand the cosine term artificially (using an index substitution $k \mapsto -k$ in the sum):

$$(2w \cos k + \mu) \tilde{c}_k^\dagger \tilde{c}_k \quad \mapsto \quad \frac{1}{2} [(2w \cos k + \mu) \tilde{c}_k^\dagger \tilde{c}_k + (2w \cos k + \mu) \tilde{c}_{-k}^\dagger \tilde{c}_{-k}] \quad (5.9)$$

\rightarrow

$$\hat{H}_{MC} = -\frac{1}{2} \sum_{k \in \text{BZ}} \left[(2w \cos k + \mu) \tilde{c}_k^\dagger \tilde{c}_k + (2w \cos k + \mu) \tilde{c}_{-k}^\dagger \tilde{c}_{-k} + i 2\Delta \sin(k) \tilde{c}_k \tilde{c}_{-k} - i 2\Delta \sin(k) \tilde{c}_{-k}^\dagger \tilde{c}_k^\dagger \right] \quad (5.10)$$

Introduce $**$ *Nambu spinors*

$$\Psi_k := \begin{pmatrix} \tilde{c}_k \\ \tilde{c}_{-k}^\dagger \end{pmatrix} \quad (5.11)$$

Note that the degrees of freedom described by the components of the Nambu spinor are *not* independent but related by particle-hole symmetry. This is different from the introduction of other pseudo-spinors in the situation of multiple DOFs per unit cell (like sublattices or internal DOFs).

→ Rewrite the Hamiltonian (up to a constant)

$$\hat{H}_{\text{MC}} = \frac{1}{2} \sum_{k \in \text{BZ}} \begin{pmatrix} \tilde{c}_k^\dagger & \tilde{c}_{-k} \end{pmatrix} \cdot \underbrace{\begin{pmatrix} -2w \cos k - \mu & -2\Delta i \sin k \\ 2\Delta i \sin k & 2w \cos k + \mu \end{pmatrix}}_{H_{\text{BdG}}(k)} \cdot \begin{pmatrix} \tilde{c}_k \\ \tilde{c}_{-k}^\dagger \end{pmatrix} \quad (5.12a)$$

$$= \frac{1}{2} \sum_{k \in \text{BZ}} \Psi_k^\dagger H_{\text{BdG}}(k) \Psi_k \quad (5.12b)$$

with $\ast\ast$ Bogoliubov-de Gennes Hamiltonian

$$H_{\text{BdG}}(k) = -(2w \cos k + \mu) \sigma^z + 2\Delta \sin k \sigma^y = \vec{d}(k) \cdot \vec{\sigma} \quad (5.13)$$

and

$$\vec{d}(k) = \begin{pmatrix} 0 \\ 2\Delta \sin k \\ -2w \cos k - \mu \end{pmatrix} \quad (5.14)$$

The BdG Hamiltonian is a *redundant* matrix encoding of the MB Hamiltonian \hat{H}_{MC} . It exists for all quadratic fermion Hamiltonians, but is non-trivial (= not diagonal) – and therefore useful – only for Hamiltonians with superconducting pairing terms. As the above construction demonstrates, its existence is rooted in the algebra of the fermion operators.

4 | Bogoliubov transformation:

To diagonalize Eq. (5.12), we must diagonalize the BdG Hamiltonian:

$$U_k^\dagger H_{\text{BdG}}(k) U_k = \begin{pmatrix} E(k) & 0 \\ 0 & -E(k) \end{pmatrix} \quad (5.15)$$

U_k : unitary rotation in Nambu space

The symmetry of the spectrum follows from PHS of the BdG Hamiltonian (→ below).

Define new fermion modes → $\ast\ast$ Bogoliubov quasiparticles:

$$\tilde{\Psi}_k \equiv \begin{pmatrix} \tilde{a}_k \\ \tilde{a}_{-k}^\dagger \end{pmatrix} := U_k^\dagger \Psi_k \stackrel{\circ}{=} \begin{pmatrix} u_k \tilde{c}_k + v_k \tilde{c}_{-k}^\dagger \\ v_{-k}^* \tilde{c}_k + u_{-k}^* \tilde{c}_{-k}^\dagger \end{pmatrix} \quad (5.16)$$

The coefficients u_k and v_k satisfy certain constraints to ensure that the new modes \tilde{a}_k obey fermionic anticommutation relations:

$$\{\tilde{a}_k, \tilde{a}_k^\dagger\} \stackrel{\circ}{=} |u_k|^2 + |v_k|^2 \stackrel{!}{=} 1, \quad (5.17a)$$

$$\{\tilde{a}_k, \tilde{a}_{-k}\} \stackrel{\circ}{=} v_k u_{-k} + u_k v_{-k} \stackrel{!}{=} 0. \quad (5.17b)$$

That this structure for U_k is possible is again a consequence of the PHS of the BdG Hamiltonian (→ below). Note that this additional structure is necessary because the Bogoliubov transformation mixes particles and holes. By contrast, for the diagonalization of a non-superconducting Bloch Hamiltonian, any unitary U_k yields a canonical transformation (because there one does not mix annihilation with creation operators).

For Eq. (5.12) in the important special case $\Delta = w$ and $\mu = 0$ (→ later), one finds the explicit expressions

$$u_k \stackrel{\circ}{=} i \sin \frac{k}{2} \quad \text{and} \quad v_k \stackrel{\circ}{=} \cos \frac{k}{2}. \quad (5.18)$$

5 | Spectrum: Eqs. (2.9) and (5.14) →

$$E(k) = |\vec{d}(k)| = \sqrt{(2w \cos k + \mu)^2 + 4\Delta^2 \sin^2 k} \quad (5.19)$$

Because of the redundancy of the BdG Hamiltonian, the second band (and therefore the second eigenenergy $-|\vec{d}(k)|$ of H_{BdG}) is “fake” ...

...because

$$\hat{H}_{\text{MC}} = \frac{1}{2} \sum_{k \in \text{BZ}} \begin{pmatrix} \tilde{a}_k^\dagger & \tilde{a}_{-k} \end{pmatrix} \cdot \begin{pmatrix} +E(k) & 0 \\ 0 & -E(k) \end{pmatrix} \cdot \begin{pmatrix} \tilde{a}_k \\ \tilde{a}_{-k}^\dagger \end{pmatrix} \quad (5.20a)$$

$$= \frac{1}{2} \sum_{k \in \text{BZ}} \left[E(k) \tilde{a}_k^\dagger \tilde{a}_k - E(k) \tilde{a}_{-k} \tilde{a}_{-k}^\dagger \right] \quad (5.20b)$$

$$= \sum_{k \in \text{BZ}} E(k) \tilde{a}_k^\dagger \tilde{a}_k + \text{const} \quad (5.20c)$$

where we used $E(k) = E(-k)$ and $\{\tilde{a}_k, \tilde{a}_k^\dagger\} = 1$; i.e., for every k there is only *one* mode \tilde{a}_k with energy $+E(k)$.

6 | Preliminary Phase diagram:

Let $\Delta \neq 0 \rightarrow E(k) = 0$ only possible for $k = 0, \pi \rightarrow$

$$E(0/\pi) = |\pm 2w + \mu| \stackrel{!}{=} 0 \quad \Rightarrow \quad 2|w| = |\mu| \quad (5.21)$$

→ Two gapped phases:

$$\text{Phase A: } 2|w| > |\mu| \quad \text{and} \quad \text{Phase B: } 2|w| < |\mu| \quad (5.22)$$

! In contrast to models with particle-number conservation, the gap here is not given by the separation of two bands (there is only one!), and the ground state is not obtained by “filling” the lower of two bands. Since $E(k) > 0$ for all $k \in \text{BZ}$, Eq. (5.20c) implies that the many-body ground state is the state with all modes \tilde{a}_k empty (\rightarrow *next*), and excited states are characterized by occupied modes (\uparrow *Bogoliubov quasiparticles*) with a finite (system-size independent) energy. This is the gap of the system (induced by superconductivity); the quasiparticle excitations are “particle-hole excitations” (superpositions of a fermion above and a hole in the condensate) and can be thought of as “broken” Cooper pairs.

7 | Many-body ground state $|\Omega\rangle$ with

$$\tilde{a}_k |\Omega\rangle \stackrel{!}{=} 0 \quad \forall k \in \text{BZ} \quad (5.23)$$

→ *Unique* BCS ground state (unique in *both* phases, i.e., no symmetry breaking!)

$$|\Omega\rangle \propto \prod_{k: \tilde{a}_k |0\rangle \neq 0} \tilde{a}_k |0\rangle \stackrel{5.16}{\propto} \stackrel{5.18}{\underset{\substack{w=\Delta \\ \mu=0}}{\propto}} \prod_{k \in (-\pi, \pi)} \tilde{a}_k |0\rangle \overset{\circ}{\propto} \tilde{a}_0 \prod_{k \in (0, \pi)} (u_k + v_k \tilde{c}_{-k}^\dagger \tilde{c}_k^\dagger) |0\rangle \quad (5.24a)$$

- This ground state is called *quasiparticle vacuum* ($\tilde{a}_k |\Omega\rangle = 0$) and is different from the *physical vacuum* ($\tilde{c}_k |\Omega\rangle \neq 0$), i.e., $|\Omega\rangle$ contains superpositions of states with different particle numbers of c_i -fermions (this is true as long as $\Delta \neq 0$, i.e., in the presence of a superconducting condensate).

- As we will see → *below*, the parameter choice $w = \Delta$ and $\mu = 0$ corresponds to the fixpoint in Phase A (which is topological). That the model simplifies at this point is apparent from the spectrum (5.19) which becomes flat.
- Notice that in phase A (for $w = \Delta$ and $\mu = 0$) $|\Omega\rangle$ has *negative* fermion parity because of the zero-mode \tilde{a}_0 (the other TRIM mode \tilde{a}_π annihilates $|0\rangle$ and must not be applied). This can be shown by deriving u_k and v_k explicitly for this case [Eq. (5.18)].

5.3. Symmetries and topological indices

Our next goal is to characterize (and distinguish) the two gapped phases A and B by topological features of the BdG Hamiltonian:

8 | \triangleleft Time-reversal symmetry:

- i | *w.l.o.g.* Δ real $\rightarrow \mathcal{T} := \mathbb{1}\mathcal{K} \rightarrow [\hat{H}_{\text{MC}}, \mathcal{T}] = 0 \rightarrow \text{TRS} \checkmark$
 More precisely: $\mathcal{T}i\mathcal{T}^{-1} = -i$ and $\mathcal{T}c_i^{(\dagger)}\mathcal{T}^{-1} = c_i^{(\dagger)}$.

$\xrightarrow{\circ}$ After a Fourier transform, TRS is represented as (acting on “Nambu space”) [\leftarrow Eq. (2.31d)]

$$\mathbb{1} H_{\text{BdG}}^*(k) \mathbb{1} = H_{\text{BdG}}(-k) \tag{5.25}$$

$\rightarrow \tilde{T} = \mathbb{1}\mathcal{K} \rightarrow \text{TRS with } \tilde{T}^2 = +\mathbb{1}$

Systems with a TRS that squares to $+\mathbb{1}$ are combined into the ...

\rightarrow $\ast\ast$ Symmetry class **AI** [\rightarrow Chapter 6]

The label has historical/mathematical meaning but is of no importance to us.

\uparrow Cartan’s classification of symmetric spaces

- ii | Eqs. (5.13) and (5.25) \rightarrow Constraints on the BdG vector:

$$d_x(-k) = d_x(k) \tag{5.26a}$$

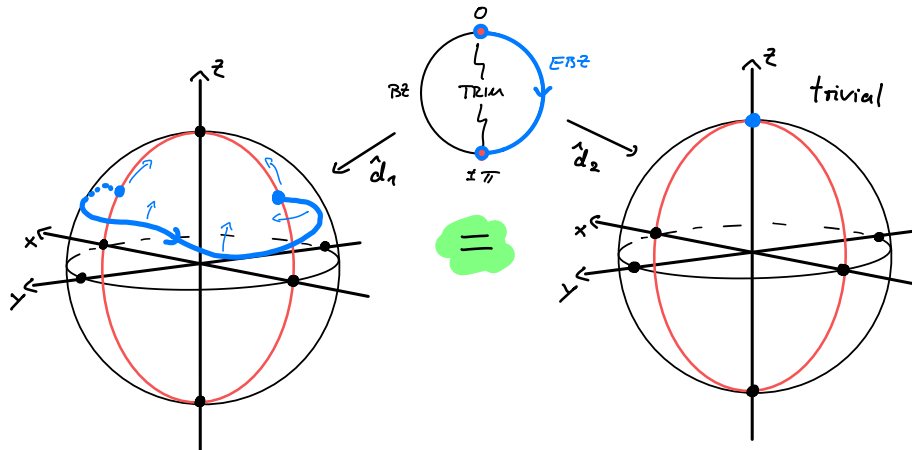
$$d_y(-k) = -d_y(k) \tag{5.26b}$$

$$d_z(-k) = d_z(k) \tag{5.26c}$$

$\rightarrow \vec{d}(k)$ on EBZ $[0, \pi]$ determines $H_{\text{BdG}}(k)$ completely

- iii | $\triangleleft K^* \in \{0, \pi\}$ TRIM $\rightarrow d_y(K^*) = 0$

\rightarrow Image $\hat{d}(\text{EBZ})$ [$\hat{d}(k) = \frac{\vec{d}(k)}{|\vec{d}(k)|}$] on S^2 must start & end on great circle:



- All paths (= gapped & symmetric Hamiltonians) can be continuously contracted
- No topological phases ☹

Note that a BdG vector pointing in z -direction corresponds to the Hamiltonian (5.6) with $w = 0 = \Delta$ and only a chemical potential $\mu \neq 0$, which is obviously a trivial band insulator with all modes either empty or filled (depending on the sign of μ).

- iv | Boldly generalizing these findings, we could hypothesize:

One-dimensional systems of symmetry class **AI** do not allow for TPs.

This is true in general; → Chapter 6 on the classification of topological insulators & superconductors.

- v | Conclusion for the Majorana chain:

TRS alone is not sufficient to characterize the phases of the Majorana chain.

→ We need something else ...

- 9 | < Particle-hole “symmetry”:

- i | < Eqs. (2.31d), (5.1b) and (5.13)

The BdG Hamiltonian (matrix) has an *intrinsic* PHS:

$$\sigma^x H_{\text{BdG}}^*(k) \sigma^x = -H_{\text{BdG}}(-k) \tag{5.27}$$

In real space this would read $UH_{\text{BdG}}^*U^\dagger = -H_{\text{BdG}}$, where U acts as σ^x on the Nambu subspace spanned by c_i and c_i^\dagger . Above we had no need to explicitly define H_{BdG} in real space.

→ $\tilde{C} := \sigma^x \mathcal{K} \rightarrow$ PHS with $\tilde{C}^2 = +\mathbb{1}$

→ $\ast\ast$ Symmetry class **D** [→ Chapter 6]

- This “symmetry” is tautological in the sense that it derives solely from the fermion algebra. It does *not* correspond to a physical many body symmetry \mathcal{C} of \hat{H}_{MC} , so that some authors do not call it a “symmetry” altogether. However, it is a valid antiunitary *pseudosymmetry* of the BdG Hamiltonian – and this is all that matters for the discussion that follows. Whether the algebraic constraint Eq. (5.27) on $H_{\text{BdG}}(k)$ derives from a *physical symmetry* or from the *algebraic structure* of the fermion algebra is irrelevant for the topological classification of $H_{\text{BdG}}(k)$.

If this all seems a bit cryptic: ☹ Problemset 8

- This teaches us something important: The “symmetry classes” we started to introduce (like **AI** and **D**) should be thought of as classes/ensembles of *matrices* with certain constraints. If these matrices derive from a many-body Hamiltonian (like a Bloch-order BdG Hamiltonian), these constraints *can* descend from real symmetries of the many-body Hamiltonian. However, this is not always the case (as for the PHS of superconductors). This explains the somewhat opaque statement that **D** describes the family of superconductors *without* symmetries – where “symmetries” refers to *physical* symmetries of the many-body Hamiltonian.

Note that the proper concept of “particle-hole symmetry” has not yet been fully settled in the community [143], partially due to the tautological nature of the PHS above (which is then referred to as *charge conjugation* instead of *particle-hole transformation*).

ii | Eqs. (5.13) and (5.27) → Constraints on the BdG vector:

$$d_x(-k) = -d_x(k) \tag{5.28a}$$

$$d_y(-k) = -d_y(k) \tag{5.28b}$$

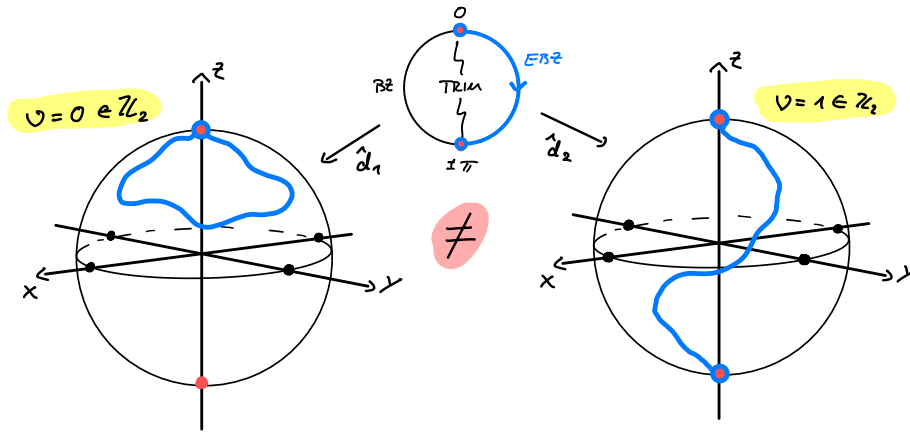
$$d_z(-k) = d_z(k) \tag{5.28c}$$

→ Again $\vec{d}(k)$ on EBZ $[0, \pi]$ determines $H_{\text{BdG}}(k)$ completely

iii | $\langle K^* \in \{0, \pi\}$ TRIM → $d_x(K^*) = 0 = d_y(K^*)$

Note that these are now *two* constraints as compared to TRS!

→ Image \hat{d} (EBZ) on S^2 must start & end either on “north” or “south pole”:



→ Two topologically distinct classes of paths
(Only one of which can be continuously contracted to a point.)

→ One topological phase possible ☺ → \mathbb{Z}_2 -index

Note that the orientation of the Bloch sphere (and therefore the position of the poles) has no physical meaning as it can be changed continuously by $SU(2)$ rotations in Nambu space (as we did with the Bogoliubov transformation). Consequently, a path attached to the *south* pole is unitarily equivalent to the shown path attached to the north pole.

iv | Boldly generalizing these findings, we could hypothesize:

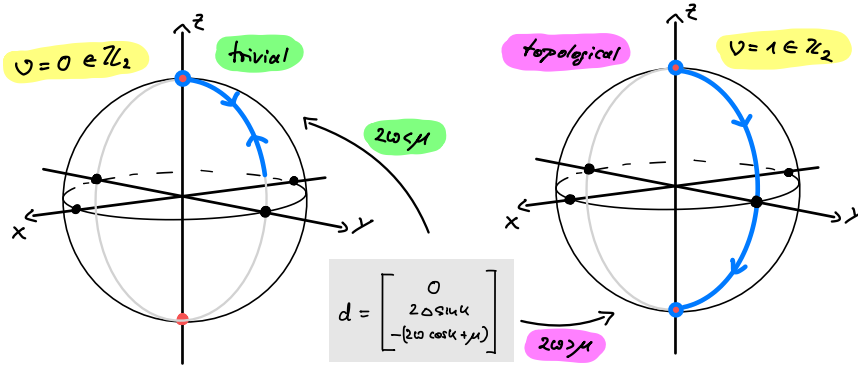
In 1D, systems of class **D** allow for a single TP labeled by a \mathbb{Z}_2 -index.

Again, this is true in general; → Chapter 6 on the classification of topological insulators & superconductors.

↓ Lecture 16 [20.06.25]

v | Conclusion for the Majorana chain:

The \mathbb{Z}_2 -index classifies the phase for $2|w| < |\mu|$ as *trivial* and $2|w| > |\mu|$ as *topological*:



→

Phase A: $2|w| > |\mu| \rightarrow$ topological

Phase B: $2|w| < |\mu| \rightarrow$ trivial

(5.29)

In his original paper [139], Kitaev classified the two phases differently (using the Pfaffian to distinguish two classes of quadratic fermion Hamiltonians). The classification presented here, based on the BdG Hamiltonian, is conceptually very different. However, it can be shown that the two approaches lead to the same notion of trivial and topological phases [144].

We could be satisfied at this point, but there is actually more to be learned if we *combine* both PHS and TRS ...

10 | < PHS & TRS:

- i | As argued above, PHS is intrinsic to the form of the BdG Hamiltonian (it cannot be broken). Furthermore, for an open chain we can always find a TRS representation by gauging away complex phases. Hence it is reasonable to consider the situation where both symmetries are preserved.

< TRS with $\tilde{T}^2 = +1$ and PHS with $\tilde{C}^2 = +1$

→ * Symmetry class **BDI** [→ Chapter 6]

- ii | Eqs. (5.26) and (5.28) → Constraints on the BdG vector:

$$d_x(-k) = 0 \tag{5.30a}$$

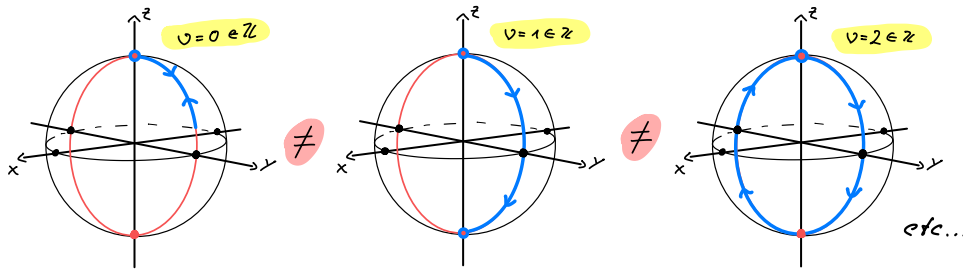
$$d_y(-k) = -d_y(k) \tag{5.30b}$$

$$d_z(-k) = d_z(k) \tag{5.30c}$$

→ Still $\vec{d}(k)$ on EBZ $[0, \pi]$ determines $H_{\text{BdG}}(k)$ completely

- iii | Image \hat{d} (EBZ) on S^2 ...

- ... is constrained to the great circle with $d_x = 0$
- ... and must start & end either on “north” or “south pole”:



→ Infinitely many topologically distinct classes of paths
(distinguished by their winding number)

→ Infinitely many topological phases possible → \mathbb{Z} -index

iv | **Boldly generalizing these findings, we could hypothesize:**

In 1D, systems of class **BDI** allow for many TPs labeled by a \mathbb{Z} -index.

Again, this is true in general; → Chapter 6 on the classification of topological insulators & superconductors.

v | Conclusion for the Majorana chain:

Although TRS is not useful on its own, in combination with PHS it boosts the \mathbb{Z}_2 -index of **D** to a \mathbb{Z} -index of **BDI**. For a single Majorana chain, this has the only benefit that we can use either the topological index of **D** or the winding number of **BDI** to characterize the topological phase; in this situation, they are equivalent. This is different if one considers *stacks* of multiple parallel Majorana chains, where one can create infinitely many different SPT phases when TRS is present (**BDI**) but only one if it is broken (**D**).

On ↻ Problemset 8 you study stacks of time-reversal symmetric Majorana chains in class **BDI**. There you show that *interactions* modify the \mathbb{Z} -index constructed here to a \mathbb{Z}_8 -index (see also → Section 6.4).

vi | Final note: For the SP Hamiltonian having PHS *and* TRS means:

$$\text{PHS: } U_C H^* U_C^\dagger \stackrel{5.1b}{=} -H \tag{5.31a}$$

$$\text{TRS: } U_T H^* U_T^\dagger \stackrel{2.31b}{=} +H \tag{5.31b}$$

which implies

$$U_S H U_S^\dagger = -H \quad \text{with} \quad U_S = U_T U_C^* \tag{5.32}$$

→ Sublattice symmetry [Eq. (4.4)]

This is true in general and will be important → *later* (Chapter 6).

5.4. Majorana fermions

Why do we call the Majorana chain “Majorana chain” in the first place?

To answer this, we need a bit of algebra. As a bonus, we will find an unexpected relation between the Majorana chain and the SSH chain discussed in Chapter 4:

11 | < Set of fermion L operators $\{c_1, c_2, \dots, c_L\}$ and define $2L$ *Majorana operators*

$$\gamma_{2i-1} = c_i + c_i^\dagger \quad \text{and} \quad \gamma_{2i} = i(c_i^\dagger - c_i) \quad (5.33)$$

→ There are *two* Majorana operators per fermion mode.

12 | → Properties:

$$\gamma_n^\dagger = \gamma_n \quad \text{and} \quad \{\gamma_n, \gamma_m\} = 2\delta_{nm} \quad \text{for} \quad n, m \in \{1, \dots, 2L\} \quad (5.34)$$

- Up to a normalization, Majorana fermions behave like *self-adjoint* or *real* fermions. The name originates from a similar concept in high-energy physics due to ETTORE MAJORANA (namely, real-valued solutions of the Dirac equation in Majorana representation). In condensed matter physics, however, the properties Eq. (5.34) should be seen as the defining relations of *Majorana operators*.
- While the γ_n describe “real” (Majorana) fermions, the c_i describe “complex” (Dirac) fermions. Eq. (5.33) demonstrates that the two Majoranas γ_{2i-1} and γ_{2i} can be thought of as the “real” and “imaginary part” of the complex fermion c_i .
- We stress that Majorana fermions are *not* → *anyons*, they are fermionic quasiparticles (as the name clearly states); only → *Majorana zero modes* can make their hosts (like vortices in 2D $p_x + ip_y$ -superconductors) behave like anyons under adiabatic deformations of the Hamiltonian.

13 | Pairs of Majoranas can be recombined to form a complex fermion:

$$c_i \stackrel{5.33}{=} \frac{1}{2}(\gamma_{2i-1} + i\gamma_{2i}) \quad \text{and} \quad c_i^\dagger \stackrel{5.33}{=} \frac{1}{2}(\gamma_{2i-1} - i\gamma_{2i}) \quad (5.35)$$

Observation: We do not have to combine the original pairs of Majoranas! Actually, it is possible to combine *any* pair of Majoranas to form a new fermion mode (→ *below*). This follows from Eq. (5.34) which shows that all $2L$ Majorana modes “are made equal.”

14 | We can now rewrite the Majorana chain Hamiltonian in terms of Majorana operators:

Eqs. (5.6) and (5.35) →

$$\hat{H}_{\text{MC}} \stackrel{\circ}{=} \frac{i}{2} \sum_{i=1}^{L'} [(\Delta + w) \gamma_{2i} \gamma_{2i+1} + (\Delta - w) \gamma_{2i-1} \gamma_{2i+2}] - \frac{i}{2} \sum_{i=1}^L \mu \gamma_{2i-1} \gamma_{2i} \quad (5.36)$$

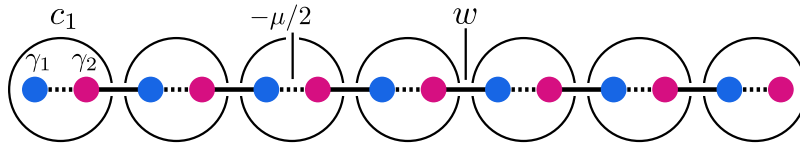
;! Note that the factors of i are needed for Hermiticity.

15 | < Special case $\Delta = w$ (this simplifies expressions but still allows us to access both phases)

$$\rightarrow \hat{H}_{\text{MC}} = -\frac{\mu}{2} \sum_{i=1}^L (i \gamma_{2i-1} \gamma_{2i}) + w \sum_{i=1}^{L'} (i \gamma_{2i} \gamma_{2i+1}) \quad (5.37)$$

Remember that the choice $\Delta = w$ also simplified the Bogoliubov transformation [e.g. Eq. (5.18)].

→ SSH-like dimerization:



16 | Comparison to the SSH chain:

The connection to the SSH chain is more than superficial. If one identifies $-\mu/2 \leftrightarrow t$ and $w \leftrightarrow w$ [where t and w are the alternating hopping amplitudes of the SSH chain, Eq. (4.10)], then the gapless points coincide: $|\mu| = 2|w|$ for the Majorana chain [Eq. (5.21)] and $|t| = |w|$ for the SSH chain [Section 4.3].

One can consider a hybrid model of Majorana and SSH chain and study their competing phases on the same footing [145]. This approach is also didactically valuable as it contrasts the different symmetries of the two models quite nicely.

5.5. Edge modes

Due to the SSH-like dimerization, we should again expect topologically protected *zero-energy modes* on the boundary of an open Majorana chain (in the topological phase). As usual, it is most instructive to focus on the fixpoints of the two phases with zero correlation length:

17 | Trivial phase (Phase B):

Let $w = \Delta = 0$ and $\mu > 0 \xrightarrow{5.37}$

$$\hat{H}_{MC} = -\frac{\mu}{2} \sum_{i=1}^L (i \gamma_{2i-1} \gamma_{2i}) \stackrel{5.33}{=} -\mu \sum_{i=1}^L \left(c_i^\dagger c_i - \frac{1}{2} \right) \quad (5.38)$$

→ Pairing of Majorana modes *on* each site

→ Unique ground state (with all physical fermion modes c_i filled)

It is useful to keep in mind that $i \gamma_2 \gamma_1 = 1 - 2c^\dagger c = (-1)^n = P$ is the *parity operator* of the fermion mode $c = \frac{1}{2}(\gamma_1 + i \gamma_2)$.

18 | Topological phase (Phase A):

Let $w = \Delta > 0$ and $\mu = 0 \xrightarrow{5.37}$

$$\hat{H}_{MC} = w \sum_{i=1}^{L'} (i \gamma_{2i} \gamma_{2i+1}) \stackrel{\text{OBC}}{=} w \sum_{i=1}^{L-1} (i \gamma_{2i} \gamma_{2i+1}) \quad (5.39)$$

→ Pairing of Majorana modes *between* adjacent sites

→ Unique ground state for PBC but 2-fold degenerate ground state space for OBC

Let us try to understand the (claimed) degeneracy for OBC in more detail:

i | Define new fermion modes ($i = 1, \dots, L - 1$):

$$a_i := \frac{1}{2}(\gamma_{2i} + i \gamma_{2i+1}) \quad \text{and} \quad a_i^\dagger = \frac{1}{2}(\gamma_{2i} - i \gamma_{2i+1}) \quad (5.40)$$

;! Compare this pairing of Majorana modes with Eq. (5.35).

Check that these are indeed fermions: $\{a_i, a_j^\dagger\} = \delta_{ij}$.

Eq. (5.39) \rightarrow

$$\hat{H}_{\text{MC}} = 2w \sum_{i=1}^{L-1} \left(a_i^\dagger a_i - \frac{1}{2} \right) \quad (5.41)$$

ii | Observation: **There is One fermion mode missing!**

Note that γ_1 and γ_{2L} do not show up in Eq. (5.39), so we can use them to construct another fermion mode:

$$e := \frac{1}{2}(\gamma_{2L} + i\gamma_1) \quad \text{and} \quad e^\dagger = \frac{1}{2}(\gamma_{2L} - i\gamma_1) \quad (5.42)$$

Note that the $L - 1$ modes a_i together with e obey the algebra of L fermionic modes, e.g., $\{e, e^\dagger\} = 1$ and $\{e, a_i\} = 0$.

→ One fermionic edge mode

Indeed, e describes a single fermion *delocalized* between the two endpoints of the chain:

$$e \stackrel{5.33}{=} \frac{i}{2} \left(\underbrace{c_L^\dagger - c_L}_{\text{Right edge}} + \underbrace{c_1^\dagger + c_1}_{\text{Left edge}} \right) \quad (5.43)$$

iii | Ground states for OBC:

$$|\Omega_n\rangle \text{ GS of } \hat{H}_{\text{MC}} \Leftrightarrow a_i |\Omega_n\rangle \stackrel{!}{=} 0 \quad \forall i = 1 \dots L - 1 \quad (5.44)$$

$[\hat{H}_{\text{MC}}, e] = 0 \rightarrow$ *Two ground states:*

$$\underbrace{e^\dagger e |\Omega_0\rangle = 0}_{\text{Edge mode empty}} |\Omega_0\rangle \quad \text{and} \quad \underbrace{e^\dagger e |\Omega_1\rangle = 1}_{\text{Edge mode occupied}} |\Omega_1\rangle \quad (5.45)$$

with $|\Omega_1\rangle = e^\dagger |\Omega_0\rangle$

$e^\dagger e$ measures the occupancy of the edge mode.

19 | Comments:

- Comparison to the SSH chain:

Remember that the SSH chain also has edge modes (Section 4.6). However, these are *fermionic*, i.e., the SSH chain (in the topological phase) has one independent (complex) fermion on *each edge*. Consequently, the ground state degeneracy for an open chain is *four-fold*. By contrast, the Majorana chain as a *Majorana* fermion per edge (and a Majorana fermion can be thought of as “half” a fermion because it is the real/imaginary part of a complex fermion). Both edges *combined* form a single (complex) fermion, so that the ground state degeneracy is only *two-fold*.

- Many-body ground states (in detail):

As for the SSH chain, the two-fold degeneracy survives beyond the fixpoint for $\mu = 0$ as long as $|\mu| < 2|w|$ (up to finite-size effects). However, at the fixpoint, the two states $|\Omega_0\rangle$ and $|\Omega_1\rangle$ have a particularly simple description that makes their condensate nature clear and also explains the robustness of their degeneracy (\uparrow [126] for details):

$$|\Omega_0\rangle \propto \sum_{n: |n| \text{ odd}} |n\rangle \quad \text{and} \quad |\Omega_1\rangle \propto \sum_{n: |n| \text{ even}} |n\rangle \quad (5.46)$$

with

$$|\mathbf{n}\rangle \equiv (c_1^\dagger)^{n_1} (c_2^\dagger)^{n_2} \dots (c_L^\dagger)^{n_L} |0\rangle \quad (5.47)$$

and $|\mathbf{n}|$ the number of fermions in configuration \mathbf{n} .

- The ground states are the *equal-weight superposition* of all fermion configurations with a fixed parity, in particular, of fermion configurations with different particle number. This is the many-body manifestation of the superconducting condensate (note that $\langle c_i c_{i+1} \rangle \neq 0$ for $|\Omega_n\rangle$).
- Locally, the states $|\Omega_0\rangle$ and $|\Omega_1\rangle$ “look” the same. They can only be distinguished by a *global* measurement of the total fermion parity. To lift their degeneracy, one has to add the term $e^\dagger e$ to the Hamiltonian \hat{H}_{MC} . But for an open chain, this operator is highly *non local* [as can be seen from Eq. (5.43)].

This scenario, namely multiple orthogonal ground states that are *indistinguishable by local operators*, is actually the hallmark of \leftarrow *topological order* (\rightarrow Part III).

- There is actually another way to lift the degeneracy. Note that $\gamma_1 e = -e^\dagger \gamma_1$ so that $|\Omega_1\rangle = \gamma_1 |\Omega_0\rangle$, i.e., $\langle \Omega_1 | \gamma_1 | \Omega_0 \rangle \neq 0$ so that the Hamiltonian $\hat{H}_{\text{MC}} + \gamma_1$ lifts the degeneracy (recall that $\gamma_1^\dagger = \gamma_1$). In contrast to $e^\dagger e$, γ_1 is localized on the left endpoint of the chain. However, γ_1 violates fermion parity and it is believed that in nature only Hamiltonians that commute with the parity operator are realizable (this is known as \uparrow *parity superselection*), so this modification is mathematically sound but physically impossible (\rightarrow *comment below*).

- Classification and the role of symmetries:

The above arguments have shown that the degeneracy of $|\Omega_0\rangle$ and $|\Omega_1\rangle$ is actually very robust and does not rely on any symmetry (note that this does not contradict the topological classification of \hat{H}_{MC} as part of symmetry class **D** because of the discussed tautological nature of the PHS). Consequently, the topological phase of the Majorana chain is *not* an SPT phase but a topologically ordered phase (of the invertible kind) [29, 35, 44]. This is in stark contrast to the SSH chain which *is* an SPT phase protected by sublattice symmetry.

[Remember (Section 4.5) that we had no trouble connecting the two phases of the SSH chain with a chemical potential that breaks SLS. You cannot do the same thing with a single Majorana chain! (Try it!) However, you *can* connect the two phases with *two* parallel chains, which demonstrates the invertibility of the topological order.]

- A note on fermion parity:

The statement that the Majorana chain does not require any symmetry is subtle. To see this, one can check that the Majorana edge modes $\gamma_l = \gamma_1$ and $\gamma_r = \gamma_{2L}$ act on the ground states as follows:

$$\gamma_l |\Omega_0\rangle = |\Omega_1\rangle \quad \text{and} \quad \gamma_r |\Omega_0\rangle = -i |\Omega_1\rangle. \quad (5.48)$$

Since these operators are Hermitian and can be constructed from local fermion modes, we could add them to the Hamiltonian as a perturbation, e.g., $\tilde{H}_{\text{MC}} = \hat{H}_{\text{MC}} + \gamma_l$. This perturbation lifts the degeneracy such that the ground state of \tilde{H}_{MC} is unique, namely $|\Omega_1\rangle - |\Omega_0\rangle$. This is not surprising as γ_l *violates* the fermion parity symmetry $\mathbb{Z}_2^f = \{\mathbb{1}, \mathcal{P}\}$.

So the Majorana chain *is* protected by a symmetry after all: fermion parity. However, this “symmetry” should not be counted as a real symmetry but as an implicit feature of fermionic Hamiltonians (for instance, quadratic Hamiltonians automatically commute with \mathcal{P}) due to the following reason:

Assume that the Hermitian (and unitary) operators γ_l and γ_r were admissible observables of the theory. Make the length L of the chain large and assume that Alice can measure $\gamma_l = c_1 + c_1^\dagger$ on the left endpoint while Bob can apply the unitary gate $\gamma_r = i(c_L^\dagger - c_L)$ on the right endpoint. Define the basis $|x\rangle \equiv |\Omega_1\rangle + (-1)^x |\Omega_0\rangle$ and let the system be

initialized in the symmetric state $|x = 0\rangle$ so that Alice measures $+1$ with certainty. Now Bob can send Alice a classical bit $x \in \mathbb{Z}_2$ of information by flipping or not flipping this state with γ_r :

$$(\gamma_r)^x |0\rangle \propto \begin{cases} |0\rangle & \text{for } x = 0 \\ |1\rangle & \text{for } x = 1. \end{cases} \quad (5.49)$$

This clearly violates causality since the bit x can be transmitted instantaneously over arbitrary distances L ; this really is a “spooky action at a distance” and should not be possible with *local* measurements and operations. Therefore γ_l and γ_r are actually *non-local* operators, despite their local appearance in terms of fermion modes!

The reason is that fermions are intrinsically non-local objects due to their statistics, and this non-locality becomes relevant for operators that violate fermion parity. The upshot is that the parity symmetry required for the Majorana chain (or any other fermion Hamiltonian) is a logical consequence of *locality* – and not an additional symmetry constraint.

5.6. ‡ Application as topological quantum memory

Here we focused on the “condensed-matter side” of the Majorana chain (since this is a course on topological quantum phases). However, the topological robustness of the ground state degeneracy suggests the use of this system for quantum information storage (and processing):

- 1 | < Topological phase @ $\mu = 0$ and $\Delta = w = 1$ & Open boundary conditions:

$$\hat{H}_{\text{MC}} = \sum_{j=1}^{L-1} (i\gamma_{2j}\gamma_{2j+1}) \equiv - \sum_{j=1}^{L-1} S_j \quad (5.50)$$

with $\ast\ast$ stabilizer generators S_j that satisfy

$$[S_i, S_j] = 0, \quad S_j^\dagger = S_j, \quad S_j^2 = \mathbb{1} \quad (5.51)$$

→ $\ast\ast$ Stabilizer group $\mathcal{S} := \langle \{S_1, \dots, S_{L-1}\} \rangle$

- Here (•) denotes the (abelian) group generated by •.
- You study the stabilizer formalism on ↻ Problemset 11.
- The stabilizer generators $S_j = -i\gamma_{2j}\gamma_{2j+1} \doteq (-1)^{a_j^\dagger a_j}$ measure the parity of the quasiparticle modes a_i defined in Eq. (5.40).

- 2 | Ground state space of Eq. (5.50):

$$\mathcal{C} = \{ |\Psi\rangle \in \mathcal{H} \mid \forall S \in \mathcal{S} : S|\Psi\rangle = |\Psi\rangle \} = \text{span} \{ |\Omega_0\rangle, |\Omega_1\rangle \} \quad (5.52)$$

Here $|\Omega_0\rangle$ and $|\Omega_1\rangle$ denote the two degenerate many-body ground states introduced in Eq. (5.44) and explicitly written in Eq. (5.46).

→ $\dim \mathcal{C} = 2$ → Use ground state space to store a qubit:

$$|0\rangle \equiv |\Omega_0\rangle \quad \text{and} \quad |1\rangle \equiv |\Omega_1\rangle \quad (5.53)$$

→ Ground state space $\mathcal{C} = \ast\ast$ Code space

In quantum information theory, a code space is a linear subspace of a larger Hilbert space that is used to encode quantum information.

3 | Qubit = Representation of U(2)

A qubit is a two-dimensional representation of U(2) which is generated by three Pauli matrices $\Sigma^x, \Sigma^y, \Sigma^z$ (and the identity Σ^0) which satisfy $\Sigma^a \Sigma^b = \delta_{ab} \mathbb{1} + i \varepsilon_{abc} \Sigma^c$ and therefore $[\Sigma^a, \Sigma^b] = 2i \varepsilon_{abc} \Sigma^c$.

→ Pauli matrices acting on \mathcal{C} :

$$\Sigma^z \equiv -i \gamma_{2L} \gamma_1 \stackrel{\circ}{=} (-1)^{e^\dagger e} \quad \text{with} \quad \begin{cases} \Sigma^z |0\rangle = +|0\rangle \\ \Sigma^z |1\rangle = -|1\rangle \end{cases} \quad (5.54a)$$

$$\Sigma^x \equiv \gamma_{2L} = e^\dagger + e = i(c_L^\dagger - c_L) \quad \text{with} \quad \begin{cases} \Sigma^x |0\rangle = |1\rangle \\ \Sigma^x |1\rangle = |0\rangle \end{cases} \quad (5.54b)$$

$$\Sigma^y \equiv \gamma_1 = i(e^\dagger - e) = c_1^\dagger + c_1 \quad \text{with} \quad \begin{cases} \Sigma^y |0\rangle = +i|1\rangle \\ \Sigma^y |1\rangle = -i|0\rangle \end{cases} \quad (5.54c)$$

→ Satisfy all properties of Pauli matrices ✓

Indeed, it is easy to check that $(\Sigma^a)^\dagger = \Sigma^a$ and $\Sigma^a \Sigma^b = \delta_{ab} \mathbb{1} + i \varepsilon_{abc} \Sigma^c$ using the properties Eq. (5.34) of Majorana operators.

The operators Σ^a are called **** logical operators** as they operate on the encoded (= logical) qubit. To emphasize this, we denote them by Σ^a and not σ^a .

4 | Observation:

$$[\Sigma^a, S_j] = 0 \quad \forall a, j \quad (5.55)$$

→ Measuring S_j does not destroy the qubit encoded in \mathcal{C} ☺

This feature is crucial to combat errors (→ below).

↓ Lecture 17 [26.06.25]

5 | Error model:

We assume that random errors on the Majorana chain can be described by unitary operators with the following properties:

- *Local*

This is a basic assumption of most error models: the environment acts *locally* on the system that encodes quantum information (here the Majorana chain). Note that essentially all Hamiltonians we study in physics have a locality structure.

- *Parity-symmetric*

In superconductors, fermionic parity is considered a natural symmetry that can be enforced to high precision because fermions are created by breaking Cooper pairs (which costs energy).

This is not a fundamental symmetry and it can be violated by ↑ *quasiparticle poisoning* [146, 147].

- *Rare & Uncorrelated*

We assume that local errors happen independently of each other with a low probability $p \ll 1$ per site $j = 1, \dots, L$ and timestep (iid = independent and identically distributed). This is often (but not always) a good approximation.

→ Elementary (= physical) errors: $E_j = -i\gamma_{2j-1}\gamma_{2j}$ ($j = 1, \dots, L$)

! Note that pairs shifted by a single site ($-i\gamma_{2j}\gamma_{2j+1}$) are *stabilizer operators* that act trivially on the code space [Eq. (5.52)]. If such an error occurs on a state $|\Psi\rangle \in \mathcal{C}$ it doesn't do anything and we can ignore it.

With Eq. (5.38) we can write elementary errors as $E_j = 1 - 2c_j^\dagger c_j = (-1)^{n_j}$. Measuring this Hermitian operator therefore means that one observes whether a physical fermion site (mode) c_i is occupied or not. Unitarily applying this operator imprints phases on the many-body wave function depending on the occupancy of the fermion modes.

6 | Logical errors induced by combinations of physical errors?

Logical errors are errors that affect the state of the logical qubit encoded in the codes space \mathcal{C} .

- < Bit-flip errors: $\Sigma^x = \gamma_{2L}$ or $\Sigma^y = \gamma_1$

Not parity-symmetric → *Cannot occur* ☹

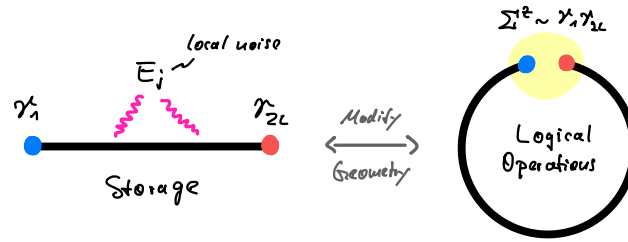
- < Phase errors: $\Sigma^z = -i\gamma_{2L}\gamma_1$

Parity-symmetric but Non-local → *Cannot occur* ☹...

...except elementary errors accumulate:

$$\underbrace{\prod_{j=1}^L E_j}_{\text{All errors}} \stackrel{5.50}{=} -i\gamma_1 \underbrace{\left[\prod_{i=1}^{L-1} S_i \right]}_{=1 \text{ on } \mathcal{C}} \gamma_{2L} = -\Sigma^z \quad \ominus \quad (5.56)$$

To prevent a logical phase error Σ^z due to a *single* elementary (physical) error, it is crucial that the two endpoints of the chain are far apart from each other (otherwise Σ^z is not non-local and therefore a permissible error!). However, sometimes one might need to measure (or apply) the logical operator Σ^z (after all, we want to do quantum computing with the encoded qubit). This means that the endpoints of the Majorana chain must be moved close to operate on the encoded qubit, but must remain far apart when storing the qubit for future use:



Modifying the geometry to apply controlled unitary operations while suppressing unwanted perturbations is a characteristic feature of → *topological quantum memories* and → *topological quantum computing*.

→ How can we prevent elementary errors from accumulating?

→ Solution:

7 | Quantum error correction (QEC) protocol:

QEC protocols are classically controlled algorithms (no Hamiltonian dynamics!) with the goal to systematically remove errors from quantum systems to protect quantum information. Their job is to “pump entropy” out of the system.

◀ Encoded qubit:

$$|\Psi_0\rangle = \alpha|0\rangle + \beta|1\rangle \in \mathcal{C} \tag{5.57}$$

$\alpha, \beta \in \mathbb{C}$: Logical amplitudes (this is the information we want to protect!)

- i | Assume that since initialization in $|\Psi_0\rangle$, a few elementary errors occurred on random positions of the chain:

$$|\Psi_0\rangle \xrightarrow[\text{on sites with } x_j = 1]{\text{Unknown errors}} |\tilde{\Psi}_0\rangle = \underbrace{\prod_j (E_j)^{x_j}}_{\equiv E(\mathbf{x})} |\Psi_0\rangle \notin \mathcal{C} \tag{5.58}$$

$\mathbf{x} = (x_1, \dots, x_L) \in \{0, 1\}^L$: unknown error pattern

Our goal is to figure out if and where errors occurred so that we can remove them before they have the chance to accumulate and destroy the encoded qubit [like in Eq. (5.56)].

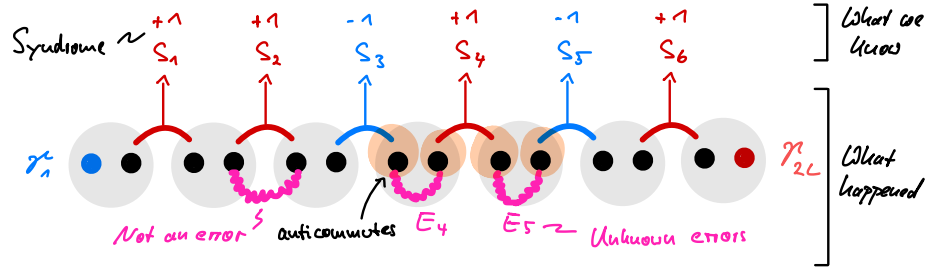
Due to the errors, the state above is no longer in the code space: $|\tilde{\Psi}_0\rangle \notin \mathcal{C}$. [In condensed matter parlance, it is no longer a ground state of Eq. (5.50) but an excited state.] Note, however, that the amplitudes α and β are still hidden in $|\tilde{\Psi}_0\rangle$! The problem is that they were “shuffled around” in an unknown way because of the error operations ...

- ii | **Observation:** $S_k E_j = -E_j S_k$ if $k = j - 1$ or $k = j$

This follows from Eq. (5.34) and the fact that adjacent errors and syndromes share a *single* Majorana fermion.

→ Measuring S_k yields information (negative eigenvalues) about the locations of errors!

→ Measure all stabilizers S_j :



→ \ast Error syndrome $s = (s_1, \dots, s_{L-1}) \in \{\pm 1\}^{L-1}$

! Since $S_j^2 = 1$ this yields one bit $s_j = \pm 1$ of information per stabilizer generator. It is crucial that [due to Eq. (5.55)] these measurements cannot destroy the encoded qubit [i.e., they cannot reveal the amplitudes α and β in Eq. (5.57)].

Question: Can we use s to compute x ?

If we *knew* the error pattern x , we could simply undo the (unitary) error operators E_j and recover the state $|\Psi_0\rangle$. The hitch is that we *don't know* x (that's what errors are, after all!).

iii | Decoding algorithm:

A decoding algorithm is a *classical algorithm* that tries to guess the actual error pattern based on the syndrome information:

$$\text{Syndrome } s \xrightarrow{\text{Decoding}} \text{Predicted error pattern } x' = \mathcal{D}(s) \quad (5.59)$$

\mathcal{D} : (Classical) decoding algorithm (to be constructed)

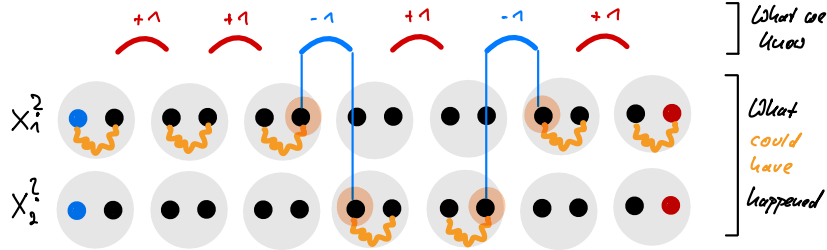
- ! Note that $\mathcal{D} : \{\pm 1\}^{L-1} \rightarrow \{0, 1\}^L$ cannot be surjective because there are only $L - 1$ bits of syndrome data but L bits in an error pattern. This immediately tells us that there must be error patterns that the decoder cannot predict because they give rise to the same syndrome data. Hence there must be situations (= error patterns) where the decoder *fails* and the encoded quantum information is lost. This is not bad luck but intrinsic to any quantum error correction protocol. (Because physical errors can always conspire to act as a logical operation that one cannot detect without destroying the encoded qubit.)
- This can be seen from Eq. (5.56) where we showed that the error pattern $x = (1, \dots, 1)$ leads to a logical Σ^z operation. But $[\Sigma^z, S_j] = 0$ for all $j = 1, \dots, L - 1$ so that syndrome measurements cannot detect this type of error: $s(\Sigma^z) = (+1, \dots, +1)$. [Had no error occurred, the syndrome would be the same: $s(\mathbb{1}) = (+1, \dots, +1)$.] A decoder has to make a decision whether to decode $s = (+1, \dots, +1)$ to $x' = (0, \dots, 0)$ or $x' = (1, \dots, 1)$ (if errors are rare, the first choice is the better one!). In any case, there will be situations where the decoder chooses wrong and fails to predict the actual error string: $x' \neq x$.

So which decoding algorithm should be pick for our “Majorana chain quantum code”?

For a given quantum code, there are many possible decoding algorithms. Which one to pick depends on many factors: the probability distribution of errors, how efficient the algorithm runs (on classical hardware), and, most importantly, its \uparrow *threshold* (the microscopic error rate that must be reached for the QEC scheme to become useful).

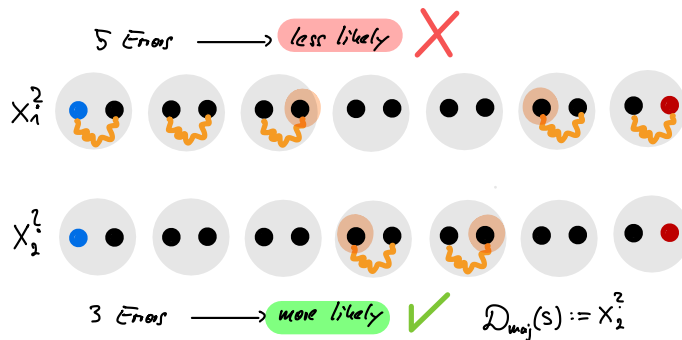
Suggestion: “Majority voting” \mathcal{D}_{maj} :

Step 1: Construct the (only) *two* error patterns $x_1^?$ and $x_2^?$ consistent with the given syndrome s :



⚠ Note that syndromes adjacent to *two* errors yield +1 when measured as they anticommute *twice* and the minus cancels. This means that syndrome measurements detect *boundaries of error chains*.

Step 2: Return the pattern with *fewer* errors:



- The rationale of this choice is that for low error probabilities (actually: $p < 0.5$) the error pattern with the smaller number of errors is the more likely one.
- \mathcal{D}_{maj} is provably optimal for the Majorana chain quantum code if syndrome measurements are perfect (it is the so called \uparrow *maximum-likelihood decoder*).

iv | Apply corrective operations:

As a last step, we apply the inverse error operations on the locations predicted by $x^?$ (since here errors are Hermitian, it is $E_j^{-1} = E_j^\dagger = E_j$):

$$|\tilde{\Psi}_0\rangle \xrightarrow[\text{= Undo errors}]{\text{Apply corrections}} E^{-1}(x^?)|\tilde{\Psi}_0\rangle \tag{5.60a}$$

$$= E^{-1}(x^?)E(x)|\Psi_0\rangle \tag{5.60b}$$

$$= E(x^? \oplus x)|\Psi_0\rangle \tag{5.60c}$$

$$\begin{cases} x^? \equiv x & |\Psi_0\rangle \rightarrow \text{Success } \checkmark \text{ 😊} \\ x^? \equiv \bar{x} & -\Sigma^z|\Psi_0\rangle \rightarrow \text{Failure } \times \text{ 😞} \end{cases} \tag{5.60d}$$

Here \bar{x} denotes the complementary pattern obtained from x by exchanging $0 \leftrightarrow 1$, and \oplus denotes bit-wise modulo-2 addition, i.e., $\bar{x} \oplus x = (1, 1, \dots, 1)$.

- ⚠ Note that the quantum memory controller does *not know* whether the correction was successful or not. Otherwise, it could have applied the “correct correction” in the first place. A failed QEC cycle therefore leads to a “silent” logical operation on the encoded qubit which (most likely) screws up the quantum algorithm that follows.

- If the decoding is successful, the QEC protocol gains at no point knowledge about the encoded amplitudes α and β . That this is possible in principle was the seminal insight by PETER SHOR in 1995 [148]. It is one of the foundations upon which the promise of scalable quantum computing rests (and, by now, several billions of market cap).
- In reality, it is often more convenient to compute and accumulate all correction strings and adapt only the final read-out stage of the quantum circuit (or apply the corrections in classical post-processing). If possible, this is advantageous because applying corrective unitaries takes time and can introduce new errors.

Together, these four steps make up a **quantum error correction cycle** and are repeated periodically (in the range of microseconds to milliseconds) to ensure that the number of errors accumulated between consecutive correction cycles remains small (which is necessary for the decoder to function properly).

This means in particular that the decoding algorithm must be *computationally efficient*. This becomes a formidable task for larger and more complicated quantum error correction codes (like the *toric code*), and explains why quite a lot of effort is put into making decoders both better at guessing x and doing so *quickly* and without much classical overhead [149].

- 8 | This procedure hints at a much more general recipe to construct quantum error correction codes:
 ◀ Topologically ordered phase of matter:

Robustly degenerate ground state space → Code space
 Excitations of Hamiltonian → Errors
 Local Hermitian terms in Hamiltonian → Syndrome observables

→ **Topological Quantum Error Correction (TQEC)**

We will study a two-dimensional topological quantum code that does not rely on fermion parity as a symmetry in ?? (→ *toric code*).

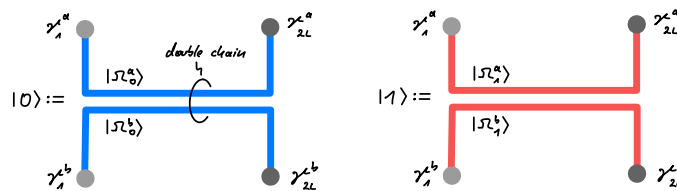
The concept of TQEC belongs to the fascinating intersection of condensed matter physics, topology, and quantum information theory teased in the Venn diagram of Section 0.2.

9 | Comments:

- Pairs of chains:

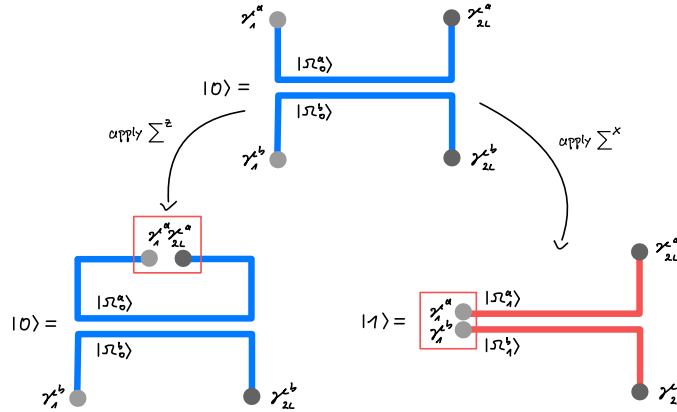
Recall that we assumed the logical operators Σ^x and Σ^y to be forbidden as physical errors due to fermionic parity symmetry (which might or might not be a good assumption in a particular setting). But if parity-violating unitaries cannot be physically realized, then *we* as operators should also not be capable of these operations! We can't have our cake and eat it too!

So in an "honest" setting with fermion parity symmetry, we should implement *all* logical operators as parity-symmetric operators as well. The trick is to encode a single logical qubit not in one but in a *pair of chains*, e.g., by associating the negative parity of both to $|0\rangle$ and positive parity of both to $|1\rangle$:



Importantly, the *total* fermion parity of the system is now fixed (even, in this case) and does not have to be changed when flipping the qubit state. To make sure that no logical operators are affected by errors, we must now completely rely on the *locality* argument. This means in particular, that “storage mode” is achieved by moving the endpoints of all chains far apart from each other to prevent local (parity-preserving) operators from coupling them (as shown above).

Logical operators can then be applied by moving two endpoints close together and applying (or measuring) a parity-symmetric (!) product of two Majorana modes:

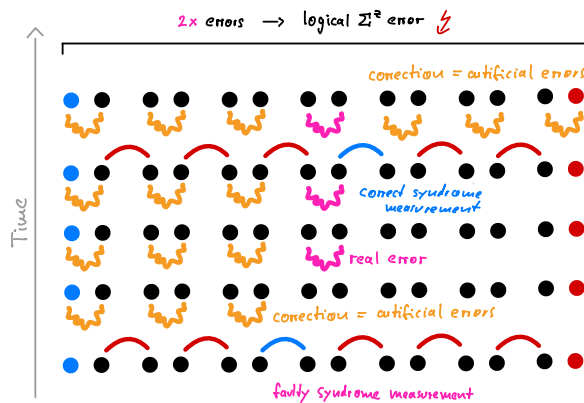


Crucially, the application of $\Sigma^x \propto \gamma_1^a \gamma_1^b$ (which essentially tunnels fermions from one chain to the other) does *not* violate fermion parity but switches the “subsystem parities” of the two chains (thereby flipping the logical qubit). (Note that applying a local pair of Majoranas between the two chains *away* from the endpoints creates quasiparticle excitations in both chains – which can be detected by syndrome measurements.) Encoding qubits in the sub-parities of multiple chains is the basic principle of Majorana-based quantum computing architectures [147, 150, 151].

- Imperfect stabilizer measurements:

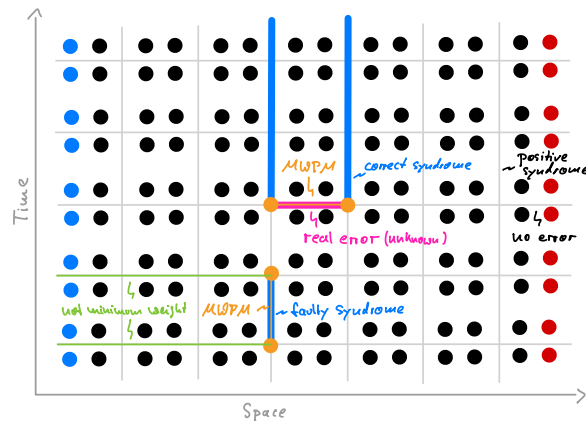
In a realistic setup, there is noise *everywhere*, in particular, the syndrome measurements *themselves* are not always correct: Sometimes a measurement might return $s_j = -1$, although no error occurred on the chain. Conversely, a measurement might miss an actual error and return $s_j = +1$. Projective measurements in a quantum experiment *always* come with a rate that quantifies how noisy they are (and this rate is non-zero)!

As we will see now, this is not just a minor inconvenience that can be “abstracted away.” That one must take these additional errors into account can be seen from the following process that is triggered by only *two* errors (one on the chain and one affecting the syndrome). Most importantly, the process (and therefore its probability) is *independent* of the length of the chain:



The crucial point is that a *single* faulty syndrome measurement can trick our decoder into applying an extensive number of artificial errors (“corrections”). A single true error is then enough to tip the scales and destroy the encoded information.

Every realistic quantum error correction protocol must be designed to withstand noise not only on the quantum code itself but also on the syndrome measurement routine. To achieve this, one can employ decoding algorithms that operate on “spacetime” by taking into account not only the current pattern of syndromes but also their history:



For the Majorana chain code, it is convenient to draw a square lattice in spacetime where syndrome measurements are associated to vertical edges and $s_j = -1$ outcomes are highlighted. Next, one identifies the *endpoints* of these highlighted paths (orange above). To reconstruct the (unknown) error pattern (now including both errors on the quantum code and faulty stabilizer measurements), the decoder performs a procedure called *minimum-weight perfect matching* (MWPM) [152, 153]. The idea is to connect all endpoints pairwise (via paths that can include horizontal and vertical edges and can terminate on the boundaries) such that no endpoints remain unpaired (this is the “perfect matching”). Every path is assigned a “weight” computed from the probabilities of errors and faulty stabilizer measurements, such that smaller weights correspond to more likely paths (for low error probabilities, these are typically the shortest paths). The perfect matching with the smallest total weight (“minimum-weight”) is then selected and used to guess the errors that occurred: every *horizontal* line traversed by the paths that connect the endpoints corresponds to an *error* that occurred, and every *vertical* line to a *faulty stabilizer measurement*.

A similar approach can be used to decode two-dimensional topological codes like the *toric code* [154–156] (the spacetime pattern is then three-dimensional). Note that the MWPM decoder sketched above is no longer the maximum-likelihood decoder [157, 158], i.e., it does not necessarily construct the corrective operations that are most likely correct (this is not obvious).

- The Majorana chain can be mapped via a *Jordan-Wigner transformation* from fermions to spins (⊕ Problemset 8). This elucidates its relation to the *transverse-field Ising model* discussed in Section 0.3. On the level of quantum codes [and in the language of stabilizers, Eq. (5.51)] this mapping yields a degenerate version of the *toric code* (on a lattice of size $L \times 1$) [149], which is *not* a quantum- but a classical memory (a *repetition code*). The Majorana chain code is therefore a “topological quantum memory with caveats:” One type of error (phase errors) are kept in check due to the locality structure of the code – this is the hallmark of *topological* quantum codes. By contrast, the other type of errors (bit-flip errors) cannot be corrected. In the “spin-world” of the toric code, this cannot be argued away and one is left with a classical error correction code. In the “fermion world” of the Majorana chain, one can – on purely physical grounds – argue that such errors violate fermion parity

symmetry and are therefore suppressed. True topological quantum codes (like the toric code) do not rely on such symmetry-protection arguments. The price to pay is that such codes are at least two-dimensional (because there is no topological order in one-dimensional spin systems [6]).

- Starting from Majorana fermions, one can construct more general quantum error correction codes called ↑ *Majorana fermion codes* [159].
- The concepts we explored suggest an intriguing possibility: The Majorana chain Hamiltonian Eq. (5.50) is a quantum phase with a ground state manifold that has the properties of a quantum error correction code! The local terms in the Hamiltonian correspond to syndrome operators, and a non-trivial syndrome (indicating the presence of an error) corresponds to an *excitation* of this Hamiltonian. This motivates the following question:

*Can we suppress errors energetically (by lowering the temperature)
instead of applying active error corrections (by a classical decoding algorithm)?*

A Hamiltonian with these properties is called a ↑ *self-correcting quantum memory*. Unfortunately, the Majorana chain is *not* self-correcting for the same reason the one-dimensional classical Ising model has no phase transition at finite temperatures: While the initial *creation* of an error indeed costs energy, its subsequent *movement* is not energetically penalized (in the classical Ising model, the creation of a domain wall costs energy, but its proliferation through the chain does not). This mechanism prevents a thermodynamically stable phase at finite temperature in which the quantum information encoded in the thermal Gibbs state $\rho = e^{-\beta H} / Z$ (density matrix!) would survive exponentially long in the system size.

The quest for finding a truly self-correcting system in three spatial dimensions or less is an active area of research. For example, it is known that a wide class of systems based on stabilizer codes (under some additional constraints) *cannot* be self-correcting [160, 161] (due to the presence of point-like excitations). There are interesting proposals with partially self-correcting properties [162, 163]; however, to the best of my knowledge, all of them have some drawbacks and do not qualify as true self-correcting systems.

Fun fact: In *four* spatial dimensions, a self-correcting quantum memory is known to exist, namely the 4D generalization of the toric code [164]. The problem is that our world is not four dimensional ☹.

- Braiding in wire networks:

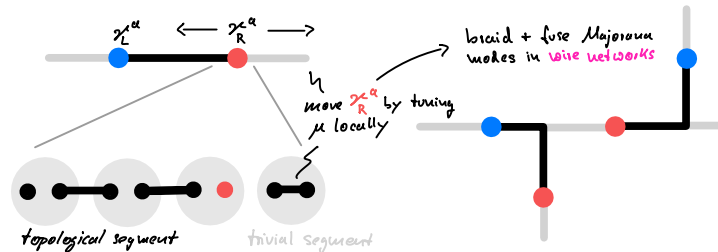
Majorana modes located at extrinsic defects can exhibit → *non-abelian anyonic statistics* (so called ↑ *(projective) Ising anyons* [165, 166]). Note that these are not quasiparticle excitations but high-energy deformations of the Hamiltonian! As we have seen in this chapter, Majorana modes naturally occur on the endpoints of *p*-wave superconducting wires (they can also appear in the vortices of two-dimensional $p_x + ip_y$ superconductors [167]).

Measuring the parity of a fermion mode given by two Majorana modes (recall $\Sigma^z \propto \gamma_2 \gamma_1$) can then be interpreted as the ↑ *fusion* of two “Ising anyons.” The non-abelian nature of these anyons is reflected in the fact that there are two consistent outcomes of this measurement: the fermion mode can be empty or occupied. Formally, one writes $\sigma \times \sigma = 1 + \Psi$ where σ denotes an Ising anyon (realized by a Majorana mode), 1 corresponds to an empty fermion mode and Ψ to an occupied fermion mode.

It turns out that moving Ising anyons adiabatically (= slowly) around each other effects non-trivial unitary operations on the degenerate subspace that encodes the different fusion outcomes. This process is called ↑ *braiding* and can be used to manipulate the encoded qubits (like the ones in our Majorana chain quantum code) *without decoding them*. This is the rationale of → *topological quantum computation*, an intrinsically robust quantum computing architecture.

But how can one braid the Majorana modes at the endpoints of Majorana chains around each other? The idea is to use *wire networks* with locally tunable chemical potentials (by applying

local gate voltages) [150]. By tuning the chemical potential, one can make segments of the wire network topological, while other parts remain in the trivial phase [recall Eq. (5.22)]. The boundaries between topological and trivial segments then host Majorana modes that can be shuffled around by changing the local gate voltages. If one adds T-junctions to connect these wires, one can start braiding Majorana modes around each other:



This is the basic idea behind a Majorana-based topological quantum computer. However, there are two caveats to be aware of: First, the braiding rules of Ising anyons cannot realize a universal gate set [168] so that one needs additional (non-topological) gates to construct a full-fledged quantum computer. And second, from an engineering perspective, it is simpler to replace the dynamical *braiding* by meticulously designed sequences of *projective measurements* [147, 169]; this architecture is known as \uparrow *measurement-based topological quantum computing* and is actively pursued by Microsoft [151].

5.7. ‡ Experiments

- The first evidence for Majorana zero modes at the boundaries of quantum wires was reported in 2012 by Mourik *et al.* [141]. They fabricated a semiconducting nanowire with strong spin-orbit coupling that opens a band gap when a magnetic field is applied (to enter a “spinless” regime). This nanowire is then coupled to a normal *s*-wave superconductor which induces effective *p*-wave pairing in the nanowire [170, 171]. The emergence of zero-energy Majorana modes can then be probed by \uparrow *tunnel spectroscopy*. These results were later substantiated by many follow-up studies (e.g. [172, 173]), see also Ref. [174] for a review.

Characterizing the topological nature of Majorana zero modes is notoriously difficult because their signatures are often hard to distinguish from non-topological phenomena. This has led to several controversial reports, including complete retractions of papers [142].

- As discussed in Section 5.6, Majorana chains can in principle be used as quantum memories. Beyond that, “braiding” Majorana zero modes (either by adiabatically moving them around each other or projectively measuring them) can be used to affect unitary gates on the encoded qubits (these unitaries are not universal, though). This led to proposals for Majorana-chain based quantum computing architectures [147, 150] which are actively pursued by Microsoft’s quantum computing division. In 2025, first experimental results of parity measurements of Majorana qubits were reported [151] – and immediately criticized as unreliable [175].

The future will tell whether Majorana modes are a feasible approach to build a quantum computer ...

6. Classification of Non-Interacting Fermionic Topological Phases

A good introduction to the classification of topological insulators and superconductors is given by Ludwig [92] (this section is partly based on his paper). A more technical description of the scheme with examples is given by Ryu *et al.* [122] (their detailed introduction is quite useful). A completely different angle on the classification is provided by Kitaev [57] (be warned: this paper looks “simple” as it is extremely high-level but the underlying mathematical framework is very deep).

Goal: By now we have seen various models of non-interacting fermions in one and two dimensions that are classified by different topological indices and protected by different symmetries (or none at all). Since all of these models are described by *band structures*, the question arises whether one can find a *unifying scheme* to classify the topological phases of non-interacting fermions.

The description of such an approach is the goal of this section.

6.1. Generic symmetries and the tenfold way

Our final goal is to fit all discussed topological models into a single classification scheme.

As a preliminary step, we must first decide on the *symmetries* to use for this classification:

- 1 | **Goal:** Classify TPs of non-interacting fermions

Approach: Use SP Hamiltonian H to describe & classify MB Hamiltonian \hat{H}

Here, H can either be a “standard” SP Hamiltonian or a Bogoliubov-de Gennes Hamiltonian if superconductivity is present.

→ We are interested in *constraints* on the matrix H that arise from the symmetries of \hat{H} .

- 2 | *Which symmetries of \hat{H} to use?*

Remember: \mathcal{X} symmetry of $\hat{H} : \Leftrightarrow [\mathcal{X}, \hat{H}] = 0$

← *Wigner’s theorem* → \mathcal{X} unitary or antiunitary (remember ⇨ Problemset 1)

→ Four possibilities on Fock space:

In Chapters 2, 4 and 5, we encountered four distinct *classes* of symmetries that can act on Fock space:

Unitary:	$\mathcal{U}i\mathcal{U}^{-1} = +i,$	$\mathcal{U}c_i\mathcal{U}^{-1} = U_{ij}c_j$	(6.1a)
(unitary MB sym.)	$[\mathcal{U}, \hat{H}] = 0$	$\Leftrightarrow [U, H] = 0$	(unitary SP sym.)
Time-reversal:	$\mathcal{T}i\mathcal{T}^{-1} = -i,$	$\mathcal{T}c_i\mathcal{T}^{-1} = U_{ij}c_j$	(6.1b)
(antiunitary MB sym.)	$[\mathcal{T}, \hat{H}] = 0$	$\Leftrightarrow [U\mathcal{K}, H] = 0$	(antiunitary SP sym.)
Particle-hole:	$\mathcal{C}i\mathcal{C}^{-1} = +i,$	$\mathcal{C}c_i\mathcal{C}^{-1} = U_{ij}c_j^\dagger$	(6.1c)
(unitary MB sym.)	$[\mathcal{C}, \hat{H}] = 0$	$\Leftrightarrow \{U\mathcal{K}, H\} = 0$	(antiunitary SP pseudosym.)
Sublattice:	$\mathcal{S}i\mathcal{S}^{-1} = -i,$	$\mathcal{S}c_i\mathcal{S}^{-1} = U_{ij}c_j^\dagger$	(6.1d)
(antiunitary MB sym.)	$[\mathcal{S}, \hat{H}] = 0$	$\Leftrightarrow \{U, H\} = 0$	(unitary SP pseudosym.)

Note that the unitary *mixing* of particles (c_i^\dagger) and holes (c_i) is not necessarily canonical, i.e., does not preserve the fermionic anticommutation relations in general (remember the \leftarrow *Bogoliubov transformation* in Chapter 5). By contrast, here we only mix annihilation operators among themselves or map them to creation operators only.

Using *unitary* symmetries of \hat{H} (H) is possible but not universal!

In the sense that the classification would be “infinite” because there are infinitely many unitarily realized symmetries and the classification depends on the specific symmetry (representation); \rightarrow *extended note below*.

\rightarrow \triangleleft TRS, PHS and SLS ...

This is a conceptually important but subtle point: The decision to “factor out” all unitary symmetries is not so much physically motivated but more a decision based on systematics. One *can* classify fermionic SPTs with unitary symmetries, but this is a question that cannot really be conclusively answered because there are infinitely many possible symmetry groups. Thus the most systematic approach asks whether there is anything below that sprawling complexity that is simpler and more systematic. After all, one should first understand these basics before plunging into the never ending story that lies beyond. To put this into context: There *are* classifications for certain unitary symmetry groups for free fermions [176–179] (but only “certain” not “all”). Also for *bosonic* SPTs one considers unitary symmetries [47]. So there is nothing inherently “bad” about them. The difference becomes clear when one compares the classification table below (the “periodic table”) with similar tables for bosonic SPTs [47]: The latter always have an exemplary character in that one must hope that the unitary symmetry one is interested in is listed; these lists are not exhaustive (they cannot be). However, once one throws all unitary symmetries away (= allows them to be explicitly broken), what is left is, quite unexpectedly, (1) *non-trivial* and (2) *finite* so that the classification introduced in the following *is* exhaustive (although in a more restricted sense).

...and only SP Hamiltonians without unitary symmetries:

$$H \text{ ** irreducible} \quad :\Leftrightarrow \quad \left([U, H] = 0 \Rightarrow U = e^{i\lambda} \mathbf{1} \right) \quad (6.2)$$

These irreducible Hamiltonians without unitary symmetries can be understood as the “atomic building blocks” of all Hamiltonians. To see this, consider an arbitrary Hamiltonian H with symmetry group G_0 that is unitarily realized on the SP Hilbert space \mathcal{H} . As always, we can

decompose the Hilbert space into irreducible representations λ of G_0 (with possible multiplicities):

$$\mathcal{H} = \bigoplus_{\lambda} \mathcal{H}_{\lambda} . \quad (6.3)$$

Each subspace \mathcal{H}_{λ} is composed of equivalent copies of the same irrep λ (“equivalent” in the sense of “isomorphic”):

$$\mathcal{H}_{\lambda} = \bigoplus_{\alpha=1}^{m_{\lambda}} \mathcal{H}_{\lambda}^{(\alpha)} \simeq \tilde{\mathcal{H}}_{\lambda} \otimes \mathcal{V}_{\lambda} \quad (6.4)$$

where $\mathcal{H}_{\lambda}^{(\alpha)} \simeq \mathcal{V}_{\lambda}$ for all α with the irrep \mathcal{V}_{λ} and $\tilde{\mathcal{H}}_{\lambda} = \mathbb{C}^{m_{\lambda}}$. It is $d_{\lambda} = \dim \mathcal{V}_{\lambda}$ the dimension of the irrep λ and m_{λ} the multiplicity of the irrep λ in \mathcal{H} . The \mathcal{H}_{λ} are known as G_0 -isotypic components of \mathcal{H} [180].

Since $[H, U_g] = 0$ for all $g \in G_0$ (with unitary representation U_g) and \mathcal{V}_{λ} is irreducible, it is

$$H = \bigoplus_{\lambda} H_{\lambda} \otimes \mathbb{1}_{d_{\lambda}} \quad \text{and} \quad U_g = \bigoplus_{\lambda} \mathbb{1}_{m_{\lambda}} \otimes U_g^{(\lambda)} . \quad (6.5)$$

The Hamiltonian blocks H_{λ} act on $\tilde{\mathcal{H}}_{\lambda}$ and have no longer any unitary symmetry left, they are the “irreducible building blocks” of all Hamiltonians, just as the $U_g^{(\lambda)}$ are the irreducible building blocks of all representations of the symmetry group G_0 . It is these irreducible Hamiltonians that we will focus on below (just like mathematicians study groups in terms of their irreducible representations $U_g^{(\lambda)}$).

3 | For a given irreducible SP Hamiltonian H check (henceforth we forget about \hat{H}) ...

$$\exists U_T ? : [U_T \mathcal{K}, H] = 0 \quad \text{and if so:} \quad U_T U_T^* \stackrel{?}{=} \pm \mathbb{1} \quad (6.6a)$$

$$\exists U_C ? : \{U_C \mathcal{K}, H\} = 0 \quad \text{and if so:} \quad U_C U_C^* \stackrel{?}{=} \pm \mathbb{1} \quad (6.6b)$$

$$\exists U_S ? : \{U_S, H\} = 0 \quad (6.6c)$$

→ Define:

$$\text{TRS:} \quad T \equiv U_T \mathcal{K} \quad (\text{antiunitary symmetry}) \quad (6.7a)$$

$$\text{PHS:} \quad C \equiv U_C \mathcal{K} \quad (\text{antiunitary pseudosymmetry}) \quad (6.7b)$$

$$\text{SLS:} \quad S \equiv U_S \quad (\text{unitary pseudosymmetry}) \quad (6.7c)$$

! Here we switch from our previous notation $T_U = U \mathcal{K}$ to $T \equiv T_{U_T} = U_T \mathcal{K}$ (similarly for $C = C_U$ and $S = S_U$) because we will mix T, C and S below and then it is important to distinguish the unitaries U_T, U_C and U_S .

→ Labeling scheme:

$$[T, H] \neq 0 \quad \Leftrightarrow \quad T = 0 \quad (6.8a)$$

$$[T, H] = 0 \quad \text{with} \quad T^2 = +1 \quad \Leftrightarrow \quad T = +1 \quad (6.8b)$$

$$[T, H] = 0 \quad \text{with} \quad T^2 = -1 \quad \Leftrightarrow \quad T = -1 \quad (6.8c)$$

$$\{C, H\} \neq 0 \quad \Leftrightarrow \quad C = 0 \quad (6.8d)$$

$$\{C, H\} = 0 \quad \text{with} \quad C^2 = +1 \quad \Leftrightarrow \quad C = +1 \quad (6.8e)$$

$$\{C, H\} = 0 \quad \text{with} \quad C^2 = -1 \quad \Leftrightarrow \quad C = -1 \quad (6.8f)$$

$$\{S, H\} \neq 0 \quad \Leftrightarrow \quad S = 0 \quad (6.8g)$$

$$\{S, H\} = 0 \quad \Leftrightarrow \quad S = 1 \quad (6.8h)$$

Note that this is an abuse of notation: In the left column, $T/C/S$ denote the *operators* of Eq. (6.7), whereas in the right column they are simply *variables* used to label the situation on the left. From the context it is always clear which use is intended.

→ Triple (T, C, S) encodes answers to classification in Eq. (6.6)

Note:

These constraints on the SP level can also be constructed quite systematically without deriving them from MB symmetries:

Imagine you are given a gapped SP Hamiltonian (= Hermitian matrix) H and a unitary U , and your job is to formulate a linear/antilinear constraint on H using only U and complex conjugation. The constraint can be written in the form

$$f(H, U) \stackrel{!}{=} H. \quad (6.9)$$

We want f to be linear/antilinear in H and its result must be Hermitian because H is; hence it should be $f(H, U) = \alpha UH^{(*)}U^\dagger$ with $\alpha \in \mathbb{R}$. Now note that $\det(H) = \det(\alpha UH^{(*)}U^\dagger) = \alpha^N \det(H)$; since H is gapped we can *w.l.o.g.* shift the Fermi energy (= zero energy) into the gap so that $\det(H) \neq 0$ and we have $\alpha^N = 1$.

In general, this leaves only four possibilities:

$$f(H, U) = \begin{cases} +1 \cdot UHU^\dagger & \text{(unitary symmetry)} \\ -1 \cdot UHU^\dagger & \text{(unitary pseudosymmetry} \rightarrow \text{SLS)} \\ +1 \cdot UH^*U^\dagger & \text{(antiunitary symmetry} \rightarrow \text{TRS)} \\ -1 \cdot UH^*U^\dagger & \text{(antiunitary pseudosymmetry} \rightarrow \text{PHS)} \end{cases} \quad (6.10)$$

Since for an irreducible Hamiltonian (by construction) there is no unitary symmetry (except the trivial one), we are left with the latter three constraints that are nothing but the three symmetries (on the MB level) we have discussed before.

4 | Important:

For a given irreducible Hamiltonian, TRS T_U , PHS C_U and SLS S_U are *unique* (if present)

To see this, assume T_{U_1} and T_{U_2} were two *different* time-reversal symmetries:

$$[T_{U_1}, H] = 0 \quad \text{and} \quad [T_{U_2}, H] = 0 \quad (6.11)$$

Then $\tilde{U} := T_{U_1}T_{U_2} = U_1U_2^*$ is a *unitary* symmetry of H :

$$[\tilde{U}, H] = 0 \xrightarrow{H \text{ irreducible}} \tilde{U} = e^{i\lambda} \mathbb{1}, \quad (6.12)$$

and therefore $T_{U_1} = U_1 \mathcal{K} = e^{i\lambda} U_2^{*\dagger} \mathcal{K} \propto T_{U_2}^{-1}$. So we can replace T_{U_1} by T_{U_2} or vice versa.

The same argument applies to PHS and similarly to SLS.

5 | Sublattice symmetry:

As already mentioned previously in Sections 4.1 and 5.3:

$$S = T \circ C = U_T U_C^* \quad \text{unitary operator with (w.l.o.g.)} \quad S^2 = +\mathbb{1} \quad (6.13)$$

One the many-body level: $\mathcal{S} = \mathcal{T} \circ \mathcal{C}$.

In particular:

$$\left. \begin{array}{l} \text{TRS:} \quad [T, H] = 0 \\ \text{PHS:} \quad \{C, H\} = 0 \end{array} \right\} \begin{array}{l} \Rightarrow \\ \Leftarrow \end{array} \{S, H\} = 0 \quad (6.14)$$

→ C cannot be eliminated in favor of T since S is not a unitary symmetry (but a pseudosymmetry)

! This means that despite “factoring out” all unitary symmetries of the SP Hamiltonian H , there can still be a unitary PHS symmetry \mathcal{C} of the MB Hamiltonian \hat{H} left because (1) C is antiunitary on the SP level and (2) $\mathcal{S} = \mathcal{T} \circ \mathcal{C}$ is a pseudosymmetry on the SP level.

→ Keep T , C , and S

6 | The “Tenfold way”:

Eq. (6.14) → (here T, C, S are used in their function as labels)

$$(T \neq 0 \vee C \neq 0) \Rightarrow S = |TC| \tag{6.15a}$$

$$\text{but: } T = 0 = C \Rightarrow \begin{cases} \text{either } S = 0 \\ \text{or } S = 1 \end{cases} \tag{6.15b}$$

This is easy to understand: If T and/or C are present, the relation $S = T \circ C$ determines the absence/presence of S automatically. Only if both T and C are absent, the absence/presence of S is not determined. (Note that $\mathcal{T} \circ \mathcal{C}$ can be a symmetry even if \mathcal{T} and \mathcal{C} are not symmetries separately!)

→ $3 \times 3 + 1 = 10$ symmetry classes:

Class	T	C	S
A	0	0	0
AII	0	0	1
AI	+1	0	0
BDI	+1	+1	1
D	0	+1	0
DII	-1	+1	1
AII	-1	0	0
CII	-1	-1	1
C	0	-1	0
CI	+1	-1	1

Remember: We encountered the classes AI, D and BDI before; the Kane-Mele model belonged to AII and the Chern insulator to A.

As mentioned before, the names of the classes go back to the mathematician ÉLIE CARTAN who assigned them to so called (large) symmetric spaces (of compact type); in the present context, the labels are typically taken “as is” without assigning any deeper meaning to them. The order in the above table seems arbitrary but is actually not – this will become clear later.

6.2. The periodic table of topological insulators and superconductors

We are finally prepared to fit all our discussed topological models into a *single classification scheme*:

7 | \leftarrow Gapped Hamiltonians H of class X in dimension d

Question: How to label the topological phases that can be realized by these systems?

Note that a *specific system H in X* may have *additional symmetries* (both unitary and antiunitary). However, the classification below does not *rely* on these symmetries, so that they can be broken by perturbations without leaving the phase.

8 | Answer:

Periodic table of topological insulators & superconductors:

		Symmetries			Dimensions							
Class		T	C	S	0D	1D	2D	3D	...	8D	...	
Complex (w/o T & C)	A	0	0	0	\mathbb{Z}	0	\mathbb{Z}	0	2-periodic →	\mathbb{Z}	...	
	AII	0	0	1	0	\mathbb{Z}	0	\mathbb{Z}		0	0	...
Real (w/ T or C)	AI	+1	0	0	\mathbb{Z}	0	0	0	"Bott periodicity" ↕ real U-groups	\mathbb{Z}	...	
	BDI	+1	+1	1	\mathbb{Z}_2	\mathbb{Z}	0	0		\mathbb{Z}_2	...	
	D	0	+1	0	\mathbb{Z}_2	\mathbb{Z}_2	\mathbb{Z}	0		\mathbb{Z}_2	...	
	DIII	-1	+1	1	0	\mathbb{Z}_2	\mathbb{Z}_2	\mathbb{Z}		0	0	...
	AII	-1	0	0	$2\mathbb{Z}$	0	\mathbb{Z}_2	\mathbb{Z}_2	8-periodic →	$2\mathbb{Z}$...	
	CII	-1	-1	1	0	$2\mathbb{Z}$	0	\mathbb{Z}_2		0	0	...
	C	0	-1	0	0	0	$2\mathbb{Z}$	0		0	0	...
	CI	+1	-1	1	0	0	0	$2\mathbb{Z}$		0	0	...

This course:

- Chern number**
 - IQHE
 - QWZ
 - Haldane
- Phaffian index**
 - Wu-Mele model
 - No Kramers pairs \mathcal{P} (Wu-Mele model)
- Winding number**
 - SSH-chain
 - All paths contractible \mathcal{P} (Majorana chains)
- Endpoints = Poles**
 - Majorana chain
 - Winding number
 - Majorana chain

Remember, remember...

The entries denote the classification of topological phases. 0 means “no TPs possible.” \mathbb{Z} means that there is an infinite number of different TPs labeled by an integer etc.

→ In every dimension, 5 out of 10 symmetry classes support TPs!

- The classification is referred to as “periodic table” because of its periodic structure for $d = 0, 1, \dots$ where the period for the “complex” classes is 2 and for the “real” classes 8.
- There are several equivalent ways to derive this table (and its periodicity), none of which is trivial. We will *sketch* one of the approaches below.

These methods were developed around 2008–2009 by different researchers [56, 57, 122].

- In case you wonder about the column for $d = 0$:* One should think of these systems as “blobs” without spatial structure. Mathematically, this column follows naturally and is not really special (actually, it is simpler because the constraints on the Hamiltonians are easier to implement). The Brillouin zone is simply T^0 (which is a point).

9 | Recipe:

If one studies a particular model (specified by a SP Hamiltonian H) and wants to find out whether any of its phases are topological, the standard procedure goes as follows:

- i | Check whether the SP Hamiltonian H features TRS, PHS, and/or SLS and (if so) whether TRS/PHS square to ± 1 .
 $\rightarrow (T, C, S) \rightarrow \text{Class } \mathbf{X}$
- ii | Use the periodic table above to check whether \mathbf{X} supports topological phases in the spatial dimension d of the given system.
- iii | Look up the associated topological invariant I for (\mathbf{X}, d) in Ref. [122].
- iv | Compute $I = I[H]$ as a function of the control parameters of the system and check whether it non-zero in (some of) the phases.

Without knowing about the periodic table and the systematic approach of Ref. [122] to construct topological invariants, we nevertheless succeeded for the Chern insulator (Class **A**) with the Chern number, the Kane-Mele model (Class **AII**) with the Pfaffian index, the SSH chain (Class **AIII**) with the winding number, and the Majorana chain (Class **D**) with the \mathbb{Z}_2 -index constructed from the BdG-Hamiltonian ☺.

Note: The symmetry classes are not exclusive. E.g., every system in class **BDI** can also be considered a member of the classes **AI**, **D**, or **AIII**. We encountered this ambiguity for the Majorana chain which generically is considered a representative of **D** even if the “clean” Majorana chain Hamiltonian does not break TRS. In this situation, TRS is considered an “accidental” symmetry that one does not want to rely on. If, however, one considers the Majorana chain a representative of **BDI**, TRS becomes a crucial symmetry that must not be broken. This may seem arbitrary but is perfectly valid as the choice of a protecting symmetry essentially specifies which perturbations we consider allowed and which forbidden. This situation is typical for all SPT phases as they do not have intrinsic topological order (recall our discussion of SPTs in ← Section 0.5). In → Section 6.4 we discuss *stacks* of Majorana chains where this concept should become clear.

6.3. Frameworks for classification

There are different frameworks that can be used to derive the periodic table above. Unfortunately, none of them is straightforward and all of them make heavy use of highly non-trivial physical and/or mathematical facts. A deep study of any of these approaches would easily fill its own course, so we keep it simple and sketch only one of the approaches exemplarily:

- Anderson localization on the boundary (Details: ↑ Refs. [56, 122])
Rationale: Study field theories (↑ *non-linear sigma models*) that describe the *boundary* of the system and determine when they retain delocalized states in the presence of disorder (i.e., whether they avoid ↑ *Anderson localization*). Mathematically, this happens if certain topological terms can be added to the action; the existence (and properties) of these terms depends on \mathbf{X} and d and provides the periodic table.
- Quantum anomalies on the boundary (Details: ↑ Ref. [181])
Rationale: Study ↑ *anomalous field theories* that can emerge as effective descriptions on the *boundaries* of the system (this approach relates to the one based on Anderson localization above). To cite Ludwig [92]:

“[The approach] relies on the notion that the boundary of a topological insulator (superconductor) cannot exist as an isolated system in its own dimensionality. Rather it must always be attached to a higher dimensional bulk.”

We encountered such an anomaly before when we discussed the IQHE and realized that its chiral edge modes are in conflict with the \leftarrow *Nielsen-Ninomiya theorem*. These edge modes can only be consistently formulated on the boundary of a two-dimensional bulk.

- **K-Theory:** (Details: \uparrow Ref. [57])

In contrast to the other two frameworks which (1) do not require translational invariance, and (2) focus on the boundary of the system, the K-theory approach pioneered by Kitaev assumes *translational invariance* and describes the *bulk* of the system. Let us briefly sketch the rationale of this (very mathematical) approach to get a feeling how the classification problem can be tackled on a very high level:

\uparrow (*Topological*) *K-theory* is a very general mathematical framework that is used to study vector bundles over topological spaces. It goes back to the influential 20th-century mathematician ALEXANDER GROTHENDIECK. In its application to classify topological phases, the topological base space is essentially the Brillouin torus and the system/Hamiltonian is described by a (potentially non-trivial) vector bundle over this space. Before its application to topological phases, K-theory had already found applications in string theory.

1 | \triangleleft Gapped (*translation invariant*) system with n filled (m empty) bands described by Bloch Hamiltonian $H(\mathbf{k})$

2 | Spectral flattening:

In this first step, we simplify the Hamiltonian without leaving the quantum phase to classify:

$$H(\mathbf{k}) \xrightarrow{\text{Continuous deformation}} \mathfrak{S}(\mathbf{k}) \quad (6.16a)$$

$$\text{with } \sigma(\mathfrak{S}(\mathbf{k})) = \underbrace{(-1, \dots, -1)}_{n \text{ filled bands}}, \underbrace{+1, \dots, +1}_{m \text{ empty bands}} \quad (6.16b)$$

$\sigma(A)$ denotes the spectrum (eigenvalues) of the operator A .

3 | \triangleleft Simplest case: Class **A** \rightarrow

(Hence we do not have to implement any symmetry constraint in the following.)

$$\mathfrak{S}(\mathbf{k}) = \underbrace{\mathcal{U}(\mathbf{k}) \begin{pmatrix} \mathbb{1}_m & 0 \\ 0 & -\mathbb{1}_n \end{pmatrix}}_{\mathbb{X}} \mathcal{U}^\dagger(\mathbf{k}) \quad \text{with } \mathcal{U}(\mathbf{k}) \in U(m+n) \quad (6.17)$$

$U(m+n)$ is the matrix group of unitary $(m+n) \times (m+n)$ -matrices.

4 | “Gauge symmetry”:

The decomposition in Eq. (6.17) is not unique:

$$\mathcal{U} \sim \mathcal{U}' \quad :\Leftrightarrow \quad \mathcal{U} = \mathcal{U}' \cdot \begin{pmatrix} \mathcal{U}_1 & 0 \\ 0 & \mathcal{U}_2 \end{pmatrix} \quad \text{for } \mathcal{U}_1 \in U(m), \mathcal{U}_2 \in U(n) \quad (6.18)$$

since then

$$\mathfrak{S}(\mathbf{k}) = \mathcal{U}(\mathbf{k}) \mathbb{X} \mathcal{U}^\dagger(\mathbf{k}) = \mathcal{U}'(\mathbf{k}) \mathbb{X} \mathcal{U}'^\dagger(\mathbf{k}) \quad (6.19)$$

That is, the \mathfrak{S} -encoding unitary \mathcal{U} is only defined up to unitaries from $U(m) \times U(n)$.

→

$$\mathfrak{S} : T^d \ni k \mapsto \mathfrak{S}(k) \hat{=} [\mathcal{U}(k)]_{\sim} \in \frac{U(m+n)}{U(m) \times U(n)} = G_{m,n+m}(\mathbb{C}) \quad (6.20)$$

$G_{m,n+m}(\mathbb{C})$: ↑ complex Grassmannian

In mathematics, Grassmannians are differentiable manifolds that parametrize the set of m -dimensional linear subspaces of an $n + m$ -dimensional vector space. The concept was introduced by mathematician HERMANN GRASSMANN in the 19th century.

→ $G_{m,n+m}(\mathbb{C})$ is the $\ast\ast$ classifying space C_0 for symmetry class **A** (and one of Cartan's symmetric spaces, which is where the label "A" comes from)

This statement is not completely correct, actually it is

$$C_0 = \bigcup_{k \in \mathbb{Z}} \lim_{s \rightarrow \infty} \frac{U(2s)}{U(s+k) \times U(s-k)} \simeq \lim_{n,m \rightarrow \infty} \frac{U(m+n)}{U(m) \times U(n)} \times \mathbb{Z}. \quad (6.21)$$

The idea behind this is that SP Hamiltonians of different sizes should be comparable (and the classification should not depend on system-specific parameters like m and n). In particular, for systems with $d > 0$ it should not matter whether one adds additional trivial bands to the system (like those from closed atomic shells). This leads to the concept of ↑ stable equivalence which has its counterpart in K -theory where one considers vector bundles modulo trivial bundles.

5 | Classifying spaces:

Similar arguments [taking the constraints (6.1) imposed by symmetries on the SP Hamiltonian into account] lead to the following table of classifying spaces:

	Class	T	C	S	Classifying Space	Name
Complex classes $UHU^t = -H$	A	0	0	0	$U(m+n) / U(m) \times U(n)$	C_0
	AIII	0	0	1	$U(n) \times U(n) / U(n)$	C_1
Real classes $UH^*U^t = H$	AI	+1	0	0	$O(n+m) / O(m) \times O(n)$	R_0
	BDI	+1	+1	1	$O(n) \times O(n) / O(n)$	R_1
	D	0	+1	0	$O(2n) / U(n)$	R_2
	DIII	-1	+1	1	$U(2n) / Sp(2n)$	R_3
	AII	-1	0	0	$Sp(n+m) / Sp(m) \times Sp(n)$	R_4
	CII	-1	-1	1	$Sp(n) \times Sp(n) / Sp(n)$	R_5
	C	0	-1	0	$Sp(2n) / U(n)$	R_6
	CI	+1	-1	1	$U(n) / O(n)$	R_7

- $Sp(n)$ denotes the compact symplectic group which is the analog of the unitary group $U(n)$ if one replaces the field \mathbb{C} by quaternions \mathbb{H} .
- The distinction between the two complex classes **A** and **AIII** and the remaining eight real classes follows from the reality constraints (that is, the constraint on the SP Hamiltonian includes a complex conjugate) on the Hamiltonians for real classes, and the missing of such for complex classes. On the mathematical level, this leads to the distinction between complex and real vector bundles and henceforth complex and real K -theory with classifying spaces C_q ($q \bmod 2$) and R_q ($q \bmod 8$), respectively.

- 6 | < Simplification: $T^d \mapsto S^d$ (we did this before when discussing Skyrmions in Section 2.1.1)

! This simplification is done for pedagogic reasons; it is undone → below and not part of the full classification.

→

$$\{ \text{Topological phases} \} \stackrel{\text{Physics}}{=} \left\{ \begin{array}{l} \text{Equivalence classes of continuous maps} \\ \mathfrak{S} : S^d \rightarrow C_0 \text{ that can be continuously} \\ \text{deformed into each other} \end{array} \right\} \quad (6.22a)$$

$$\stackrel{\text{Math}}{=} \langle d \text{th } \uparrow \text{ Homotopy group of } C_0 \rangle \equiv \pi_d(C_0) \quad (6.22b)$$

The homotopy group $\pi_d(X)$ is the group of equivalence classes (= homotopy classes) of (base-point-preserving) homeomorphisms (= continuous maps) from the d -dimensional sphere S^d to the topological space X . The special group $\pi_1(X)$ is called \uparrow *fundamental group* and describe the topologically different ways closed loops can be drawn on the space X , where two loops are equivalent if they can be continuously deformed into each other (this is the homotopy).

Example for $d = 2$: $\pi_2(C_0) \stackrel{*}{=} \mathbb{Z} \rightarrow$ Chern number ☺

Remember that the IQHE (and relatives) belong to class **A** (classified by C_0) and we identified the \mathbb{Z} -valued Chern number as label for possible topological phases.

- 7 | Undo simplification ($S^d \mapsto T^d$) & Include symmetry constraints

(Here we focus on the eight real classes, i.e., $\mathbf{X} \neq \mathbf{A}, \mathbf{AIII}$.)

Kitaev & K-Theory [57] $\xrightarrow{*}$

$$\{ \text{Topological phases of } (\mathbf{X}, d) \} = \underbrace{\pi(\bar{T}^d, R_q)}_{K_{\mathbb{R}}^{-q}(\bar{T}^d)} \stackrel{K\text{-theory}}{=} \underbrace{\pi_0(R_{q-d})}_{\substack{\text{** Strong topological index} \\ \rightarrow \text{Periodic table}}} \oplus \underbrace{\bigoplus_{s=0}^{d-1} \binom{d}{s} \pi_0(R_{q-s})}_{\substack{\text{** Weak topological indices} \\ \text{(not part of the periodic table)}}} \quad (6.23)$$

- $\pi_0(X)$ is the 0th homotopy group of X ; its elements label the *connected components* of X . Since the connectivity of the symmetric spaces R_q is known, the right-hand side of Eq. (6.23) can be looked up in the literature.
- $\pi(\bar{T}^d, R_q)$ describes the equivalence classes of all maps $\mathfrak{S}(\mathbf{k})$ from the BZ T^d into an appropriately restricted matrix space (which depends on the symmetry class \mathbf{X} , \uparrow Table 1 in Ref. [92]; for $d = 0$ the target space is the classifying space R_q that belongs to \mathbf{X} , for $d > 0$ this is only true at the TRIMs) that, in addition, satisfy the symmetry constraints on momenta demanded by the symmetry class \mathbf{X} (the latter constraint is indicated by the bar of \bar{T}^d); this object is known in K -theory as the “real K -group $K_{\mathbb{R}}^{-q}(\bar{T}^d)$ of \bar{T}^d .” Remember, for example, that TRS relates the Bloch Hamiltonian at momentum \mathbf{k} to the Bloch Hamiltonian at momentum $-\mathbf{k}$, Eq. (2.31d). These constraints are hidden in the precise definition of $\pi(\bar{T}^d, R_q)$.

→ Computing $\pi_0(R_{q-d})$ (= strong topological indices) ...

- for $q = 0, \dots, 7$ (real symmetry classes = rows)

- and $d = 0, 1, \dots$ (dimensions of space = columns)

...yields the periodic table (more precisely: the eight rows of the real symmetry classes)

Comments:

- There is an analog expression for the two *complex* classes **A** and **AIII** (first two rows of the periodic table).
- The contributions labeled “weak topological indices” are not part of the periodic table.

These additional indices have physical consequences, e.g., for ↑ *weak topological insulators* [57, 96, 97].

- The indices of the classifying spaces R_{q-d} and R_{q-s} are defined modulo 8; for the complex classes, the periodicity is 2 (this is known in K-theory as ↑ *Bott periodicity*). This leads to the periodicity of the *periodic* table in the dimension d and finally explains its name.

In contrast to the more famous periodic table in chemistry, this one is *really* periodic ☺.

8 | Example for $q = 4$ (**AII**) and $d = 2$ (e.g. ← *Kane-Mele model*):

$$\pi(\bar{T}^2, R_4) = \pi_0(R_2) \oplus 1 \times \pi_0(R_4) \oplus 2 \times \pi_0(R_3) \quad (6.24)$$

$$= \underbrace{\mathbb{Z}_2}_{\text{Pfaffian index}} \oplus \underbrace{\mathbb{Z}}_{\# \text{ Valence bands}} \oplus \underbrace{2 \times 0}_{\text{No weak indices}} \quad (6.25)$$

The values for $\pi_0(R_q)$ are provided in Table 2 of Ref. [57] but can also be read off from the $d = 0$ column of the periodic table (replacing $2\mathbb{Z}$ by \mathbb{Z}).

6.4. Consequences of interactions

In this part, we focused on *non-interacting* fermions. The crucial feature of such theories is that their MB Hamiltonian \hat{H} can be encoded by a SP Hamiltonian H so that their MB spectrum can be built from the SP spectrum; this makes them exactly (or efficiently) solvable. The periodic table is built on the SP Hamiltonians and is therefore only valid for systems that can be reasonably described by such theories.

The natural question is then of course:

What happens to the periodic table if *interactions* are included?

It is clear that interactions allow for more “paths” to connect gapped Hamiltonians, so that the classification must become “coarser” (i.e., phases that are separated without interactions may no longer be if interactions are allowed).

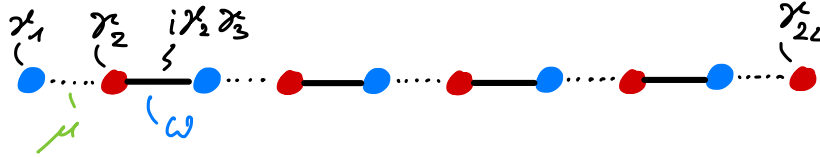
Quick answer:

- A full classification is known for *quartic* interactions (↑ Ref. [182]).
- In $d = 1$ dimensions, (interacting) fermions can be mapped to (interacting) *bosons* and fully classified via techniques that we discuss in Part II (↑ Refs. [29, 183, 184]).
- There is no complete classification known for arbitrary interactions and dimensions (as far as I know).
- This is a topic of ongoing research ... (e.g. ↑ Refs. [185, 186])

However, there is an *example* that demonstrates that (and how) the periodic table is modified by interactions for a specific (X, d) :

This was worked out by Fidkowski and Kitaev in 2010 [187]. You study this example on Problemset 8.

- 1 | Majorana chain for $w = \Delta > 0$ and $\mu = 0$: [Remember Eq. (5.39) in Section 5.5]



TRS & PHS → Symmetry class **BDI** in $d = 1$ → \mathbb{Z} -index

Remember the \mathbb{Z} -valued winding number defined in Section 5.3 which is quantized if TRS is present.

! Here we do *not* consider the Majorana chain as representative of class **D** *without* TRS; it turns out that the corresponding \mathbb{Z}_2 -index is stable under interactions [29].

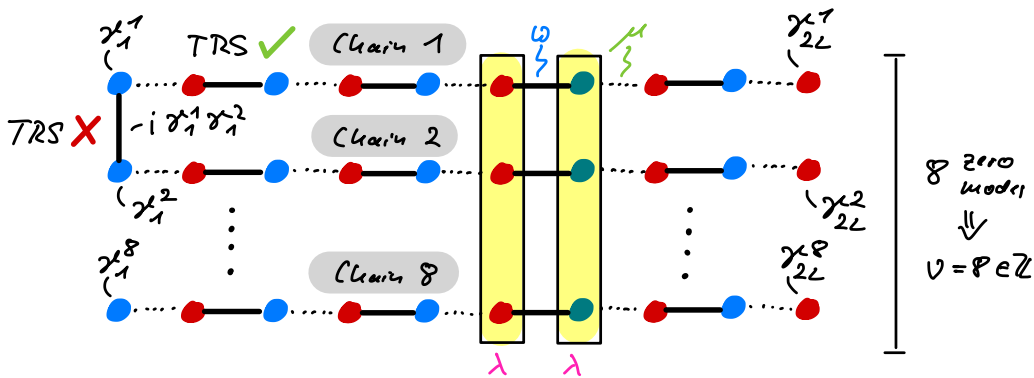
- 2 | Time-reversal symmetry:

$$\mathcal{T}i\mathcal{T}^{-1} = -i \quad \text{and} \quad \mathcal{T}\gamma_{2i-1}\mathcal{T}^{-1} = +\gamma_{2i-1}, \quad \mathcal{T}\gamma_{2i}\mathcal{T}^{-1} = -\gamma_{2i} \quad (6.26)$$

This follows from the “standard” TRS for *spinless* fermions: $\mathcal{T}c_i\mathcal{T}^{-1} = c_i$ and Eq. (5.33).

→ Only quadratic couplings between *even* (red) and *odd* (blue) Majorana modes allowed!

- 3 | Stack of Majorana chains in the topological phase:



Note that one could gap out the edge modes with $i\gamma_1^\alpha\gamma_1^{\alpha+1}$ but these terms *break* TRS (the coupled modes are both either even or odd)!

→ \mathbb{Z} -index = # dangling Majorana modes γ_1^α (on one end of the stack)

The chains are *oriented* in that they start with an odd and end with an even mode (which transform differently under TRS). Reversing the orientation of a chain therefore gives a negative index and indeed, a pair of chains with opposite orientation can be gapped out without breaking TRS because the two Majorana modes on one end are even and odd.

8 topological chains → **BDI**-index $\nu = 8$

Note that if there is an *odd* number of dangling Majorana modes on one end, you cannot gap them out completely even when breaking TRS because after gapping out all pairs a single mode will be left. This distinguishes the situations with an even and an odd number of Majorana zero modes and corresponds to the \mathbb{Z}_2 -index of class **D** that does not require TRS.

4 | **Idea:** Connect topological to trivial phase via quartic interaction:

$$\hat{H}(\mu, w, \lambda) = \hat{H}_{\text{MC}}(\mu, w) + \lambda \sum_{n=1}^{2L} W_n \tag{6.27}$$

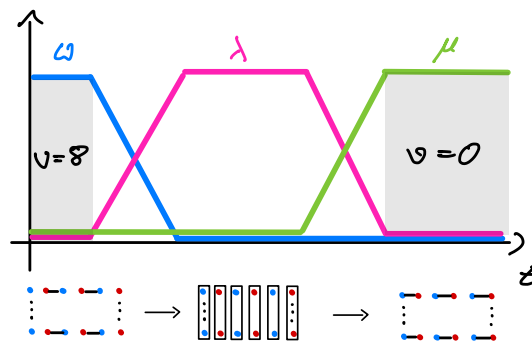
with quartic interaction between the 8 chains

$$W_n = \gamma_n^1 \gamma_n^2 \gamma_n^3 \gamma_n^4 \pm \dots \text{many more quartic terms} \tag{6.28}$$

See ↑ Eq. (8) in Ref. [187] for the full term and its derivation.

! The interaction terms W_n commute with the TRS in Eq. (6.26).

< Protocol:



On this continuous path ...

- the bulk gap remains open ...
This can be shown by exact diagonalization on a unit cell (which contains 8 fermion modes that span a $2^8 = 256$ dimensional Fock space).
You show this numerically on ⇨ Problemset 8.
- and TRS is not broken.
This is easily checked by inspection.

5 | Conclusion:

With *interactions* $\nu = 0$ and $\nu = 8$ are the *same* phase in **BDI**!

(6.29)

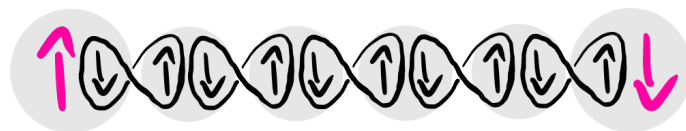
→ \mathbb{Z} -index of **BDI** in $d = 1$ reduces to \mathbb{Z}_8 -index

→ *With interactions* there are not infinitely many top. 1D superconductors in **BDI** but only 8!

For an overview how quartic interactions modify the periodic table in other dimensions and for other symmetry classes see Ref. [182].

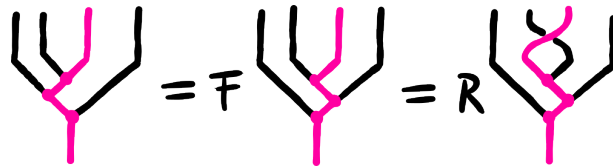
Part II.

Symmetry-Protected Topological Phases of Interacting Spin Systems



Part III.

Intrinsic Topological Order and Long-Range Entanglement



Bibliography

- [1] B. A. Bernevig and T. L. Hughes, *Topological Insulators and Topological Superconductors*, Princeton University Press, ISBN 9780691151755 (2013). (Cited on pages [v](#), [47](#), [93](#), and [131](#).)
- [2] J. K. Asbóth, L. Oroszlány and A. P. Pályi, *A Short Course on Topological Insulators: Band Structure and Edge States in One and Two Dimensions*, vol. 6 of *Lecture Notes in Physics*, Springer International Publishing, ISBN 3319256076 (2016). (Cited on pages [v](#), [116](#), and [122](#).)
- [3] M. Franz and L. W. Molenkamp, eds., *Topological insulators*, 6. Elsevier, Amsterdam, first edn., ISBN 9780444633187 (2013). (Cited on page [v](#).)
- [4] S.-Q. Shen, *Topological Insulators: Dirac Equation in Condensed Matters*, Springer Berlin Heidelberg, ISBN 9783642328589, doi:[10.1007/978-3-642-32858-9](#), [Download](#) (2012). (Cited on page [vi](#).)
- [5] R. Moessner and J. E. Moore, *Topological Phases of Matter*, Cambridge University Press, ISBN 9781107105539, doi:[10.1017/9781316226308](#) (2021). (Cited on page [vi](#).)
- [6] X. Chen, Z.-C. Gu and X.-G. Wen, *Classification of gapped symmetric phases in one-dimensional spin systems*, Physical Review B **83**, 035107 (2011), doi:[10.1103/physrevb.83.035107](#), [Download](#). (Cited on pages [vi](#), [16](#), [25](#), and [153](#).)
- [7] R. Verresen, R. Moessner and F. Pollmann, *One-dimensional symmetry protected topological phases and their transitions*, Physical Review B **96**(16), 165124 (2017), doi:[10.1103/physrevb.96.165124](#), [Download](#). (Cited on page [vi](#).)
- [8] S. H. Simon, *Topological quantum*, Oxford University Press, Oxford, ISBN 9780198886723 (2023). (Cited on page [vi](#).)
- [9] J. K. Pachos, *Introduction to Topological Quantum Computation*, Cambridge University Press, Cambridge, ISBN 9781139375498 (2012). (Cited on page [vi](#).)
- [10] X.-G. Wen, *Quantum field theory of many-body systems*, Oxford University Press, Oxford, repr. edn., ISBN 9780199227259 (2010). (Cited on page [vi](#).)
- [11] Z. Wang, *Topological Quantum Computation*, No. 112 in Regional Conference Series in Mathematics / Conference Board of the Mathematical Sciences. American Mathematical Society, ISBN 9780821849309 (2010). (Cited on page [vi](#).)
- [12] M. Nakahara, *Geometry, Topology and Physics*, CRC Press, ISBN 9781420056945 (2018). (Cited on pages [vi](#) and [93](#).)
- [13] K. v. Klitzing, G. Dorda and M. Pepper, *New method for high-accuracy determination of the fine-structure constant based on quantized Hall resistance*, Physical Review Letters **45**, 494 (1980), doi:[10.1103/physrevlett.45.494](#), [Download](#). (Cited on pages [vii](#), [19](#), [30](#), and [33](#).)
- [14] D. C. Tsui, H. L. Stormer and A. C. Gossard, *Two-dimensional magnetotransport in the extreme quantum limit*, Physical Review Letters **48**, 1559 (1982), doi:[10.1103/physrevlett.48.1559](#), [Download](#). (Cited on page [vii](#).)
- [15] R. B. Laughlin, *Anomalous quantum Hall effect: An incompressible quantum fluid with fractionally charged excitations*, Physical Review Letters **50**, 1395 (1983), doi:[10.1103/physrevlett.50.1395](#), [Download](#). (Cited on pages [vii](#) and [26](#).)
- [16] J. M. Kosterlitz and D. J. Thouless, *Ordering, metastability and phase transitions in two-dimensional systems*, Journal of Physics C: Solid State Physics **6**(7), 1181 (1973), doi:[10.1088/0022-3719/6/7/010](#), [Download](#). (Cited on page [vii](#).)
- [17] D. J. Thouless, M. Kohmoto, M. P. Nightingale and M. den Nijs, *Quantized Hall conductance in a two-dimensional periodic potential*, Physical Review Letters **49**, 405 (1982), doi:[10.1103/physrevlett.49.405](#), [Download](#). (Cited on pages [vii](#), [30](#), [33](#), [47](#), [51](#), and [57](#).)

- [18] F. D. M. Haldane, *Nonlinear field theory of large-spin Heisenberg antiferromagnets: Semiclassically quantized solitons of the one-dimensional easy-axis Néel state*, Physical Review Letters **50**, 1153 (1983), doi:[10.1103/physrevlett.50.1153](https://doi.org/10.1103/physrevlett.50.1153), [Download](#). (Cited on page vii.)
- [19] F. D. M. Haldane, *Model for a quantum Hall effect without Landau levels: Condensed-matter realization of the “parity anomaly”*, Physical Review Letters **61**, 2015 (1988), doi:[10.1103/physrevlett.61.2015](https://doi.org/10.1103/physrevlett.61.2015), [Download](#). (Cited on pages vii and 86.)
- [20] N. Lang and H. P. Büchler, *Topological networks for quantum communication between distant qubits*, npj Quantum Information **3**(1), 47 (2017), doi:[10.1038/s41534-017-0047-x](https://doi.org/10.1038/s41534-017-0047-x), [Download](#). (Cited on pages 1 and 128.)
- [21] F. Böttcher, J.-N. Schmidt, M. Wenzel, J. Hertkorn, M. Guo, T. Langen and T. Pfau, *Transient supersolid properties in an array of dipolar quantum droplets*, Physical Review X **9**(1), 011051 (2019), doi:[10.1103/physrevx.9.011051](https://doi.org/10.1103/physrevx.9.011051), [Download](#). (Cited on page 10.)
- [22] L. Tanzi, E. Lucioni, F. Famà, J. Catani, A. Fioretti, C. Gabbanini, R. Bisset, L. Santos and G. Modugno, *Observation of a dipolar quantum gas with metastable supersolid properties*, Physical Review Letters **122**(13), 130405 (2019), doi:[10.1103/physrevlett.122.130405](https://doi.org/10.1103/physrevlett.122.130405), [Download](#). (Cited on page 10.)
- [23] L. Chomaz, D. Petter, P. Ilzhöfer, G. Natale, A. Trautmann, C. Politi, G. Durastante, R. van Bijnen, A. Patscheider, M. Sohmen, M. Mark and F. Ferlaino, *Long-lived and transient supersolid behaviors in dipolar quantum gases*, Physical Review X **9**(2), 021012 (2019), doi:[10.1103/physrevx.9.021012](https://doi.org/10.1103/physrevx.9.021012), [Download](#). (Cited on page 10.)
- [24] C. Liu and G. G. Emch, *Explaining quantum spontaneous symmetry breaking*, Studies in History and Philosophy of Science Part B: Studies in History and Philosophy of Modern Physics **36**(1), 137 (2005), doi:[10.1016/j.shpsb.2004.12.003](https://doi.org/10.1016/j.shpsb.2004.12.003), [Download](#). (Cited on page 15.)
- [25] D. J. Baker and H. Halvorson, *How is spontaneous symmetry breaking possible? Understanding Wigner’s theorem in light of unitary inequivalence*, Studies in History and Philosophy of Science Part B: Studies in History and Philosophy of Modern Physics **44**(4), 464 (2013), doi:[10.1016/j.shpsb.2013.09.005](https://doi.org/10.1016/j.shpsb.2013.09.005), [Download](#). (Cited on page 15.)
- [26] N. Landsman, *Spontaneous symmetry breaking in quantum systems: Emergence or reduction?*, Studies in History and Philosophy of Science Part B: Studies in History and Philosophy of Modern Physics **44**(4), 379 (2013), doi:[10.1016/j.shpsb.2013.07.003](https://doi.org/10.1016/j.shpsb.2013.07.003), [Download](#). (Cited on page 15.)
- [27] M. B. Hastings and T. Koma, *Spectral gap and exponential decay of correlations*, Communications in Mathematical Physics **265**(3), 781 (2006), doi:[10.1007/s00220-006-0030-4](https://doi.org/10.1007/s00220-006-0030-4), [Download](#). (Cited on page 16.)
- [28] M. B. Hastings, *An area law for one-dimensional quantum systems*, Journal of Statistical Mechanics: Theory and Experiment **2007**(08), P08024 (2007), doi:[10.1088/1742-5468/2007/08/p08024](https://doi.org/10.1088/1742-5468/2007/08/p08024), [Download](#). (Cited on page 16.)
- [29] X. Chen, Z.-C. Gu and X.-G. Wen, *Complete classification of one-dimensional gapped quantum phases in interacting spin systems*, Physical Review B **84**, 235128 (2011), doi:[10.1103/physrevb.84.235128](https://doi.org/10.1103/physrevb.84.235128), [Download](#). (Cited on pages 17, 24, 143, 165, and 166.)
- [30] X. Chen, Z.-C. Gu and X.-G. Wen, *Local unitary transformation, long-range quantum entanglement, wave function renormalization, and topological order*, Physical Review B **82**, 155138 (2010), doi:[10.1103/physrevb.82.155138](https://doi.org/10.1103/physrevb.82.155138), [Download](#). (Cited on pages 17 and 25.)
- [31] G. Semeghini, H. Levine, A. Keesling, S. Ebadi, T. T. Wang, D. Bluvstein, R. Verresen, H. Pichler, M. Kalinowski, R. Samajdar, A. Omran, S. Sachdev *et al.*, *Probing topological spin liquids on a programmable quantum simulator*, Science **374**(6572), 1242 (2021), doi:[10.1126/science.abi8794](https://doi.org/10.1126/science.abi8794), [Download](#). (Cited on page 19.)
- [32] R. Acharya, D. A. Abanin, L. Aghababaie-Beni, I. Aleiner, T. I. Andersen, M. Ansmann, F. Arute, K. Arya, A. Asfaw, N. Astrakhantsev, J. Atalaya, R. Babbush *et al.*, *Quantum error correction below the surface code threshold*, Nature **638**(8052), 920 (2024), doi:[10.1038/s41586-024-08449-y](https://doi.org/10.1038/s41586-024-08449-y), [Download](#). (Cited on page 19.)
- [33] S. Trebst and C. Hickey, *Kitaev materials*, Physics Reports **950**, 1 (2022), doi:[10.1016/j.physrep.2021.11.003](https://doi.org/10.1016/j.physrep.2021.11.003), [Download](#). (Cited on page 19.)
- [34] Z. Liu and E. J. Bergholtz, *Recent developments in fractional Chern insulators*, pp. 515–538, Elsevier, ISBN 9780323914086, doi:[10.1016/b978-0-323-90800-9.00136-0](https://doi.org/10.1016/b978-0-323-90800-9.00136-0), [Download](#) (2024). (Cited on page 19.)
- [35] X.-G. Wen, *Colloquium: Zoo of quantum-topological phases of matter*, Reviews of Modern Physics **89**, 041004 (2017), doi:[10.1103/revmodphys.89.041004](https://doi.org/10.1103/revmodphys.89.041004), [Download](#). (Cited on pages 19, 20, 22, 66, 67, 86, 111, 112, 131, and 143.)

- [36] I. D. Rodríguez and G. Sierra, *Entanglement entropy of integer quantum Hall states*, *Physical Review B* **80**, 153303 (2009), doi:[10.1103/physrevb.80.153303](https://doi.org/10.1103/physrevb.80.153303), [Download](#). (Cited on pages 19 and 67.)
- [37] A. Kitaev and J. Preskill, *Topological entanglement entropy*, *Physical Review Letters* **96**, 110404 (2006), doi:[10.1103/physrevlett.96.110404](https://doi.org/10.1103/physrevlett.96.110404), [Download](#). (Cited on pages 19 and 67.)
- [38] X.-G. Wen, *Quantum orders and symmetric spin liquids*, *Physical Review B* **65**, 165113 (2002), doi:[10.1103/physrevb.65.165113](https://doi.org/10.1103/physrevb.65.165113), [Download](#). (Cited on page 19.)
- [39] X.-G. Wen, *Topological orders and Chern-Simons theory in strongly correlated quantum liquid*, *International Journal of Modern Physics B* **05**(10), 1641 (1991), doi:[10.1142/s0217979291001541](https://doi.org/10.1142/s0217979291001541), [Download](#). (Cited on pages 19 and 131.)
- [40] T. Hansson, V. Oganesyan and S. Sondhi, *Superconductors are topologically ordered*, *Annals of Physics* **313**(2), 497 (2004), doi:[10.1016/j.aop.2004.05.006](https://doi.org/10.1016/j.aop.2004.05.006), [Download](#). (Cited on pages 19 and 131.)
- [41] M. Blau and G. Thompson, *Topological gauge theories of antisymmetric tensor fields*, *Annals of Physics* **205**(1), 130 (1991), doi:[10.1016/0003-4916\(91\)90240-9](https://doi.org/10.1016/0003-4916(91)90240-9), [Download](#). (Cited on page 19.)
- [42] L. Kong and X.-G. Wen, *Braided fusion categories, gravitational anomalies, and the mathematical framework for topological orders in any dimensions*, arXiv e-prints arXiv:1405.5858 (2014), [1405.5858](https://arxiv.org/abs/1405.5858). (Cited on page 20.)
- [43] T. Lan, L. Kong and X.-G. Wen, *Theory of (2+1)-dimensional fermionic topological orders and fermionic/bosonic topological orders with symmetries*, *Physical Review B* **94**(15), 155113 (2016), doi:[10.1103/physrevb.94.155113](https://doi.org/10.1103/physrevb.94.155113), [Download](#). (Cited on page 20.)
- [44] S.-Q. Ning, Y. Qi, Z.-C. Gu and C. Wang, *Enforced symmetry breaking by invertible topological order*, *Physical Review Research* **5**(2), 023153 (2023), doi:[10.1103/physrevresearch.5.023153](https://doi.org/10.1103/physrevresearch.5.023153), [Download](#). (Cited on pages 20, 25, and 143.)
- [45] M. Cheng, Z. Bi, Y.-Z. You and Z.-C. Gu, *Classification of symmetry-protected phases for interacting fermions in two dimensions*, *Physical Review B* **97**, 205109 (2018), doi:[10.1103/physrevb.97.205109](https://doi.org/10.1103/physrevb.97.205109), [Download](#). (Cited on page 24.)
- [46] X. Chen, Z.-C. Gu, Z.-X. Liu and X.-G. Wen, *Symmetry-protected topological orders in interacting bosonic systems*, *Science* **338**(6114), 1604 (2012), doi:[10.1126/science.1227224](https://doi.org/10.1126/science.1227224), [Download](#). (Cited on page 24.)
- [47] X. Chen, Z.-C. Gu, Z.-X. Liu and X.-G. Wen, *Symmetry protected topological orders and the group cohomology of their symmetry group*, *Physical Review B* **87**, 155114 (2013), doi:[10.1103/physrevb.87.155114](https://doi.org/10.1103/physrevb.87.155114), [Download](#). (Cited on pages 24, 25, and 156.)
- [48] L. D. Landau, *Zur Theorie der Phasenumwandlungen I*, *Physikalische Zeitschrift der Sowjetunion* **11**, 26 (1937). (Cited on page 25.)
- [49] L. D. Landau, *Zur Theorie der Phasenumwandlungen II*, *Physikalische Zeitschrift der Sowjetunion* **11**, 545 (1937). (Cited on page 25.)
- [50] V. L. Ginzburg and L. D. Landau, *On the theory of superconductivity*, *Journal of Experimental and Theoretical Physics (JETP)* **20**, 1064 (1950). (Cited on page 25.)
- [51] E. Witten, *Topological quantum field theory*, *Communications in Mathematical Physics* **117**(3), 353 (1988), doi:[10.1007/bf01223371](https://doi.org/10.1007/bf01223371), [Download](#). (Cited on page 25.)
- [52] X.-G. Wen, *Topological orders in rigid states*, *International Journal of Modern Physics B* **04**(02), 239 (1990), doi:[10.1142/s0217979290000139](https://doi.org/10.1142/s0217979290000139), [Download](#). (Cited on page 25.)
- [53] D. S. Freed, *Short-range entanglement and invertible field theories* (2014), [1406.7278](https://arxiv.org/abs/1406.7278). (Cited on page 25.)
- [54] Z.-C. Gu and X.-G. Wen, *Symmetry-protected topological orders for interacting fermions: Fermionic topological nonlinear σ models and a special group supercohomology theory*, *Physical Review B* **90**, 115141 (2014), doi:[10.1103/physrevb.90.115141](https://doi.org/10.1103/physrevb.90.115141), [Download](#). (Cited on page 25.)
- [55] A. Kapustin, R. Thorngren, A. Turzillo and Z. Wang, *Fermionic symmetry protected topological phases and cobordisms*, *Journal of High Energy Physics* **2015**(12), 1 (2015), doi:[10.1007/jhep12\(2015\)052](https://doi.org/10.1007/jhep12(2015)052), [Download](#). (Cited on page 25.)
- [56] A. P. Schnyder, S. Ryu, A. Furusaki and A. W. W. Ludwig, *Classification of topological insulators and superconductors in three spatial dimensions*, *Physical Review B* **78**, 195125 (2008), doi:[10.1103/physrevb.78.195125](https://doi.org/10.1103/physrevb.78.195125), [Download](#). (Cited on pages 25, 160, and 161.)
- [57] A. Kitaev, *Periodic table for topological insulators and superconductors*, *AIP Conference Proceedings* **1134**(1), 22 (2009), doi:[10.1063/1.3149495](https://doi.org/10.1063/1.3149495), [Download](#). (Cited on pages 25, 73, 155, 160, 162, 164, and 165.)

- [58] X.-G. Wen and Q. Niu, *Ground-state degeneracy of the fractional quantum Hall states in the presence of a random potential and on high-genus Riemann surfaces*, *Physical Review B* **41**, 9377 (1990), doi:[10.1103/physrevb.41.9377](https://doi.org/10.1103/physrevb.41.9377), [Download](#). (Cited on page 26.)
- [59] D. Arovas, J. R. Schrieffer and F. Wilczek, *Fractional statistics and the quantum Hall effect*, *Physical Review Letters* **53**, 722 (1984), doi:[10.1103/physrevlett.53.722](https://doi.org/10.1103/physrevlett.53.722), [Download](#). (Cited on page 26.)
- [60] G. Moore and N. Read, *Nonabelions in the fractional quantum Hall effect*, *Nuclear Physics B* **360**(2), 362 (1991), doi:[10.1016/0550-3213\(91\)90407-o](https://doi.org/10.1016/0550-3213(91)90407-o), [Download](#). (Cited on page 26.)
- [61] A. Zee, *Quantum Hall fluids*, In *Field Theory, Topology and Condensed Matter Physics*, pp. 99–153. Springer Berlin Heidelberg, doi:[10.1007/bfb0113369](https://doi.org/10.1007/bfb0113369), [Download](#) (1995). (Cited on page 26.)
- [62] X.-G. Wen, *Chiral Luttinger liquid and the edge excitations in the fractional quantum Hall states*, *Physical Review B* **41**, 12838 (1990), doi:[10.1103/physrevb.41.12838](https://doi.org/10.1103/physrevb.41.12838), [Download](#). (Cited on page 27.)
- [63] E. Fradkin, *Field Theories of Condensed Matter Systems*, Addison-Wesley Publishing Company (1991). (Cited on pages 30, 47, 57, and 59.)
- [64] D. Tong, *Lectures on the Quantum Hall Effect*, arXiv (1606.06687) (2016), [Download](#). (Cited on pages 30, 47, 58, 64, and 65.)
- [65] R. Prange, M. Cage, K. Klitzing, S. Girvin, A. Chang, F. Haldane, R. Laughlin, A. Pruisken and D. Thouless, *The Quantum Hall Effect*, Graduate Texts in Contemporary Physics. Springer New York, ISBN 9781461233503 (2012). (Cited on page 30.)
- [66] G. W. Moore, *A comment on Berry connections*, doi:[10.48550/ARXIV.1706.01149](https://doi.org/10.48550/ARXIV.1706.01149), [Download](#) (2017). (Cited on pages 38 and 43.)
- [67] M. Born and V. Fock, *Beweis des Adiabatsatzes*, *Zeitschrift für Physik* **51**(3-4), 165 (1928), doi:[10.1007/bf01343193](https://doi.org/10.1007/bf01343193), [Download](#). (Cited on page 39.)
- [68] N. Lang, *Lecture notes on “Special and General Relativity”*, [Download](#) (2024). (Cited on page 42.)
- [69] M. V. Berry, *Quantal phase factors accompanying adiabatic changes*, *Proceedings of the Royal Society of London. A. Mathematical and Physical Sciences* **392**(1802), 45 (1984), doi:[10.1098/rspa.1984.0023](https://doi.org/10.1098/rspa.1984.0023), [Download](#). (Cited on pages 43 and 46.)
- [70] J. von Bergmann and H. von Bergmann, *Foucault pendulum through basic geometry*, *American Journal of Physics* **75**(10), 888 (2007), doi:[10.1119/1.2757623](https://doi.org/10.1119/1.2757623), [Download](#). (Cited on page 43.)
- [71] M. Berry, *Anticipations of the geometric phase*, *Physics Today* **43**(12), 34 (1990), doi:[10.1063/1.881219](https://doi.org/10.1063/1.881219), [Download](#). (Cited on page 43.)
- [72] T. Bitter and D. Dubbers, *Manifestation of Berry’s topological phase in neutron spin rotation*, *Physical Review Letters* **59**(3), 251 (1987), doi:[10.1103/physrevlett.59.251](https://doi.org/10.1103/physrevlett.59.251), [Download](#). (Cited on page 46.)
- [73] D. Suter, G. C. Chingas, R. A. Harris and A. Pines, *Berry’s phase in magnetic resonance*, *Molecular Physics* **61**(6), 1327 (1987), doi:[10.1080/00268978700101831](https://doi.org/10.1080/00268978700101831), [Download](#). (Cited on page 46.)
- [74] A. Tomita and R. Y. Chiao, *Observation of Berry’s topological phase by use of an optical fiber*, *Physical Review Letters* **57**(8), 937 (1986), doi:[10.1103/physrevlett.57.937](https://doi.org/10.1103/physrevlett.57.937), [Download](#). (Cited on page 46.)
- [75] F. D. M. Haldane, *Comment on “Observation of Berry’s topological phase by use of an optical fiber”*, *Physical Review Letters* **59**(15), 1788 (1987), doi:[10.1103/physrevlett.59.1788](https://doi.org/10.1103/physrevlett.59.1788), [Download](#). (Cited on page 46.)
- [76] Q. Niu, D. J. Thouless and Y.-S. Wu, *Quantized Hall conductance as a topological invariant*, *Physical Review B* **31**(6), 3372 (1985), doi:[10.1103/physrevb.31.3372](https://doi.org/10.1103/physrevb.31.3372), [Download](#). (Cited on pages 47, 57, and 58.)
- [77] R. Kubo, *Statistical-mechanical theory of irreversible processes. i. general theory and simple applications to magnetic and conduction problems*, *Journal of the Physical Society of Japan* **12**(6), 570 (1957), doi:[10.1143/jpsj.12.570](https://doi.org/10.1143/jpsj.12.570), [Download](#). (Cited on page 48.)
- [78] D. R. Hofstadter, *Energy levels and wave functions of bloch electrons in rational and irrational magnetic fields*, *Physical Review B* **14**(6), 2239 (1976), doi:[10.1103/physrevb.14.2239](https://doi.org/10.1103/physrevb.14.2239), [Download](#). (Cited on page 57.)
- [79] M. B. Hastings and S. Michalakis, *Quantization of Hall conductance for interacting electrons on a torus*, *Communications in Mathematical Physics* **334**(1), 433 (2014), doi:[10.1007/s00220-014-2167-x](https://doi.org/10.1007/s00220-014-2167-x), [Download](#). (Cited on pages 57 and 58.)
- [80] M. Büttiker, *Absence of backscattering in the quantum Hall effect in multiprobe conductors*, *Physical Review B* **38**(14), 9375 (1988), doi:[10.1103/physrevb.38.9375](https://doi.org/10.1103/physrevb.38.9375), [Download](#). (Cited on page 57.)

- [81] J. E. Avron, R. Seiler and B. Simon, *Homotopy and quantization in condensed matter physics*, Physical Review Letters **51**(1), 51 (1983), doi:[10.1103/physrevlett.51.51](https://doi.org/10.1103/physrevlett.51.51), [Download](#). (Cited on page 58.)
- [82] R. B. Laughlin, *Quantized Hall conductivity in two dimensions*, Physical Review B **23**, 5632 (1981), doi:[10.1103/physrevb.23.5632](https://doi.org/10.1103/physrevb.23.5632), [Download](#). (Cited on page 58.)
- [83] P. Mazur and S. de Groot, *On Onsager's relations in a magnetic field*, Physica **19**(1-12), 961 (1953), doi:[10.1016/s0031-8914\(53\)80108-4](https://doi.org/10.1016/s0031-8914(53)80108-4), [Download](#). (Cited on page 58.)
- [84] Y. Hatsugai, *Chern number and edge states in the integer quantum Hall effect*, Physical Review Letters **71**, 3697 (1993), doi:[10.1103/physrevlett.71.3697](https://doi.org/10.1103/physrevlett.71.3697), [Download](#). (Cited on page 62.)
- [85] A. M. Essin and V. Gurarie, *Bulk-boundary correspondence of topological insulators from their respective Green's functions*, Physical Review B **84**, 125132 (2011), doi:[10.1103/physrevb.84.125132](https://doi.org/10.1103/physrevb.84.125132), [Download](#). (Cited on page 62.)
- [86] T. Fukui, K. Shiozaki, T. Fujiwara and S. Fujimoto, *Bulk-edge correspondence for Chern topological phases: A viewpoint from a generalized index theorem*, Journal of the Physical Society of Japan **81**(11), 114602 (2012), doi:[10.1143/jpsj.81.114602](https://doi.org/10.1143/jpsj.81.114602), [Download](#). (Cited on page 62.)
- [87] H. Nielsen and M. Ninomiya, *Absence of neutrinos on a lattice: (I). Proof by homotopy theory*, Nuclear Physics B **185**(1), 20 (1981), doi:[10.1016/0550-3213\(81\)90361-8](https://doi.org/10.1016/0550-3213(81)90361-8), [Download](#). (Cited on page 64.)
- [88] H. Nielsen and M. Ninomiya, *Absence of neutrinos on a lattice: (II). Intuitive topological proof*, Nuclear Physics B **193**(1), 173 (1981), doi:[10.1016/0550-3213\(81\)90524-1](https://doi.org/10.1016/0550-3213(81)90524-1), [Download](#). (Cited on page 64.)
- [89] D. Tong, *Gauge theory*, Lecture notes, DAMTP Cambridge **10**(8) (2018), [Download](#). (Cited on page 64.)
- [90] C. Brouder, G. Panati, M. Calandra, C. Mourougane and N. Marzari, *Exponential localization of Wannier functions in insulators*, Physical Review Letters **98**, 046402 (2007), doi:[10.1103/physrevlett.98.046402](https://doi.org/10.1103/physrevlett.98.046402), [Download](#). (Cited on page 65.)
- [91] M. B. Hastings and T. A. Loring, *Almost commuting matrices, localized Wannier functions, and the quantum Hall effect*, Journal of Mathematical Physics **51**(1), 015214 (2010), doi:[10.1063/1.3274817](https://doi.org/10.1063/1.3274817), [Download](#). (Cited on page 65.)
- [92] A. W. W. Ludwig, *Topological phases: Classification of topological insulators and superconductors of non-interacting fermions, and beyond*, Physica Scripta **2016**(T168), 014001 (2016), doi:[10.1088/0031-8949/2015/t168/014001](https://doi.org/10.1088/0031-8949/2015/t168/014001), [Download](#). (Cited on pages 66, 74, 78, 155, 161, and 164.)
- [93] S. Rachel, *Quantum phase transitions of topological insulators without gap closing*, Journal of Physics: Condensed Matter **28**(40), 405502 (2016), doi:[10.1088/0953-8984/28/40/405502](https://doi.org/10.1088/0953-8984/28/40/405502), [Download](#). (Cited on page 67.)
- [94] S. Rachel, *Interacting topological insulators: a review*, Reports on Progress in Physics **81**(11), 116501 (2018), doi:[10.1088/1361-6633/aad6a6](https://doi.org/10.1088/1361-6633/aad6a6), [Download](#). (Cited on pages 67 and 111.)
- [95] T. H. R. Skyrme, *A non-linear field theory*, Proceedings of the Royal Society of London. Series A. Mathematical and Physical Sciences **260**(1300), 127 (1961), doi:[10.1098/rspa.1961.0018](https://doi.org/10.1098/rspa.1961.0018), [Download](#). (Cited on page 71.)
- [96] L. Fu, C. L. Kane and E. J. Mele, *Topological insulators in three dimensions*, Physical Review Letters **98**(10), 106803 (2007), doi:[10.1103/physrevlett.98.106803](https://doi.org/10.1103/physrevlett.98.106803), [Download](#). (Cited on pages 73, 107, 112, and 165.)
- [97] L. Fu and C. L. Kane, *Topological insulators with inversion symmetry*, Physical Review B **76**(4), 045302 (2007), doi:[10.1103/physrevb.76.045302](https://doi.org/10.1103/physrevb.76.045302), [Download](#). (Cited on pages 73, 93, 112, and 165.)
- [98] E. P. Wigner, *Gruppentheorie und ihre Anwendung auf die Quantenmechanik der Atomspektren*, Vieweg+Teubner Verlag, Wiesbaden, ISBN 978-3-663-00642-8, doi:[10.1007/978-3-663-02555-9](https://doi.org/10.1007/978-3-663-02555-9), [Download](#) (1931). (Cited on page 74.)
- [99] E. P. Wigner, *Über die Operation der Zeitumkehr in der Quantenmechanik* pp. 213–226 (1993), doi:[10.1007/978-3-662-02781-3_15](https://doi.org/10.1007/978-3-662-02781-3_15), [Download](#). (Cited on page 76.)
- [100] J. E. Moore and L. Balents, *Topological invariants of time-reversal-invariant band structures*, Physical Review B **75**(12), 121306 (2007), doi:[10.1103/PhysRevB.75.121306](https://doi.org/10.1103/PhysRevB.75.121306), [Download](#). (Cited on pages 79, 104, and 112.)
- [101] N. Lang, *Lecture notes on "Quantum Field Theory"*, [Download](#) (2023). (Cited on page 80.)
- [102] X.-L. Qi, Y.-S. Wu and S.-C. Zhang, *Topological quantization of the spin Hall effect in two-dimensional paramagnetic semiconductors*, Physical Review B **74**(8), 085308 (2006), doi:[10.1103/physrevb.74.085308](https://doi.org/10.1103/physrevb.74.085308), [Download](#). (Cited on page 82.)

- [103] F. D. M. Haldane, *Nobel lecture “Topological Quantum Matter”*, [Download](#) (2016). (Cited on page 86.)
- [104] R. Yu, W. Zhang, H.-J. Zhang, S.-C. Zhang, X. Dai and Z. Fang, *Quantized anomalous Hall effect in magnetic topological insulators*, *Science* **329**(5987), 61 (2010), doi:[10.1126/science.1187485](https://doi.org/10.1126/science.1187485), [Download](#). (Cited on page 92.)
- [105] C.-Z. Chang, J. Zhang, X. Feng, J. Shen, Z. Zhang, M. Guo, K. Li, Y. Ou, P. Wei, L.-L. Wang, Z.-Q. Ji, Y. Feng *et al.*, *Experimental observation of the quantum anomalous Hall effect in a magnetic topological insulator*, *Science* **340**(6129), 167 (2013), doi:[10.1126/science.1234414](https://doi.org/10.1126/science.1234414), [Download](#). (Cited on page 92.)
- [106] X. Kou, S.-T. Guo, Y. Fan, L. Pan, M. Lang, Y. Jiang, Q. Shao, T. Nie, K. Murata, J. Tang, Y. Wang, L. He *et al.*, *Scale-invariant quantum anomalous Hall effect in magnetic topological insulators beyond the two-dimensional limit*, *Physical Review Letters* **113**(13), 137201 (2014), doi:[10.1103/physrevlett.113.137201](https://doi.org/10.1103/physrevlett.113.137201), [Download](#). (Cited on page 92.)
- [107] J. G. Checkelsky, R. Yoshimi, A. Tsukazaki, K. S. Takahashi, Y. Kozuka, J. Falson, M. Kawasaki and Y. Tokura, *Trajectory of the anomalous Hall effect towards the quantized state in a ferromagnetic topological insulator*, *Nature Physics* **10**(10), 731 (2014), doi:[10.1038/nphys3053](https://doi.org/10.1038/nphys3053), [Download](#). (Cited on page 92.)
- [108] G. Jotzu, M. Messer, R. Desbuquois, M. Lebrat, T. Uehlinger, D. Greif and T. Esslinger, *Experimental realization of the topological Haldane model with ultracold fermions*, *Nature* **515**, 237 (2014), doi:[10.1038/nature13915](https://doi.org/10.1038/nature13915), [Download](#). (Cited on page 92.)
- [109] M.-C. Liang, Y.-D. Wei, L. Zhang, X.-J. Wang, H. Zhang, W.-W. Wang, W. Qi, X.-J. Liu and X. Zhang, *Realization of Qi-Wu-Zhang model in spin-orbit-coupled ultracold fermions*, *Physical Review Research* **5**(1), 012006 (2023), doi:[10.1103/physrevresearch.5.1012006](https://doi.org/10.1103/physrevresearch.5.1012006), [Download](#). (Cited on page 92.)
- [110] C. L. Kane and E. J. Mele, *Quantum spin Hall effect in graphene*, *Physical Review Letters* **95**, 226801 (2005), doi:[10.1103/physrevlett.95.226801](https://doi.org/10.1103/physrevlett.95.226801), [Download](#). (Cited on pages 93, 97, and 111.)
- [111] C. L. Kane and E. J. Mele, *Z_2 topological order and the quantum spin Hall effect*, *Physical Review Letters* **95**, 146802 (2005), doi:[10.1103/physrevlett.95.146802](https://doi.org/10.1103/physrevlett.95.146802), [Download](#). (Cited on pages 93, 97, 99, 106, 107, 108, 109, and 111.)
- [112] L. Fu and C. L. Kane, *Time reversal polarization and a Z_2 adiabatic spin pump*, *Physical Review B* **74**(19), 195312 (2006), doi:[10.1103/PhysRevB.74.195312](https://doi.org/10.1103/PhysRevB.74.195312), [Download](#). (Cited on pages 93 and 105.)
- [113] M. Fruchart and D. Carpentier, *An introduction to topological insulators*, *Comptes Rendus Physique* **14**(9-10), 779 (2013), doi:[10.1016/j.crhy.2013.09.013](https://doi.org/10.1016/j.crhy.2013.09.013), [Download](#). (Cited on pages 93, 104, and 105.)
- [114] D. Carpentier, *Topology of bands in solids: From insulators to Dirac matter*, In *Dirac Matter*, pp. 95–129. Springer, doi:[10.1007/978-3-319-32536-1_5](https://doi.org/10.1007/978-3-319-32536-1_5), [Download](#) (2017). (Cited on pages 93 and 104.)
- [115] R. M. Kaufmann, D. Li and B. Wehefritz-Kaufmann, *Notes on topological insulators*, *Reviews in Mathematical Physics* **28**(10), 1630003 (2016), doi:[10.1142/S0129055X1630003X](https://doi.org/10.1142/S0129055X1630003X), [Download](#). (Cited on page 93.)
- [116] C. Nash and S. Sen, *Topology and Geometry for Physicists*, Dover Books on Mathematics. Dover Publications, ISBN 9780486318363 (2013). (Cited on page 93.)
- [117] Y. A. Bychkov and E. I. Rashba, *Oscillatory effects and the magnetic susceptibility of carriers in inversion layers*, *Journal of Physics C: Solid State Physics* **17**(33), 6039 (1984), doi:[10.1088/0022-3719/17/33/015](https://doi.org/10.1088/0022-3719/17/33/015), [Download](#). (Cited on page 97.)
- [118] B. A. Bernevig, T. L. Hughes and S.-C. Zhang, *Quantum spin Hall effect and topological phase transition in HgTe quantum wells*, *Science* **314**(5806), 1757 (2006), doi:[10.1126/science.1133734](https://doi.org/10.1126/science.1133734), [Download](#). (Cited on page 112.)
- [119] M. König, S. Wiedmann, C. Brüne, A. Roth, H. Buhmann, L. W. Molenkamp, X.-L. Qi and S.-C. Zhang, *Quantum spin Hall insulator state in HgTe quantum wells*, *Science* **318**(5851), 766 (2007), doi:[10.1126/science.1148047](https://doi.org/10.1126/science.1148047), [Download](#). (Cited on page 112.)
- [120] D. Hsieh, D. Qian, L. Wray, Y. Xia, Y. S. Hor, R. J. Cava and M. Z. Hasan, *A topological Dirac insulator in a quantum spin Hall phase*, *Nature* **452**, 970 (2008), doi:[10.1038/nature06843](https://doi.org/10.1038/nature06843), [Download](#). (Cited on page 112.)
- [121] X.-L. Qi and S.-C. Zhang, *Topological insulators and superconductors*, *Reviews of Modern Physics* **83**, 1057 (2011), doi:[10.1103/revmodphys.83.1057](https://doi.org/10.1103/revmodphys.83.1057), [Download](#). (Cited on page 112.)
- [122] S. Ryu, A. P. Schnyder, A. Furusaki and A. W. W. Ludwig, *Topological insulators and superconductors: Tenfold way and dimensional hierarchy*, *New Journal of Physics* **12**(6), 065010 (2010), doi:[10.1088/1367-2630/12/6/065010](https://doi.org/10.1088/1367-2630/12/6/065010), [Download](#). (Cited on pages 112, 155, 160, and 161.)

- [123] R. Roy, *Topological phases and the quantum spin Hall effect in three dimensions*, Physical Review B **79**(19), 195322 (2009), doi: [10.1103/PhysRevB.79.195322](https://doi.org/10.1103/PhysRevB.79.195322), [Download](#). (Cited on page 112.)
- [124] J. L. Gross, J. Yellen and P. Zhang, eds., *Handbook of graph theory*, Discrete mathematics and its applications. CRC Press, Boca Raton, second edn., ISBN 9781498761369 (2014). (Cited on page 115.)
- [125] W. P. Su, J. R. Schrieffer and A. J. Heeger, *Solitons in polyacetylene*, Physical Review Letters **42**, 1698 (1979), doi: [10.1103/physrevlett.42.1698](https://doi.org/10.1103/physrevlett.42.1698), [Download](#). (Cited on page 116.)
- [126] N. Lang, *One-Dimensional Topological States of Synthetic Quantum Matter*, Verlag Dr. Hut, München, ISBN 978-3-8439-4157-0, [Download](#) (2019). (Cited on pages 116, 131, and 142.)
- [127] J. Zak, *Berry's phase for energy bands in solids*, Physical Review Letters **62**, 2747 (1989), doi: [10.1103/physrevlett.62.2747](https://doi.org/10.1103/physrevlett.62.2747), [Download](#). (Cited on page 121.)
- [128] M. Atala, M. Aidelsburger, J. T. Barreiro, D. Abanin, T. Kitagawa, E. Demler and I. Bloch, *Direct measurement of the Zak phase in topological Bloch bands*, Nature Physics **9**, 795 (2013), doi: [10.1038/nphys2790](https://doi.org/10.1038/nphys2790), [Download](#). (Cited on pages 121 and 128.)
- [129] E. J. Meier, F. A. An and B. Gadway, *Observation of the topological soliton state in the Su-Schrieffer-Heeger model*, Nature Communications **7**(1) (2016), doi: [10.1038/ncomms13986](https://doi.org/10.1038/ncomms13986), [Download](#). (Cited on page 128.)
- [130] P. St-Jean, V. Goblot, E. Galopin, A. Lemaître, T. Ozawa, L. Le Gratiet, I. Sagnes, J. Bloch and A. Amo, *Lasing in topological edge states of a one-dimensional lattice*, Nature Photonics **11**(10), 651 (2017), doi: [10.1038/s41566-017-0006-2](https://doi.org/10.1038/s41566-017-0006-2), [Download](#). (Cited on page 128.)
- [131] R. Chaunsali, E. Kim, A. Thakkar, P. Kevrekidis and J. Yang, *Demonstrating an in situ topological band transition in cylindrical granular chains*, Physical Review Letters **119**(2), 024301 (2017), doi: [10.1103/physrevlett.119.024301](https://doi.org/10.1103/physrevlett.119.024301), [Download](#). (Cited on page 128.)
- [132] T. Tian, Y. Zhang, L. Zhang, L. Wu, S. Lin, J. Zhou, C.-K. Duan, J.-H. Jiang and J. Du, *Experimental realization of nonreciprocal adiabatic transfer of phonons in a dynamically modulated nanomechanical topological insulator*, Physical Review Letters **129**(21), 215901 (2022), doi: [10.1103/physrevlett.129.215901](https://doi.org/10.1103/physrevlett.129.215901), [Download](#). (Cited on page 128.)
- [133] T. Yuan, C. Zeng, Y.-Y. Mao, F.-F. Wu, Y.-J. Xie, W.-Z. Zhang, H.-N. Dai, Y.-A. Chen and J.-W. Pan, *Realizing robust edge-to-edge transport of atomic momentum states in a dynamically modulated synthetic lattice*, Physical Review Research **5**(3), 032005 (2023), doi: [10.1103/physrevresearch.5.032005](https://doi.org/10.1103/physrevresearch.5.032005), [Download](#). (Cited on page 128.)
- [134] S. de Léséleuc, V. Lienhard, P. Scholl, D. Barredo, S. Weber, N. Lang, H. P. Büchler, T. Lahaye and A. Browaeys, *Observation of a symmetry-protected topological phase of interacting bosons with Rydberg atoms*, Science **365**(6455), 775 (2019), doi: [10.1126/science.aav9105](https://doi.org/10.1126/science.aav9105), [Download](#). (Cited on page 128.)
- [135] S. Elitzur, *Impossibility of spontaneously breaking local symmetries*, Physical Review D **12**, 3978 (1975), doi: [10.1103/physrevd.12.3978](https://doi.org/10.1103/physrevd.12.3978), [Download](#). (Cited on page 131.)
- [136] J. Fröhlich, G. Morchio and F. Strocchi, *Higgs phenomenon without symmetry breaking order parameter*, Nuclear Physics B **190**(3), 553 (1981), doi: [10.1016/0550-3213\(81\)90448-x](https://doi.org/10.1016/0550-3213(81)90448-x), [Download](#). (Cited on page 131.)
- [137] M. Greiter, *Is electromagnetic gauge invariance spontaneously violated in superconductors?*, Annals of Physics **319**(1), 217 (2005), doi: [10.1016/j.aop.2005.03.008](https://doi.org/10.1016/j.aop.2005.03.008), [Download](#). (Cited on page 131.)
- [138] S. Friederich, *Gauge symmetry breaking in gauge theories—in search of clarification*, European Journal for Philosophy of Science **3**(2), 157 (2012), doi: [10.1007/s13194-012-0061-y](https://doi.org/10.1007/s13194-012-0061-y), [Download](#). (Cited on page 131.)
- [139] A. Y. Kitaev, *Unpaired Majorana fermions in quantum wires*, Physics-Uspekhi **44**(10S), 131 (2001), doi: [10.1070/1063-7869/44/10s/s29](https://doi.org/10.1070/1063-7869/44/10s/s29), [Download](#). (Cited on pages 131 and 138.)
- [140] N. Lang, *Phase transitions and topological phases by driven dissipation*, Master's thesis, University of Stuttgart (2013). (Cited on page 131.)
- [141] V. Mourik, K. Zuo, S. M. Frolov, S. R. Plissard, E. P. A. M. Bakkers and L. P. Kouwenhoven, *Signatures of Majorana fermions in hybrid superconductor-semiconductor nanowire devices*, Science **336**(6084), 1003 (2012), doi: [10.1126/science.1222360](https://doi.org/10.1126/science.1222360), [Download](#). (Cited on pages 132 and 154.)
- [142] H. Zhang, C.-X. Liu, S. Gazibegovic, D. Xu, J. A. Logan, G. Wang, N. van Loo, J. D. S. Bommer, M. W. A. de Moor, D. Car, R. L. M. Op het Veld, P. J. van Veldhoven *et al.*, *Quantized Majorana conductance*, Nature **556**, 74 (2018), doi: [10.1038/nature26142](https://doi.org/10.1038/nature26142), [Download](#). (Cited on pages 132 and 154.)
- [143] M. R. Zirnbauer, *Particle-hole symmetries in condensed matter*, Journal of Mathematical Physics **62**(2), 021101 (2021), doi: [10.1063/5.0035358](https://doi.org/10.1063/5.0035358), [Download](#). (Cited on page 136.)

- [144] J. C. Budich and E. Ardonne, *Equivalent topological invariants for one-dimensional Majorana wires in symmetry class D*, Physical Review B **88**(7), 075419 (2013), doi:[10.1103/PhysRevB.88.075419](https://doi.org/10.1103/PhysRevB.88.075419), [Download](#). (Cited on page 138.)
- [145] R. Wakatsuki, M. Ezawa, Y. Tanaka and N. Nagaosa, *Fermion fractionalization to Majorana fermions in a dimerized Kitaev superconductor*, Physical Review B **90**(1), 014505 (2014), doi:[10.1103/PhysRevB.90.014505](https://doi.org/10.1103/PhysRevB.90.014505), [Download](#). (Cited on page 141.)
- [146] D. Rainis and D. Loss, *Majorana qubit decoherence by quasiparticle poisoning*, Physical Review B **85**, 174533 (2012), doi:[10.1103/physrevb.85.174533](https://doi.org/10.1103/physrevb.85.174533), [Download](#). (Cited on page 146.)
- [147] T. Karzig, C. Knapp, R. M. Lutchyn, P. Bonderson, M. B. Hastings, C. Nayak, J. Alicea, K. Flensberg, S. Plugge, Y. Oreg, C. M. Marcus and M. H. Freedman, *Scalable designs for quasiparticle-poisoning-protected topological quantum computation with Majorana zero modes*, Physical Review B **95**, 235305 (2017), doi:[10.1103/physrevb.95.235305](https://doi.org/10.1103/physrevb.95.235305), [Download](#). (Cited on pages 146, 151, and 154.)
- [148] P. W. Shor, *Scheme for reducing decoherence in quantum computer memory*, Physical Review A **52**, R2493 (1995), doi:[10.1103/physreva.52.r2493](https://doi.org/10.1103/physreva.52.r2493), [Download](#). (Cited on page 150.)
- [149] N. Lang and H. P. Büchler, *Strictly local one-dimensional topological quantum error correction with symmetry-constrained cellular automata*, SciPost Physics **4**, 007 (2018), doi:[10.21468/scipostphys.4.1.007](https://doi.org/10.21468/scipostphys.4.1.007), [Download](#). (Cited on pages 150 and 152.)
- [150] J. Alicea, Y. Oreg, G. Refael, F. von Oppen and M. P. A. Fisher, *Non-abelian statistics and topological quantum information processing in 1D wire networks*, Nature Physics **7**, 412 (2011), doi:[10.1038/nphys1915](https://doi.org/10.1038/nphys1915), [Download](#). (Cited on pages 151 and 154.)
- [151] M. Aghaee, A. Alcaraz Ramirez, Z. Alam, R. Ali, M. Andrzejczuk, A. Antipov, M. Astafev, A. Barzegar, B. Bauer, J. Becker, U. K. Bhaskar, A. Bocharov *et al.*, *Interferometric single-shot parity measurement in InAs–Al hybrid devices*, Nature **638**(8051), 651 (2025), doi:[10.1038/s41586-024-08445-2](https://doi.org/10.1038/s41586-024-08445-2), [Download](#). (Cited on pages 151 and 154.)
- [152] J. Edmonds, *Paths, trees, and flowers*, Canadian Journal of Mathematics **17**, 449 (1965), doi:[10.4153/cjm-1965-045-4](https://doi.org/10.4153/cjm-1965-045-4), [Download](#). (Cited on page 152.)
- [153] V. Kolmogorov, *Blossom v: a new implementation of a minimum cost perfect matching algorithm*, Mathematical Programming Computation **1**(1), 43 (2009), doi:[10.1007/s12532-009-0002-8](https://doi.org/10.1007/s12532-009-0002-8), [Download](#). (Cited on page 152.)
- [154] E. Dennis, A. Kitaev, A. Landahl and J. Preskill, *Topological quantum memory*, Journal of Mathematical Physics **43**(9), 4452 (2002), doi:[10.1063/1.1499754](https://doi.org/10.1063/1.1499754), [Download](#). (Cited on page 152.)
- [155] G. Duclos-Cianci and D. Poulin, *Fast decoders for topological quantum codes*, Physical Review Letters **104**, 050504 (2010), doi:[10.1103/physrevlett.104.050504](https://doi.org/10.1103/physrevlett.104.050504), [Download](#). (Cited on page 152.)
- [156] A. G. Fowler, A. C. Whiteside and L. C. L. Hollenberg, *Towards practical classical processing for the surface code*, Physical Review Letters **108**, 180501 (2012), doi:[10.1103/physrevlett.108.180501](https://doi.org/10.1103/physrevlett.108.180501), [Download](#). (Cited on page 152.)
- [157] S. Bravyi, M. Suchara and A. Vargo, *Efficient algorithms for maximum likelihood decoding in the surface code*, Physical Review A **90**(3), 032326 (2014), doi:[10.1103/physreva.90.032326](https://doi.org/10.1103/physreva.90.032326), [Download](#). (Cited on page 152.)
- [158] F. Roser, H. P. Büchler and N. Lang, *Decoding the projective transverse field ising model*, Physical Review B **107**(21), 214201 (2023), doi:[10.1103/physrevb.107.214201](https://doi.org/10.1103/physrevb.107.214201), [Download](#). (Cited on page 152.)
- [159] S. Bravyi, B. M. Terhal and B. Leemhuis, *Majorana fermion codes*, New Journal of Physics **12**(8), 083039 (2010), doi:[10.1088/1367-2630/12/8/083039](https://doi.org/10.1088/1367-2630/12/8/083039), [Download](#). (Cited on page 153.)
- [160] S. Bravyi and B. Terhal, *A no-go theorem for a two-dimensional self-correcting quantum memory based on stabilizer codes*, New Journal of Physics **11**(4), 043029 (2009), doi:[10.1088/1367-2630/11/4/043029](https://doi.org/10.1088/1367-2630/11/4/043029), [Download](#). (Cited on page 153.)
- [161] B. Yoshida, *Feasibility of self-correcting quantum memory and thermal stability of topological order*, Annals of Physics **326**(10), 2566 (2011), doi:[10.1016/j.aop.2011.06.001](https://doi.org/10.1016/j.aop.2011.06.001), [Download](#). (Cited on page 153.)
- [162] J. Haah, *Local stabilizer codes in three dimensions without string logical operators*, Physical Review A **83**, 042330 (2011), doi:[10.1103/physreva.83.042330](https://doi.org/10.1103/physreva.83.042330), [Download](#). (Cited on page 153.)
- [163] S. Bravyi and J. Haah, *Quantum self-correction in the 3D cubic code model*, Physical Review Letters **111**, 200501 (2013), doi:[10.1103/physrevlett.111.200501](https://doi.org/10.1103/physrevlett.111.200501), [Download](#). (Cited on page 153.)

- [164] R. Alicki, M. Horodecki, P. Horodecki and R. Horodecki, *On thermal stability of topological qubit in Kitaev's 4D model*, *Open Systems & Information Dynamics* **17**(01), 1 (2010), doi:[10.1142/s1230161210000023](https://doi.org/10.1142/s1230161210000023), [Download](#). (Cited on page 153.)
- [165] A. Kitaev, *Anyons in an exactly solved model and beyond*, *Annals of Physics* **321**(1), 2 (2006), doi:[10.1016/j.aop.2005.10.005](https://doi.org/10.1016/j.aop.2005.10.005), [Download](#). (Cited on page 153.)
- [166] M. Barkeshli, C.-M. Jian and X.-L. Qi, *Twist defects and projective non-abelian braiding statistics*, *Physical Review B* **87**, 045130 (2013), doi:[10.1103/physrevb.87.045130](https://doi.org/10.1103/physrevb.87.045130), [Download](#). (Cited on page 153.)
- [167] N. Read and D. Green, *Paired states of fermions in two dimensions with breaking of parity and time-reversal symmetries and the fractional quantum Hall effect*, *Physical Review B* **61**, 10267 (2000), doi:[10.1103/physrevb.61.10267](https://doi.org/10.1103/physrevb.61.10267), [Download](#). (Cited on page 153.)
- [168] S. Bravyi, *Universal quantum computation with the $\nu = 5/2$ fractional quantum hall state*, *Physical Review A* **73**(4), 042313 (2006), doi:[10.1103/physreva.73.042313](https://doi.org/10.1103/physreva.73.042313), [Download](#). (Cited on page 154.)
- [169] P. Bonderson, M. Freedman and C. Nayak, *Measurement-only topological quantum computation*, *Physical Review Letters* **101**(1), 010501 (2008), doi:[10.1103/physrevlett.101.010501](https://doi.org/10.1103/physrevlett.101.010501), [Download](#). (Cited on page 154.)
- [170] R. M. Lutchyn, J. D. Sau and S. Das Sarma, *Majorana fermions and a topological phase transition in semiconductor-superconductor heterostructures*, *Physical Review Letters* **105**, 077001 (2010), doi:[10.1103/PhysRevLett.105.077001](https://doi.org/10.1103/PhysRevLett.105.077001), [Download](#). (Cited on page 154.)
- [171] Y. Oreg, G. Refael and F. von Oppen, *Helical liquids and Majorana bound states in quantum wires*, *Physical Review Letters* **105**, 177002 (2010), doi:[10.1103/PhysRevLett.105.177002](https://doi.org/10.1103/PhysRevLett.105.177002), [Download](#). (Cited on page 154.)
- [172] S. M. Albrecht, A. P. Higginbotham, M. Madsen, F. Kuemmeth, T. S. Jespersen, J. Nygård, P. Krogstrup and C. M. Marcus, *Exponential protection of zero modes in Majorana islands*, *Nature* **531**, 206 (2016), doi:[10.1038/nature17162](https://doi.org/10.1038/nature17162), [Download](#). (Cited on page 154.)
- [173] F. Nichele, A. C. Drachmann, A. M. Whiticar, E. C. O'Farrell, H. J. Suominen, A. Fornieri, T. Wang, G. C. Gardner, C. Thomas, A. T. Hatke, P. Krogstrup, M. J. Manfra et al., *Scaling of Majorana zero-bias conductance peaks*, *Physical Review Letters* **119**(13), 136803 (2017), doi:[10.1103/physrevlett.119.136803](https://doi.org/10.1103/physrevlett.119.136803), [Download](#). (Cited on page 154.)
- [174] R. M. Lutchyn, E. P. A. M. Bakkers, L. P. Kouwenhoven, P. Krogstrup, C. M. Marcus and Y. Oreg, *Majorana zero modes in superconductor-semiconductor heterostructures*, *Nature Reviews Materials* **3**(5), 52 (2018), doi:[10.1038/s41578-018-0003-1](https://doi.org/10.1038/s41578-018-0003-1), [Download](#). (Cited on page 154.)
- [175] H. F. Legg, *Comment on "Interferometric single-shot parity measurement in InAs-Al hybrid devices"*, *Microsoft Quantum, Nature* **638**, 651-655 (2025), doi:[10.48550/ARXIV.2503.08944](https://doi.org/10.48550/ARXIV.2503.08944), [Download](#) (2025). (Cited on page 154.)
- [176] L. Fu, *Topological crystalline insulators*, *Physical Review Letters* **106**, 106802 (2011), doi:[10.1103/physrevlett.106.106802](https://doi.org/10.1103/physrevlett.106.106802), [Download](#). (Cited on page 156.)
- [177] C.-K. Chiu, H. Yao and S. Ryu, *Classification of topological insulators and superconductors in the presence of reflection symmetry*, *Physical Review B* **88**, 075142 (2013), doi:[10.1103/physrevb.88.075142](https://doi.org/10.1103/physrevb.88.075142), [Download](#). (Cited on page 156.)
- [178] T. Morimoto and A. Furusaki, *Topological classification with additional symmetries from Clifford algebras*, *Physical Review B* **88**, 125129 (2013), doi:[10.1103/physrevb.88.125129](https://doi.org/10.1103/physrevb.88.125129), [Download](#). (Cited on page 156.)
- [179] K. Shiozaki and M. Sato, *Topology of crystalline insulators and superconductors*, *Physical Review B* **90**, 165114 (2014), doi:[10.1103/physrevb.90.165114](https://doi.org/10.1103/physrevb.90.165114), [Download](#). (Cited on page 156.)
- [180] P. Heinzner, A. Huckleberry and M. Zirnbauer, *Symmetry classes of disordered fermions*, *Communications in Mathematical Physics* **257**(3), 725 (2005), doi:[10.1007/s00220-005-1330-9](https://doi.org/10.1007/s00220-005-1330-9), [Download](#). (Cited on page 157.)
- [181] S. Ryu, J. E. Moore and A. W. W. Ludwig, *Electromagnetic and gravitational responses and anomalies in topological insulators and superconductors*, *Physical Review B* **85**(4), 045104 (2012), doi:[10.1103/PhysRevB.85.045104](https://doi.org/10.1103/PhysRevB.85.045104), [Download](#). (Cited on page 161.)
- [182] T. Morimoto, A. Furusaki and C. Mudry, *Breakdown of the topological classification for gapped phases of noninteracting fermions by quartic interactions*, *Physical Review B* **92**(12), 125104 (2015), doi:[10.1103/PhysRevB.92.125104](https://doi.org/10.1103/PhysRevB.92.125104), [Download](#). (Cited on pages 165 and 167.)

- [183] L. Fidkowski and A. Kitaev, *Topological phases of fermions in one dimension*, Physical Review B **83**, 075103 (2011), doi:[10.1103/physrevb.83.075103](https://doi.org/10.1103/physrevb.83.075103), [Download](#). (Cited on page 165.)
- [184] A. M. Turner, F. Pollmann and E. Berg, *Topological phases of one-dimensional fermions: An entanglement point of view*, Physical Review B **83**, 075102 (2011), doi:[10.1103/physrevb.83.075102](https://doi.org/10.1103/physrevb.83.075102), [Download](#). (Cited on page 165.)
- [185] S. Rachel, *Interacting topological insulators: a review*, Reports on Progress in Physics **81**(11), 116501 (2018), doi:[10.1088/1361-6633/aad6a6](https://doi.org/10.1088/1361-6633/aad6a6), [Download](#). (Cited on page 165.)
- [186] Q.-R. Wang and Z.-C. Gu, *Towards a complete classification of symmetry-protected topological phases for interacting fermions in three dimensions and a general group supercohomology theory*, Physical Review X **8**, 011055 (2018), doi:[10.1103/physrevx.8.011055](https://doi.org/10.1103/physrevx.8.011055), [Download](#). (Cited on page 165.)
- [187] L. Fidkowski and A. Kitaev, *Effects of interactions on the topological classification of free fermion systems*, Physical Review B **81**, 134509 (2010), doi:[10.1103/physrevb.81.134509](https://doi.org/10.1103/physrevb.81.134509), [Download](#). (Cited on pages 166 and 167.)